TECHNICAL REPORT STANDARD PAGE

1. Title and Subtitle
Internal Friction Angle of Sands with High Fines Content

2. Author(s)
Murad Abu-Farsakh, Ph.D., P.E.; Salman S. Abusalman

3. Performing Organization Name and Address
Louisiana Transportation Research Center
4101 Gourrier Avenue
Baton Rouge, LA 70808

4. Sponsoring Agency Name and Address
Louisiana Department of Transportation and Development
P.O. Box 94245
Baton Rouge, LA 70804-9245

5. Report No.
FHWA/LA.24/699

6. Report Date
October 2024

7. Performing Organization Code
LTRC Project Number: 21-1GT
SIO Number: DOTLT1000375

8. Type of Report and Period Covered
Final Report
Mar 2021 – Mar 2024

9. No. of Pages
314

10. Supplementary Notes
Conducted in Cooperation with the U.S. Department of Transportation, Federal Highway Administration.

11. Distribution Statement
Unrestricted. This document is available through the National Technical Information Service, Springfield, VA 21161.

12. Key Words
Internal friction angle; high fines content; SPT; CPT; mechanical behavior; shear strength.

13. Abstract
A comprehensive laboratory testing program that included small and large direct shear tests (DST) was performed in this study to evaluate the effect of fines content on the internal friction angle (ϕ) of sand mixed with fines, as well as the interface friction angle (δ) between sand soils mixed with fines and the concrete pile face. Small DSTs were performed to evaluate the ϕ for sand soils mixed with different fines contents (10% to 70%), different relative densities, and different moisture contents (omc, omc+2%, omc+4%, omc+6%), while large DSTs were conducted to evaluate the δ between sand soils mixed with fines and the concrete pile surface. Four different soils (Soil 2 to Soil 5) were employed to mix the original sand soil (Soil 1) with fines at different fines contents. Scanning Electron Microscope (SEM) tests were performed to examine the particle shapes and measure the roundness (R) for the different sand-fines samples. The results of DSTs showed that the ϕ and δ for the sand-fines mixtures decreased when increasing the fines content (mainly silt content), decreased when increasing the fine sand content, decreased when increasing the moisture content, and decreased when decreasing the relative density. The coefficient of interface friction between the sand soil mixtures and concrete

surface ranged from 0.65 to 0.76, with an average of 0.69. A reduction factor (ψ) was introduced and calculated to account for the effect of silt and fine sand, which represents the ratio between the interface coefficient of friction for clean sand and sand with fines content, and the results suggest that a sand mixture with approximately 60% silt or approximately 20% fine sand will reduce the interface coefficient of friction to approximately 80% of the value for clean sand. This study also focused on modifying the Schmertmann and Japan Road Association (JRA) of SPT-ϕ correlation equations and charts to estimate the ϕ considering fines content and other soil parameters. Non-linear regression analysis was performed using the fines (silt) content, fine sand content, relative density, moisture content, and R to modify the Schmertmann and JRA equations to estimate the ϕ angle for sand-fines mixtures. Artificial Neural Network (ANN) models were also developed to estimate the ϕ of the sand-fines mixtures. The developed regression equations were verified using two problematic sites in Louisiana with sand mixed with high fines content (mainly silts), which showed an error of ≤5% at one site and <10% at the second site. The results from selected literature and this study were also explored to provide guidelines to evaluate the threshold percentage of fines content (silt or clay) beyond which sand soils mixed with fines behave differently than clean sand with <5% fines.

Project Review Committee

Each research project will have an advisory committee appointed by the LTRC Director. The Project Review Committee is responsible for assisting the LTRC Administrator or Manager in the development of acceptable research problem statements, requests for proposals, review of research proposals, oversight of approved research projects, and implementation of findings.

LTRC appreciates the dedication of the following Project Review Committee Members in guiding this research study to fruition.

LTRC Administrator/Manager

Zhongjie "Doc" Zhang, Ph.D., P.E.

Pavement and Geotechnical Research Manager

Members

Jesse Rauser, James Chatagnier, Jess Thurman, Kevin Mai, Gavin Gautreau, Sergio Aviles, Richie Charoenpap, Xin Peng, and Arturo Aguirre

Directorate Implementation Sponsor

Chad Winchester, P.E.

DOTD Chief Engineer

Internal Friction Angle of Sands with High Fines Content

By

Murad Y. Abu-Farsakh, Ph.D., P.E.
Salman S. Abusalman

Louisiana Transportation Research Center
4101 Gourrier Avenue
Baton Rouge, LA 70808

LTRC Project No. 21-1GT
SIO No. DOTLT1000375

conducted for
Louisiana Department of Transportation and Development
Louisiana Transportation Research Center

October 2024

Abstract

A comprehensive laboratory testing program that included small and large direct shear tests (DST) was performed in this study to evaluate the effect of fines content on the internal friction angle (ϕ) of sand mixed with fines, as well as the interface friction angle (δ) between sand soils mixed with fines and the concrete pile face. Small DSTs were performed to evaluate the ϕ for sand soils mixed with different fines contents (10% to 70%), different relative densities, and different moisture contents (omc, omc+2%, omc+4%, omc+6%), while large DSTs were conducted to evaluate the δ between sand soils mixed with fines and the concrete pile surface. Four different soils (Soil 2 to Soil 5) were employed to mix the original sand soil (Soil 1) with fines at different fines contents. Scanning Electron Microscope (SEM) tests were performed to examine the particle shapes and measure the roundness (R) for the different sand-fines samples. The results of DSTs showed that the ϕ and δ for the sand-fines mixtures decreased when increasing the fines content (mainly silt content), decreased when increasing the fine sand content, decreased when increasing the moisture content, and decreased when decreasing the relative density. The coefficient of interface friction between the sand soil mixtures and concrete surface ranged from 0.65 to 0.76, with an average of 0.69. A reduction factor (ψ) was introduced and calculated to account for the effect of silt and fine sand, which represents the ratio between the interface coefficient of friction for clean sand and sand with fines content, and the results suggest that a sand mixture with approximately 60% silt or approximately 20% fine sand will reduce the interface coefficient of friction to approximately 80% of the value for clean sand. This study also focused on modifying the Schmertmann and Japan Road Association (JRA) of SPT-ϕ correlation equations and charts to estimate the ϕ considering fines content and other soil parameters. Non-linear regression analysis was performed using the fines (silt) content, fine sand content, relative density, moisture content, and R to modify the Schmertmann and JRA equations to estimate the ϕ for sand-fines mixtures. Artificial Neural Network (ANN) models were also developed to estimate the ϕ of the sand-fines mixtures. The developed regression equations were verified using two problematic sites in Louisiana with sand mixed with high fines content (mainly silts), which showed an error of $\leq$5% at one site and <10% at the second site. The results from selected literature and this study were also explored to provide guidelines to evaluate the threshold percentage of fines content (silt or clay) beyond which sand soils mixed with fines behave differently than clean sand with <5% fines.

Acknowledgments

This research project was funded by the Louisiana Department of Transportation and Development (DOTD) and the Louisiana Transportation Research Center (LTRC). The help and support of Dr. Zhongjie Zhang at LTRC is gratefully acknowledged.

Implementation Statement

The accurate evaluation of the internal friction angle (ϕ) of cohesion-less soils, such as sand, is very important in the design of infrastructure and other geotechnical engineering problems. Unfortunately, it is very difficult to obtain undisturbed sand samples to evaluate the ϕ from laboratory tests. Therefore, correlation equations are often used to estimate ϕ from in-situ tests, such as standard penetration tests (SPT) or cone penetration tests (CPT). However, almost all correlations available in literature between the ϕ and SPT/CPT results were developed for clean sand with <5% fines. Nevertheless, sand soil mixtures with significant fines contents (clay and/or silt) are frequently encountered in many project sites, where the developed ϕ-SPT (or ϕ-CPT) correlations are not valid. Several project sites in Louisiana featuring driven piles in sandy soils with a high percentage of non-plastic fines (silt) or fine sand were tested to have lower capacities than the design values, which led to the underestimation of pile lengths. This is primarily due to a higher estimation of the ϕ values from available ϕ-SPT correlations.

The results of this study demonstrated the potential benefits of improving the existing ϕ-SPT correlations for local Louisiana soils, which can be realized in various geotechnical areas. The developed non-linear ϕ-SPT(N_{60}) regression equations of modified Schmertmann and Japan Road Association (JRA) models, as well as the developed Artificial Neural Network (ANN) models for estimating ϕ of sand-fines mixtures considering silt content, fine sand content, water content, and roundness, can help DOTD engineers perform better analyses and obtain a more accurate design of infrastructure and other geotechnical engineering problems.

The findings of this research study can be implemented by DOTD design engineers in the analysis, design, and performance evaluation of various geotechnical engineering applications, including:

1. Better characterization of the subsurface soil conditions of sites with cohesion-less soils using the modified ϕ-SPT(N_{60}) correlations and ANN models.
2. Faster and better assessment of the selected soil mechanical properties using the modified ϕ-SPT(N_{60}) correlations and ANN models.
3. More accurate and safer design of piles driven into subsurface soil of sand with high fines content using the modified ϕ-SPT(N_{60}) correlations and ANN models.

4. Better assessment of the threshold of fines content (silt or clay) beyond which sand soils mixed with fines behave as silty soil or cohesive clayey soils.

Table of Contents

List of Tables

List of Figures

Introduction

The internal friction angle (ϕ) of a soil is an important parameter used in the strength limit state design of infrastructure from a geotechnical standpoint. It can be determined either by conducting laboratory tests on retrieved soil samples, such as direct shear tests (DST) and triaxial tests, or from correlations with in-situ test results. Unfortunately, it is very difficult to obtain undisturbed sandy soil samples; as a result, the ϕ for sandy soils cannot be accurately estimated directly from laboratory tests. Therefore, correlations are necessary to estimate the values of the ϕ for sandy soils from in-situ testing parameters, such as the standard penetration test (SPT) or the cone penetration test (CPT). Several correlation equations and charts were developed in the literature for clean sand using SPT or CPT data. However, sand soil mixtures (with fines content), such as silty sands and clayey sands, are more frequently encountered in geotechnical engineering projects than clean sand soils. Consequently, the variability of the ϕ estimation remains significant, and a shortcoming of these methods is that the effect of fines content on the ϕ is not properly considered in the literature. The Louisiana Department of Transportation and Development (DOTD) uses the correlation recommended by the Federal Highway Administration (FHWA) to obtain the ϕ for sandy soils, which are only developed for clean sand with fines content <5%. This major shortcoming creates many problematic concerns in DOTD geotechnical engineering design concerning sand with fines content. Several projects featuring piles driven in sandy soils with a high percentage of non-plastic fines (i.e., silt) or fine sand that were tested in the field have lower resistance than the anticipated design values, which led to the underestimation of pile lengths. The design pile length was 15-30 feet less than the actual pile length needed. This is due to the higher internal friction values estimated from current SPT correlations. DOTD geotechnical engineers tend to reduce the values of the ϕ of sandy soils with fines content and be more cautious whenever they encounter sites with sand and high non-plastic fines or fine sand.

The primary objective of this study was to evaluate the effect of fines content and fine sand on the value of the internal friction angle (ϕ) of silty/clayey sand or fine sand soils typically encountered in local Louisiana soils. Additionally, because concrete is a common material used to manufacture driven piles in Louisiana, researchers aimed to evaluate the effect of fines content and fine sand on the interface friction angle (δ) between the sandy soils with fines content and concrete piles. Furthermore, they investigated the threshold of fines content beyond which the sand soils mixed with fines (silt and clay) will behave differently than clean sand (i.e., cohesive soil behavior).

In this study, small and large direct shear tests were performed to evaluate the internal friction angle (ϕ) for sandy soils mixed with fines, while large direct shear tests were conducted to investigate the interface friction angle (δ) between sandy soils mixed with fines and the concrete pile surface. Different fines contents (silt/clay), relative densities, moisture contents, soil particle shapes, gradations, and confining stresses were considered to determine their effects on the ϕ and δ. The results of these tests were used to develop the relationships between relative density, fines content, moisture content, and the ϕ (or δ). These relationships were used to modify the correlation charts and equations typically used to evaluate the ϕ of sandy soil using the SPT in order to consider the contribution of the fines contents. Statistical regression analysis and an Artificial Neural Network (ANN) were used to develop equations and models to account for the effects of fines content and other parameters on the ϕ.

Objectives

The primary objectives of this study were to:

- Evaluate the effect of fines content and fine sand content on the value of the internal friction angle (ϕ) of sand soils mixed with fines typically encountered in Louisiana.
- Evaluate the effect of fines content and fine sand content on the interface friction angle (δ) between sand soils mixed with fines and concrete interface.
- Determine the threshold percentage of fines content beyond which sand soils mixed with fines (i.e., fine-grained or cohesive soils) behave differently than cohesion-less soils. This will have a direct impact on the design of pile foundations, since different static design methods are used for piles driven in different soil types (i.e., sand or clay).

Scope

In this study, the small direct shear test was performed to evaluate the internal friction angle (ϕ) for sand soils mixed with fines, while the large direct shear test was conducted to evaluate the interface friction angle (δ) between sand soils mixed with fines and the concrete pile surface. Different fines contents (silt/clay), relative densities, moisture contents, soil particle shapes, gradations, and confining stresses were considered to determine the effect of these parameters on the values of the ϕ and δ. The results of these tests were used to develop regression relationships between relative density, fines content, moisture content, and the ϕ (or δ). These relationships were used to modify the correlation equations and charts used to evaluate the ϕ of sand using the standard penetration tests (SPT) to consider the contribution of the fine contents. A statistical regression analysis and neural network were used to develop equations and models to estimate the ϕ considering the fines content and other parameters.

Literature Review

This study was focused on evaluating the effect of fines contents and their gradations on the overall soil mechanical behavior and the interface mechanical behavior between sand-fines mixtures and pile materials (e.g., concrete). The experimental work in this study aimed at investigating the mechanical behavior of sand-fine mixtures under monotonic loading and drained conditions. For this purpose, a comprehensive literature review was performed on previous research studies related to laboratory and field tests, analytical analysis, correlation with in-situ tests, effect of fines content, and liquefaction behavior of sand-fine mixtures to better understand the performance of sand-silt composition.

The literature review is divided into three parts. The first part features studies focused on the estimation of the internal friction angle (ϕ) based on in-situ SPT and CPT tests. The second part features studies focused on the influence of fines on the behavior of sand-fine mixtures. This is related to the soil mechanical behavior of the soil mixture itself, and the primary experimental approach used is the direct shear test. Finally, the third part features studies focused on the influence of fines on interface behavior and shear strength between sand mixtures and concrete/steel piles, with the primary experimental approach again being the direct shear test.

Internal Friction Angle Estimation Based On SPT and CPT

Most of the available in-situ SPT/CPT correlations with the internal friction angle (ϕ) in the literature were developed for clean sand with low fine content (<5%). The correlations between the ϕ and SPT data were the earliest work of these correlations (e.g., [1], [2], [3], [4], [5], [6], [7], [8]). Dunham [1] presented three equations between the ϕ and SPT N-values for different particle shapes. Peck et al. [2] provided a correlation between the corrected $(N_1)_{60}$ and the ϕ in graphical form (i.e., chart). Wolff [6] approximated this graph into the form of an equation. Shiori and Fukui [5] proposed three equations between the ϕ and N_{70} for roads, building, and general use. Schmertmann [4] gave a correlation between N_{60}, vertical effective stress, and the ϕ, which was later approximated by Kulhawy and Mayne [8]. Hatanka and Uchida [9] also presented a correlation between the ϕ and $(N_1)_{60}$.

For correlations with CPT, studies by Villet and Mitchell [10], as well as Robertson and Campanella [11], were the earliest efforts to develop a correlation between the ϕ and the cone tip resistance (q_c).

Almost all of the proposed correlations in the literature were developed based on approximation and an assumption that the soil is clean sand with a low percentage of fines content (<5%). However, some correlations were developed for sands with greater than 5% fines content. One correlation was proposed by Ricceri et al. [12] based on the results of CPT tests on the soil in the Venice Lagoon, Italy. He claimed that these correlations are for soil classification of SP-SM. According to the Unified Soil Classification System (USCS), SP-SM are considered as silty sand with 5-12% fines. However, their ϕ-q_c correlation (see below) did not address the contribution of fines in this correlation.

$$\phi = \tan^{-1}(0.38 + 0.27 \log \frac{q_c}{\sigma_{v0}{}'}) \quad [1]$$

Lee et al. [13] proposed a correlation between the peak friction angle (ϕ'_p) obtained from triaxial test results and the normalized cone tip resistances $q_c/\sigma_{h'}$. This correlation can be used to estimate the peak friction angle for both clean and silty sands with silt content ranging from 0 to 20%. This correlation showed good agreement, as reported by Robertson and Campanella [11], when it was compared with measured values. However, when the $q_c/\sigma_{h'}$ reached 300, the ϕ produced higher values.

$$\phi'_p = 15.575(\frac{q_c}{\sigma h'})^{0.1714} \quad [2]$$

Searla [14] developed an empirical equation for soil parameters including the drained angle of friction (ϕ) at a given relative density for mixed soils. Based on the Schmertmann [4] chart and using computer programming, his work resulted in the following equation:

$$\phi = \frac{\log_{10}(R_f) - 2.87 + \log_{10}(q_c)}{0.021 \log_{10}(q_c) - 0.88} \quad [3]$$

Where,
R_f is the ratio of skin resistance (f_s) to the cone tip resistance of the Begemann friction cone in percent (q_c), and
ϕ is the drained angle of friction in degrees.

This equation does not clearly explain the effect of overburden pressure, which is an essential parameter in the internal friction correlations. According to Kulhawy and Mayne [8], the effective friction angle (ϕ') for clean sand can be estimated using the CPT parameters as follows:

$$\phi' = 17.6° + 11.0° \log(q_{t1}) \qquad [4]$$

Where,

$q_{t1} = (q_t/p_a) / (\sigma_{v0}'/p_a)^{0.5}$ is the stress-normalized cone tip resistance,

$p_a = 1\ bar = 100\ kPa$, and

σ_{v0}' is the effective overburden pressure.

Murley [15] proposed direct correlations between the field N-values, c′, and ϕ' for mixed sandy soil. He used the energy-balance approach to determine the resistance of the soil to SPT penetration by the sampler. Houston and Mitchell [16] developed the relationship between ϕ' and q_c in which he included the liquidity index and remolded shear strength in the correlations. These correlations did not consider the unit weight, clay fraction, and uniformity of the coarse-grained portion. Some assumptions and limitations were also accounted for. Therefore, field testing should be conducted to verify these relationships. Hettiarachchi and Brown [17] developed the same energy balance approach, but they derived an equation to estimate the friction angle for sand alone.

Lee et al. [18] performed several investigations on CPT correlations for sandy soil with fine content (mainly silt). They used the dilatancy relationship that was proposed by Bolton [19] to calculate the internal friction angle (ϕ) and compared it with the measured friction angle from triaxial tests. It was observed that the ϕ obtained from CPT relations showed reasonable agreement with the measured values from triaxial test results. The dilatancy index was introduced with its variables in the CPT correlations. Regression analysis was performed for these variables to study the effect of fine (silt) content, which showed consistent values for all silt contents.

$$I_{R,CPT} = I_D \left(Q_{CPT} - \mathrm{In}\left(\frac{100 q_c}{P_a}\right)\right) - R_{CPT} \qquad [5]$$

$$\phi'_P = \phi'_C + R_D . I_{R.CPT*} \qquad [6]$$

Wener [20] developed several correlations between the SPT $(N_1)_{60}$ values and the internal friction angle (ϕ) for Las Vegas soils, which are composed of different mixtures of sand with fines, such as clayey sand and silt sand. The ϕ was measured by direct shear tests from samples collected from the field. Regression analysis was performed to obtain these relationships. The results showed that the ϕ did not increase relative to the increasing of soil consistency and N_{60} values when compared with the tables from Meyerhof [3]. Moh et al. [21] presented a correlation for a silty sand deposit in Taipei between the ϕ and the SPT values. The values of ϕ were estimated from direct shear tests conducted at small normal stresses. The developed correlations did not consider the effect of overburden pressure and were established only from the local data in Taipei.

Salari et al. [22] provided multiple equations for internal friction angle (ϕ) with SPT-N values for gravels with sand and clayey gravels with sand (GC and GW). The ϕ values were determined by direct shear tests. The results of the ϕ showed agreement with the Peck et al. [2] equations, but were mostly lower than the value from the Meyerhof [3] equation. In another study, Salari et al. [22] performed the same procedure, but on different types of soils for sand and clayey sand (SP and SC). The results and comparison with other empirical equations showed the same conclusion obtained in GC and GW soil as follows:

$$\phi = 0.7732\ (N) + 10.201 \qquad [7]$$

Mujtaba et al. [23] proposed correlations for the internal friction angle (ϕ) and SPT-N values for soil samples classified as poorly graded sand (SP), poorly graded sand with silt (SP-SM), and silty sand (SM) with fine content up to 40%. The values of ϕ were determined by direct shear tests. Linear regression analysis was conducted to obtain this correlation. The equation was compared with that proposed by Hatanaka and Uchida [9] using the same data. The Hatanaka and Uchida [9] equations showed overestimation and underestimation for different relative densities. This variation was explained by the difference in obtaining the ϕ using triaxial results in Hatanaka and Uchida [9] and due to the different SPT procedures conducted in both studies. The same explanation was proposed when compared to the Peck et al. [2] and Japan Road Association [7] values. The contribution of fines in the ϕ was not stated when compared with other studies conducted on clean sand for the same equation that was adopted in the study.

$$\phi = 0.7N_{60} + 18.0 \qquad [8]$$

The various SPT correlations between the SPT N-values versus the internal friction angle (ϕ) and relative density are tabulated in Table 1 and Table 2, respectively.

Table 1. SPT correlation with the internal friction angle (ϕ)

Name	Correlation	Soil Type
Dunham [1]	$\phi = \sqrt{12N} + 20$ $\phi = \sqrt{12N} + 25$ $\phi = \sqrt{12N} + 15$	Round and well-graded or angular and uniformly graded Angular and well graded Round and uniformly graded sand
Ohsaki	$\phi = \sqrt{20N} + 15$	Sand
Shioi and Fukui [5]	$\phi = \sqrt{18N_{70}} + 15$ $\phi = 0.36N_{70} + 27$ $\phi = 0.45N_{70} + 20$	Roads Bridges Buildings
Schmertmann [4]	$\phi = \tan^{-1}\left(\frac{N_{60}}{12.2 + 20.3\left(\frac{\sigma_0}{p_a}\right)}\right)^{0.34}$	Sand
Hatanka and Uchida [9]	$\phi = \sqrt{15.4(N_1)_{60}} + 20$	Sand
Japan Road Association [7]	$\phi = (20(N_1)_{60})^{0.5} + 20 \leq 45$ For SPT-N >5	Sand
Salari et al. [22]	$\phi = 0.7732\ \text{SPT} + 10.201$	Sand and clayey sand
Mujtaba et al. [23]	$\phi = 0.7N_{60} + 18.0$	Sand (SP), SP-SM, and silty sand (SM) with fine content up to 40%,

Table 2. SPT N-value versus friction angle and relative density [3]

SPT N [Blows/0.3 m]	Soil packing	Relative Density [%]	Friction angle [°]
< 4	Very loose	< 20	< 30
4-10	Loose	20-40	30-35
10-30	Compact	40-60	35-40
30-50	Dense	60-80	40-45
> 50	Very Dense	> 80	> 45

As the literature reveals, limited correlations considered the effect of fines content, and none of them explained the contribution of fines between the internal friction angle (ϕ) and the SPT/CPT parameters. On the other hand, many studies were performed between the ϕ and the SPT/CPT parameters alone. These studies are mostly related to the liquefaction of sand and its undrained shear strength. The SPT N-values depend heavily on grain size, and clean sand will always have higher values than sand mixed with fines [24]. Meyerhof [3] claimed that the appearance of silty and fine sandy soil will result in higher SPT-N values than clean sand. When dynamic loads are applied on silty and fine sandy soils in a saturated state, the developed excess pore pressure will be difficult to dissipate due to low permeability, thus giving more resistance and dilation to the dynamic load. This leads to a higher SPT value, which is not an actual representation of soil strata. Meyerhof [3] proposed the dilatancy correction factor for these phenomena. When SPT is performed in saturated silts/fine sands, if the observed N-value is more than 15, a correction must be applied to reduce the observed values. This correction is applied on the N-value corrected for overburden pressure as follows:

$$(\mathrm{N}_1)'_{60} = 15 + \frac{1}{2}((\mathrm{N}_1)_{60} - 15))\ ,\ (\mathrm{N}_1)_{60} > 15 \qquad [9]$$

$$(\mathrm{N}_1)'_{60} = 15\ ,\ (\mathrm{N}_1)_{60} < 15 \qquad [10]$$

The relationship between SPT and CPT was proposed by several researchers using a numerical relation of q_c/N ratio. This ratio is shown to have a trend relation with the grain size. Jamoilkowski [25] studied the effect of fines content on the q_c/N ratio. Kulhawy and Mayne [8] collected extensive data from many researchers and obtained the same trend as presented in Jamiolkowski [25].

The most important soil property strongly connected to the internal friction angle (ϕ) for cohesion-less soil is the relative density (D_r). The fines content of soil, as well as other soil properties such as grain size, shape, soil grading, and mineralogy, can significantly change the soil's relative density, thus resulting in a different ϕ. This presents a challenge for geotechnical engineers in determining the real value of relative density and proposing an accurate correlation that fits different types of soil at various conditions. There are several correlations proposed in the literature between the soil's relative density and the SPT/CPT data. Gibbs and Holtz [26] proposed a correlation between D_r and N_{60} in a graphical form, which can be approximated as follows [3]:

$$D_r = \left(\frac{N_{60}}{\left(17 + 24\left(\frac{\sigma_{vo}'}{p_a}\right)\right)}\right)^{0.5} \quad [11]$$

Halder and Tang [27] approximated the Gibbs and Holtz [26] correlation and expressed it as follows:

$$N_{60} = 20{D_r}^{2.5} + 0.21\left(\frac{\sigma_{vo}'}{p_a}\right){D_r}^2 \quad [12]$$

Peck and Bazaraa [28] proposed two equations between D_r and N_{60} at different effective overburden pressures as follows:

$$(\text{For } \sigma_{vo}'<72) \quad D_r = \left(\frac{N_{60}}{\left(20+84\left(\frac{\sigma_{vo}'}{p_a}\right)\right)}\right)^{0.5} \quad [13]$$

$$(\text{For } \sigma_{vo}'\geq 72) \quad D_r = \left(\frac{N_{60}}{\left(65+21\left(\frac{\sigma_{vo}'}{p_a}\right)\right)}\right)^{0.5} \quad [14]$$

Skempton [29] observed a positive relationship between SPT values and particle size at constant density and overburden pressure. He also found out that the aging effect could produce different SPT values, resulting in higher penetration resistance. He developed a correlation between D_r and N_{60} that takes into account the effect of pre-consolidation pressure as follows:

$$D_r = \left(\frac{N_{60}}{a + C_{OC}.b.\sigma_0'}\right)^{0.5} \quad [15]$$

Where,
C_{OC} is the over consolidation coefficients.

The a and b are constants that vary depending on the soil type.

Tokimatsu and Yoshimi [30] proposed an equation between D_r and N_{60} considering the effect of fines content expressed as follows:

$$Dr = 0.21\left(\frac{N_{60}}{0.7 + \frac{\sigma_{vo}'}{98}} + \frac{\Delta N}{1.7}\right)^{0.5} \quad [16]$$

Where,
ΔN is the correction factor for the effect of fines.

The increase of the fines content will increase the relative density based on this correlation. Kulhawy and Mayne [8] considered the effect of grain size, aging, and over consolidation in their correlations as follows:

$$Dr = \left(\frac{N_{60}}{C_p C_A C_{OCR}}\right)^{0.5} \quad [17]$$

Cubrinovski and Ishihara [31] included the effect of fines content and grain size in his correlation between relative density (D_r) and SPT values. They proposed the parameter C_D that accounts for the effect of grain size and could be measured for the range of $(e_{max} - e_{min})$. For sand with fines content, it produced a large range of $(e_{max} - e_{min})$, which can lead to a decrease in penetration resistance.

$$C_D = \frac{9}{(e_{max} - e_{min})^{1.7}} \quad [18]$$

$$N = \frac{9\, {D_r}^2}{(e_{max} - e_{min})^{1.7}}\left(\frac{\sigma_{vo}'}{98}\right)^{\frac{1}{2}} \quad [19]$$

For the correlation between D_r and cone tip resistance (q_c), Baldi et al. [32] proposed an equation based on chamber tests. These correlations were developed using Hukksund and Ticino sand as follows:

$$Dr = \frac{1}{C_2}\ln\left(\frac{q_c}{C_o {\sigma_0}^{C_1}}\right) \quad [20]$$

Several other correlations were developed in the literature between D_r and q_c (e.g., [33], [34], [8], [35]). None of the developed correlations between D_r and q_c mentioned above are always reliable and may differ based on varying soil properties and soil conditions.

Ghali et al. [36] proposed a new correlation between D_r and $(N_1)_{60}$ based on experimental results. These correlations involved the coefficient of uniformity (C_u), mean grain size (D_{50}), and two-dimensional angularity. Sand with fines content less than 5% fine are applicable to these correlations. Any sand with high fines content will overestimate the SPT values. The influence of water content is also neglected in these correlations.

$$\frac{N_{1_{60}}}{Dr^2} = a_f . S_u{}^{0.5} . \log(100D_{50}) . \exp(\frac{-2A_{2D}}{1000}) \qquad [21]$$

Where,

S_u is the undrained shear strength, and

a_f is an amplitude multiplication factor which ranges between (50-70), with variation of (S_u, D_{50}).

Influence of Fines on the Mechanical Behavior of Sand-Fine Mixtures

Many research studies in the literature used laboratory tests, such as direct shear tests and triaxial tests, to investigate the mechanical behavior of sand containing fines, attempt to determine the threshold of fines content that changes the behavior of the sand mixed with fines (silt/clay) from cohesion-less soil to cohesive soil behavior, and explain the influence of fine content on internal friction angle (ϕ) and shear strength. Several contradictory interpretations were observed due to differences in the parameters used to measure and quantify the soil density (i.e., the concepts of void ratio, granular void ratio, void skeleton, and relative densities) and the sample preparation method used [37]. The soil floating fabric of fines within coarse grains is illustrated in Figure 1 by Carraro et al. [37].

Figure 1. a) Non-floating fabric, and b) floating fabric [37]

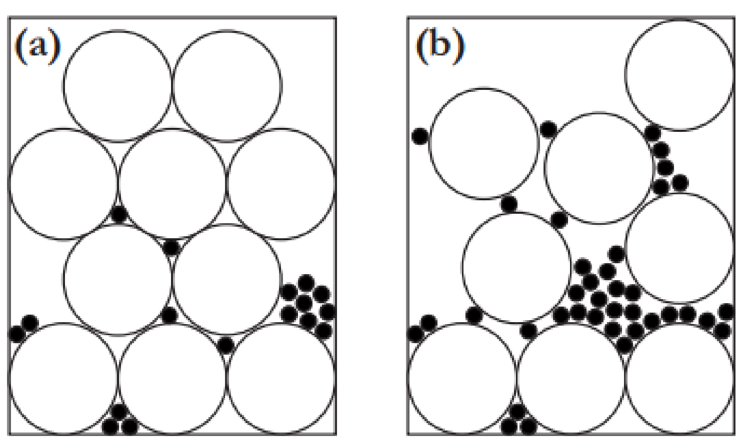

These parameters can be used to evaluate the behavior of sand with fines content in the transition or threshold point and below (where no floating fabric is present, sand particles controls). Each parameter, when used, has a different interpretation of the effect of fines [37]. Yamamuro et al. [38] showed that the soil fabric of sand and silt particles in a soil mixture could be highly affected by the sampling method and could obtain different shear strength values.

The shear strength depends on the structure of the soil skeleton. When the soil is faced with an external loading, an internal force is formed from the particles' frictional contact, which allows sliding, rolling, and other interactions between the soil particles. This internal force and frictional contact needs to be represented by an index that can characterize the shear strength of soil and explain the soil skeleton behavior [39]. If the void ratio is used as an index to quantify the density of the soil particles, it will not consider the heterogeneous composition of the sand containing different particles and shapes, assuming that all particles contribute in sustaining the shear forces. Most of the research related to the shear strength of sand containing fines used the concept of inter-granular void ratio (e_g) (e.g., [39], [40], [41], [42]) or void skeleton (e.g., [43], [44], [45]). The latter concept assumes that fines do not participate in transferring the friction between particles and are only considered as voids.

Vinayagam [39] conducted undrained triaxial compression tests on silty sand to study the effect of fines content on the internal friction forces between the soil particles. The soil mixture behaved like silt when the fines content reached 30%. Vanayagam [39] also concluded that transition fine content is reached when the inter-granular void ratio (e_g) is equal to the maximum void ratio (e_{max}). These interpretations are highly dependent on the confining stress and the initial density of soil. The mixture would require high fines content in order for the silt particles to dominate the soil mixture in very dense soils. At a loose state with high fines content, the mixture is very sensitive to confining stress, thus allowing the sand particles to dominate. In summary, the shear strength of silty sand depends on the inter-granular friction contact density, which is a function of fines content, confining stress, and void ratio.

Monkul and Ozden [46] investigated the transitional fines content value and its effect on the shear strength using the concept of inter-granular void ratio (e_g). They conducted direct shear tests on kaolinite-sand mixtures and observed a decrease of shear strength when the mixtures exceeded the transition fine content. A study by Monkul and Ozden [46] revealed the influence of effective stress and the initial condition of soil on the transition fines content. Their results showed that the transition fines content increased when increasing the effective stress. The relationship between the inter-granular void ratio, fines content, and effective stress (in the third plane), which can capture the transition zone from sand to clay behavior, is shown in Figure 2. The bold line represents the third plane when the inter-granular void ratio equals the maximum void ratio of sand in Figure 2. The curves of approximately 20-30% of fines content intersect the transitional plane, which agrees with the previous studies in the literature.

Figure 2. Variation of inter-granular void ratio with effective stress for various fine contents [46]

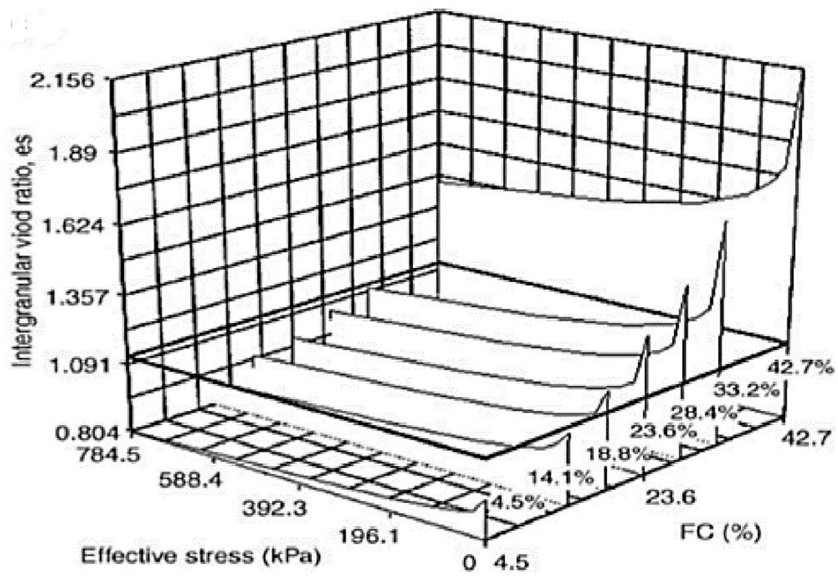

Vinayagam et al. [39] established an inter-granular soil mix classification explaining the microstructure of sand-silt mixtures and proposed a new density index called the equivalent void ratio (e_{eq}), which accounts for the secondary role of fines content (FC) in the transfer of contact frictional forces by a parameter b, as shown in the following equation:

$$(\mathrm{e})_{eq} = \frac{e + (1-b).FC}{1-(1-b).FC}\ ;\ \ 1 > b > 0 \qquad [22]$$

Where,

b is defined as the portion of fines that contributes to the active inter-grain contacts.

The value of b is zero when the contribution of fines on the force chain is neglected and assumed as voids, similar to the concept of inter-granular void ratio. When b is one, however, the fines will participate in supporting the coarse grain, and the concept of global void ratio will prevail. The value of b depends on the disparity ratio and grain characteristics.

Ni et al. [47] used the equivalent granular void ratio on both plastic and non-plastic fines. They found out that the kaolin fine had a negative effect on the soil mixture, causing instability in the undrained shear strength; therefore, the range of b for the plastic fine was $-\infty \leq b \leq 0$, suggesting that the plastic fine will act like voids at their best. These ranges depend on the stress history of the soil. The fines will act as voids in the over consolidated samples. However, in normally consolidated samples, the clay minerals will be stacked between the sand particles, causing instability. The critical friction angle values did not change with the presence of kaolin fine due to the fact that clay minerals have been driven out of the coarse grain. The range of b for non-plastic fines is $0 \leq b \leq 1$, suggesting a positive influence on the undrained shear strength. The ranges for both plastic and non-plastic fines are an expression of the relative stiffness and size of the fines to the host sand. Silt has a similar hardness to sand, while clay minerals are much softer in nature. The void size distribution of silt and sand particles was expressed by (X= d_{10} sand/d_{50} silt) and correlated well with the b values. When X increases, the pore space also increases, allowing more fine particles not to be involved in the force chain, resulting in lower b values.

Kim [48] conducted an experimental study to investigate the effect of fines content on the shear behavior of sand/clay mixtures with 0-100% fines content under monotonic loading. Several drained and undrained shear tests were performed. For mixtures that had 0-19.6% of fines content, the results showed that increasing the fine content in dense sand decreases the shear strength, while for loose sand, the strength increases. The skeleton of dense sand lost when increasing fines content, resulting in a decrease in shear strength. However, for loose sand, the fines increase the density of soil, which gives higher shear strength values. For FC ≥ 29.4%, the shear strength had an almost constant value with increasing fine content. It was also observed that clay particles control the soil matrix at a fines content of FC = 29.6%.

Ismael et al. [49] examined the contribution of fines on arid climate sand deposits with medium dense conditions using direct shear tests. An increase of the internal friction angle (ϕ) was observed for mixtures with 0-20% fines content following a large drop in the friction angle when the fines exceeded 30%.

Salgado et al. [45] conducted a series of triaxial tests on Ottawa sand/silt samples with fines content in the range of 5–20% by weight to study the effect of non-plastic fines on the small shear modulus and shear strength. Bender elements were used in triaxial test samples to measure the effect of silt on the small-shear modulus. It was observed that the small-strain stiffness (10^{-4} to10^{-3} strain) decreased with the increase of small percentages of silt. Another observation was the increase in both the peak friction angle and the critical state friction angle when adding silt to the non-floating fabric silty sand. The values of critical-state friction angles were 29.7° for clean Ottawa sand, 30.57° for sand with 5% fines content, 32.7° for sand with 10% fines content, 32.57 ° for sand with 15% fines content, and 33.7 ° for sand with 20% fines content. These results are for the case of low silt content and a fabric mostly governed by sand-to-sand contact; therefore, adding silt to the non-floating fabric silty sand increases interlocking between the soil particles, making the mixture stronger and more dilative.

Carraro et al. [37] conducted 72 drained triaxial compression tests on the static behavior of gap-graded mixtures of silica sand mixed with fines, kaolin clay, and silt to study the effect of plasticity and the type of fine on the shear strength of sandy soil. The results included only small fine content up to 15% and showed that the addition of non-plastic fines to sand increases both the critical and peak friction angles of the sand in both loose and dense conditions. In loose sand, it became more contractive with increasing silt, while in dense sand, it became more dilative, which agrees with the findings of Salgado et al. [45]. The addition of plastic fine (clay) to sand at the same relative density of 83% decreases the critical and peak friction angles of sand, making it more contractive. These behaviors were clearly examined using the environmental Scanning Electron Microscope (SEM), which showed that clay lubricates and smooths the asperities on the surface of the sand grains. This reduces the friction between the sand particles, while the angularity of silt aids interactions with the asperities on the surface of sand grains, increasing the jamming effect during shearing.

Xiao et al. [50] studied the effect of non-plastic fine content (silt) on the strength-dilatancy relationships for sand. Bolton's strength-dilatancy equation and the test data from Salgado et al. [45] and Carraro et al. [37] were used to analyze and modify the strength-dilatancy relationship as a function of fine content. The ratio of excess angle, which is the difference between the peak friction angle and critical state friction angle, to the relative dilatancy was found to increase to a peak value, then decrease with an increase in fine content.

Lupini et al. [41] conducted ring shear tests on sand-clay mixtures at large displacement to study the effect of clay fraction on residual strength in drained conditions, as shown in Figure 3. The drop of the internal friction angle (ϕ) from peak $\left(\phi_P\right)$ to residual value $\left(\phi_R\right)$ was not observed for clay fractions lower than 20%. However, for clay fractions of 20-

40%, the drop was very significant. Based on these results, three modes of residual shear behavior that are dependent on particle shape and inter-particle friction were observed. Turbulent shearing mode at low clay fraction occurs, resulting in high residual strength, due to the rotation and movement of soil particles. Sliding shearing mode occurs at high clay fractions. The clay particles start to dominate the soil separating the contact of the rotund sand particles, which results in low residual strength. The transitional mode contains both sliding and turbulent shearing simultaneity and occurs in mixtures with no dominant particles.

Figure 3. Variation of residual friction angle with the clay fraction [41]

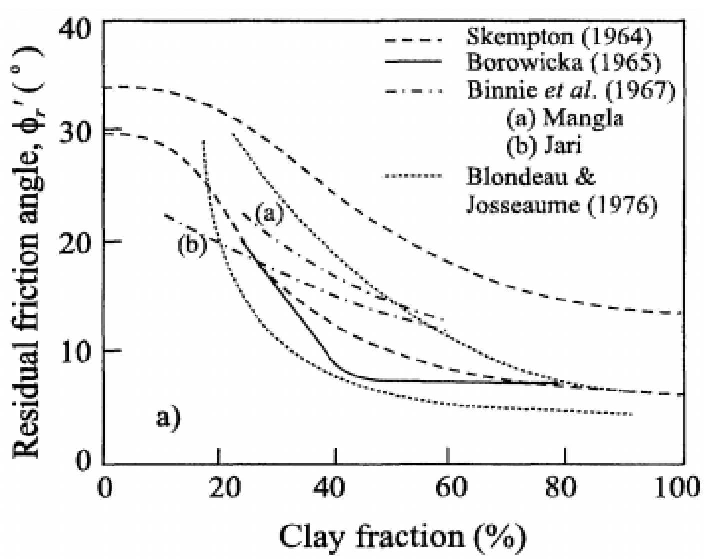

Yin [51] studied the influence of clay content on the internal friction angle (ϕ) of Hong Kong marine sand deposits. The results of triaxial compression tests revealed a similar trend to that reported by Lupini et al. [41]. Mollins et al. [52] performed an experimental study on the drained strength of bentonite-enhanced sand with bentonite mixture up to 20% (see Figure 4). They used the concept of granular void ratio on the stress-dilatancy equation from Bolton [19] in estimating the relative density of sand in mixture $(I_D)_S$. It was found that the strength of bentonite sand mixture could be analyzed by three modes of behavior. Mixtures with granular relative density above (10 – In(p′)) will have friction peak angle similar to clean sand. When $0 \leq (I_D)_S \leq$ (10 – In p′), the dilation will decrease, and the friction angle will drop to the critical friction angle of sand alone. The friction angle will exhibit the residual shear strength of clay when negative values of $(I_D)_S$ are reached. These shear modes did not include mixtures with 20% bentonite, because this approach ignores the role of the clay particles in transferring the frictional forces. Stewart et al. [53] took the data of Molins et al. [52] to design a model for landfill liner. The drained strength was estimated using Bolton's dilatancy equation. They concluded that the friction transported by the bentonite is neglected. The sand that was investigated in the model is silty fine angular quartz sand with 7% fines.

Figure 4. Graph showing the variation in the drained strength (ϕ) of bentonite-sand mixtures with the initial relative density of the sand in the mixtures [52]

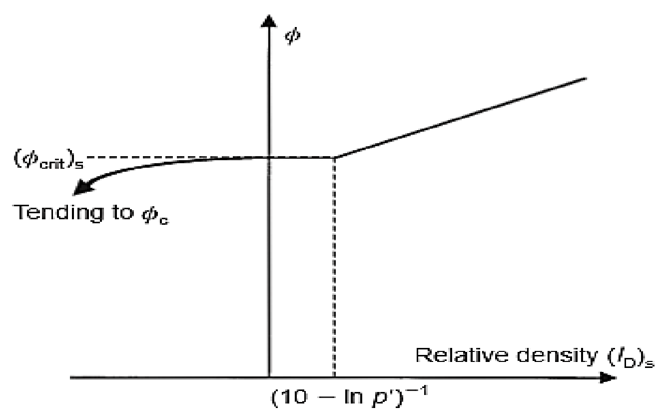

Haider et al. [54] studied the drained shear strength of fine sand mixed with decomposed granite soil through triaxial tests. The shear strength of the mixture was controlled by the fractional contact of sand providing more interlocking at sand content above 20%. The silt particles' inter-fine contact governed the mixture at sand content lower than 10%. The inter-granular void ratio was used to quantify the mixture density.

Mahmoudi et al. [55] conducted direct shear tests on sand-silt mixtures with fines content up to 30% for loose and dense samples. The concept of equivalent void ratio and equivalent relative density was used to quantify the soil sample, which are only applicable to sand dominating mixtures with fine content less than the threshold fine content. These parameters showed good correlation with the peak friction angle.

Li et al. [56] studied the influence of fine content on binary mixtures of kaolin clay and glass beads using direct shear tests. Their results showed that the residual friction angle correlated well with the results from Lupini et al. [41]. It was reported that the effect of water content distribution and the difference of water content inside and outside the shear zone represented the change of void ratio during shearing. Positive difference indicated dilative that exhibited at low clay fractions. Having higher water content in the outer shear zone leads to contractive behavior that is exhibited at high clay fractions. Slickensides shear surfaces occurred, resulting in sliding mode and a lower friction angle at high fine content.

Li [57] proposed an equation that accounts for the effect of particle shape and size distribution on the critical friction angle (ϕ_{cr}). Direct shear tests were conducted on different mixtures of fines (silt and clay) and coarse fraction (CRF). Two parameters were used to represent the particle shape: elongation (EL) and convexity (CON). Elongation is an estimate of particle symmetry, and convexity is related to surface roughness. Elongated particles developed higher shear surface area and roughness producing higher friction angle. Increasing convexity will decrease the surface roughness that results in lower friction angles. Fine particles started to govern the mixture at high normal stress due to the large face interaction of the platy particles, thus causing lower friction angles to be developed. The equation for ϕ_{cr} is:

$$\phi_{cr} = 12.7\text{CRF} - 2\text{CON} + 13.2\text{EL} + 23{:}1 \qquad [23]$$

The effect of particle shape on the internal friction angle (ϕ) was studied using different approaches through the literature. Bareither et al. [58] established an equation to determine the ϕ of compacted sand based on effective particle size (D_{10}), maximum dry unit weight (γ_{dmax}), and roundness (R). Multivariate regression analysis was used to develop the following equation:

$$\phi = 1.89 + 20.56\, D_{10} + 2.35(\gamma_{dmax}) - 24.1(R) \qquad [24]$$

Ueda et al. [59] conducted a series of discrete element simulations and direct shear tests on binary mixtures of small and large particles with medium and fine sand particle sizes. A model was developed to measure the threshold of small particle content at which the frictional resistance transformed by the small particles becomes negligible, and the threshold content at which the friction resistance of the large particles becomes small. These values were highly dependent on the ratio of large particle to small particle diameter. The study found that the force transported by the large particles could be ignored if the spacing between the large particles was more than two times the small particle size. Arasan et al. [60] showed that the high fractional dimensions are obtained with an increase in the angularity of the sand particles, which resulted in higher ϕ values for sand particles of 177 to 710 µm.

Stark et al. [61] concluded that flat, elliptic sand particles obtain larger internal friction angles (ϕ) than rounded particles due to the special reorientation of the flat particles during shearing. This results in greater strength and higher ϕ.

Vallejo and Mawby [62] conducted direct shear testing on sand-clay mixtures and found that the shear strength of the mixture is the same as that of clean sand when the fines content is below 25%, which was governed by the friction resistance of sand particles alone. For fine content of 25-60%, the shear strength was governed by sand and clay particles together. When the fines content was above 60%, the shear strength was dominated by clay only. Those findings showed a similar trend to that obtained by the Lupini et al. [41] and Georgianou et al. [42] studies. Porosity values were found to be significantly related to these limits of shear strength. The minimum porosity value represented the boundary between the sand-controlled and clay-controlled mixtures. Monkul and Ozden [46] showed that the concept of minimum porosity, which is a function of void ratio, is not always valid, and that the value of minimum void ratio could be higher than anticipated beyond the transition fine content value.

Influence of Fines on Interface Behavior and Shear Strength Between Sand and Concrete/Steel

Simple ring and direct shear interface tests have been used in the literature to measure the interface friction angle (δ) between clean sand and different solid materials (e.g., concrete, steel). Abderrahim and Tisot [63] evaluated the δ in cohesion-less soil-structure interface through performing tests using direct shear box, ring shear apparatus, and mini pressure meter. The highest values of the δ were obtained from the direct shear tests, and the lowest values were obtained from the ring shear tests. No difference in the ϕ values were observed between triaxial and direct shear tests. The small size apparatus has some limitations, which could produce unreliable results. However, the literature shows that the size of apparatus had no significant effect on the interface friction mobilized between soil and other materials (e.g., [64], [65], [66]).

Several authors have contradicting views about the effects of relative density on interface friction. Some stated that the δ increases when increasing relative density (e.g., [67], [68], [64], [69], [70]), while others stated that relative density is not an important factor contributing to the δ, and its effect is negligible (e.g., [71], [72], [73], [74]). Tiwari et al. [75] observed an increase in the interface friction angle (δ) for soil-concrete interface when increasing the relative density, but the effect of relative density on the δ between soil and steal or wood were unpredictable and inconsistent in their studies.

The influence of particle size on interface friction angle (δ) was studied by several investigators (e.g., [73], [76], [77]). Particles with more angular and elongated shapes usually have higher δ values (e.g., [64], [77], [78]).

The mode of shearing could also play a role in influencing the interface friction angle (δ) value. Subba Rao et al. [79] showed different results of the δ due to changing the procedure for preparing the interface. Two modes of shear types (Type A and Type B) were proposed. Type A placed the sand in the lower half shear box, and solid material was placed over the sand. Type B, the most common shear type, prepared the sand over the solid material bed. Studies showed that the value of the δ is independent of the soil density in the Type A condition, but increases with increasing density in the Type B condition. The maximum value of the δ was obtained when increasing the surface roughness in Type B to the peak internal friction angle (ϕ) of sand, while for Type A, the interface friction angle (δ) reached only the critical friction angle. For both types, the values of the δ were equal for different surfaces of roughness.

The influence of normal stress on the interface friction angle (δ) was also investigated. Potyondy [80] and Acar et al. [67] showed that the δ decreases when increasing the normal stress. Uesugi and Kishida [66] and O'Rourke et al. [64] claimed that it had no effect. Quinteros et al. [81] showed that the effect of normal stress on the δ depends on the roughness of the interface and soil material. An increase of the δ with decreasing normal stress was observed in polished and painted steel interfaces, while no increase was obtained in rough steel. It was concluded that the δ is independent of the normal stress when it exceeded 100 kPa. This trend was also seen in several experiments in the literature (e.g., [82], [83]).

The shear test can be performed in either stress-controlled or strain-controlled conditions. Throughout the literature, it was concluded that there is no difference between the stress-controlled and strain-controlled interface test results (e.g., [84], [85]). The only difference is that in the strain-controlled-condition, the stress path between the peak strength and ultimate strength can be observed and plotted, while for the stress-controlled-condition, only the peak can be obtained. Liu et al. [86] applied shearing rates from 0.007 mm/min to 500 mm/min, and only a decrease of (1˚) was observed.

Han et al. [77] performed direct interface shear tests to study the effects of roughness, gradation, particle size, and particle shape on the sand-steel interface friction angle (δ). After presenting the roughness value by the normalized roughness parameter introduced by Uesugi and Kishida [66], they made several conclusions. Uniform sand obtained higher δ values than well-graded sand with increasing roughness. The rate of increase in the δ/ϕ ratio in uniform sand was much higher than that in well-graded sand. Smaller mean particle sizes (D_{50}) obtained higher values of the δ, which substantiated other findings (e.g., [73], [76]). This increase in the δ is due to the decrease in the normalized roughness parameter, which is related to the particle size. Higher values were observed in angular and elongated shapes. Han et al. [77] also showed that the ϕ increased when increasing the (D_{50}).

Potynedy [80] used sand mixed with fines content of up to 50% clay content to measure the interface friction angle (δ) with steel and concrete as a function of grain distribution, moisture content, and roughness. He found out that the value of the interface friction angle (δ) increased with increasing roughness and decreasing moisture content. The value of the δ decreased when increasing the clay content, especially when it exceeded a ratio of 15%. Ferreira et al. [87] investigated the influence of moisture content and relative density on soil-geosynthetic interfaces. The results showed that the interface shear strength decreased when increasing the moisture content. The effect of the moisture content was found to be dependent on the normal stress, material type, and relative density. Canakci et al. [88] studied the effect of water content on the δ of organic soil with different construction materials. The δ was found to be inversely related to the water content for steel and wood. However, the δ for smooth concrete remained nearly constant at all moisture contents.

Yoshimi [89] conducted ring shear tests on dry sands with steel surfaces of varying roughness. He expressed the interface friction angle (δ) as the coefficient of friction. The results demonstrated that the surface roughness was a factor contributing significantly to the coefficient of friction, not the density as stated previously. Uesugi and Kishida [76] studied the coefficient of friction using simple direct shear interface tests with more properties involved, such as the mean particle diameter, sand density, and mineralogy. He proposed the normalized roughness parameter, which was used thereafter by other researchers. It represents the ratio of relative surface roughness to the mean particle size (D_{50}). This parameter was introduced due to the unique relationship obtained between the surface roughness and (D_{50}).

Many investigators studied the relationship between D_{50} and the δ, but very few studied the effect of fine contents (FC) on the interface friction angle (δ). Quinteros et al. [81]

performed ring shear tests on North Sea silica fine sands to silty sands with fine content varying from 0-42%. His results did not capture any clear correlations between FC and the δ, and he concluded that the effect of FC is insignificant on the δ. They found out that the effect of normal stress is more significant on the δ than on the roughness and D_{50} parameters. This contradictory finding, which is different than other studies, was primarily due to the narrow range of D_{50} presented in his study. Su et al. [90] results also showed that the effect of D_{50} on the soil-structure interface friction angles (δ) is not significant, but it is more pronounced at the internal friction angle (ϕ) of the soil.

Liu et al. [86] collected a very large database of Bishop's ring shear steel-interface tests on silty sand with 0-20% of non-plastic (silt) fines to study the effect of fines content, D_{50}, and surface roughness on the interface friction angle (δ). His study showed that the δ had high values for soil with higher fines content. A clear correlation was observed between the δ and normal stress above 30 kPa, which showed that the δ is highly dependent on the normal stress. A study by Liu et al. [86] followed the Inductively Coupled Plasma (ICP) procedures during the ring shear testing, which applies pre-shearing up to 3 ft. (1 m) to represent the field conditions in driven piles before obtaining full drainage conditions. This led to grain crushing and interface smoothing, and consequently, higher values of the δ were observed in low normalized roughness ranges.

Tsubakihara and Hideaki [91] conducted laboratory interface shear tests on sand-clay mixtures with mild steel of various surface roughness using a direct simple shear test. The sand-clay mixtures had a ratio of sand to clay of 0.2, 0.4, 0.6, 0.8, and 1.0. The results showed that there is no difference in the maximum coefficient of interface friction for all mixtures of different ratios, frictional behavior of soil deformation, and sliding at the interface. They classified the frictional behavior into three zones (or modes), as described in Figure 5: shear deformation within the soil sample (Mode 1), sliding interface with shear deformation within the soil at the same time (Mode 2), and full sliding at the interface (Mode 3). The boundaries between these zones were measured using the critical roughness value [92]. The effect of fine content on sand-clay mixtures increased the critical roughness value with low clay content, thus allowing shearing to occur both in the interface and within the soil, as shown in Figure 5 [91]. The behavior of the three modes of failure at the interface was found to be dependent on the soil skeleton. If the soil skeleton was dominated by sand, then sand controlled the soil behavior, allowing full sliding at the interface. However, as the clay content increased, it allowed floating fabric in the soil skeleton, and thus no sand skeleton was formed, leading to shear failure within the clay soil. They demonstrated the existence of these modes by studying the relationship of sand content as a function of water content with respect to clay fraction.

Figure 5. Three modes of failure with respect to steel roughness and fine percentages [91]

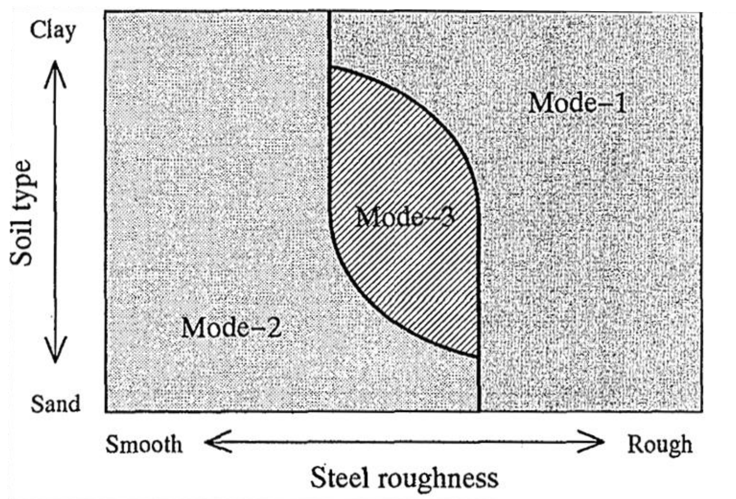

Chik and Vallejo [93] conducted laboratory experiments on binary mixtures of fine and coarse sand to measure the internal friction angle (ϕ) and the interface friction angle (δ). Glass plate and porous stone were used to represent the smooth surface and rough surface, respectively. The results showed that for coarse dominated sand, higher interface friction values were developed at rough surfaces due to better interlocking, while for smooth surfaces, the friction developed at the interface was controlled by fine sand due to a large contact area with the glass plate.

Methodology

The primary objectives of this study were to evaluate the effect of fines content and fine sand content on the value of internal friction angle (ϕ) of sand soils mixed with fines; to evaluate the effect of fines content and fine sand content on the interface friction angle (δ) between sand soils mixed with fines and the concrete interface; and to determine the threshold percentage of fines content beyond which the sand soils mixed with fines will behave as cohesive soils. For this purpose, an extensive laboratory testing program was executed, which included specific gravity, Atterberg limits, maximum and minimum void ratios, particle size distribution, standard proctor, small-size direct shear tests, and large-size direct shear tests.

Laboratory Testing Preparation and Planning

Material Selection

Different types of local sand and silt soils were collected in this study from various locations in Louisiana for the preparation of sand-fine mixtures. Sand types of different angularity and roundness, gradations, and particle sizes were collected. Sand-fine mixture samples from different project locations in Louisiana, where there are discrepancies in estimating the pile capacity, were collected and also tested in this study. Conventional soil tests were conducted to evaluate the different soil parameters, including specific gravity, maximum and minimum void ratios, particle size distribution, maximum dry density and optimum moisture content, and Atterberg limits [liquid limit (LL), plastic limit (PL), and plasticity index (PI)]. Extensive small-size and large-size direct shear tests were conducted to evaluate the shear strength parameters (c and ϕ) of sand-fines mixtures, and the interface friction parameters (c_a and δ) between sand-fines mixtures and the concrete surface.

Five different soil types were used in this study, designated as Soils 1, 2, 3, 4, and 5. For example, Soil 1 was classified as poorly graded sand according to the Unified Soil Classification System (USCS). Soil 1 was mixed with the other four soils to produce different sand-fines mixtures. The physical properties for the different soils are presented in Table 3. The particle size distribution of the five soils is presented in Figure 6.

Table 3. Material properties for the tested soil

Soil Properties	Soil No.1	Soil No.2	Soil No.3	Soil No.4	Soil No.5
USCS Classification	SP	CL	CL-ML	ML	ML
Specific Gravity (G_s)	2.67	2.75	2.71	2.68	2.65
Plastic limit	-	25.0	17.0	15.8	14.9
Liquid limit	-	38.0	24.6	20.1	17.1
Plasticity index	-	13.0	7.6	4.3	2.2
FC%	1.0	80.2	70.1	61.0	50.1
Sand%	99.0	18.8	29.9	39.0	49.9
Clay%	-	56.0	8.5	6.4	5.0
Silt%	-	24.2	61.6	54.6	45.1

Figure 6. Size distribution of the tested material

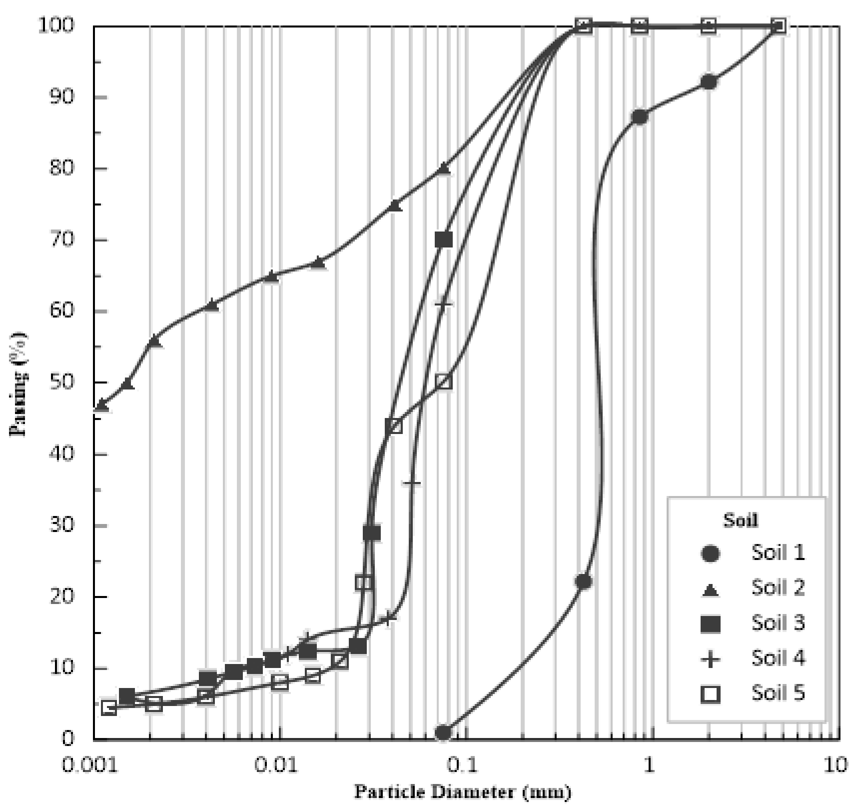

A concrete box with the same roughness of concrete piles was taken from a contracting company in Baton Rouge, Louisiana, to simulate the concrete pile surface. The size of the concrete box is 16’’ × 16’’ × 2’’. One of the sides was reduced to 12’’, and the thickness was increased to 4’’ by adding soil below the concrete box to fit inside the lower shear box device.

Sample Preparation

The soils were first oven dried for 24 hours and sieved through No. 4 to remove any gravels or rocks within the soil. Atterberg limits and particle size distribution tests were performed to determine the percent of sand, silt, and clay contents, and for soil classification. The four soils (Soils 2, 3, 4, and 5) were mixed with the sand Soil 1 to produce sand-fine mixtures with 10%, 20%, 30%, 40%, 50%, 60%, and 70% of fines contents by weight in the study . Fine soils were blended carefully to ensure particle distribution while mixing it with Soil 1. A mixer machine was used to mix the Soil 1 sand material with the fine materials. The proportions of both materials were estimated on an Excel sheet to ensure mixtures with accurate fines content. The mixing time was set to 10 minutes with a constant speed for all the samples to ensure the same uniformity and distribution between the particles, thus achieving a homogeneous mixture for all samples. The fine soil was placed first into the mixer, then the sand was placed over it. This was done on all mixtures in order to obtain consistent results in the direct shear test. Soil 2 was mixed with Soil 1 to produce sand-fine mixtures of 10%, 20%, 30%, and 40% of fines contents. Soil 3 was mixed with Soil 1 to produce sand-fine mixtures of 10%, 30%, 50%, and 70% of fines contents. Soils 4 and 5 were mixed with Soil 1 to produce sand-fine mixtures of 10%, 20%, 30%, 40%, 50%, 60%, and 70% of fines contents. Since Soil 2 contained fines that were mainly dominated by clay, which requires more time for consolidation when increasing the clay content, only up to 40% of fines content for Soil 2 was mixed with Soil 1. Figure 7 illustrates an example of this mixing process.

Figure 7. Mixture device; a) after placing the fine soil, b) after placing the sand

(a)

(b)

Laboratory Direct Shear Testing Plan

An extensive direct shear testing program was carried out using both the small-size and large-size direct shear testing devices available in LTRC lab facilities. For mixtures with relatively small fines content, a vibrator was used to achieve the target relative density. For mixtures with relatively high fines contents, moisture tamping was applied to achieve the targeted compaction. Before conducting the direct shear tests, standard proctor tests were carried out to determine the optimum moisture content and maximum dry density for each sand-fine soil mixture. Atterberg limit tests were performed to select the right method for sample preparation. The non-plastic soil mixtures were prepared using a vibrator, while soil mixtures with high plasticity index (PI) were prepared using moist tamping. The minimum and maximum void ratio tests were conducted on each mixture to achieve a certain relative density when preparing the specimen. Different water contents for each mixture were mixed to evaluate the effect of water content in the study. The sand-fine mixtures were mixed at the optimum moisture content, as a starting value, then increased at a constant increment until the soil became more of a liquid and difficult to prepare. Sample preparation for combining the Soils 1 and 2, Soils 1 and 3, Soils 1 and 4, and Soils 1 and 5 mixtures are presented in Table 4, Table 5, Table 6, and Table 7, respectively.

Table 4. Sample preparation for combined Soil 1 and Soil 2 mixtures

Soil Mixture	Sand	Sand with 10% fine	Sand with 20% fine	Sand with 30% fine	Sand with 40% fine
Specimen preparation	Vibration	Vibration	Vibration	Moist tamping	Moist tamping

Table 5. Sample preparation for combined Soil 1 and Soil 3 mixtures

Soil Mixture	Sand	Sand with 10% fine	Sand with 30% fine	Sand with 50% fine	Sand with 70% fine
Specimen preparation	Vibration	Vibration	Vibration	Moist tamping	Moist tamping

Table 6. Sample preparation for combined Soil 1 and Soil 4 mixtures

Soil Mixture	Sand	Sand with 10% fine	Sand with 20% fine	Sand with 30% fine	Sand with 40% fine	Sand with 50% fine	Sand with 60% fine	Sand with 70% fine
Specimen preparation	Vibration	Vibration	Vibration	Vibration	Moist tamping	Moist tamping	Moist tamping	Moist tamping

Table 7. Sample preparation for combined Soil 1 and Soil 5 mixtures

Soil Mixture	Sand	Sand with 10% fine	Sand with 20% fine	Sand with 30% fine	Sand with 40% fine	Sand with 50% fine	Sand with 60% fine	Sand with 70% fine
Specimen preparation	Vibration	Vibration	Vibration	Vibration	Moist tamping	Moist tamping	Moist tamping	Moist tamping

According to ASTM D-4253 and D-4254, the index parameters of different relative densities can be measured. Therefore, the index parameters of the different sand-clay/silt mixtures in this study were evaluated. The relative densities were estimated using the following equations:

$$Dr = \frac{emax - e_o}{emax - emin} \quad [25]$$

$$e_{0=} \frac{G_S y_w}{y_d} - 1 \quad [26]$$

$$y_d = \frac{W_s}{V} \quad [27]$$

The tests were performed according to the ATSM D-3080, thus allowing consolidated drained conditions. The soil was first mixed with water and allowed to stand for at least three hours inside plastic bags to achieve a target void ratio and initial relative density conditions. A known mass was placed inside the shear box, then vibrated to achieve a certain volume. For sand samples with a high percentage of fines, tamping was used inside the shear box to compact the soil in a process of two or more layers, until the accumulative mass placed in the shear box was compacted to known volume. The tamper used to compact the material must have an area in contact with the soil equal or less than ½ the area of the shear box (ATSM D-3080). The magnitude of the estimated displacement at failure depends on many factors, including the type and stress history of the soil. As a guide, the ASTM suggests using displacement at failure of 0.5 in. if the material is normally or lightly over consolidated fine-grained soil. After reaching consolidation, the soil was sheared for three hours in all mixtures under a shearing rate of 0.00278 in./mm. Each mixture was first prepared at an optimum moisture content and maximum dry density to perform the direct shear test. Then direct shear tests were performed on the same mixture with higher moisture contents and lower relative densities. Thus the samples were only sheared on the wet state with different relative densities.

The primary objective for conducting small-size direct shear tests was to investigate the influence of non-plastic fines content (silt) and fine sand on the peak and critical state internal friction angles (ϕ) of the sand-fine mixtures under various initial conditions, moisture contents, and stress states. The stress-strain response was also examined in the study. The experimental variables include the following: 1) angularity and roundness of the sand particles; 2) different normal stresses (10 psi, 16 psi, 22 psi); 3) different moisture contents [optimum moisture content (omc), omc+2%, omc+4%, omc+6%]; 4) different relative densities (loose, medium dense, dense); and 5) different fine (silt/clay) contents by weight (10%, 20%, 30%, 40%, 50%, 60%, and 70%).

Soil mixtures for combined Soil 1 and Soil 2

The soil properties of different soil mixtures prepared by combining Soils 1 and 2 are presented in Table 8. These mixtures were prepared with fine contents (FC) (silt/clay) of 10%, 20%, 30%, and 40%. The standard Proctor compaction curves for the combined Soil 1 and Soil 2 mixtures are presented in Figure 8, and the results of maximum dry unit weight and optimum moisture contents are presented in Table 9.

Table 8. Soil properties for combined Soil 1 and Soil 2 mixtures

Soil Properties	**Soil 1**	**Mixture 1 (10% fines)**	**Mixture 2 (20% fines)**	**Mixture 3 (30% fines)**	**Mixture 4 (40% fines)**	**Soil 2**
USCS Classification	SP	SP	SM	SC	SC	CL
Specific Gravity (G_s)	2.67	2.71	2.72	2.73	2.74	2.75
Plastic limit	-	-	15.0	17.0	19.0	25.0
Liquid limit	-	-	17.0	24.0	31.0	38.0
Plasticity index	-	-	2.0	7.0	12.0	13.0
FC%	1.0	10.0	20.0	30.0	40.0	82.0
Sand%	99.0	90.0	80.0	70.0	60.0	18.0
Fine Sand%	21.2	21.0	20.8	20.6	20.3	21.0
Clay%	0.1	6.9	14.6	22.3	37.7	6.9
Silt%	0.8	3.0	5.3	7.6	12.2	3.0

Figure 8. Standard Proctor compaction curves for combined Soil 1 and Soil 2 mixtures

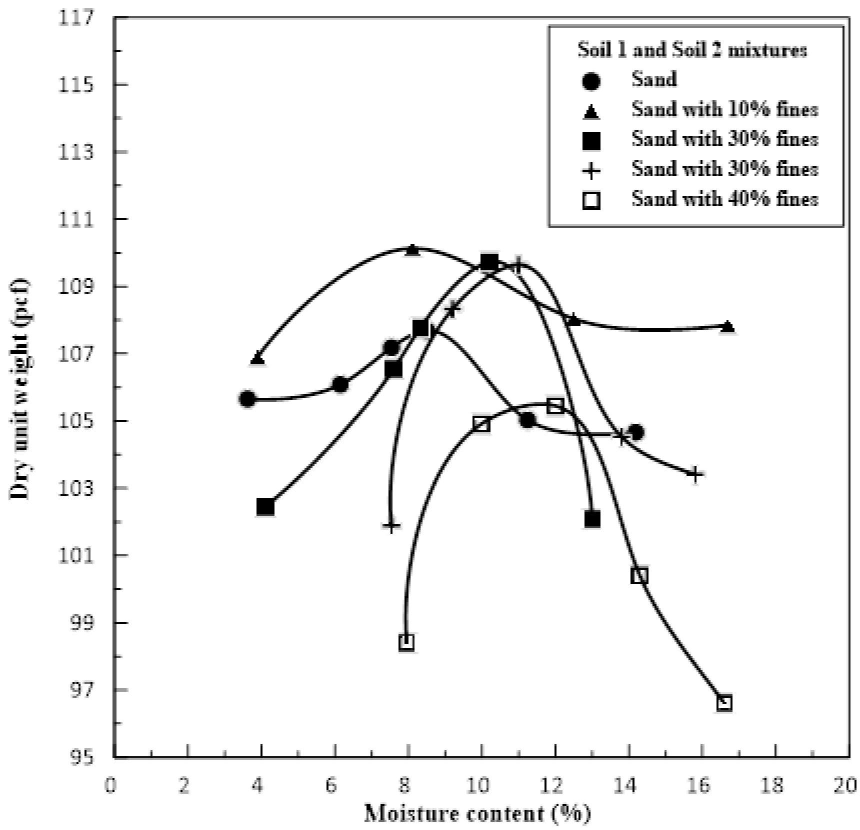

Table 9. Results of standard Proctor tests for combined Soil 1 and Soil 2 mixtures

Properties	Soil 1	Mixture 1 (10% fines)	Mixture 2 (20% fines)	Mixture 3 (30% fines)	Mixture 4 (40% fines)
Maximum dry unit weight, γ_{dm} (pcf)	107.7	110.2	109.8	109.6	105.5
Optimum moisture content, %	8.0	8.0	10.0	11.0	12.0

Soil mixtures for combined Soil 1 and Soil 3

The properties of different soil mixtures for combined Soils 1 and 3 with fines contents of 10%, 30%, 50% and 70% are presented in Table 10. The corresponding standard Proctor compaction curves for the different mixtures of combined Soil 1 and Soil 3 are presented in Figure 9. The results of maximum dry unit weight and optimum moisture contents for the four soil mixtures are presented in Table 11.

Table 10. Soil properties for combined Soil 1 and Soil 3 mixtures

Soil Properties	Soil 1	Mixture 1 (10% fines)	Mixture 2 (30% fines)	Mixture 3 (50% fines)	Mixture 4 (70% fines)
USCS Classification	SP	SP	SM	SM-ML	CL
Specific Gravity (G_s)	2.67	2.69	2.70	2.70	2.71
Plastic limit	-	-	12.9	13.4	17.0
Liquid limit	-	-	13.2	15.4	24.6
Plasticity index	-	-	0.3	2.00	7.6
FC%	1.0	10.0	30.0	50.0	70.0
Sand%	99.0	90.0	70.0	50.0	30.0
Fine Sand%	21.2	22.3	24.8	27.3	29.8
Clay%	0.1	1.1	3.5	6.0	8.4
Silt%	0.8	8.8	26.4	43.9	61.5

Figure 9. Standard Proctor compaction curves for combined Soil 1 and Soil 3 mixtures

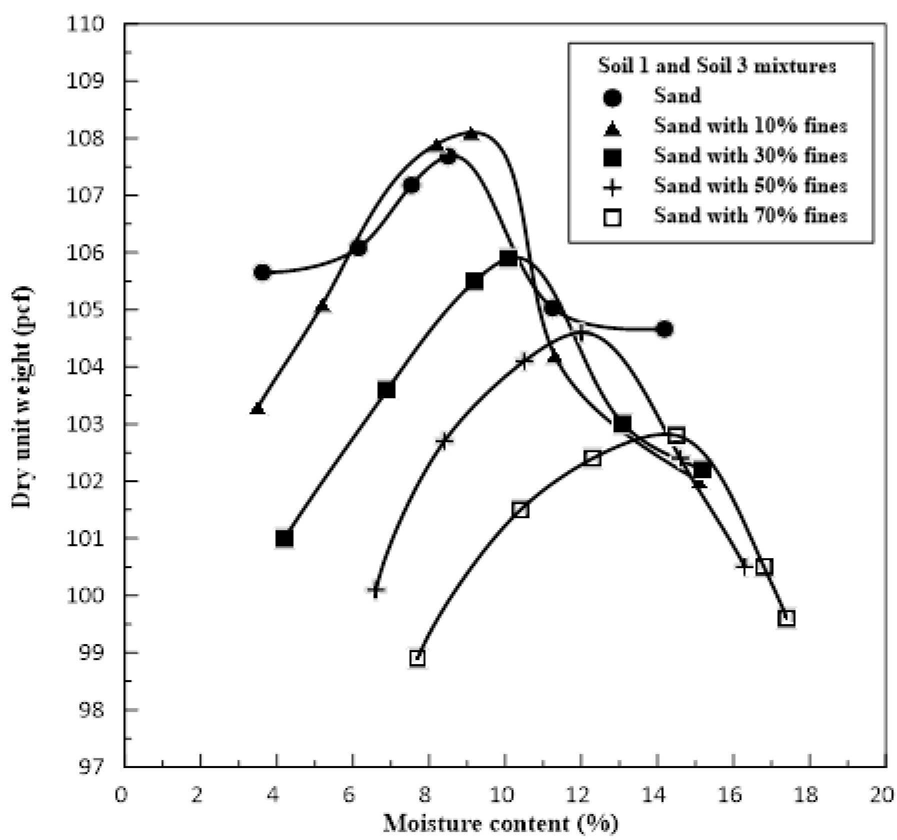

Table 11. Results of standard Proctor for combined Soil 1 and Soil 3 mixtures

Properties	Soil 1	Mixture 1 (10% fines)	Mixture 2 (30% fines)	Mixture 3 (50% fines)	Mixture 4 (70% fines)
Maximum dry unit weight γ_{dm} (pcf)	107.6	108.1	105.9	104.6	102.8
Optimum moisture content, %	8.0	9.1	10.1	12.0	14.5

Soil mixtures for combined Soil 1 and Soil 4

Seven soil mixtures were prepared by combining Soils 1 and 4 at different fines contents (silt/clay) of 10%, 20%, 30%, 40%, 50%, 60%, and 70%, and the soil properties of these soil mixtures are presented in Table 12. The compaction curves obtained from standard Proctor tests for the combined Soil 1 and Soil 4 mixtures are presented in Figure 10 for mixtures of 10%, 30%, 50%, and 70% fines contents, and in Figure 11 for mixtures of 20%, 40%, and 60% fines contents. The corresponding maximum dry unit weight and optimum moisture contents for the different mixtures are presented in Table 13.

Table 12. Soil properties for combined Soil 1 and Soil 4 mixtures

Soil Properties	Mixture 1 (10% fines)	Mixture 2 (20% fines)	Mixture 3 (30% fines)	Mixture 4 (40% fines)	Mixture 5 (50% fines)	Mixture 6 (60% fines)	Mixture 7 (70% fines)
USCS Classification	SP	SM	SM	SM	SC-ML	CL-ML	CL
Plastic limit	-	10.2	15.7	16.3	17.1	19.2	21.4
Liquid limit	-	12.3	19.8	21.8	24.2	27.2	30.3
Plasticity index	-	2.1	4.1	5.5	7.1	8.0	8.9
FC%	10.0	20.0	30.0	40.0	50.0	60.0	70.0
Sand%	90.0	80.0	70.0	60.0	50.0	40.0	30.0
Fine Sand%	23.8	26.6	29.8	32.6	35.7	38.5	41.6
Clay%	1.0	1.9	3.0	4.5	5.2	6.6	7.4
Silt%	9.0	18.1	26.9	35.5	44.7	53.4	62.6

Figure 10. Standard Proctor compaction curves for combined Soil 1 and Soil 4 mixtures of 10%, 30%, 50%, and 70% fines contents

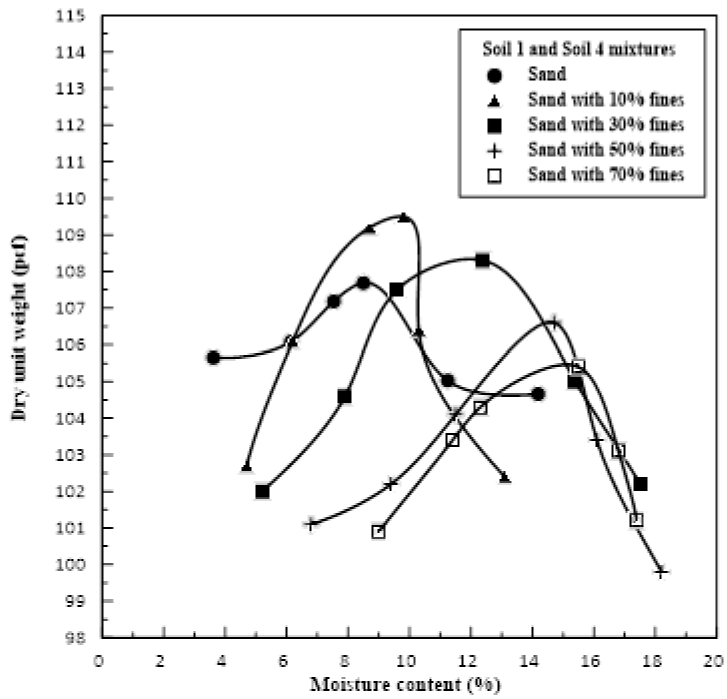

Figure 11. Standard Proctor compaction curves for combined Soil 1 and Soil 4 mixtures of 20%, 40%, and 60% fines contents

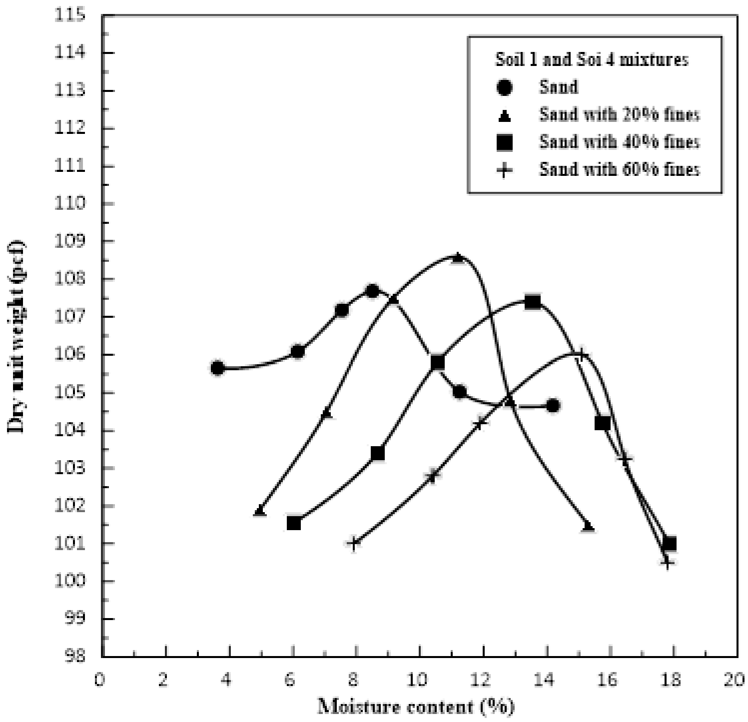

Table 13. Results of standard tests for combined Soil 1 and Soil 4 mixtures

Properties	**Mixture 1 (10% fines)**	**Mixture 2 (20% fines)**	**Mixture 3 (30% fines)**	**Mixture 4 (40% fines)**	**Mixture 5 (50% fines)**	**Mixture 6 (60% fines)**	**Mixture 7 (70% fines)**
Maximum dry unit weight, γ_d (pcf)	109.5	18.6	108.3	107.4	106.6	106.0	105.4
Optimum moisture content, %	10.0	11.2	12.4	13.5	14.7	15.1	15.5

Soil mixtures for combined Soil 1 and Soil 5

Seven soil mixtures were prepared by combining Soils 1 and 5 at different fines contents (silt/clay) of 10%, 20%, 30%, 40%, 50%, 60%, and 70%. Table 14 presents the soil properties of the different soil mixtures. The results of standard Proctor compaction tests for the combined Soil 1 and Soil 5 are presented in Figure 12 for mixtures with 10%, 30%, 50%, and 70% fines contents, while **Error! Reference source not found.** presents the standard Proctor compaction curves for mixtures with 20%, 40%, and 60% fines contents. The maximum dry unit weight and optimum moisture contents for the seven Soil 1 and Soil 5 mixtures are presented in Table 15.

Table 14. Soil properties for combined Soil 1 and Soil 5 mixtures

Soil Properties	Mixture 1 (10% fines)	Mixture 2 (20% fines)	Mixture 3 (30% fines)	Mixture 4 (40% fines)	Mixture 5 (50% fines)	Mixture 6 (60% fines)	Mixture 7 (70% fines)
USCS Classification	SP	SM	SM	SM	SM-ML	CL-ML	CL-ML
Plastic limit	-	8.5	12.8	13.8	14.9	16.1	17.0
Liquid limit	-	9.2	13.9	15.6	17.11	21.4	25.2
Plasticity index	-	0.7	1.1	1.8	2.21	5.3	8.2
FC%	10.0	20.0	30.0	40.0	50.0	60.0	70.0
Sand%	90.0	80.0	70.0	60.0	50.0	40.0	30.0
Fine Sand%	9.0	18.3	27.0	29.5	45.0	53.8	62.9
Clay%	0.91	2.1	2.9	4.2	4.9	5.8	7.0
Silt%	9.0	9.9	27.0	27.8	45.0	54.2	62.9

Figure 12. Standard Proctor compaction curves for combined Soil 1 and Soil 5 mixtures of 10%, 30%, 50%, and 70% fines contents

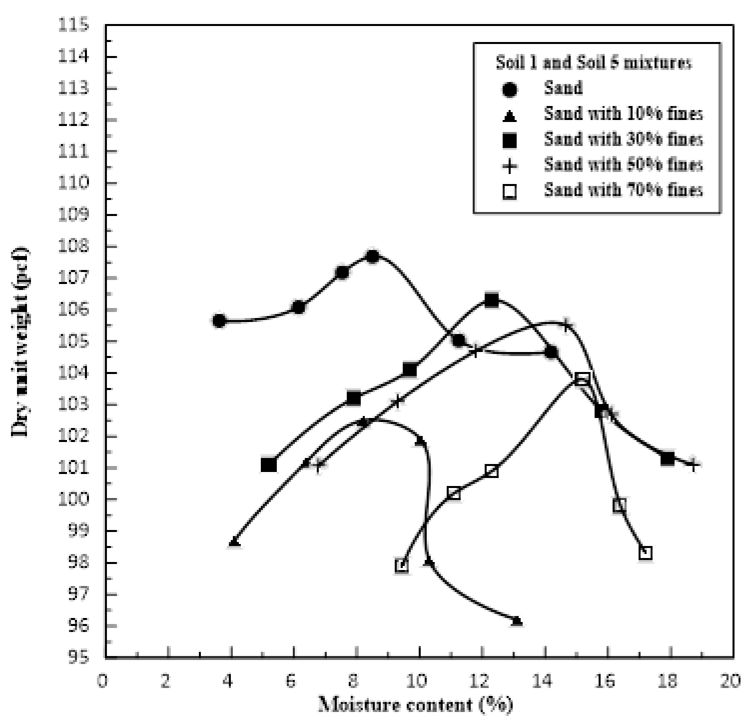

Figure 13. Standard Proctor compaction curves for combined Soil 1 and Soil 5 mixtures of 20%, 40%, and 60% fines contents

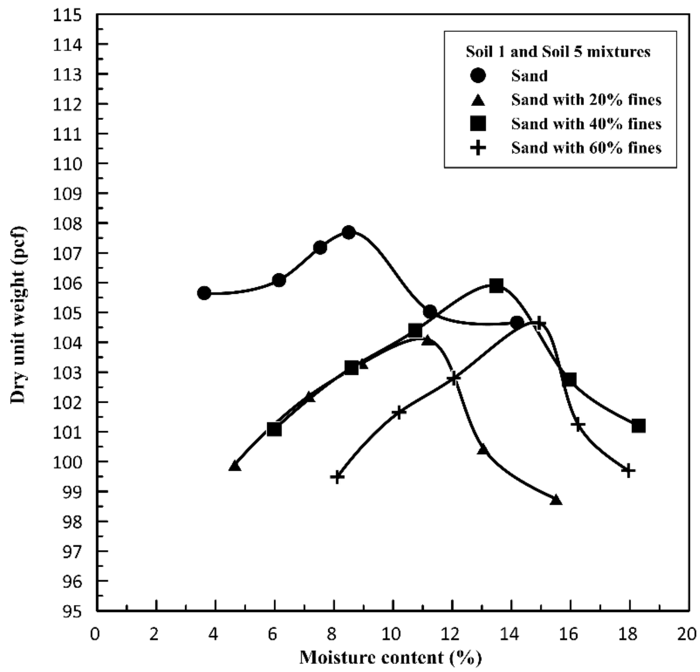

Table 15. Results of standard Proctor tests for combined Soil 1 and Soil 5 mixtures

Properties	**Mixture 1 (10% fines)**	**Mixture 2 (20% fines)**	**Mixture 3 (30% fines)**	**Mixture 4 (40% fines)**	**Mixture 5 (50% fines)**	**Mixture 6 (60% fines)**	**Mixture 7 (70% fines)**
Maximum dry unit weight, γ_d (pcf)	102.5	104.1	106.3	105.8	105.5	104.6	103.8
Optimum moisture content, %	8.2	11.2	12.3	13.4	14.6	14.9	15.2

Scanning Electron Microscope (SEM)

The Scanning Electron Microscope (SEM) is a test process that scans a sample with an electron beam to produce a magnified image for analysis. The method is also known as SEM analysis and SEM microscopy, and it is used very effectively in the microanalysis and failure analysis of solid inorganic materials. SEM is performed at high magnifications, generates high-resolution images, and precisely measures very small features and objects.

The picture of SEM starts at 25×, approximately 6 mm across the whole field of view, and zooms in to 12,000×, approximately 12 µm resolution across the whole field of view. This high resolution level can capture the size of coarse sand (2-4.25 mm) till clay (>0.075 mm). In this study, the sample preparation for SEM analysis was pre-formed carefully through the following steps:

1. Oven dry the soil samples at 110°F for 24 hours.
2. Sieve the samples into four different ranges (coarse sand, medium sand, fine sand, and fine soil grained) for testing.
3. Using a brush, apply the conductive graphite coating to a carbon stud.
4. Carefully set the selected soil on the painted stud and allow it to air-dry. Drying should take no longer than five minutes after air-drying.
5. Place the samples in the spaces available on the testing platform located in the chamber of the sputter coater.
6. Specify the coating element and desired thickness using the touch screen control.
7. Allow the machine to run until the coating of the samples is complete. Time of coating depends on the amount of the sample and its coating thickness.
8. During SEM, the chamber will emit a glowing light. Carefully remove samples from the sputter coater and place in a petri dish for easy transportation to the SEM equipment.

Particle Shape Analysis

The Image J Software was used to estimate the particle shape of the soil particles for Soils 3, 4, and 5. The images of SEM were imported into the software. The scale of the image was selected, and the particle shape was recognized through free-hand selection manually for each particle. The software calculated the circularity, roundness, and aspect ratio of the soil particles. These parameters were calculated using the following equations:

$$\text{Circularity} = \frac{4\pi\ (\text{Area of the particles})}{(\text{Perimeter of the particle})^{2}} \qquad [28]$$

$$\text{Aspect ratio} = \frac{\text{Major axis of the particle}}{\text{Minor axis of the particle}} \qquad [29]$$

$$\text{Roundness (R)} = \frac{4\ (\text{Area of the particle})}{\pi\ (\text{Major axis})^{2}} \qquad [30]$$

A value of 1.0 for roundness indicates a perfectly spherical particle. As the value approaches 0, it indicates an increasingly elongated shape. Values may not be valid for very small particles. The SEM image results for Soils 3, 4, and 5 are presented in Figure 14.

Figure 14. Results of SEM for a) Soil 3, b) Soil 4, and c) Soil 5

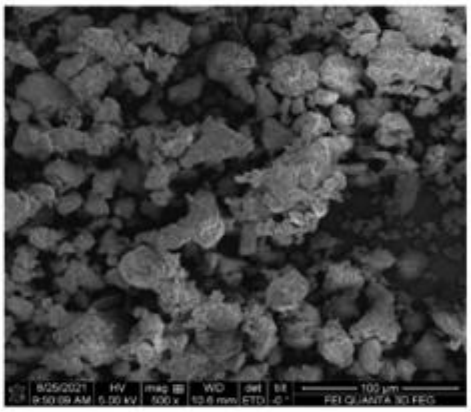

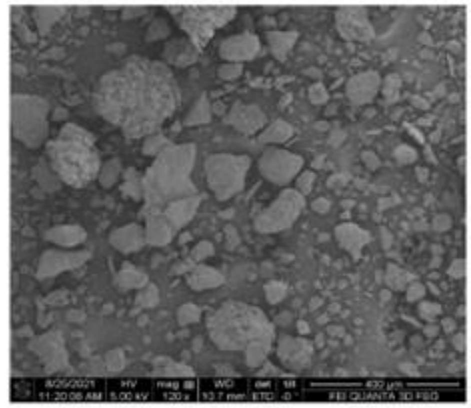

(a)

Fines

Roundness, (R) = 0.71

Fine Sand

Roundness, (R) = 0.78

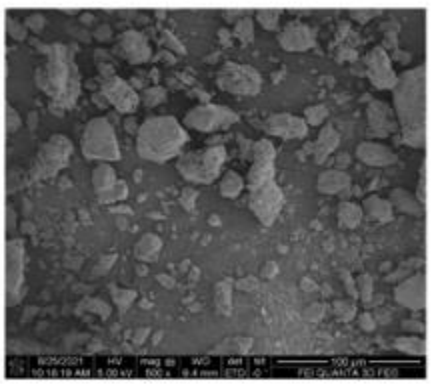

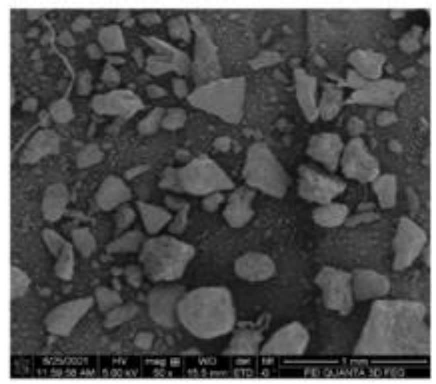

(b)

Fines

Roundness, (R) = 0.66

Fine Sand

Roundness, (R) = 0.65

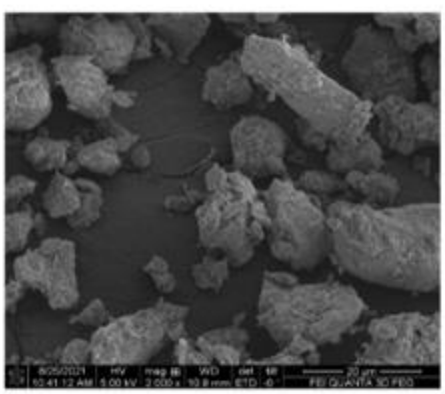

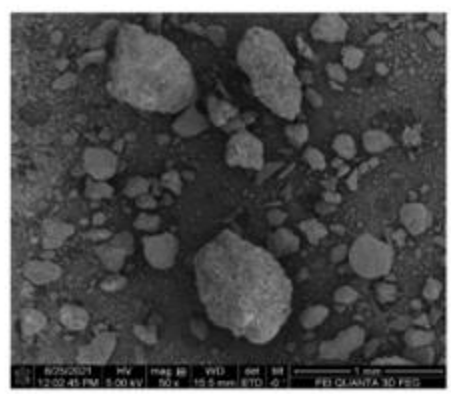

(c)

Fines

Roundness, (R) = 0.68

Fine Sand

Roundness, (R) = 0.83

Discussion of Results

The effects of silt and clay contents on the internal friction angle (ϕ) are distinctly different. Most geotechnical engineers consider the behavior of silts to be a median between clays at one end and sand at the other. This approach of approximation is not practical due to the different shear behaviors of clay and sand. The generation of friction between sand particles is completely different from that of clay particles. For cohesion-less soils, the forces between the soil particles arise from friction between the particles as they have relative movement. For clayey soils, on the other hand, the primary forces arise from electric repulsion through the absorbed water layer that exists between clay particles. Therefore, the mixtures in this study could be categorized in two types: 1) soil mixtures with fines dominated by clay, and 2) soil mixtures with fines dominated by silt particles. Type one soil mixtures were prepared by combining Soils 1 and 2, while type two soil mixtures were prepared by combining Soil 1 with either Soil 3, Soil 4, or Soil 5. The application of testing silt or clay alone was not possible because of the difficulty in obtaining silt or clay particles alone in natural soil. Additionally, there is a procedure that separates silt particles from clay particles in laboratory testing.

Results of Small Direct Shear Tests

Small direct shear tests were conducted to evaluate the shear strength parameters (cohesion [c] and internal friction angle [ϕ]) for the different soil mixtures prepared by combining Soil 1 (sand) with Soil 2, Soil 3, Soil 4, or Soil 5 to achieve different fines contents (FC) from 10% to 70% and different moisture contents (optimum moisture content [omc], omc+2%, omc+4%, omc+6%).

For the combined Soil 1 and Soil 2 mixtures, the internal friction angle (ϕ) obtained at the optimum moisture content and maximum dry unit weight increased when increasing the fines contents (primarily clay content) until reaching 30% fines, then decreased slightly. The results of all small direct shear tests for combined Soil 1 and Soil 2 mixtures with fines contents of 10%, 20%, 30% and 40% are also presented in Table 16. Figure 15 summarizes the results of a direct shear test for combined Soil 1 and Soil 2 mixtures prepared using 10% fines at optimum moisture content (omc). The results of all other direct shear tests are presented in Appendix A. As shown in Table 16, the ϕ determined from small direct shear tests increased from 38° to 41.6° when increasing the fines content, then dropped to 40°. This trend was also consistent at different water contents. These findings are similar to the results reported by Vallejo and Mawby [62]. Sand-clay soil mixtures with 40-75% sand content are likely to have higher shear strength than the sand soil alone, as stated by Vallejo and Mawby [62]. The shear strength for soil mixtures with these proportions is provided by frictional resistance both from clay and sand particles. Increasing the water content led to the decrease in both the cohesion and the ϕ for all combined Soil 1 and Soil 2 mixtures.

Table 16. Results of small direct shear for combined Soil 1 and Soil 2 mixtures

Soil	Dry unit weight, γ_d (pcf)	Water content (%)	Relative Density (%)	Friction angle (ϕ) (degree)	Cohesion (psi)
Sand with 10% fine (Fine sand%=3.5) (Clay%=6.1) (Silt%= 3.9)	110.1	7.8	70.4	38.3°	1.15
	107.2	13	62.4	36.8°	0.8
	104.4	15.9	41.4	34.9°	-
Sand with 20% fine (Fine sand%=7.2) (Clay%=12.2) (Silt%= 7.8)	122.7	10.3	84	41.3°	2.16
	116.4	13.2	63.4	39.3°	1.8
	112.5	16.6	53.4	37.3°	1.41
Sand with 30% fine (Fine sand%=9.2) (Clay%=18.3) (Silt%= 11.7)	121.5	11.2	81.3	41.6°	3
	115.5	13.1	61.7	40.3°	2.4
	111.9	15.8	54	39.7°	2.1
Sand with 40% fine (Fine sand%=11.2) (Clay%=24.4) (Silt%= 15.6)	117.3	12.3	71.5	40°	5.1
	113.1	14.1	63	39.2°	4.12
	109.1	16.3	42.7	39.3°	3.7

Figure 15. Results of small direct shear tests for combined Soil 1 and Soil 2 mixtures at FC=10%, D_r =41.4%, W_c = 15.9%: (a) shear stress vs normal stress; (b) shear stress vs horizontal displacement; (c) vertical displacement vs horizontal displacement

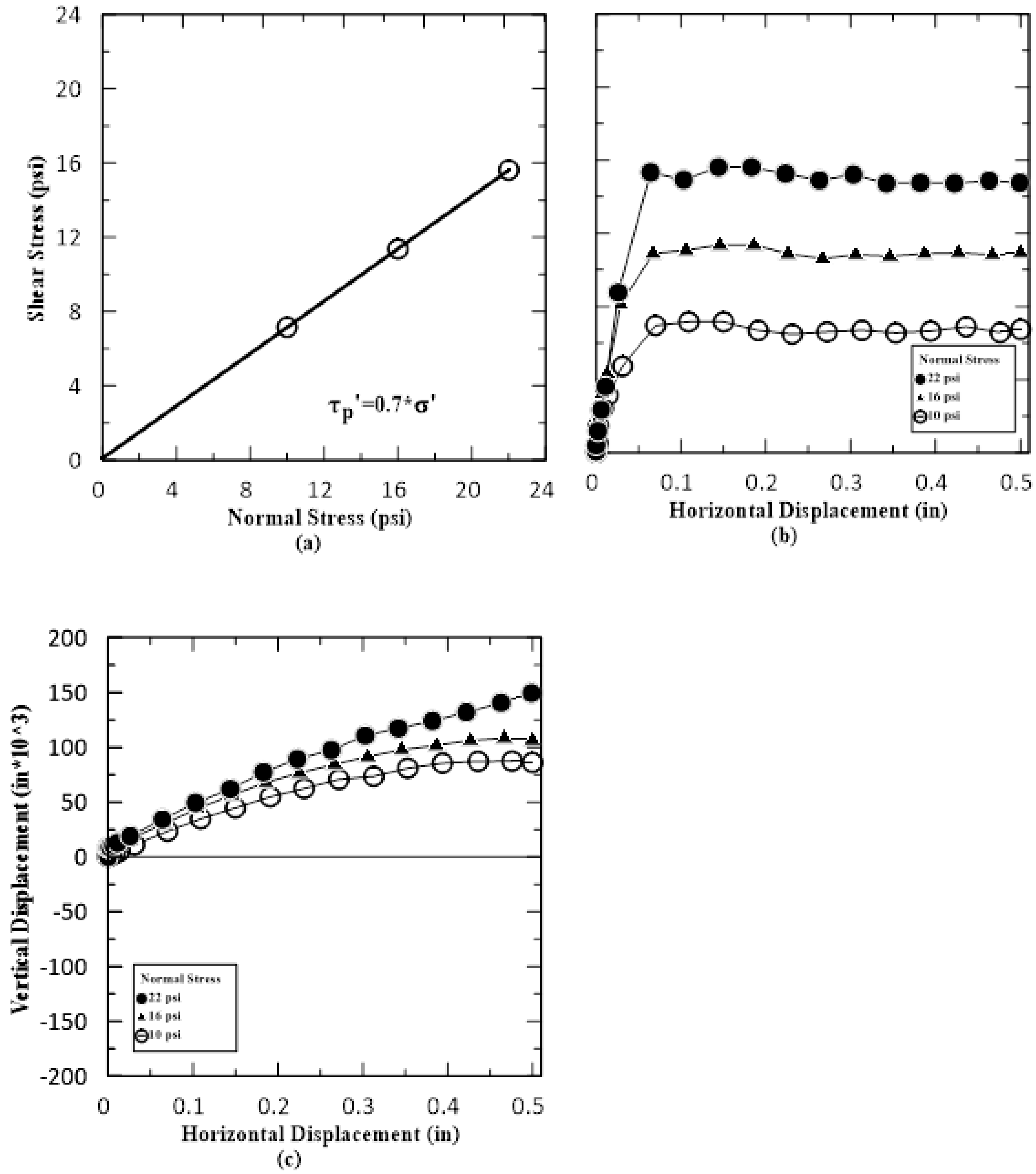

Figure 16 presents the results of the small direct shear test for combined Soil 1 and Soil 3 mixtures prepared using 10% fines and omc. The results of the other direct shear tests with fines contents of 10%, 30%, 50% and 70% and different moisture contents are presented in Appendix A. Additionally, the results of all other small direct shear tests for combined

Soil 1 and Soil 3 mixtures are summarized in Table 17. The internal friction angle (ϕ) for combined Soil 1 and Soil 3 mixtures prepared at optimum moisture content and maximum dry unit weight dropped significantly when increasing the fines content (primarily silt content). The value of the ϕ decreased from 41.2° to 29° when reaching a fine content of 70%, while cohesion increased from 1.1 psi to 4.2 psi, as shown in Table 17. These observations are similar to the results of a study by Phan et al. [94], which showed that silt was allowed to mobilize the cohesive strength and thus slip between the sand particles. Increasing the water content led to a decrease in both the cohesion and ϕ for all soil mixtures. Similar observations were also made for combined Soil 1 and Soil 4 (or Soil 5) mixtures. An additional reason for the significant drop in the ϕ can also be attributed to the content of fine sand. Large soil particles in cohesion-less soil tend to have high friction than fine particles, as reported by Bareither et al. [58].

Small direct shear tests were performed by combining Soil 1 with Soil 4 to evaluate the shear strength parameters (c, ϕ) for mixtures with fines contents of 10%, 20%, 30%, 40%, 50%, 60% and 70%, and for different moisture contents (omc, omc+2%, omc+4%, omc+6%). Figure 17 presents the results of the small direct shear test for combined Soil 1 and Soil 4 mixtures prepared using 10% fines and omc. The results of the other small direct shear tests with fines contents of 10%, 20%, 30%, 40%, 50%, 60%, and 70% and different moisture contents are presented in Appendix A. Additionally, the results of all other small direct shear tests for combined Soil 1 and Soil 4 mixtures are summarized in Table 18. Similar to the combined Soil 1 and Soil 3 mixtures, the internal friction angle (ϕ) for combined Soil 1 and Soil 4 mixtures prepared at optimum moisture content and maximum dry unit weight decreased when increasing the fines content (mainly silt content). The ϕ decreased from 41.4° to 27.7° when the fine content increased from 10% to 70%, while the cohesion (c) increased from 1.47 psi to 5.0 psi, as shown in Table 18. Again, these observations are similar to the results of a study by Phan et al. [94], which showed that silt was allowed to mobilize the cohesive strength and thus slip between the sand particles. The increase in water content from omc to omc+6% resulted in a decrease in both the cohesion and ϕ for all combined Soil 1 and Soil 4 mixtures. The decrease in ϕ can also be attributed to the content of fine sand in the soil mixture.

Figure 16. Results of small direct shear tests for combined Soil 1 and Soil 3 mixtures at FC=10%, Dr =33.3%, Wc = 18.1%: (a) shear stress vs normal stress; (b) shear stress vs horizontal displacement; (c) vertical displacement vs horizontal displacement

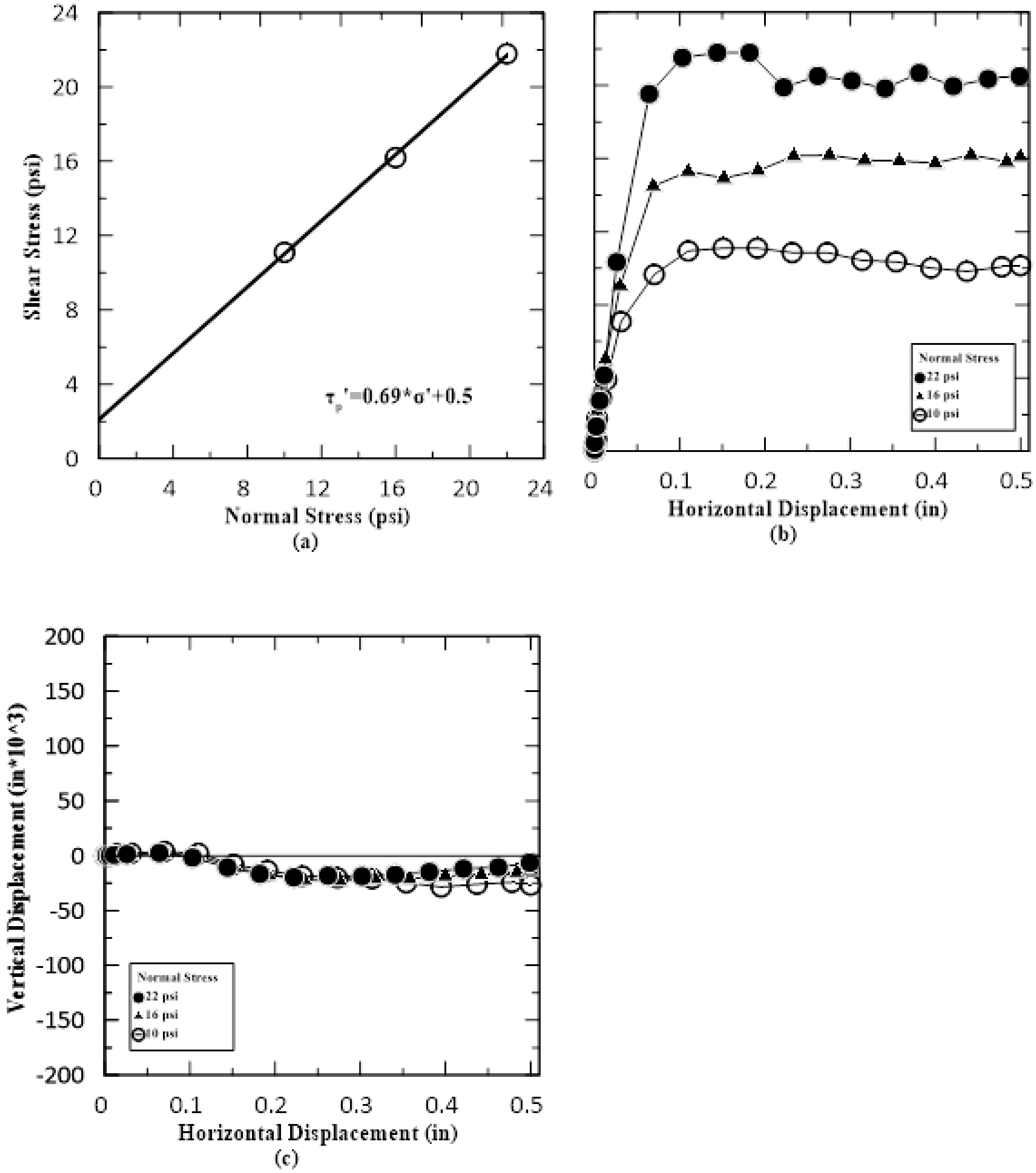

Table 17. Results of small direct shear tests for combined Soil 1 and Soil 3 mixtures

Soil	Dry unit weight, γ_d (pcf)	Water content (%)	Relative Density (%)	Friction angle (ϕ) (degree)	Cohesion (psi)
Sand with 10% fine (Fine sand%=4.1) (Clay%=1.96) (Silt%= 8)	113.4	10.1	74.1	41.2°	1.1
	111.2	12.0	65.5	38.6°	0.97
	107.4	15.3	51.4	35.7°	0.76
	102.1	18.1	43.4	34.6°	0.5
Sand with 30% fine (Fine sand%=9) (Clay%=5.9) (Silt%= 24.1)	119.1	11.0	82.1	38°	2
	116.9	14.3	73.1	36.1°	1.6
	111.0	16.6	57.0	33.7°	1.36
	108.5	18.9	39.1	32°	1.1
Sand with 50% fine (Fine sand%=14.2) (Clay%=9.9) (Silt%= 40.1)	121.7	13.0	88.7	34°	3.1
	117.5	15.2	73.1	32.6°	2.56
	112.8	17.3	55.5	31.3°	1.8
	108.0	19.0	42.3	29.8°	1.47
Sand with 70% fine (Fine sand%=15.2) (Clay%=14) (Silt%= 57)	117.9	16.1	91.8	29°	4.2
	114.3	18.2	76.6	26.5°	3.8
	110.1	20.3	61.5	24.2°	2.9
	106.6	22.0	43.3	22.6°	2.4

Figure 17. Results of small direct shear tests for combined Soil 1 and Soil 4 mixtures at FC =10%, Dr =41%, Wc = 15.2%: (a) shear stress vs normal stress; (b) shear stress vs horizontal displacement; (c) vertical displacement vs horizontal displacement

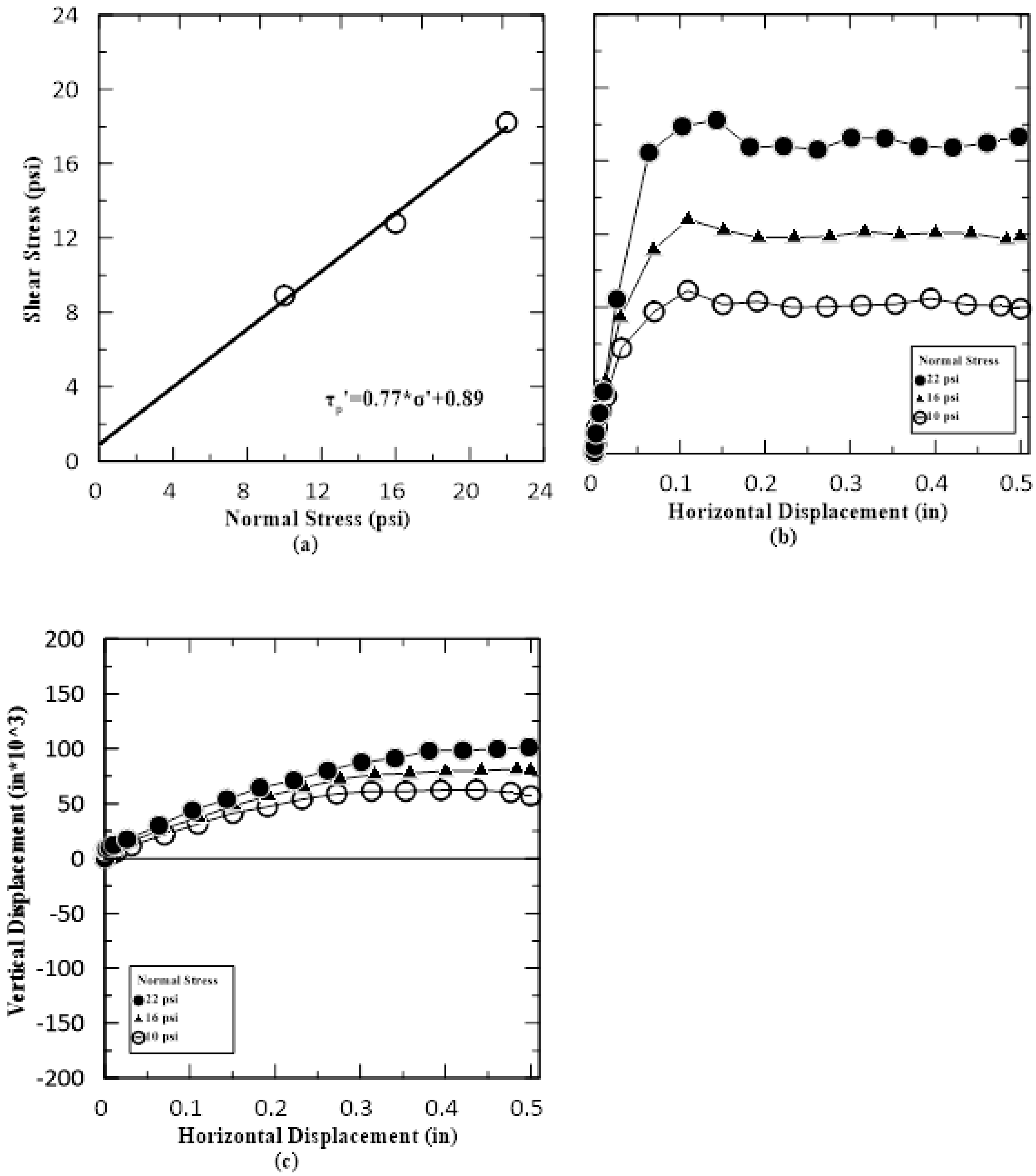

Table 18. Results of small direct shear tests for combined Soil 1 and Soil 4 mixtures

Soil	Dry unit weight (pcf)	Water content (%)	Relative density (%)	Friction angle (ϕ) (degree)	Cohesion (psi)
Sand with 10% fine (Fine sand%=5.1) (Clay%=2.3) (Silt%= 7.7)	103.1	9.1	87.3	41.4	1.47
	100.7	11.3	76.5	40.3	1.33
	99.8	13	62.9	38.9	1.23
	96.5	15.2	49.3	37.4	1
Sand with 20% fine (Fine sand%=21.3) (Clay%=1.9) (Silt%= 18.1)	104.2	9.6	86.9	39.5	0
	101.9	11.3	75.4	38.5	0
	99.8	13.5	63.3	37.4	0
	97.4	15.5	50.6	35.5	0
Sand with 30% fine (Fine sand%=11.1) (Clay%=6.6) (Silt%= 23.1)	105.1	10.2	86.5	38.0	2.5
	103.2	12.1	74.6	36.5	2.33
	100	14.3	64.2	35.6	1.76
	97.9	16	51.7	34.0	1.26
Sand with 40% fine (Fine sand%=19.6) (Clay%=4.5) (Silt%= 35.5)	106.4	11.3	87.6	36.1	0
	103.7	13.2	76.1	34.7	0
	100.1	15.3	63.8	33.6	0
	98.3	17.4	52.4	31.8	0
Sand with 50% fine (Fine sand%=16.2) (Clay%=11.5) (Silt%= 38.5)	107.8	12	88.3	34.6	3.26
	104	14.4	78.3	33.0	3.1
	100.1	16	63.9	31.6	2.7
	98.3	18.6	53.2	29.8	2.2
Sand with 60% fine (Fine sand%=15.4) (Clay%=6.6) (Silt%= 53.4)	108.8	13.3	89.1	30.5	0
	106.3	15.5	79.3	29.2	0
	102.5	17.5	65.2	27.7	0
	99.8	19.5	54.1	26.0	0
Sand with 70% fine (Fine sand%=19.2) (Clay%=16.1) (Silt%= 53.9)	110.2	14.5	90.5	27.7	5
	108.7	16.3	80.0	25.7	4.6
	105.2	18.6	66.7	24.2	4.1
	101.6	20.2	54.4	21.8	3.9

The results of the small direct shear test for combined Soil 1 and Soil 5 mixture prepared using 10% fines and omc are presented in Figure 18. The results of the rest of the direct shear tests prepared by combining Soil 1 and Soil 5 to achieve fines contents of 10%, 20%, 30%, 40%, 50%, 60%, and 70%, and for different moisture contents are presented in Appendix A. Additionally, the results of all other small direct shear tests for combined Soil 1 and Soil 5 mixtures are summarized in Table 17. The internal friction angle (ϕ) for combined Soil 1 and Soil 5 mixtures prepared at optimum moisture content and maximum dry unit weight decreased from 40° to 30.9° as the fines content (mainly silt content) increased from 10% to 70%. Meanwhile, cohesion increased from 0.9 psi to 3.5 psi, as shown in Table 19. Increasing the water content from omc to omc+6% resulted in decreasing both the cohesion and ϕ for all mixtures; this was similar to observations for combined Soil 1 and Soil 3 (or Soil 4) mixtures. Again, the significant drop in the ϕ can be also attributed to the content of fine sand in the mixtures.

Figure 18. Results of small direct shear tests for combined Soil 1 and Soil 5 mixtures at FC =10%, Dr =33.3%, Wc = 18.1%: (a) shear stress vs normal stress; (b) shear stress vs horizontal displacement; (c) vertical displacement vs horizontal displacement

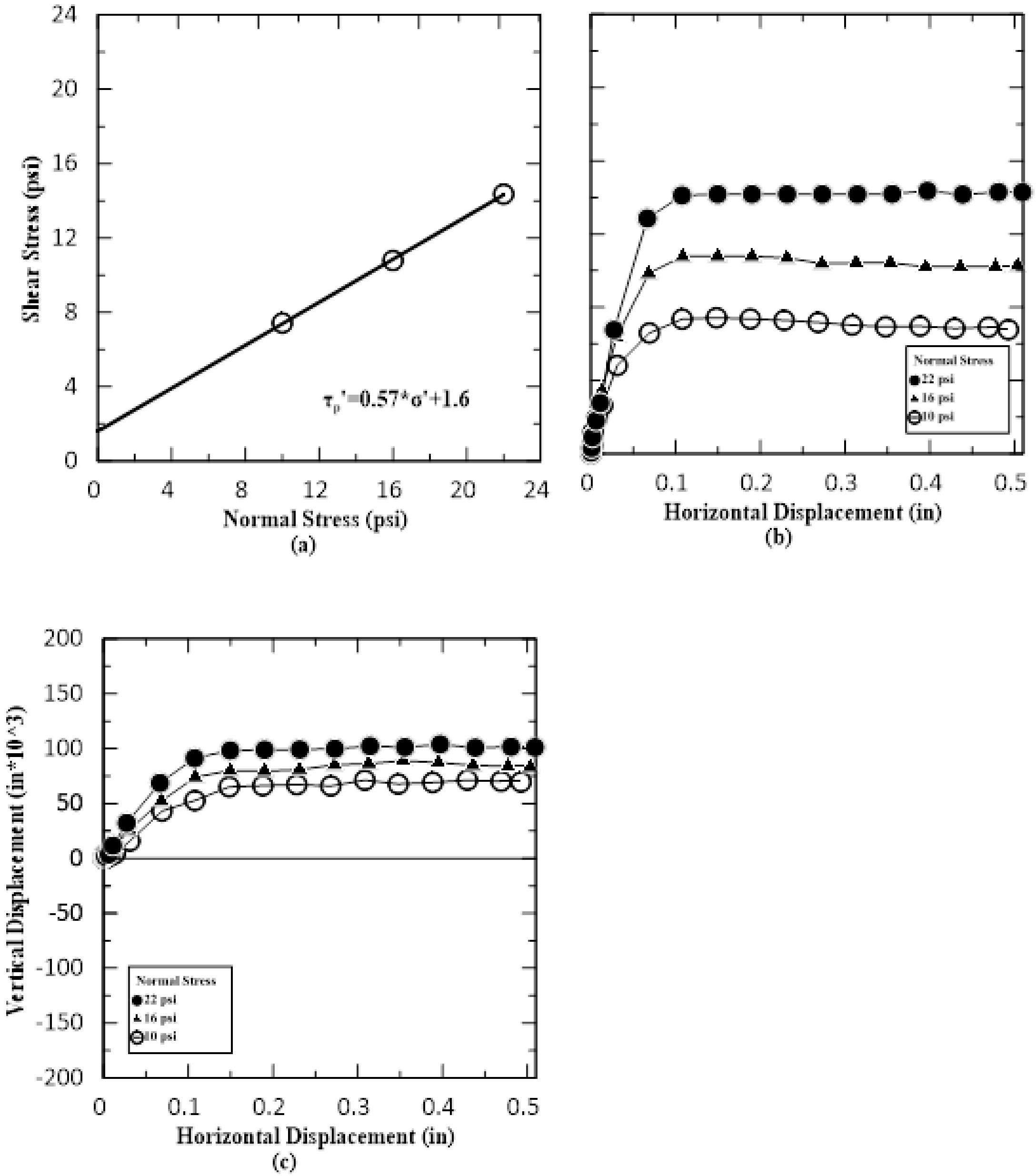

Table 19. Results of small direct shear tests for combined Soil 1 and Soil 5 mixtures

Soil	Dry unit weight, γ_d (pcf)	Water content (%)	Relative density (%)	Friction angle (ϕ) (degree)	Cohesion (psi)
Sand with 10% fine (Fine sand%=7.2) (Clay%=2.1) (Silt%= 7.9)	113.4	10.1	81.6	40°	0.9
	111.2	12	71.9	37.7°	0.8
	107.4	15.3	60.4	36.8°	0.6
	102.1	18.1	44.7	35.3°	0.56
Sand with 20% fine (Fine sand%=14.6) (Clay%=2.1) (Silt%= 9.9)	116.2	10.6	83.9	39.6°	0
	114.0	12.8	73.0	37.7°	0
	109.3	15.4	61.2	35.8°	0.63
	105.4	17.4	47.0	34.7°	0.20
Sand with 30% fine (Fine sand%=13.1) (Clay%=6.3) (Silt%= 23.7)	119.1	11	86.7	38.9°	1.47
	116.9	14.3	76.2	37.4°	1.3
	111	16.6	63.0	35°	1
	108.5	18.9	50.7	33.3°	0.33
Sand with 40% fine (Fine sand%=17.7) (Clay%=4.2) (Silt%= 27.8)	120.4	12.2	87.3	37.4°	0.14
	117.3	14.6	77.3	35.0°	0.18
	112.1	16.7	63.4	33.3°	0.62
	108.2	18.8	52.4	32.4°	0.68
Sand with 50% fine (Fine sand%=18.2) (Clay%=10.5) (Silt%= 39.5)	121.7	13	88.4	35.3°	2.4
	117.5	15.2	76.6	33.7°	2.3
	112.8	17.3	64.2	31.3°	2
	108	19	53.4	31.0°	1.8
Sand with 60% fine (Fine sand%=21.5) (Clay%=5.8) (Silt%= 54.2)	119.9	14.7	90.2	33.4°	0.76
	115.8	16.8	76.5	30.7°	2.0
	111.4	18.6	66.5	28.3°	1.3
	107.4	20.5	53.6	26.5°	1.3
Sand with 70% fine (Fine sand%=20.2) (Clay%=14.7) (Silt%= 55.3)	117.9	16.1	90.9	30.9°	3.5
	114.3	18.2	77.4	27.3°	3.2
	110.1	20.3	65.2	24.7°	2.9
	106.6	22	53.7	21.8°	2.6

Results of Large Direct Shear Tests

Large direct shear tests (size = 12”× 12”× 8”) were performed in this study to evaluate the interface friction angle (δ) between sandy soils mixed with different fines contents and the concrete pile surface. The effects of different parameters, including the fines contents (silt/clay), relative densities, moisture contents, and confining stresses, on the values of the δ angles were investigated.

The results of the large direct shear tests for combined Soil 1 and Soil 2 mixtures are summarized in Table 20. The results showed that the interface friction angle (δ) increased slightly when increasing the fines content. Figure 19 presents the results of the large direct shear test for combined Soil 1 and Soil 2 mixtures prepared using 10% fines and omc. The results of the other large direct shear tests prepared at different fines contents of 10%, 20%, 30%, and 40%, and different moisture contents (omc to omc+6%) are presented in Appendix B. The δ at optimum moisture content and maximum dry unit weight increased from 31.1° to 32.6° when the fines content increased from 10% to 40%.

Table 20. Results of large interface direct shear tests for combined Soil 1 and Soil 2 mixtures

Soil	Dry unit weight, γ_d (pcf)	Water content (%)	Relative Density (%)	Interface friction angle (δ) (degree)	Adhesion (psi)
Sand with 10% fine (Fine Sand%=3.5) (Clay%=6.1) (Silt%= 3.9)	110.1	7.8	70.4	31.3°	0.21
	107.2	13	62.4	30.8°	0.45
	104.4	15.9	41.4	30.1°	0.386
Sand with 20% fine (Fine Sand%=7.2) (Clay%=12.2) (Silt%= 7.8)	122.7	10.3	84	31.9°	1.02
	116.4	13.2	63.4	30.9°	1
	112.5	16.6	53.4	30.3°	0.88
Sand with 30% fine (Fine Sand%=9.2) (Clay%=18.3) (Silt%= 11.7)	121.5	11.2	81.3	32.6°	1.4
	115.5	13.1	61.7	31°	1.1
	111.9	15.8	54	30.8°	0.6
Sand with 40% fine (Fine Sand%=11.2) (Clay%=24.4) (Silt%= 15.6)	117.3	12.3	71.5	32.3°	3.76
	113.1	14.1	63	30.6°	3.55
	109.1	16.3	42.7	29.7°	3.26

Figure 19. Results of large direct shear tests for combined Soil 1 and Soil 2 mixtures at FC =10%, Dr =70.4%, Wc = 7.8%: (a) interface shear stress vs normal stress; (b) interface shear stress vs horizontal displacement; (c) vertical displacement vs horizontal displacement

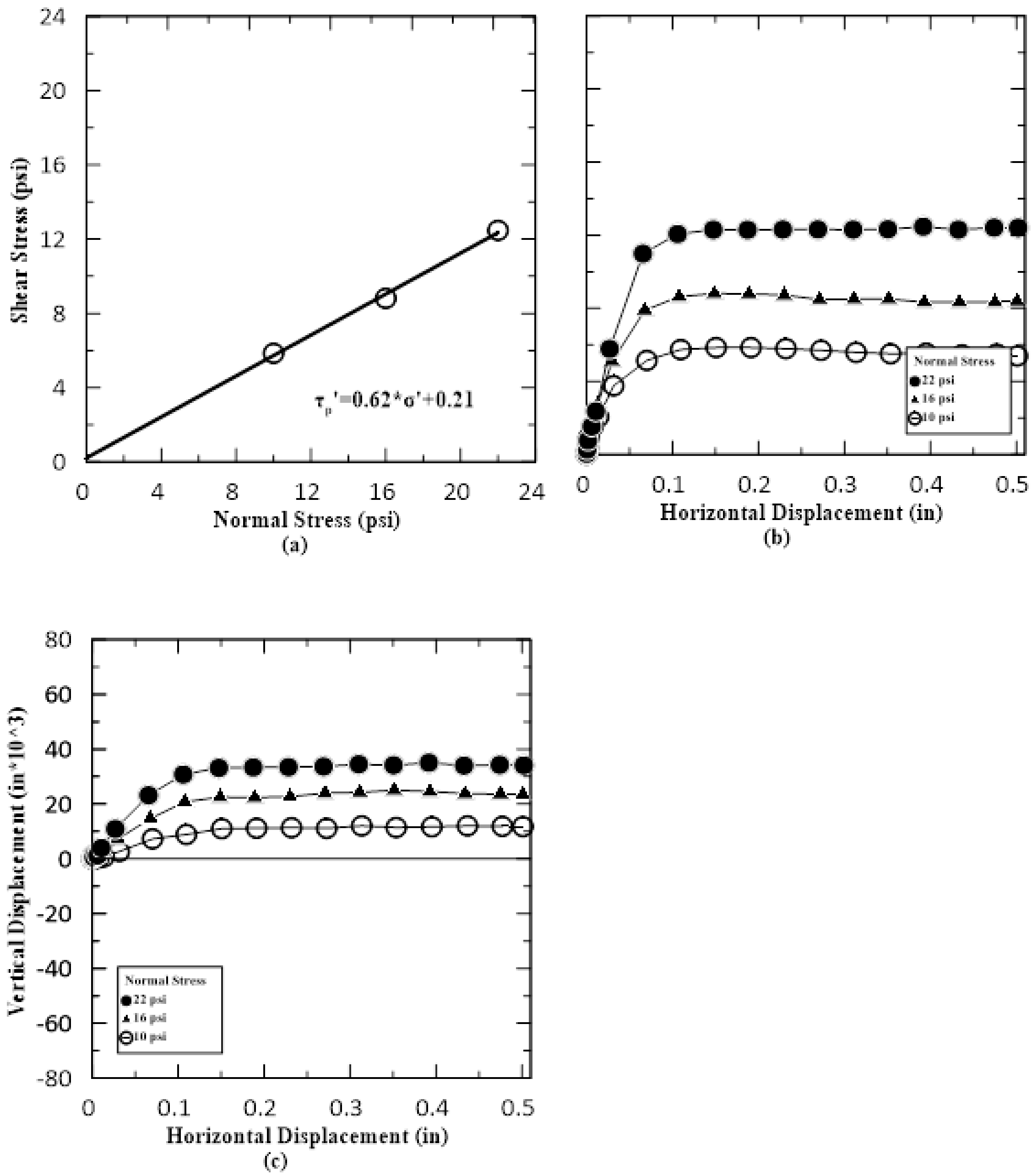

The calculated values of the coefficient of interface friction [tan(δ)/tan (ϕ)] between the soil and concrete surface did not show any trend with the increase of fines content. The interface coefficient values obtained at the optimum moisture contents for the different combined Soil 1 and Soil 2 mixtures are presented in Table 21, which ranges between 0.7 and 0.76 (average = 0.73).

Table 21. Coefficient of soil-concrete interface friction for combined Soil 1 and Soil 2 mixtures at optimum moisture contents

Soil	Internal friction angle (ϕ') (degree)	Interface friction angle (δ) (degree)	Coefficient of interface friction tan(δ)/tan (ϕ)
Sand with 10% fine	38.3°	31.3°	0.76
Sand with 20% fine	41.3°	31.9°	0.70
Sand with 30% fine	41.6°	32.6°	0.72
Sand with 40% fine	40°	32.3°	0.75

The results of the large direct shear tests for combined Soil 1 and Soil 3 mixtures are summarized in Table 22, and those of the large direct shear tests for combined Soil 1 and Soil 3 mixtures prepared using 10% fines and omc are presented in Figure 20. The results of the rest of the large direct shear tests prepared at fines contents of 10%, 50%, and 70%, and different moisture contents (omc to omc+6%) are presented in Appendix B. The results showed that the interface friction angle (δ) decreased for samples prepared at omc from 31.3° for 10% fines content soil mixture to 21° for 70% fines content soil mixture.

The coefficient of interface friction [tan(δ)/tan (ϕ)] between the soil and concrete surface for combined Soil 1 and Soil 3 mixtures were calculated, and the results for samples prepared at optimum moisture contents (Table 23) show that the values range from 0.65 for 70% fines content to 0.77 for 10% fines content (average = 0.69).

Table 22. Results of large interface direct shear tests for Soil 1 and Soil 3 mixtures

Soil	Dry density unit weight, γ_d (pcf)	Water content (%)	Relative density (%)	Interface friction angle (δ) (Degree)	Adhesion (psi)
Sand with 10% fine (Fine sand%=4.1) (Clay%=1.96) (Silt%= 8)	113.4	10.3	81.3	31.3°	-
	111.2	12.2	69.1	30.7°	-
	107.4	15	57.9	28.9°	-
Sand with 50% fine (Fine sand%=14.2) (Clay%=9.9) (Silt%= 40.1)	121.7	13	80.1	24.2°	1
	117.5	15.2	61	23°	0.8
	112.8	17.3	53.7	22.6°	0.43
Sand with 70% fine (Fine sand%=15.2) (Clay%=14) (Silt%= 57)	117.3	12	78.5	21°	1.2
	113.4	14.2	63.3	20.5°	0.8
	109.1	16.2	52.7	20.1°	0.43

Figure 20. Results of large direct shear tests for combined Soil 1 and Soil 3 mixtures at FC =10%, Dr =81.3%, Wc = 10.3%: (a) interface shear stress vs normal stress; (b) interface shear stress vs horizontal displacement; (c) vertical displacement vs horizontal displacement

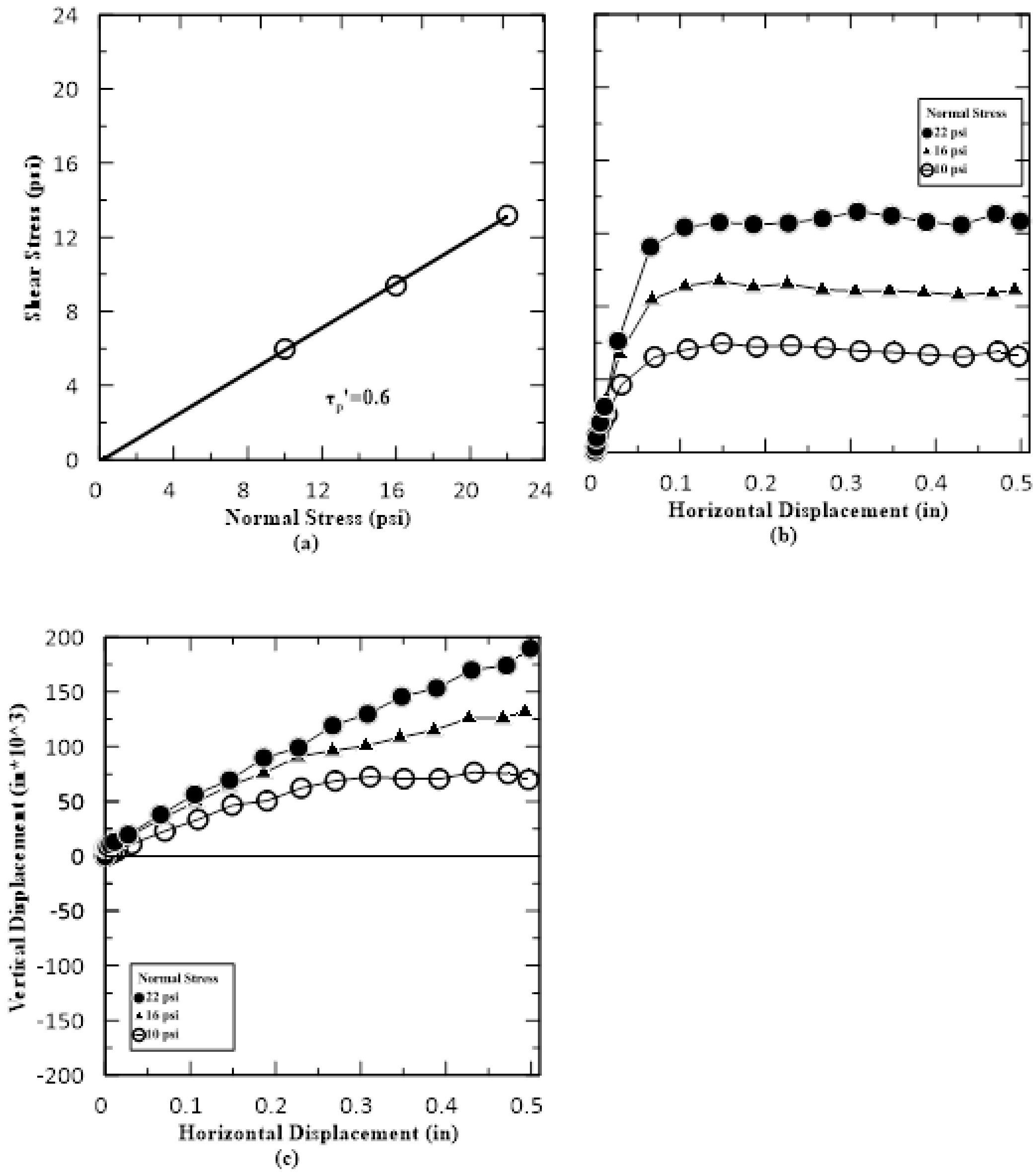

Table 23. Coefficient of soil-concrete interface friction for combined Soil 1 and Soil 3 mixtures at optimum moisture contents

Soil	Friction angle (ϕ) (degree)	Interface friction angle (δ) (degree)	Coefficient of interface friction $\tan(\delta)/\tan(\phi)$
Sand with 10% fine	38.3°	31.6°	0.77
Sand with 50% fine	34°	24.2°	0.66
Sand with 70% fine	29°	20°	0.65

The results of the large direct shear tests for combined Soil 1 and Soil 4 mixtures prepared at 10%, 50%, and 70% fines content are summarized in Table 24. The results showed that the interface friction angle (δ) decreased when increasing the fines content as well as when increasing the water content. Figure 21 presents the results of the large direct shear tests obtained for combined Soil 1 and Soil 4 mixtures prepared using 10% fines and omc. The results of the rest of the large direct shear tests prepared at different fines contents of 10%, 50%, and 70%, and different moisture contents (omc to omc+6%) are presented in Appendix B. The δ obtained at optimum moisture content and maximum dry unit weight decreased from 31.6° to 22.2° when the fines content increased from 10% to 70%.

Table 24. Results of large interface direct shear tests for combined Soil 1 and Soil 4 mixtures

Soil	Dry unit weight, γ_d (pcf)	Water content (%)	Relative density (%)	Interface friction angle (δ) (Degree)	Adhesion (psi)
Sand with 10% fine (Fine sand%=5.1) (Clay%=2.3) (Silt%= 7.7)	103.2	9.2	81.3	31.6°	-
	100.7	11.2	69.1	30.2°	-
	99.7	13.2	57.9	29.8°	-
Sand with 50% fine (Fine sand%=16.2) (Clay%=11.5) (Silt%= 38.5)	107.4	12.1	80.1	27.3°	1
	104	14.2	61	26.18°	0.5
	99.8	16.3	53.7	25.8°	-
Sand with 70% fine (Fine sand%=19.2) (Clay%=16.1) (Silt%= 53.9)	110.7	14.2	71.5	22.2°	1.3
	108.4	16.2	62.2	21.8°	1
	105	18.4	42.7	20.13°	0.3

Figure 21. Results of large direct shear tests for combined Soil 1 and Soil 4 mixtures at FC =10%, Dr =81.3%, Wc = 9.2%: (a) interface shear stress vs normal stress; (b) interface shear stress vs horizontal displacement; (c) vertical displacement vs horizontal displacement

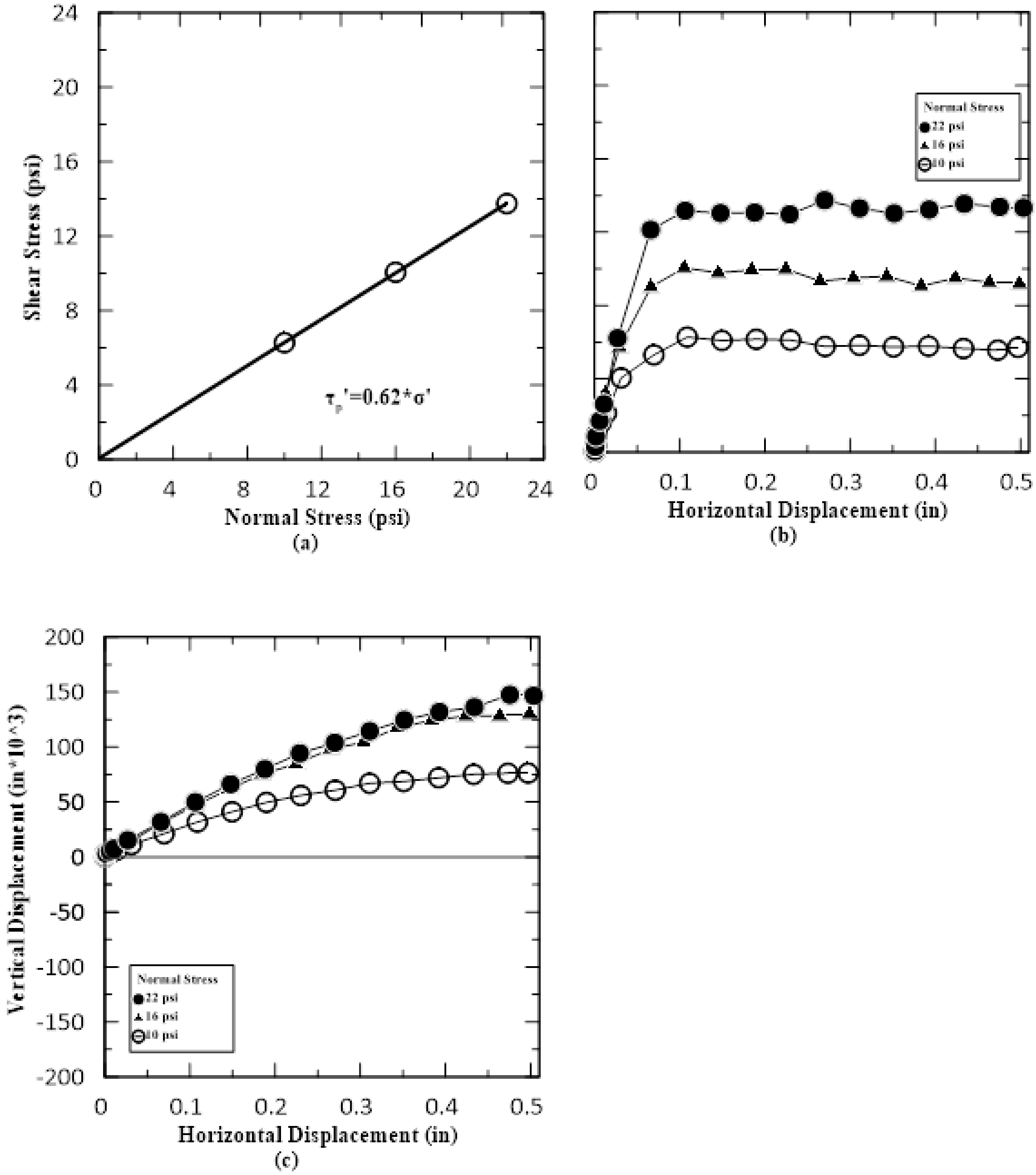

The coefficients of interface friction [tan(δ)/tan (ϕ)] between the soil and concrete surface for combined Soil 1 and Soil 4 mixtures were calculated, and the values for samples prepared at optimum moisture contents are presented in Table 25. The results show that the coefficient of interface friction values range from 0.66 for 70% fines content to 0.70 for 10% fines content (average =0.68), which is not significant.

Table 25. Coefficient of soil-concrete interface friction for combined Soil 1 and Soil 4 mixtures at optimum moisture contents

Soil	Friction angle (ϕ) (degree)	Interface friction angle (δ) (degree)	Coefficient of interface friction tan(δ)/tan(ϕ)
Sand with 10% fine	41.4°	31.6°	0.70
Sand with 50% fine	34.6°	27.3°	0.67
Sand with 70% fine	27.7°	22.2°	0.66

The results of the large direct shear tests for combined Soil 1 and Soil 5 mixtures prepared at different fines contents (10%, 50%, and 70%) and different moisture contents (omc to omc+6%) are summarized in Table 26, and those of the large direct shear tests for combined Soil 1 and Soil 5 mixtures prepared using 10% fines and omc are presented in Figure 22. The results of the rest of the large direct shear tests for combined Soil 1 and Soil 5 prepared at different fines contents and different moisture contents are presented in Appendix B. The results showed that the interface friction angle (δ) for combined Soil 1 and Soil 5 mixtures prepared at omc decreased from 30.5° for a 10% fines content mixture to 18.5° for a 70% fines content mixture.

Table 26. Results of large interface direct shear tests for combined Soil 1 and Soil 5 mixtures

Soil	Dry unit weight, γ_d (pcf)	Water content (%)	Relative density (%)	Interface friction angle (δ) (Degree)	Cohesion (psi)
Sand with 10% fine (Fine sand%=7.2) (Clay%=2.1) (Silt%= 7.9)	113.2	10	81.3	30.5°	-
	110.7	12	69.1	30.2°	-
	109.7	15.2	57.9	29.4°	-
Sand with 50% fine (Fine sand%=18.2) (Clay%=10.5) (Silt%= 39.5)	117.4	11	80.1	25.4°	1.1
	114	14.2	61	24.1°	0.57
	109.8	18.3	53.7	24°	-
Sand with 70% fine (Fine sand%=20.2) (Clay%=14.7) (Silt%= 55.3)	110.7	16.2	71.5	18.5°	1.32
	108.4	18.2	62.2	18°	0.8
	105	20.3	42.7	17.7°	0.6

Figure 22. Results of large direct shear tests for combined Soil 1 and Soil 5 mixtures at FC =10%, Dr =81.3%, Wc = 10%: (a) interface shear stress vs normal stress; (b) interface shear stress vs horizontal displacement; (c) vertical displacement vs horizontal displacement

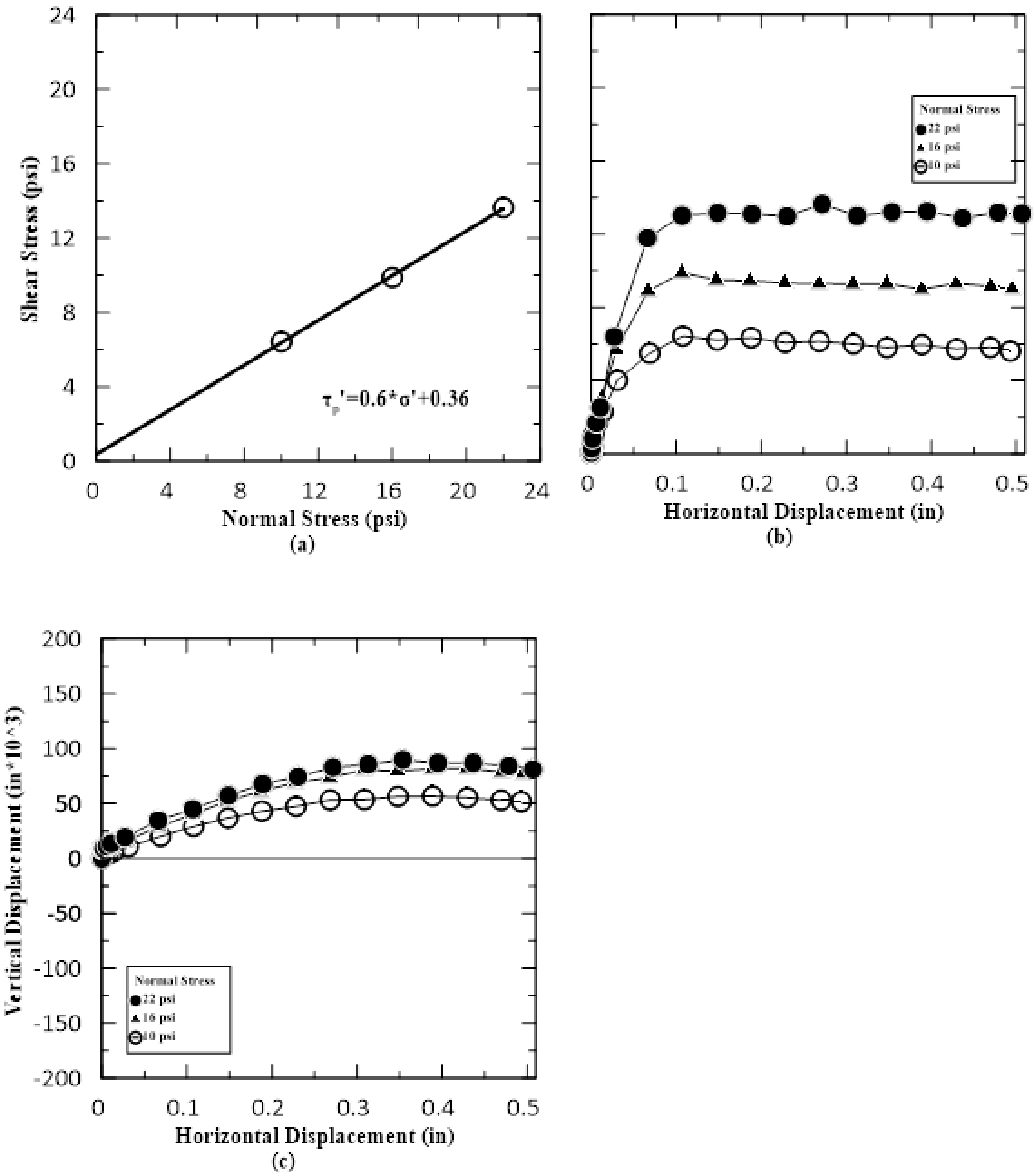

The calculated coefficient of interface friction [tan(δ)/tan (ϕ)] between the soil and concrete surface for combined Soil 1 and Soil 5 mixtures for samples prepared at optimum moisture contents are presented in Table 27. These results show that the values range from 0.66 for 70% fines content to 0.70 for 10% fines content (average = 0.68).

Table 27. Coefficient of soil-concrete interface friction for combined Soil 1 and Soil 5 mixtures at optimum moisture contents

Soil	Friction angle (ϕ) (degree)	Interface friction angle (δ) (degree)	Coefficient of interface friction tan(δ)/tan(ϕ)
Sand with 10% fine	40°	30.°	0.70
Sand with 50% fine	35.3°	25.4°	0.67
Sand with 70% fine	27°	18.5°	0.66

SPT Correlations

Most available correlations between the strength of the soil and the results of in-situ tests, such as standard penetration tests (SPT) and cone penetration tests (CPT), have been developed for either sand soils or clay soils, and these correlations have not been found to be useful for soils having low-plasticity silts. The Schmertmann charts and correlations adopted by the Federal Highway Administration (FHWA) are the most common methods used to evaluate the internal friction angle (ϕ) of soils from SPT tests. Unfortunately, these charts are only applicable to clean sand soils with low fines content (< 5%). This study focused on updating these charts and correlations to include sand mixed with fines content (silt and clay), with an emphasis on silt content.

Geotechnical correlations such as SPT charts are usually developed from the results of both laboratory and in-situ testing. In this study, a laboratory database was developed based on direct shear tests that were performed to measure the internal friction angle (ϕ) for sand soil mixtures prepared at different fines contents (with silt contents) and different water contents. Since the in-situ SPT testing data were not available, the semi-empirical approach is adopted in this study to estimate the SPT values. The values of the relative density (D_r) parameter for different soil mixtures evaluated from laboratory tests were used as the mediator connection between the values of SPT(N_{60}) data and the ϕ'. The direct shear tests, and corresponding ϕ values, were performed at different relative densities (D_r) and hence at different correlated SPT(N_{60}) values. The values of relative density were used in this study to calculate the corresponding SPT(N_{60}) values for the different soil mixtures at different normal stresses using the Gibbs and Holtz [95] chart, as presented in Figure 23.

Figure 23. Gibbs and Holtz correlation between relative density and SPT(N_{60}) at different vertical stresses [95]

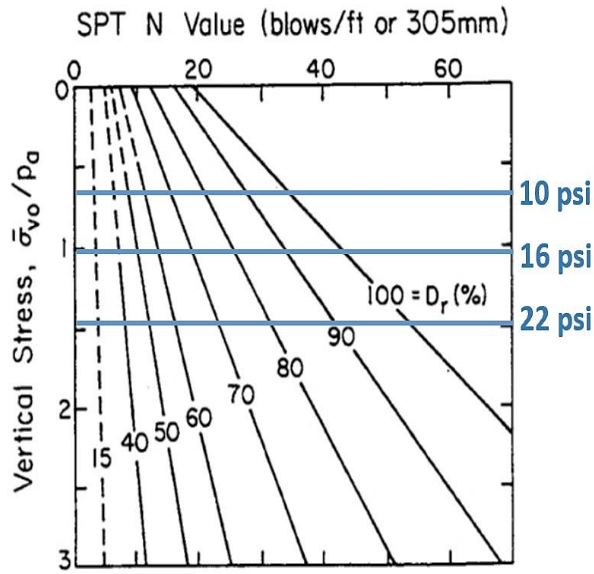

The SPT(N_{60}) values for the different soil mixtures were obtained at three normal stresses (10 psi, 16 psi and 22 psi), as shown in Figure 23. The values were selected to represent the conditions of the direct shear tests. Only the soil mixtures prepared by combining Soil 1 with either Soil 3, Soil 4, or Soil 5 at different fines contents (with high silt content) and different water contents were included for SPT correlations. The combined Soil 1 and Soil 2 mixtures (with clay content) were not used because they did not show problematic behavior when increasing the fines contents (mostly clay content).

The values of SPT(N_{60}) obtained for the different direct shear tests for the combined Soil 1 and Soil 3 mixtures prepared at different fines contents, different relative densities, and different normal stresses are summarized in Table 28. The SPT(N_{60}) correlated values for the combined Soil 1 and Soil 4 mixtures and combined Soil 1 and Soil 5 mixtures are summarized in Table 29 and Table 30, respectively.

Table 28. SPT N_{60} values for combined Soil 1 and Soil 3 mixtures

Soil	Relative density, D_r	Internal friction angle, ϕ	SPT N_{60}	SPT N_{60}	SPT N_{60}
			10 psi	16 psi	22 psi
Sand with 10% fine Fine sand%= 4.1 Sand Clay%= 1.96 Silt%= 8	43.4	34.6	8	9.5	11
	51.4	35.7	9	11	14.5
	65.5	38.6	14	17.25	20.5
	74.1	41.2	18.4	21.8	28.6
Sand with 30% fine Fine sand%= 9.0 Clay%= 5.9 Silt%= 24.1	39.1	32.0	6.3	7.2	8.13
	57.0	33.7	10.9	13.3	15.7
	73.1	36.1	18	20.5	27.6
	82.1	38.0	23	28.5	34.6
Sand with 50% fine Fine sand%= 14.2 Clay%= 9.9 Silt%= 40.1	42.3	29.8	7	7.8	9
	55.5	31.3	10	12.9	14.6
	73.1	32.6	18.4	22	26.7
	88.7	34.0	28.1	35.5	38.6
Sand with 70% fine Fine sand%=15.2 Clay%=14 Silt%= 57	43.3	22.6	7.3	8.5	9.7
	61.5	24.2	12.5	15.4	18.2
	76.6	26.5	19.5	24.2	28.8
	91.8	29.0	37	44	49

Table 29. SPT N_{60} values for combined Soil 1 and Soil 4 mixtures

Soil	Relative density, D_r	Internal friction angle, ϕ	SPT N_{60}	SPT N_{60}	SPT N_{60}
			10 psi	16 psi	22 psi
Sand with 10% fine (Fine Sand%=5.1) (Clay%=2.3) (Silt%= 7.7)	49.3	37.4	9.8	10.5	12.1
	62.9	38.9	16.4	17.4	20.5
	76.5	40.3	23.6	27.8	33.4
	87.3	41.4	29.0	36.2	42.2
Sand with 20% fine (Fine Sand%=5.1) (Clay%=2.3) (Silt%= 7.7)	50.6	35.5	11.0	12.5	13.6
	63.3	37.4	16.9	19.8	20.4
	75.4	38.5	23.8	28.1	31.3
	86.9	39.5	28.1	36.5	41.8
Sand with 30% fine (Fine Sand%=11.1) (Clay%=6.6) (Silt%= 23.1)	51.7	34	11.9	14.2	16.33
	64.2	36.5	17.3	20.9	21.2
	74.6	35.5	24.5	28.3	33.2
	86.5	38	26.5	37.4	42
Sand with 40% fine (Fine Sand%=11.1) (Clay%=6.6) (Silt%= 23.1)	52.4	31.8	12.6	15.6	16.8
	63.8	33.6	18.2	22.1	22.7
	76.1	34.7	25.2	29.5	34.0
	87.6	36.1	28.8	38.8	42.7
Sand with 50% fine (Fine Sand%=16.2) (Clay%=11.5) (Silt%= 38.5)	53.2	29.8	12.7	15.1	17.3
	63.9	31.6	18	22.3	23.4
	78.3	33	25.1	29.6	35.2
	88.3	34.6	28.0	38.3	43.1
Sand with 60% fine (Fine Sand%=18.2) (Clay%=10.5)	54.1	26.0	13.1	15.4	17.4
	65.2	27.7	18.2	23.6	24.0
	79.3	29.2	25.5	32.2	35.7
	89.1	30.5	29.5	38.7	44.3
Sand with 70% fine (Fine Sand%=19.2) (Clay%=16.1) (Silt%= 53.9)	54.4	21.8	13.3	16	17.8
	66.7	24.2	18.44	24.2	24.3
	80.0	25.7	26	30.2	35.9
	90.5	27.7	31.1	39.1	45.5

Table 30. SPT N_{60} values for combined Soil 1 and Soil 5 mixtures

Soil	Relative density, D_r	Internal friction angle, ϕ	SPT N_{60} 10 psi	SPT N_{60} 16 psi	SPT N_{60} 22 psi
Sand with 10% fine (Fine Sand%=7.2) (Clay%=2.1) (Silt%= 7.9)	44.7	35.3	8.4	10.2	11.8
	60.4	36.8	13.2	16.7	20
	71.9	37.7	22.1	25.4	28.9
	81.6	40.0	29.7	30.6	35.4
Sand with 20% fine (Fine Sand%=18.2) (Clay%=10.5)	47.0	34.7	9.1	11.4	13.5
	61.2	35.8	14.2	18.1	20.6
	73.0	37.7	21.7	24.5	29.2
	83.9	39.6	25.1	32.5	37.6
Sand with 30% fine (Fine Sand%=13.1) (Clay%=6.3) (Silt%= 23.7)	50.7	33.3	10.5	12.9	14.8
	63.0	35.0	16	20.2	21.3
	76.2	37.4	22.3	25.3	30.1
	86.7	38.9	33.2	35.5	39.3
Sand with 40% fine (Fine Sand%=18.2) (Clay%=10.5)	52.4	32.4	10.9	13.5	16.2
	63.4	33.3	14.8	19.2	21.8
	77.3	35.0	22.1	26.7	31.6
	87.3	37.4	26.3	35.0	40.8
Sand with 50% fine (Fine Sand%=18.2) (Clay%=10.5) (Silt%= 39.5)	53.4	31.0	12	14.4	16.7
	64.2	31.3	14.9	19.2	22
	76.6	33.7	24	28.5	31.9
	88.4	35.3	26.8	35.3	43
Sand with 60% fine (Fine Sand%=18.2) (Clay%=10.5)	53.6	26.5	11.5	14.8	17.2
	66.5	28.3	15.8	20.5	23.4
	76.5	30.7	23.1	27.1	33.3
	90.2	33.4	28.2	36.1	44.0
Sand with 70% fine (Fine Sand%=20.2) (Clay%=14.7) (Silt%= 55.3)	53.7	21.8	12.4	15.6	17
	65.2	24.7	18.1	23.7	23.7
	77.4	27.3	25.7	26.6	35
	90.9	30.9	30	38.6	44.7

The values of SPT(N_{60}) obtained for the different soil mixtures in Table 28, Table 29, and Table 30 were plotted in the SPT-ϕ Schmertmann chart presented in Figure 24. The values of SPT(N_{60}) versus the ϕ for the different soil mixtures of different fines contents were used to modify the Schmertmann chart to incorporate the effect of fines contents. This modification is done on soil mixtures with fines contents dominated by silt particles only due to the significant drop observed in the ϕ with increasing silt content. Figure 25 presents the modified charts for Soil 1 and Soil 3 mixtures prepared at different fines contents of 10%, 30%, 50%, and 70%. The figure shows that the internal friction angle (ϕ) corresponding to the SPT values for the different soil mixtures are lower than the values obtained from the original chart; thus, the Schmertmann chart lines are shifted to the right to capture the effects of fines content (mainly silt content) on SPT-ϕ correlations. The modified SPT-ϕ charts for the combined Soil 1 and Soil 4 mixtures are presented in Figure 26 and Figure 27 for fines contents of 10%, 30%, 50%, and 70% and fines contents of 20%, 40%, and 60%, respectively. Finally, Figure 28 and Figure 29 present the modified SPT-ϕ charts for the combined Soil 1 and Soil 5 mixtures for different fines contents of 10%, 30%, 50%, and 70% and fines contents of 20%, 40%, and 60%, respectively.

The modified SPT-ϕ charts for the different soil mixtures for both the combined Soil 1 and Soil 4 mixtures, and the combined Soil 1 and Soil 5 mixtures, also show a shift of chart lines to the right (i.e., a decrease of the ϕ) to capture the effect of fines content on the SPT-ϕ correlations.

Figure 24. Schmertmann correlation chart between internal friction angle (ϕ) and SPT (N_{60}) at different vertical stresses

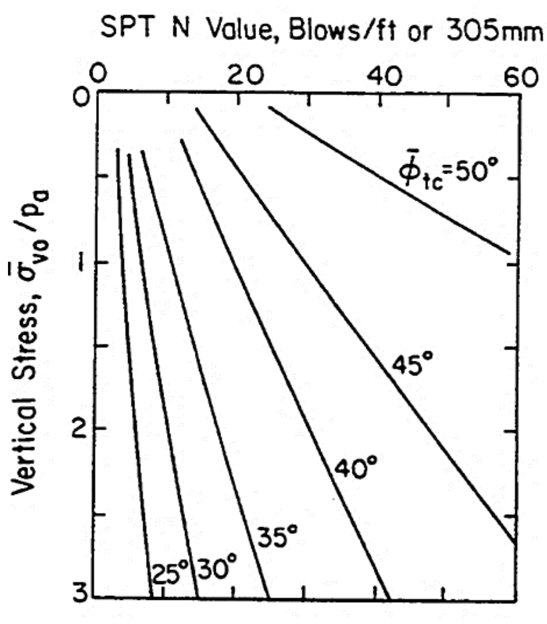

Figure 25. Modified Schmertmann charts for the combined Soil 1 and Soil 3 mixtures at different fines contents: a) 10% fines, b) 30% fines, c) 50% fines, and d) 70% fines

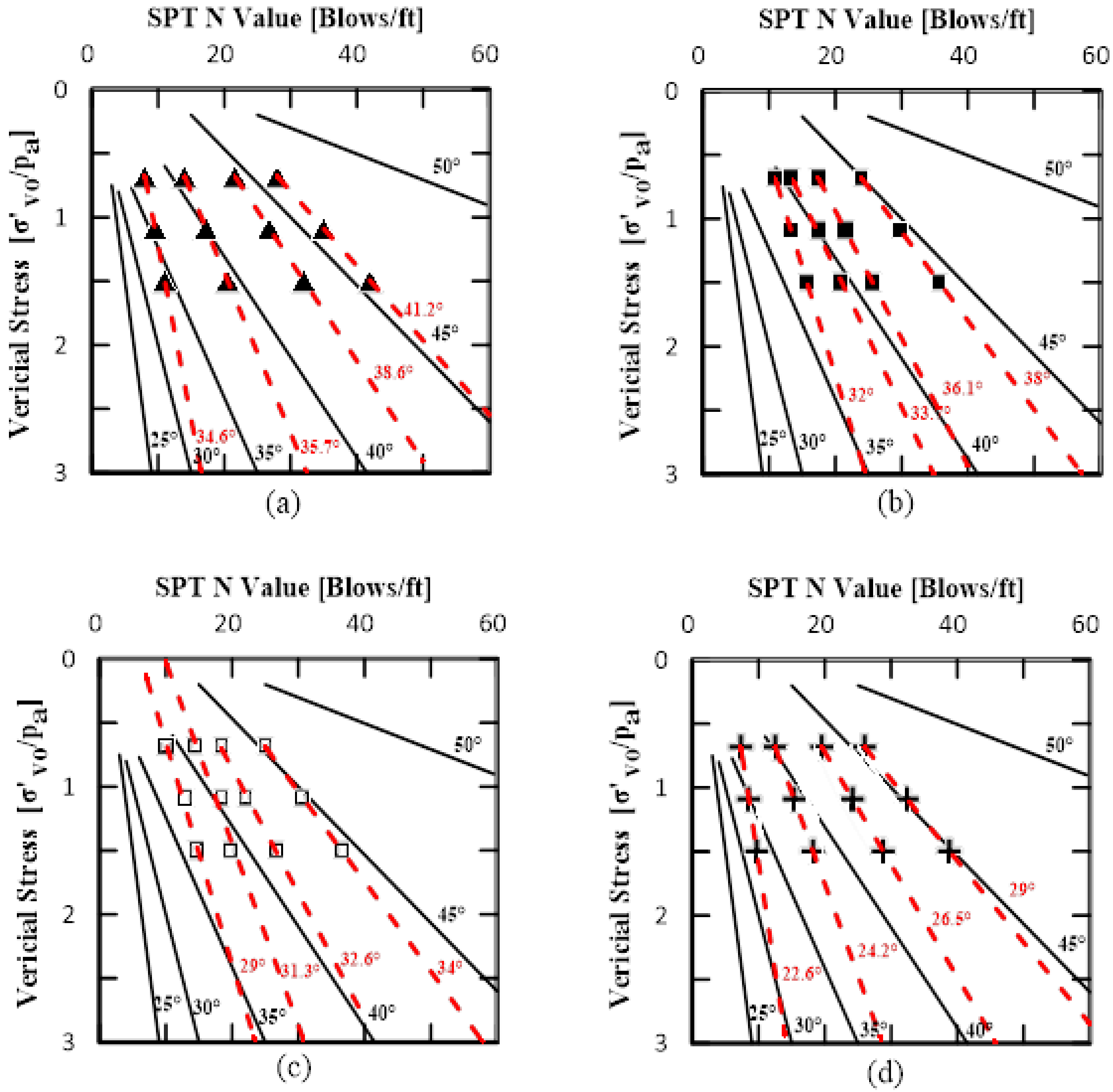

Figure 26. Modified Schmertmann charts for the combined Soil 1 and Soil 4 mixtures at different fines contents: a) 10% fines, b) 30% fines, c) 50% fines, and d) 70% fines

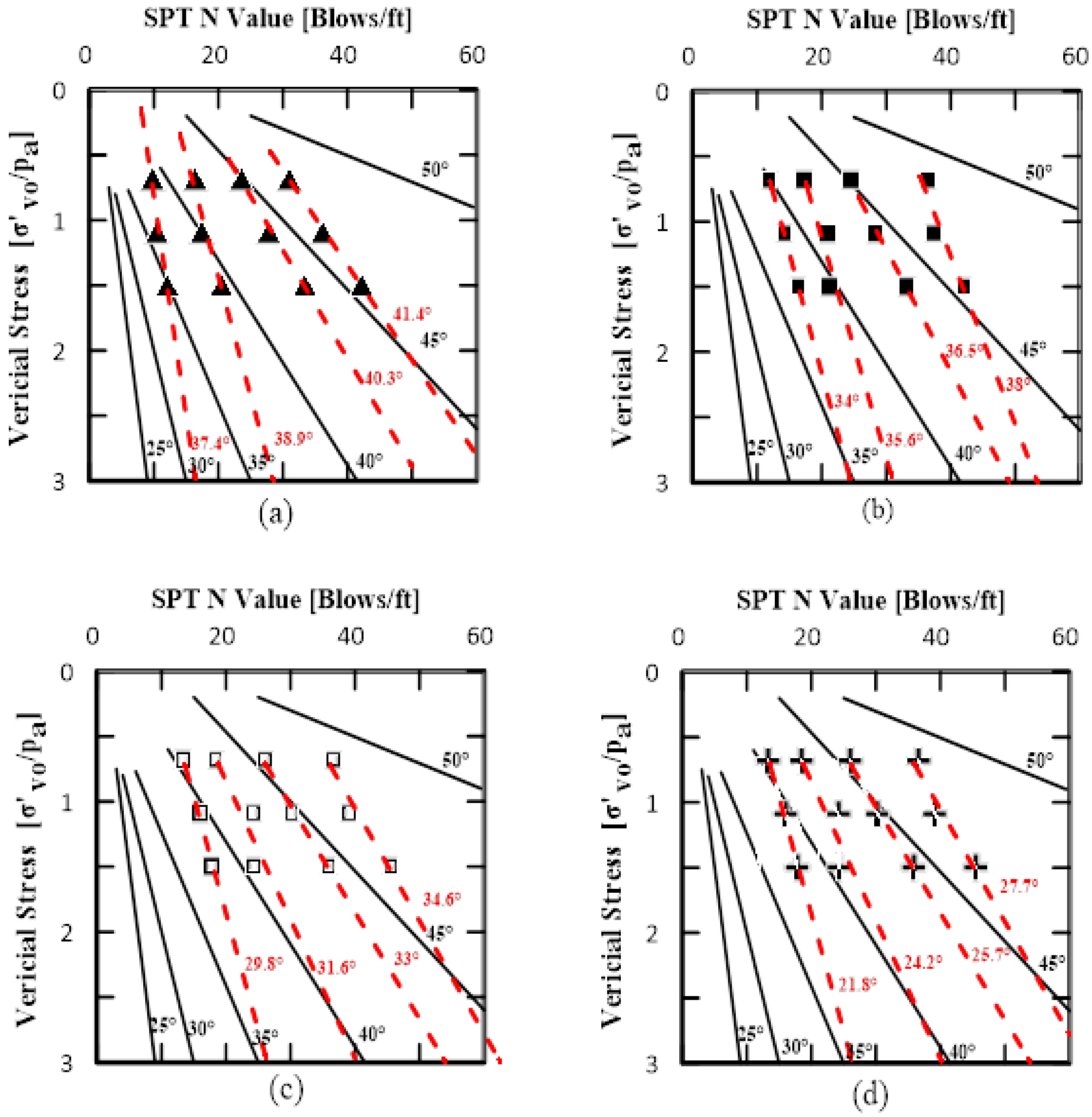

Figure 27. Modified Schmertmann charts for the combined Soil 1 and Soil 4 mixtures at different fines contents: a) 20% fines, b) 40% fines, and c) 60% fines

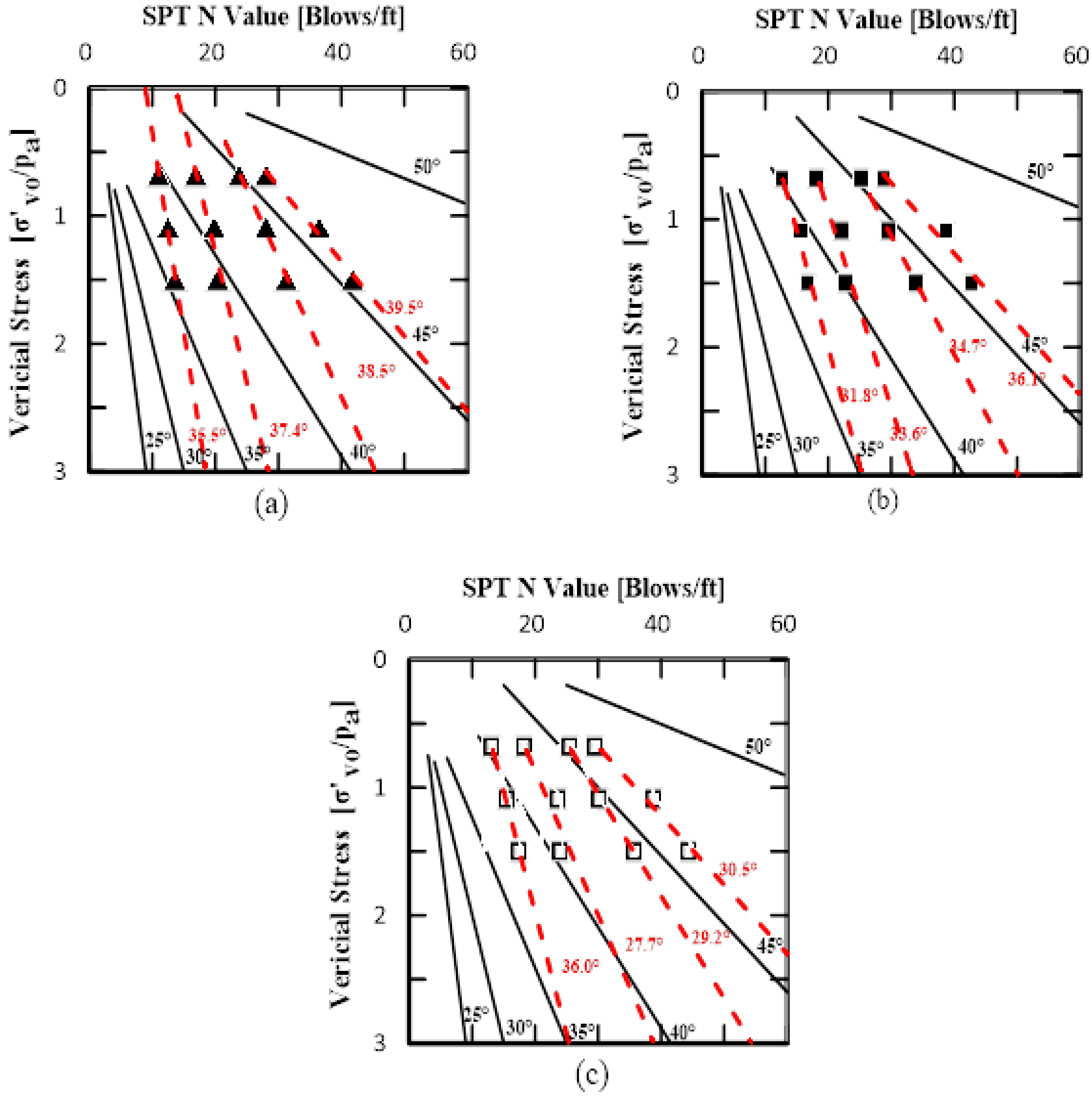

Figure 28. Modified Schmertmann charts for the combined Soil 1 and Soil 5 mixtures at different fines contents: a) 10% fines, b) 30% fines, c) 50% fines, and d) 70% fines

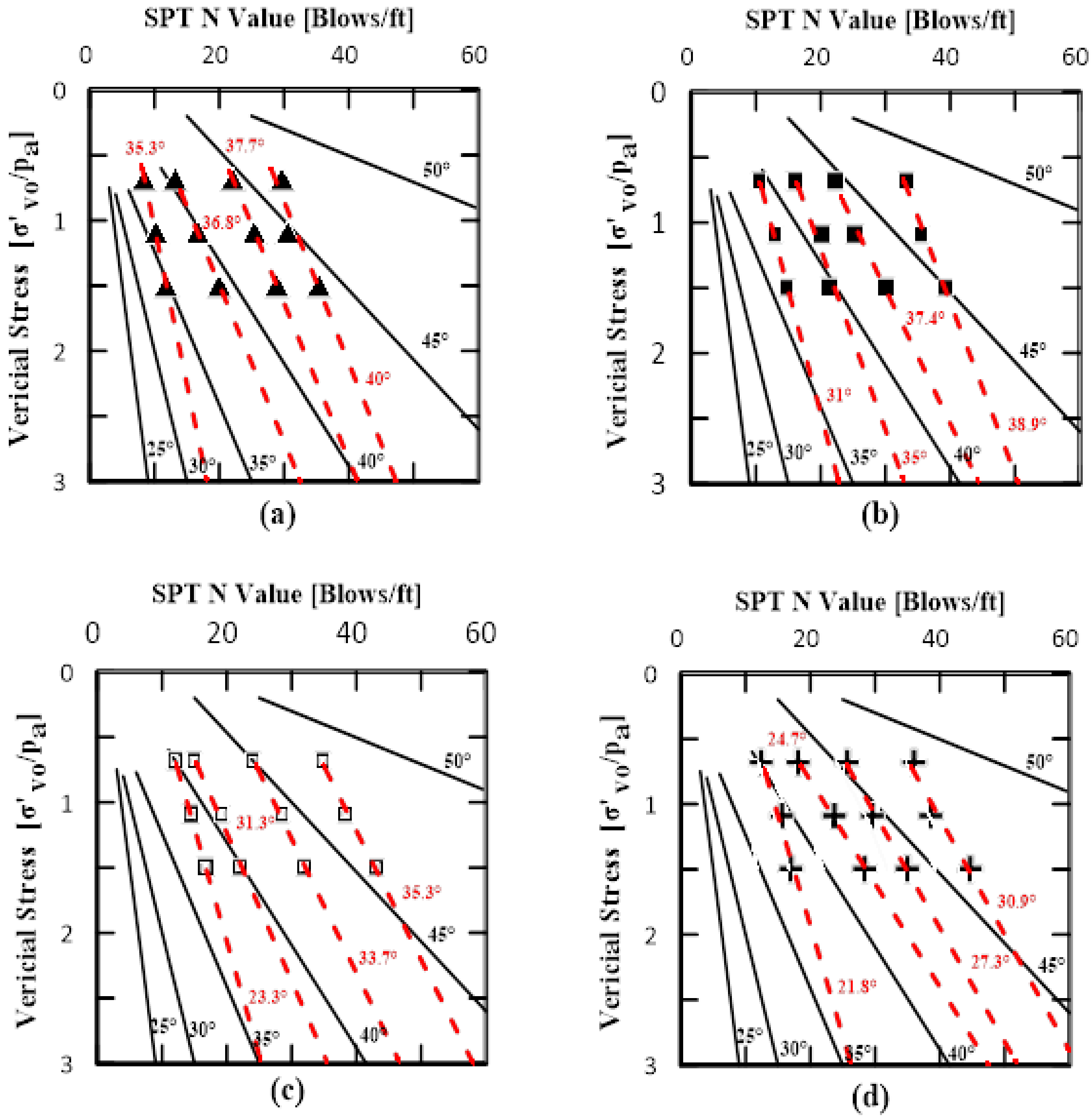

Figure 29. Modified Schmertmann charts for the combined Soil 1 and Soil 5 mixtures at different fines contents: a) 20% fines, b) 40% fines, and c) 60% fines

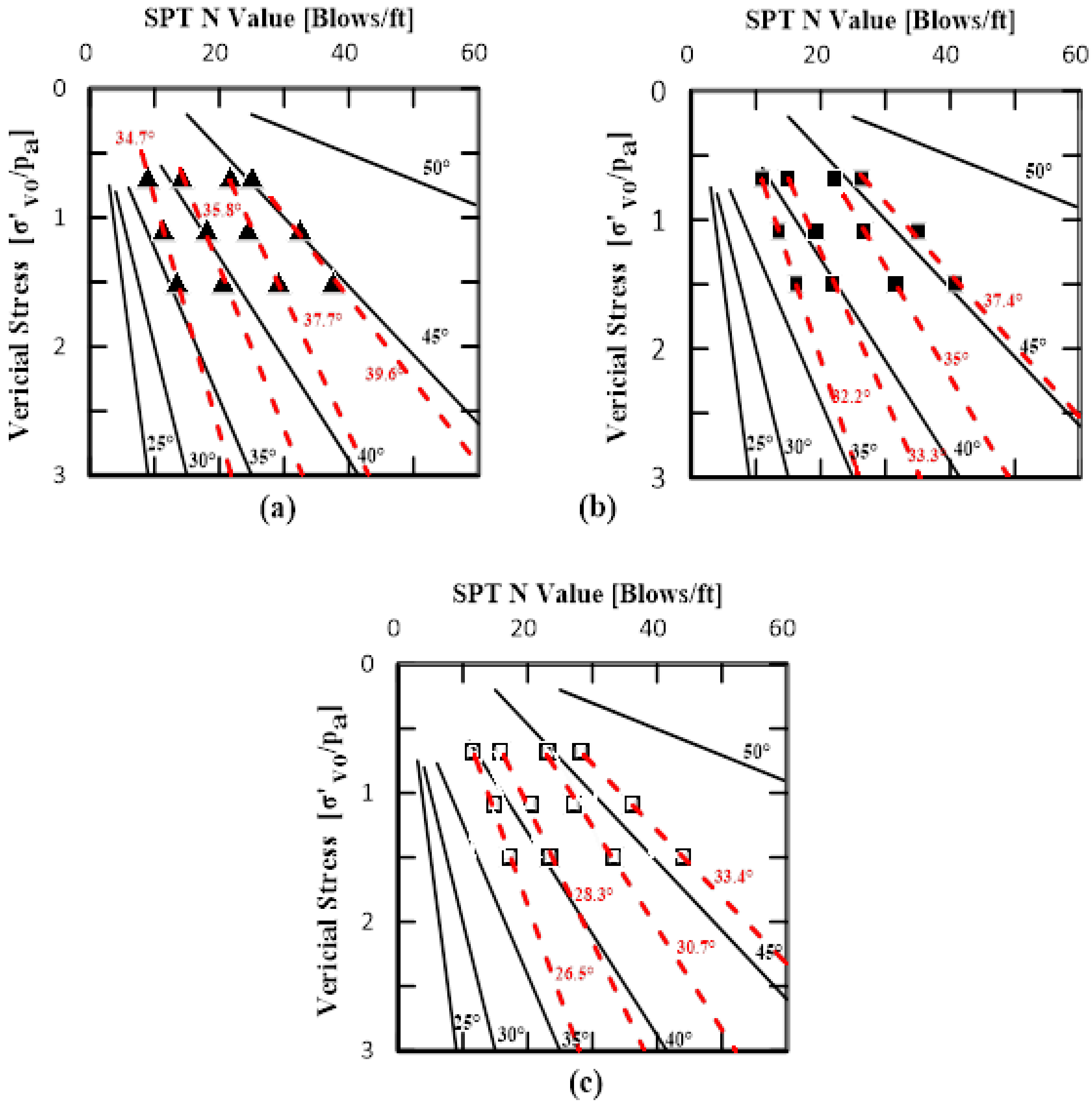

The mathematical expression of the Schmertmann chart in Figure 24 can be expressed using the following equation:

$$\phi = \tan^{-1}\left(\frac{N_{60}}{12.2 + 20.3\left(\frac{\sigma_0}{p_a}\right)}\right)^{0.34} \quad \textbf{[31]}$$

Modification of Equation 31 to account for the effects of fines content and other soil parameters was carried out through non-linear regression analysis. The experimental work was conducted at different conditions to evaluate and predict the internal friction angle (ϕ).

The input potential parameters and the structure of the modified non-linear model are shown in Figure 30.

Figure 30. Experimental input potential parameters and the structure of the modified non-linear model

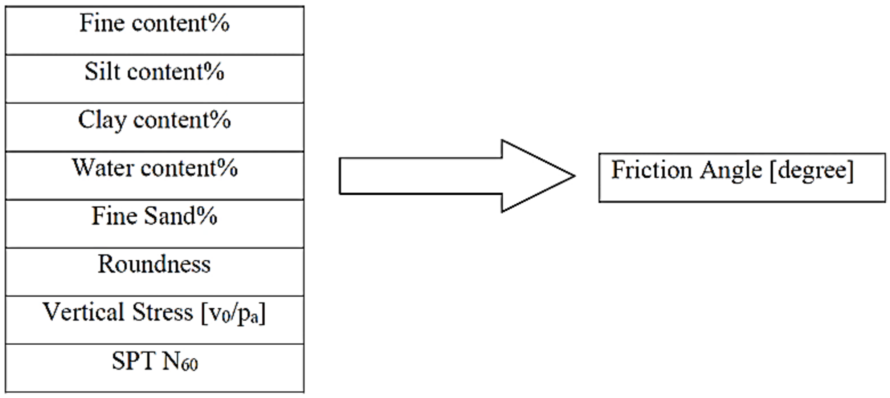

Three values of roundness parameters (R) were measured for the three different particle shapes (fines, fine sand, and medium/coarse sand) of the soil mixtures. These parameters will have different effects on the internal friction angle (ϕ) of the different sand-fines soil mixtures depending on their proportions in the tested material. Therefore, to simplify the three roundness parameters into a representative roundness parameter for the entire mixture, the weighted average roundness (R_{avg}) was introduced, which can be calculated using this equation:

$$R_{avg} = \frac{\%FC * R_{Fines} + \%Fine\ sand * R_{Fine\ sand} + \%Medium\&coarse\ sand}{100} \quad [32]$$

Where,

%FC, R_{Fines}, %Fine sand, $R_{Fine\ sand}$, %Medium&Coarse sand, $R_{m\&f\ sand}$ are the fine content, roundness of the fines, fine sand content, roundness of the fine sand, medium and coarse sand content, and roundness of the medium and coarse sand, respectively.

In statistical analysis, developing a correlation using predictor variables that express a linear relationship is a regression model; when the predictor variables in the same regression model are correlated, they cannot independently predict the value of the dependent variable. Therefore, the multi-collinearity and the significance of the input parameters must be first calculated and checked before developing any regression model. Collinearity refers to a situation when more than two explanatory variables in a multiple regression model are highly linearly related. Collinearity reduces the precision of the estimated coefficients. Bivariate correlation analysis using SPSS software was performed to measure the collinearity and the significance of the input parameters (see Table 31). The parameters used for correlation analysis include relative density, water content, dry density, average roundness (R_{avg}), fine content, clay content, silt content, fine sand content, and fine sand + silt (Si+FS) content.

Table 31. Bivariate correlation analysis using SPSS software

	Friction angle (degree)	**Silt (%)**	**Clay (%)**	**Fine Sand (%)**	**Fines (%)**	**Fine sand + silt (%)**	**Water content (%)**	**R_{avg}**
Pearson correlation	1	-0.84*	-0.34	-0.80*	-0.87*	-0.88*	-0.86*	-0.65*
Sig	<0.001	<0.001	<0.035	<0.001	<0.001	<0.001	<0.001	<0.001

'*': Significant variable

Based on an analysis of multi-collinearity and significance results, the following points can be observed:

1. The N_{60} value and the overburden pressure are essential input parameters in the Schmertmann model; therefore, they were included in bivariate correlation analysis.
2. The silt content (%) and fines content (%) are correlated to one another with a value of 0.99. To avoid collinearity, the fines content was removed from the model. The same situation is also applied for clay.
3. The silt content (%) and fine sand content (%) were added together as a single variable (Si+FS) (%) and used in the regression model.

Modified ϕ-N_{60} Schmertmann Models for Different Fines Contents

Non-linear regression analyses were first performed using the SPSS software to develop the best models to fit the N_{60}-ϕ shifted chart lines presented earlier for the sand-fine mixtures of 10%, 20%, 30%, 40%, 50%, 60%, and 70% fines. Two model coefficients (c_1 and c_2) were added to Schmertmann equation for better prediction and an optimal solution.

The model for ϕ was assumed as follows:

$$\phi = \tan^{-1}\left(\frac{c_1 + c_2 * N_{60}}{c_3 + c_4\left(\frac{\sigma_0}{p_a}\right)}\right)^{c_5} \qquad [33]$$

Where,
c_1 , c_2 , c_3 , c_4 , and c_5 are the model coefficients.

The friction angle versus SPT (ϕ-N_{60}) correlations for the different sand-fines mixtures with different fines contents are presented in Table 32.

Table 32. Correlations of ϕ-N_{60} based on fine content

Mixtures based on fine content	Correlation	R^2	RMSE
Sand with 10% Fines	$\phi = \tan^{-1}\left(\frac{46 + 6.56 * N_{60}}{46 + 6.6\left(\frac{\sigma_0}{p_a}\right)}\right)^{0.41}$	0.79	0.82
Sand with 20% Fines	$\phi = \tan^{-1}\left(\frac{22.5 + 3.41 * N_{60}}{36.4 + 8.2\left(\frac{\sigma_0}{p_a}\right)}\right)^{0.31}$	0.81	1.22
Sand with 30% Fines	$\phi = \tan^{-1}\left(\frac{0.84 + 0.1 * N_{60}}{26 + 9.2\left(\frac{\sigma_0}{p_a}\right)}\right)^{0.2}$	0.87	0.81
Sand with 40% Fines	$\phi = \tan^{-1}\left(\frac{0.46 + 1.26 * N_{60}}{26.1 + 12.4\left(\frac{\sigma_0}{p_a}\right)}\right)^{0.3}$	0.85	1.47
Sand with 50% Fines	$\phi = \tan^{-1}\left(\frac{0.364 * N_{60}}{25.8 + 15.2\left(\frac{\sigma_0}{p_a}\right)}\right)^{0.41}$	0.67	2.88

Mixtures based on fine content	**Correlation**	**R^2**	**RMSE**
Sand with 60% Fines	$\phi = \tan^{-1}(\frac{0.66 + 0.31 \ * N_{60}}{30.1 + 15.7\left(\frac{\sigma_0}{p_a}\right)})^{0.37}$	0.72	2.43
Sand with 70% Fines	$\phi = \tan^{-1}(\frac{1.2 + 0.2 * N_{60}}{33.5 + 15.9\left(\frac{\sigma_0}{p_a}\right)})^{0.33}$	0.68	2.3

By analyzing the resulting ϕ-N_{60} models in Table 32, one can recognize their limitations. Each soil with the same fines content (%) can contain different proportions of clay%, silt%, and fine sand%. Therefore, these correlations may not be realistic in estimating the friction angle of sand-fine mixtures, since they do not distinguish between the types of fines in the sand mixtures in Schmertmann's correlation. Although the ϕ-N_{60} correlations presented in Table 32 show good fit for the corresponding fines content, they cannot be used to explain the contribution of fine type.

Modified ϕ-N_{60} Schmertmann Models with Added Variables

A comprehensive non-linear regression model of Schmertmann's equation was explored by adding the effects of the different input parameters, such as roundness, silt content, fine sand content, and water content, into the equation. The relationship between the friction angle of the sand-fine mixtures and the added parameters are plotted and presented in Figure 31.

Figure 31. Relationship between friction angle and different input parameters: a) silt content; b) fine sand%; c) roundness; d) water content

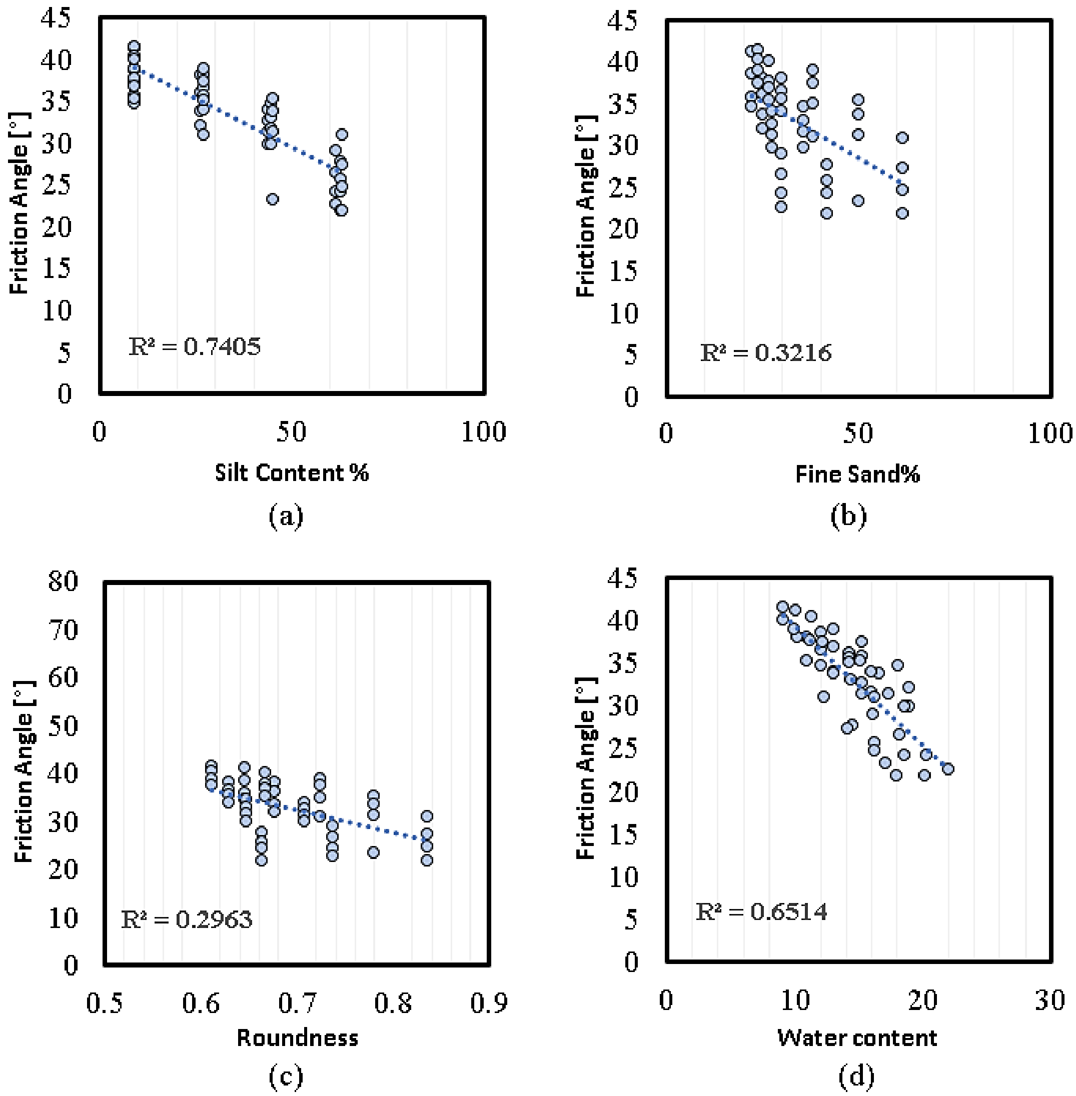

The four input parameters (i.e., roundness, silt content, fine sand content, and water content) were added to the model based on their correlations with the friction angle and the best line to fit these correlations, which was linear, as shown in Figure 31. Consequently, the general equation for the modified Schmertmann model is:

$$\phi = \tan^{-1}\left(\frac{c_1 + c_2 * N_{60}}{c_3 + c_4\left(\frac{\sigma_0}{p_a}\right)}\right)^{c_5} - c_6 * water\% - c_7 * Silt\% - c_8 * Fine\ sand\% - c_9 * Roundness \qquad [34]$$

Several non-linear regression models were generated to develop the most accurate model for estimating the friction angle (ϕ) of the sand-fines mixtures. The silt content (%) and fine sand content (%) were included in the models, either separately or together, due to the relevance of these two input parameters on the friction angle from the literature. As a result, six different regression models with different input parameters were generated, compared, and evaluated. The water content and silt content were added to all of the regression models. Fine sand was added as a single parameter or combined with the silt (Si+FS%). The models were replicated by adding the roundness parameter (R_{avg}) to measure its performance on the predicted models.

The complexity of the non-linear proposed model and the coefficients involved in the model may lead to an inaccurate solution using the local optimization rather than global optimization of dataset. A locally optimal solution (not covering all data) is one, where there is no best solution within an open neighborhood around it. Applying a local search algorithm to a model that requires a global search algorithm may deliver poor results because the local algorithm covers a limited range of possibilities. Therefore, Python platform was used in this study to provide the best possible solution for the entire input search space. This was performed through an algorithm that can run all the possible inputs for the coefficients and provide us the most accurate model with the highest R^2 and lowest RMSE.

Two category input sets were explored to develop the modified Schmertmann models of the ϕ. One set includes water content, and the other set does not. Category 1 includes all four input parameters (silt content, fine sand content, roundness, and water content); while Category 2 includes three input parameters (silt content, roundness, fine sand content). A total of six model types (Type 1 to Type 6) of different combinations of input parameters was developed for each category. Table 33 presents the input parameters used in the modified Schmertmann models for the two categories and different types.

Table 33. Input parameters used for modified Schmertmann models

	Category 1	Category 2
Model Type	**Input parameters added**	**Input parameters added**
Type 1	(W%), (Silt%), (R)	(Silt%), (R)
Type 2	(W%), (Si+FS %), (R)	(Si+FS %), (R)
Type 3	(W%),(Fine Sand%), (Silt%), (R)	(Fine Sand%), (Silt%), (R)
Type 4	(W%), (Silt%)	(Silt%)
Type 5	(W%), (Si+FS %)	(Si+FS %)
Type 6	(W%), (Silt%), (Fine Sand%)	(Silt%), (Fine Sand%)

The resulting modified Schmertmann models for the six types of Category 1 (Type 1 to Type 6) are summarized below. The values of RMSE and R^2 were calculated for the models.

$$\phi = \tan^{-1}\left(\frac{0.14 * N_{60}}{28 + 12\left(\frac{\sigma_0}{p_a}\right)}\right)^{0.1} - 0.255 * (Silt\%) - 0.16(W\%) - 0.1 * (R) \qquad \text{(Type 1) [35]}$$

RMSE=2.3, R^2= 0.86

$$\phi = \tan^{-1}(\frac{0.15 * N_{60}}{31 + 12\left(\frac{\sigma_0}{p_a}\right)})^{0.1} - 0.12 * (\mathrm{Si{+}FS})\% - 0.14(\mathrm{W}\%) - 0.09 * (\mathrm{R}) \quad \text{(Type 2) [36]}$$

RMSE=4.38, R^2= 0.88

$$\phi = \tan^{-1}(\frac{0.15 * N_{60}}{21 + 14\left(\frac{\sigma_0}{p_a}\right)})^{0.11} - 0.12 * (Si\mathrm{lt}\%) - 0.11 * (Fine\ Sand\%) - 0.14(\mathrm{W}\%) - 0.1 * (\mathrm{R}) \quad \text{(Type 3) [37]}$$

RMSE=3.4, R^2= 0.89

$$\phi = \tan^{-1}(\frac{0.14 * N_{60}}{28 + 14\left(\frac{\sigma_0}{p_a}\right)})^{0.11} - 0.256 * (Si\mathrm{lt}\%) - 0.16(\mathrm{W}\%) \quad \text{(Type 4) [38]}$$

RMSE=1.82, R^2= 0.85

$$\phi = \tan^{-1}(\frac{0.14 * N_{60}}{20 + 012\left(\frac{\sigma_0}{p_a}\right)})^{0.11} - 0.124 * (\mathrm{Si{+}FS})\% - 0.14 * (\mathrm{W}\%) \quad \text{(Type 5) [39]}$$

RMSE=2.1, R^2= 0.88

$$\phi = \tan^{-1}(\frac{0.11 * N_{60}}{31 + 15\left(\frac{\sigma_0}{p_a}\right)})^{0.1} - 0.134 * (Si\mathrm{lt}\%) - 0.08 * (Fine\ Sand\%) - 0.12(\mathrm{W}\%) \quad \text{(Type 6) [40]}$$

RMSE=2.0, R^2= 0.90

The comparison between the measured friction angles (ϕ) for the different sand-fines mixtures from direct shear tests and the predicted values for the six type models of Category 1 are presented in Figure 32. As shown in the figure, and presented in the equations, the first model (Type 1) with input parameters (Silt%, R, and W%) had an adjusted R^2 of 0.87 with an RMSE equal to 2.3. Replacing the silt content in the first model with (Si+FS)%, as shown in the Type 2 model, increased the RMSE to 4.38 (Equations 35 and 36). Between the Type 4 and Type 5 models, replacing the silt content with (Si+FS)% resulted in increasing the RMSE from 1.82 to 2.1, and reducing the R^2 from 0.88 to 0.85 (Equations 38 and 39). Among the six models, the Type 6 model with input parameters of silt content (Silt%), fine sand content (Fine sand%), and moisture content (W%) gave the lowest RMSE of 2.0 with R^2= 0.89.

The resulting modified Schmertmann models for the six types (Type 1 to Type 6) of Category 2 are summarized below. The values of RMSE and R^2 were calculated for each model.

$$\phi = \tan^{-1}\left(\frac{0.15 * N_{60}}{32 + 19.7\left(\frac{\sigma_0}{p_a}\right)}\right)^{0.11} - 0.254 * (Silt\%) - 0.1 * (\mathrm{R}) \qquad \text{(Type 1) [41]}$$

RMSE=1.7, R^2= 0.84

$$\phi = \tan^{-1}\left(\frac{0.15 * N_{60}}{16.3 + 9.8\left(\frac{\sigma_0}{p_a}\right)}\right)^{0.12} - 0.147 * (\mathrm{Si+FS})\% - 0.1 * (\mathrm{R}) \qquad \text{(Type 2) [42]}$$

RMSE=1.9, R^2= 0.89

$$\phi = \tan^{-1}\left(\frac{0.1 * N_{60}}{11.6 + 6.9\left(\frac{\sigma_0}{p_a}\right)}\right)^{0.12} - 0.19 * (Si\mathrm{lt}\%) - 0.11 * (Fine\ Sand\%) - 0.1 * (\mathrm{R}) \qquad \text{(Type 3) [43]}$$

RMSE=1.9, R^2= 0.90

$$\phi = \tan^{-1}\left(\frac{0.1 * N_{60}}{14.2 + 29.5\left(\frac{\sigma_0}{p_a}\right)}\right)^{0.1} - 0.257 * (Si\mathrm{lt}\%) \qquad \text{(Type 4) [44]}$$

RMSE=1.83, R^2= 0.85

$$\phi = \tan^{-1}\left(\frac{0.16 * N_{60}}{17.3 + 10\left(\frac{\sigma_0}{p_a}\right)}\right)^{0.12} - 0.138 * (\mathrm{Si+FS})\% \qquad \text{(Type 5) [45]}$$

RMSE=1.99, R^2= 0.89

$$\phi = \tan^{-1}\left(\frac{0.15 * N_{60}}{18.6 + 14.8\left(\frac{\sigma_0}{p_a}\right)}\right)^{0.115} - 0.2 * (Si\mathrm{lt}\%) - 0.1 * (Fine\ Sand\%) \qquad \text{(Type 6) [46]}$$

RMSE=1.7, R^2= 0.9

Figure 32. Measured ϕ from direct shear vs predicted ϕ from modified Schmertmann equations for Category 1: a) Type 1; b) Type 2; c) Type 3; d) Type 4; e) Type 5; f) Type 6

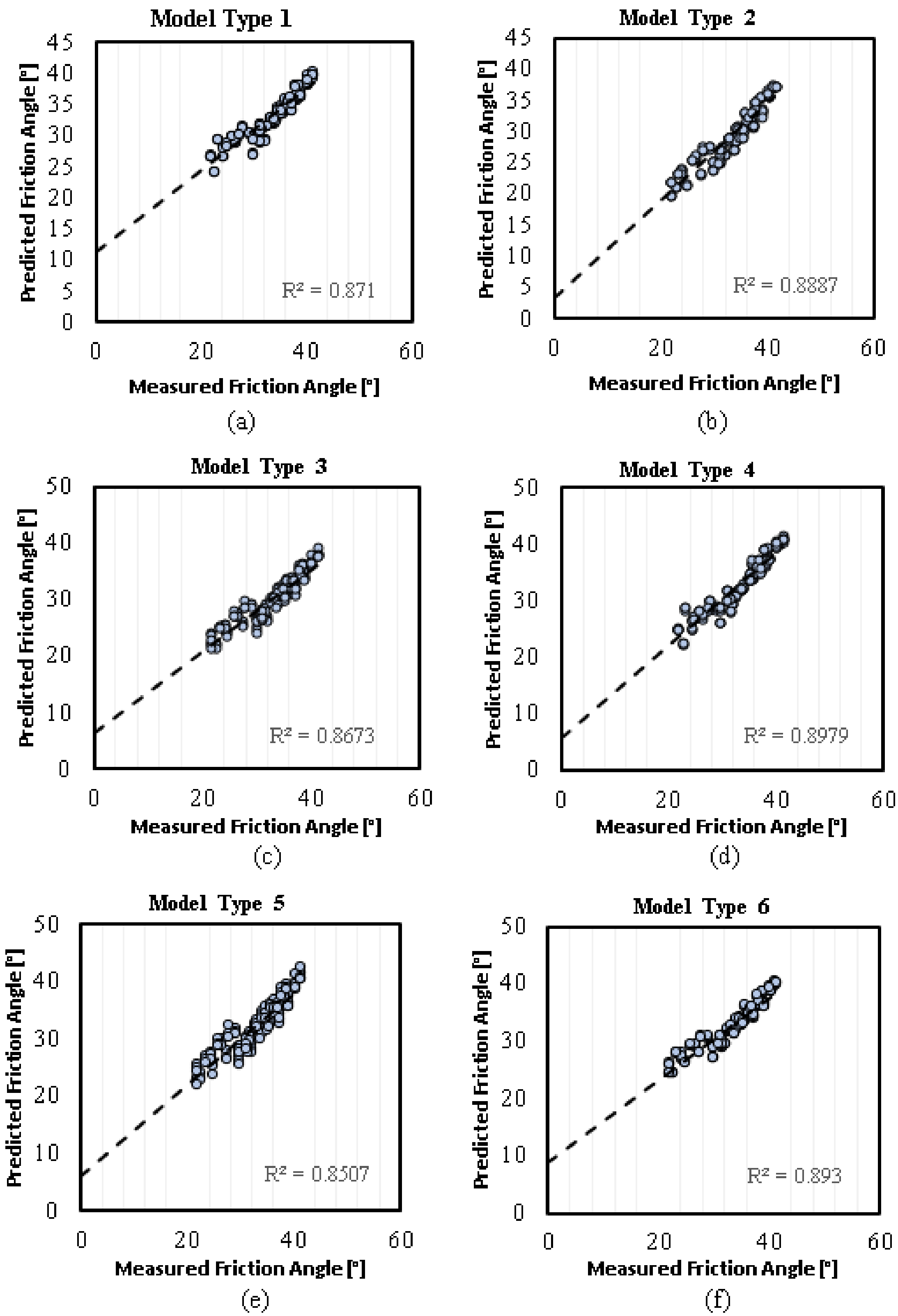

Figure 33 depicts the comparison between the measured friction angles (ϕ) for the different sand-fines mixtures obtained from the direct shear tests and the predicted ϕ values using the six type models of modified Schmertmann Category 2. Comparing the Type 1 model with input parameters (Silt% and R) with the Type 2 model with input parameters [(Si+FS)% and R] resulted in a slight increase of RMSE from 1.7 to 1.9 and an increase of R^2 from 0.86 to 0.89 (Equations 41 and 42). Separating the silt and fine sand contents in the Type 3 model (Equation 43) resulted in RMSE = 1.9 and R^2 = 0.89. Comparing the Type 4 and Type 5 models (Equations 44 and 45), replacing the silt content with (Si+FS)% resulted in increasing the RMSE from 1.83 to 1.99 and reducing the R^2 from 0.88 to 0.86. When separating the silt and fine sand contents and removing the roundness (R) in the Type 6 model (Equation 46), the RMSE reduced to 1.7, and R^2 improved to 0.90. Consequently, using the silt content, fine sand content, and water content in the modified Schmertmann Category 2 models would provide the most accurate ϕ prediction model.

Figure 33. Measured ϕ from direct shear vs predicted ϕ from modified Schmertmann equations for Category 2: a) Type 1; b) Type 2; c) Type 3; d) Type 4; e) Type 5; f) Type 6

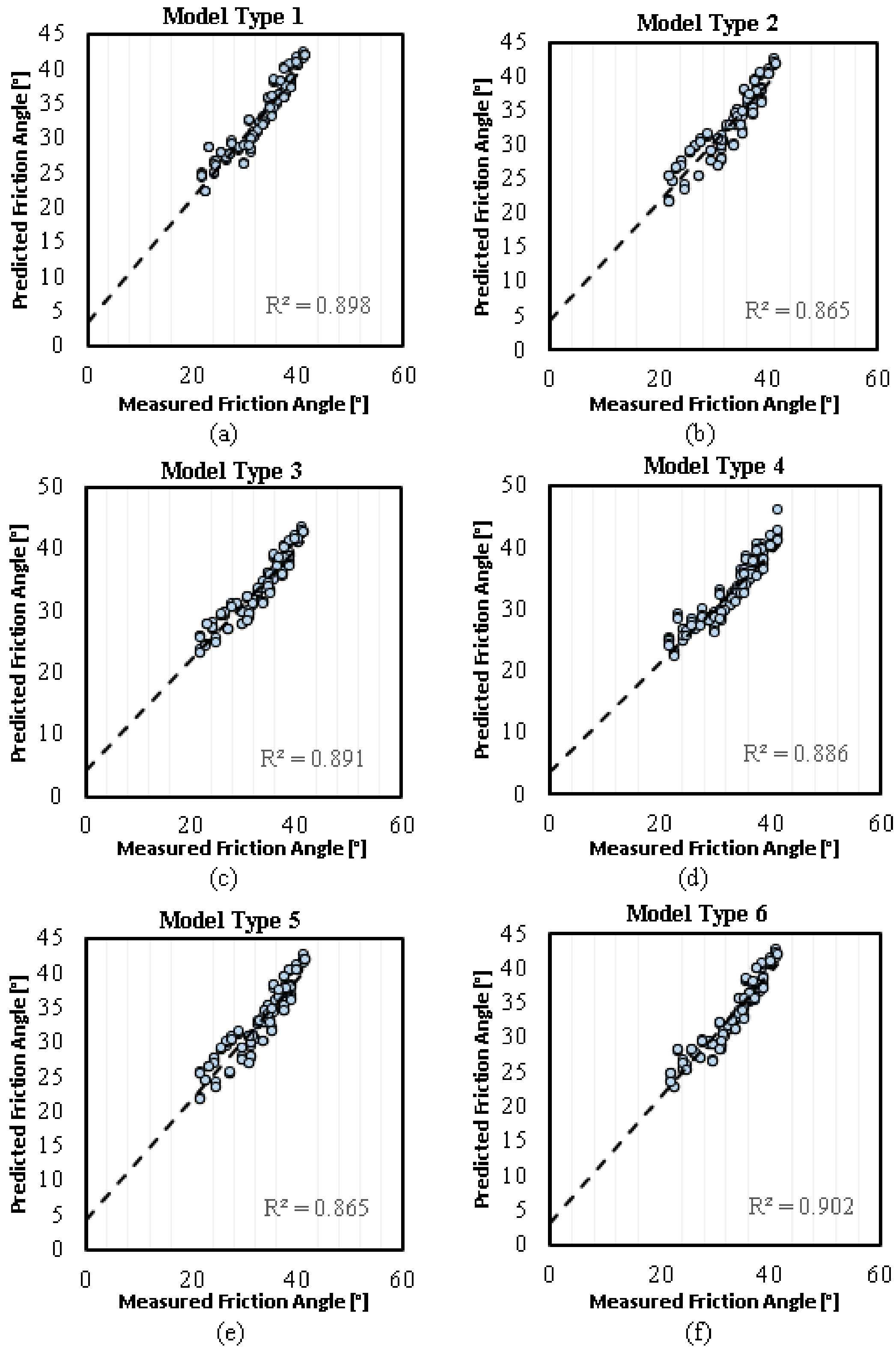

These results reveal that separating the two input parameters of silt content and fine sand content results in a better prediction model of the ϕ for sand-fines mixtures than combining the two parameters together. This may be due to the differing influence between the fine sand and silt in decreasing the friction angle.

Modified ϕ-$(N_1)_{60}$ Japan Road Association Models with Added Variables

The ϕ-$(N_1)_{60}$equation of the Japan Road Association [7] was modified to include the effect of fine contents by adding the same parameters used in the modified Schmertmann models as shown in Table 34 (Category 3 and Category 4). The general proposed model for modified Japan Road Association is:

$$\phi = (c1 * (N_1)_{60})^{0.5} - c2 * \mathrm{W\%} - c3 * \mathrm{Silt\%} - c4 * \mathrm{Fine\ Sand\%} - c5 * \mathrm{R} + \mathrm{c6} \quad [47]$$

$(N_1)_{60}$

Table 34. Input parameters used for modified Japan Road Association models

	Category 3	Category 4
Model Type	**Parameters Added**	**Parameters Added**
Type 1	(W%), (Silt%), (R)	(Silt%), (R)
Type 2	(W%), (Si+FS %), (R)	(Si+FS %), (R)
Type 3	(W%),(Fine Sand%), (Silt%), (R)	(Fine Sand%), (Silt%), (R)
Type 4	(W%), (Silt%)	(Silt%)
Type 5	(W%), (Si+FS %)	(Si+FS %)
Type 6	(W%), (Silt%), (Fine Sand%)	(Silt%), (Fine Sand%)

The Japan Road Association's model is less complex than the Schmertmann model; therefore, the model was generated through local optimal solution. Each solver with local optimal solution in fitting a model requires initial values for the coefficients in the model. The initial assumptions and the local solving algorithm significantly change the solution of the model. The local algorithm will mostly find the best objective value that is around the initial values. The model was solved using GRG non-linear algorithm, which is suitable for non-linear functions with no discontinuities. The initial values of the current coefficients (c_1 and c_6) were 15. That is generally because the solution of the modified model should be close to the original model. The other added coefficients were assumed one to provide close ranges and observe the significant of the added variable in the same condition. A constraint was given to c_1 to be larger than zero to avoid any mathematical errors while running the solver.

The resulting modified Japan Road Association models for the six types (Type 1 to Type 6) of Category 3 are summarized below. The values of RMSE and R^2 were calculated for each model.

$$\phi = (17.3 * (N_1)_{60})^{0.5} + 20.8 - 0.15 * \text{W\%} - 0.254 * \text{Silt\%} - 0.12 * \text{R}$$

RMSE=2.7, R^2= 0.84 (Type 1) [48]

$$\phi = (17.9 * (N_1)_{60})^{0.5} + 20.8 - 0.1 * \text{W\%} - 0.126 * (\text{Si} + \text{FS})\% - 0.1 * \text{R}$$

RMSE=2.25, R^2= 0.85 (Type 2) [49]

$$\phi = (17.1 * (N_1)_{60})^{0.5} + 21.3 - 0.12 * \text{W\%} - 0.168 * \text{Silt\%} - 0.1 * \text{Fine Sand} - 0.1 * \text{R}$$

RMSE=1.82, R^2= 0.89 (Type 3) [50]

$$\phi = (18.3 * (N_1)_{60})^{0.5} + 20.6 - 0.15 * \text{W\%} - 0.248 * \text{Silt\%}$$

RMSE=1.77, R^2= 0.87 (Type 4) [51]

$$\phi = (17.8 * (N_1)_{60})^{0.5} + 20.8 - 0.1 * \text{W\%} - 0.136 * (\text{Si} + \text{FS})\%$$

RMSE=2.14, R^2= 0.89 (Type 5) [52]

$$\phi = (18.3 * (N_1)_{60})^{0.5} + 20.7 - 0.1 * \text{W\%} - 0.21 * \text{Silt\%} - 0.08 * \text{Fine Sand\%}$$

RMSE=1.79, R^2= 0.90 (Type 6) [53]

The comparison between the measured friction angles (ϕ) for the different sand-fines mixtures obtained from the direct shear tests and the predicted ϕ values using the six type models of modified Japan Road Association for Category 3 are presented in Figure 34. The results show that the Type 1 model (Equation 48) with input parameters of (silt%, W%, and R) has RMSE = 2.7 and R^2 = 0.75. Replacing the silt content in the Type 1 model with

(Si+FS%) in Type 2 model (Equation 49) resulted in decreasing the RMSE to 2.25 and increasing the R^2 to 0.84. However, replacing the silt content in the Type 4 model (Equation 51) with (Si+FS%) in the Type 5 model (Equation 52) resulted in increasing the RMSE from 1.77 to 2.14 and decreasing the R^2 from 0.89 to 0.84. The results show that separating the silt and fine sand contents in Type 3 and Type 6 model (Equations 50 and 53) yielded reasonable RMSE (1.82 and 1.79) and R^2 (0.89) values. The results also show no difference in the models with or without including the roundness (R) parameter. Consequently, using the silt content, fine sand content, and water content in the modified Japan Road Association's Category 3 models give the most accurate ϕ prediction of the sand-fines mixtures.

Figure 34. Measured ϕ from direct shear vs predicted ϕ from modified Japan Road Association equations for Category 3: a) Type 1; b) Type 2; c) Type 3; d) Type 4; e) Type 5; f) Type 6

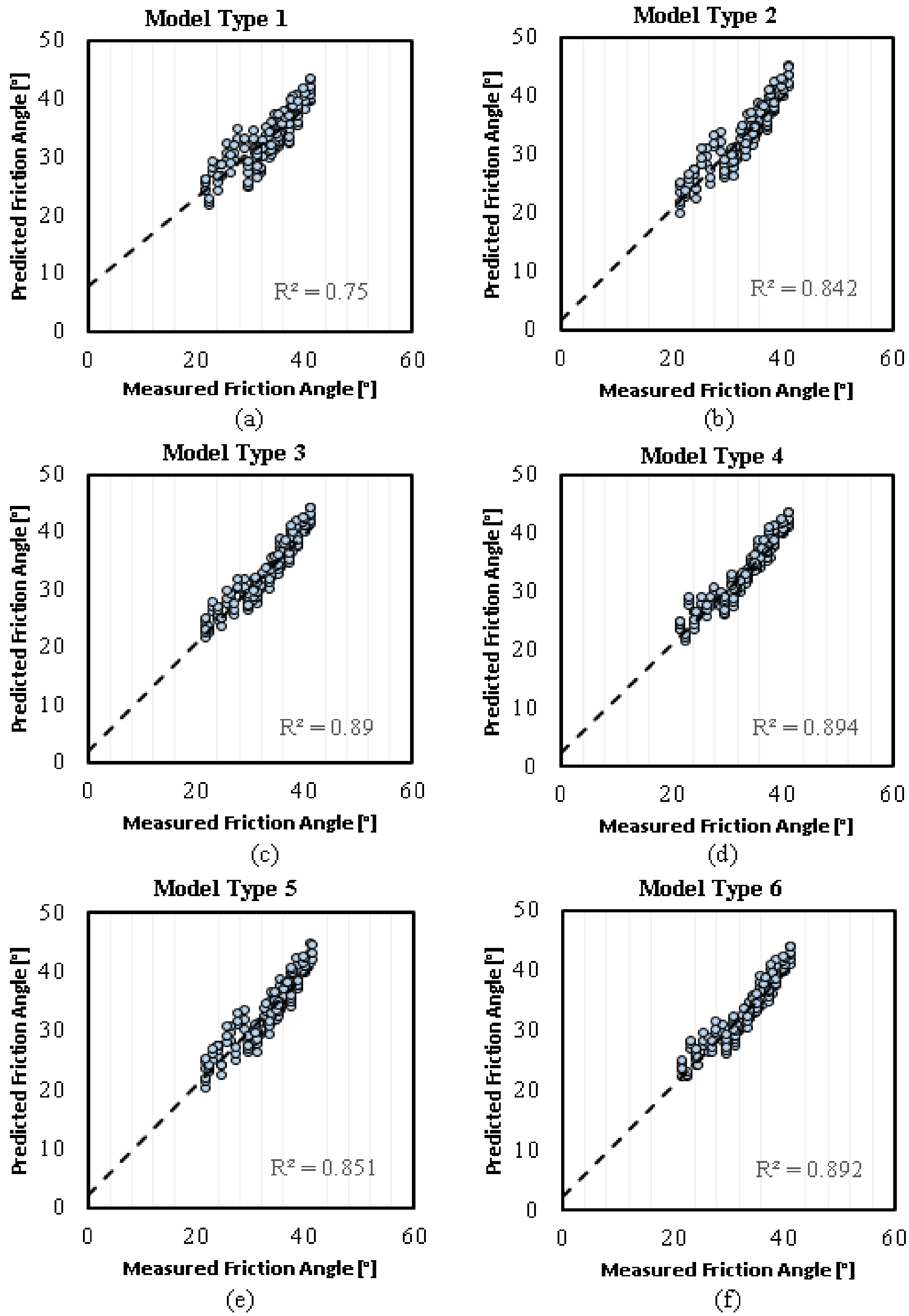

The resulting modified Japan Road Association models for the six types (Type 1 to Type 6) of Category 4 are summarized below. The values of RMSE and R^2 were calculated for each model.

$$\phi = (16.4 * (N_1)_{60})^{0.5} + 20.5 - 0.264 * \text{Silt\%} - 0.12 * \text{R}$$

RMSE=1.78, R^2= 0.87 (Type 1) [54]

$$\phi = (16.9 * (N_1)_{60})^{0.5} + 21.5 - 0.154 * (\text{Si} + \text{FS})\% - 0.1 * \text{R}$$

RMSE=2.07, R^2= 0.88 (Type 2) [55]

$$\phi = (17.1 * (N_1)_{60})^{0.5} + 21.3 - 0.175 * \text{Silt\%} - 0.12 * \text{Fine Sand\%} - 0.2 * \text{R}$$

RMSE=1.76, R^2= 0.89 (Type 3) [56]

$$\phi = (17.1 * (N_1)_{60})^{0.5} + 20.7 - 0.268 * \text{Silt\%}$$

RMSE=1.78, R^2= 0.86 (Type 4) [57]

$$\phi = (16.8 * (N_1)_{60})^{0.5} + 21.5 - 0.164 * (\text{Si} + \text{FS})\%$$

RMSE=2.07, R^2= 0.89 (Type 5) [58]

$$\phi = (18.1 * (N_1)_{60})^{0.5} + 20.7 - 0.22 * \text{Silt\%} - 0.11 * \text{Fine Sand\%}$$

RMSE=1.75, R^2= 0.91 (Type 6) [59]

Figure 35 presents the comparison between the measured friction angles (ϕ) obtained from the direct shear tests and those predicted using the six type models of modified Japan Road Association for Category 4.

Figure 35. Measured ϕ from direct shear vs predicted ϕ from modified Japan Road Association equations for category 4: a) Type 1; b) Type 2; c) Type 3; d) Type 4; e) Type 5; f) Type 6

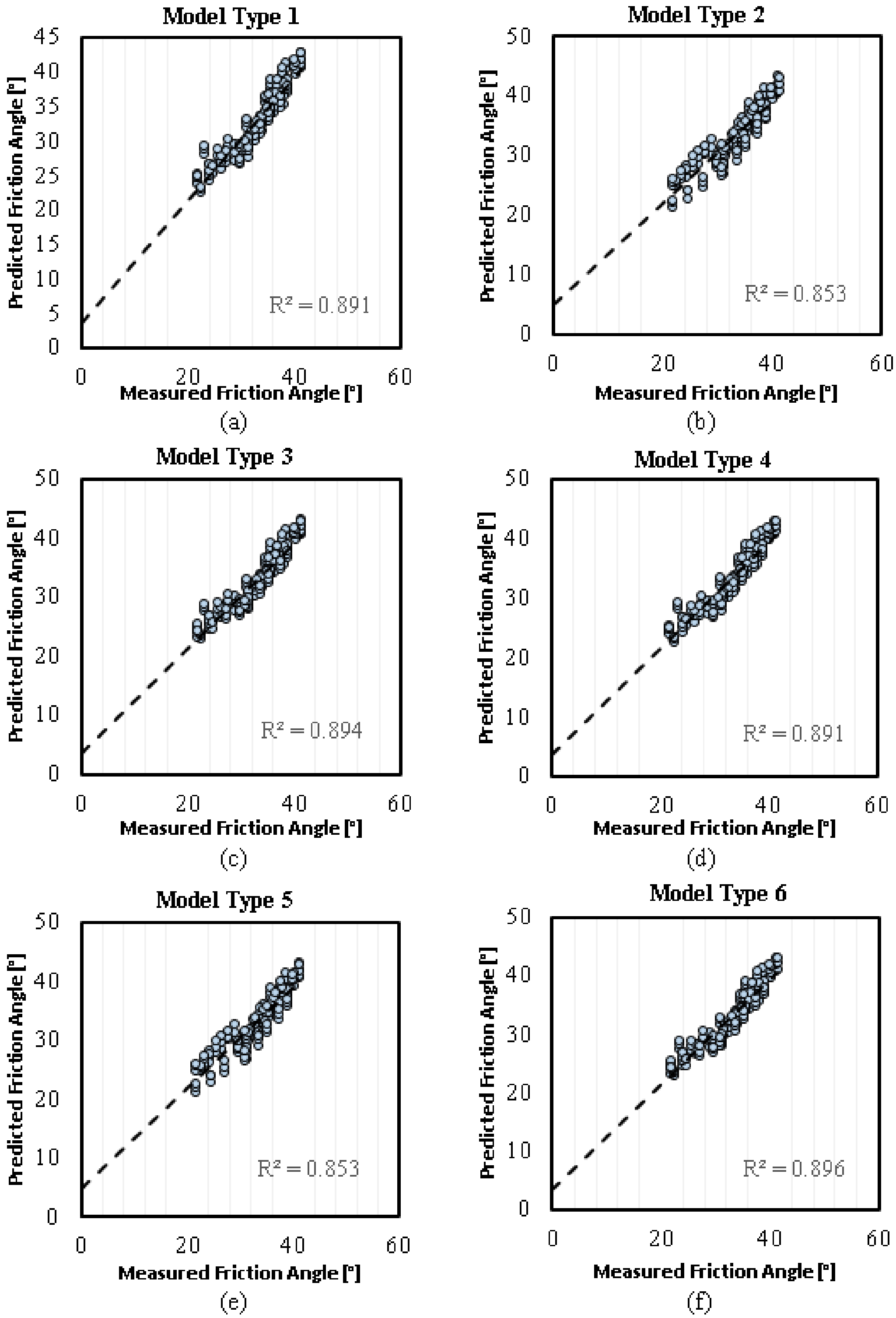

Comparing the models using the silt% input parameter (Type 1 and Type 4) and those using the (Si+FS)% input parameter (Type 2 and Type 5) showed that replacing the silt content with combination of silt and fine sand content resulted in higher RMSE (1.78 vs 2.07) and lower R^2 (0.891 vs. 0.853). The results show that separating the silt and fine sand contents in Type 3 and Type 6 models (Equations 56 and 59) slightly reduced the RMSE (1.76 and 1.75) and slightly improved R^2 (0.894 and 0.896) values. The results also show no difference in the models with or without including the roundness (R) parameter. Equations 54 through 58 demonstrated that using the silt content and fine sand content parameters only in the modified Japan Road Association's Category 4 models can result in a good estimation of the ϕ for the different sand-fines mixtures.

The summary of all ϕ-N_{60} regression models developed based on the modified Schmertmann and modified Japan Road Association equations for the four categories (Category 1 to Category 4) using different additional input parameters (silt content, fine sand content, moisture content, and roundness) are summarized in Table 35. Exploring the different regression models presented in the table, one can recognize that the best-performing regression models to estimate the internal friction angle (ϕ) for the different sand-fines mixture are obtained when only the silt content and fine sand content input parameters are used.

Reduction Factor for the Interface Coefficient of Friction

Both the internal friction angle (ϕ) and the interface friction angle (δ) between the concrete pile and sandy soils mixed with fines dominated by silt exhibited a significant drop in values with the increase in fines content, according to the results of laboratory tests and regression models. As described earlier, small direct shear tests were performed to evaluate the ϕ for sandy soils mixed with fines, while large direct shear tests were performed to evaluate the δ between sandy soils mixed with fines and the concrete pile surface. The silt and fine sand contents were the primary parameters contributing to the decrease in internal and interface frictions. A reduction factor (ψ) was introduced in this study to account for the effect of silt and fine sand contents, which represent the ratio between the interface coefficient of friction for sand soil with fine sand and silt contents compared with clean sand soil. This is described in the following equation:

$$\frac{\tan(\delta)}{\tan(\phi)} = \psi * \frac{\tan(\delta)}{\tan(\phi)_{\text{Clean sand}}} \quad [60]$$

Figure 36a, 36b, and 36c present plots between the interface reduction factor (ψ) and silt content (Silt%), fine sand content (FS%), and combined silt and fine sand content [(Si+FS)%], respectively. The best fit lines are also presented in the figures.

Table 35. Summary of all ϕ-N_{60} regression models

Model	RMSE	R^2
Modified Schmertmann Models		
(W%), (Silt%), (R)	2.3	0.87
(W%), (S+FS %), (R)	4.38	0.88
(W%),(Silt%), (Fine Sand%), (R)	3.4	0.86
(W%), (Silt%)	1.82	0.89
(W%), (S+FS %)	2.1	0.85
(W%), (Silt%), (Fine Sand%)	3.4	0.86
(Silt%), (R)	1.7	0.86
(S+FS %), (R)	1.9	0.89
(Silt%), (Fine Sand%), (R)	1.9	0.89
(Silt%)	1.83	0.88
(S-FS %)	1.99	0.86
(Silt%), (Fine Sand%)	**1.70**	**0.90**
Modified Japan Road Association Models		
(W%), (Silt%), (R)	2.7	0.75
(W%), (S+FS %), (R)	2.25	0.84
(W%),(Silt%), (Fine Sand%), (R)	1.82	0.89
(W%), (Silt%)	1.77	0.89
(W%), (S+FS %)	2.14	0.85
(W%),(Silt%), (Fine Sand%),	1.79	0.89
(Silt%), (R)	1.78	0.89
(S+FS %), (R)	2.07	0.85
(Silt%), (Fine Sand%), (R)	1.76	0.89
(Silt%)	1.78	0.89
(S+FS %)	2.07	0.85
(Silt%), (Fine Sand%)	**1.77**	**0.90**

Figure 36. Relationship between reduction factor (ψ) and silt and fine sand contents

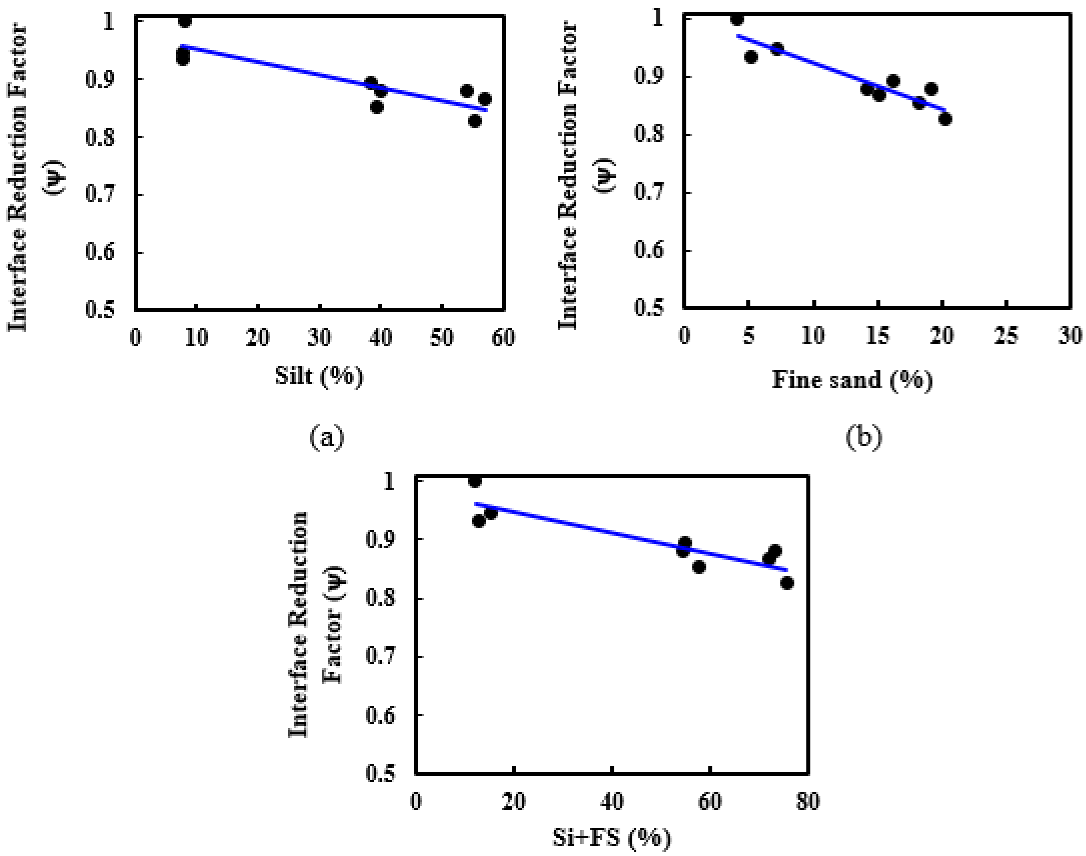

(a) (b)

(c)

Based on Figure 36, the relationship between the reduction factor (ψ) and the silt and fine sand contents can be expressed as follows.

$$\psi = 1 - 0.0025 * \text{Silt\%} - 0.0015 * \text{Fine sand\%} \qquad [61]$$

$$\psi = 1 - 0.00207 * (\text{Si} + \text{FS})\% \qquad [62]$$

Equation 61 presents the reduction factor (ψ) as a function of silt content and fine content separately, while Equation 62 presents the reduction factor as a function of combined silt and fine sand content [(Si+FS)%]. It is advised to take the minimum value obtained using the two equations to be more conservative. The two equations suggest that a sand mixture with approximately 60% silt or approximately 20% fine sand will reduce the interface coefficient of friction [tan(δ)/tan(ϕ)] to approximately 80% of the value for clean sand $[\tan(\delta)/\tan(\phi)]_{(\text{Clean sand})}$. It is highly recommended to be conservative when the sand soil is exposed to silt or fine sand contents. Poytnody [80] suggested using a coefficient of interface friction equal to 0.2-0.3 for saturated silt.

Development of ANN Models for ϕ for Sands with Fines Content

Description of ANN Algorithm

The learning mechanism of the human brain, which is composed of very complex webs of interconnected neurons, is the primary inspiration for the development of artificial neural networks (ANNs). They intend to replicate the learning process of the human brain learning through mathematical algorithms using prior cases. The ANNs can perform parallel computation for complex and massive data processing and knowledge representation.

Like the human brain, the primary element of ANN is neurons. These are also called nodes or processing elements. These processing elements are generally arranged in several layers consisting of an input layer (single layer), one or a few intermediate layers, and an output layer (single layer), as shown in Figure 37. The intermediate layers are also called hidden layers since they do not interact directly with the external environment. At least one neuron is present in each layer. The network is arranged in such a way that the output of one layer serves as the input for the following layer.

Figure 37. Typical structure ANN [96]

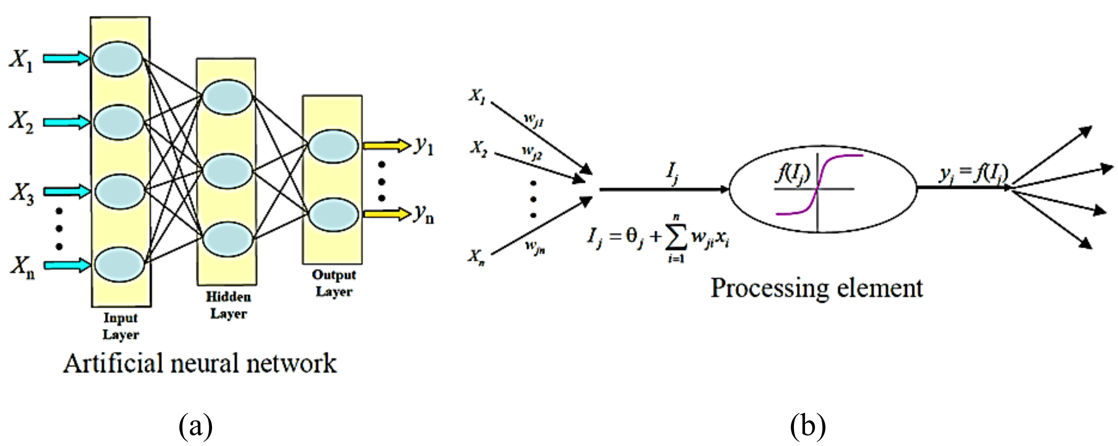

The neurons, or nodes, of each layer network are connected to other neurons through connection weights (see Figure 37b), which determine the strength of the connections between the interconnected neurons. No connection between any two neurons should have a zero weight, whereas a negative weight refers to a repressive relation. The received weighted inputs for an individual processing node are summed, aggregated, and scaled within a certain range to improve the convergence property of ANN. The results are then propagated through a transfer function (e.g., step, linear, ramp, sigmoid logistic, or hyperbolic tangent) to generate the output of the processing node (see Figure 37b). The process for any node j is summarized using the following equations:

$$I_j = \theta_j + \sum_{i=1}^{n} w_{ji} x_i \tag{63}$$

$$y_j = f(I_j) \tag{64}$$

Where,
I_j^l = activation level of node j;
w_{ji}^l = connection weight between nodes i and j;
x_i^{l-1}= input from node i;
i = 0, 1, …, n; $\theta_j^l = w_{j0}$ = bias for node j;
y_j^l = output of node j, and
$f(I_j)$ = transfer function

The hyperbolic tangent function (tanh) was used in this study, which is the hyperbolic analogue of the tan circular function. It is one of the most used functions for neural networks where the output ranges between -1 to +1. Ideally, $\tanh(I_j) = (e^{I_j} - e^{-I_j}) / (e^{I_j} + e^{-I_j})$. The network is then propagated forward leading to final output, y_j. It is then compared with the target output, y_t, and error, E, of the network, which is then calculated as $E = ½ \sum (y_t - y_j)^2$.

The backpropagation algorithm is the prime algorithm used for training ANN models [97]. The prime operation in backpropagation is searching for an error surface for point(s) with minimum error using a form of steepest descent. At each time step, the error gradient guides to a certain direction in the weight space, which reduces the local error drastically. The ANN backpropagation procedure can be described using the following steps [98]:

1. The input parameters are labeled as $x_1^0, x_1^0, x_3^0 \ldots x_m^o$.
2. The connection weights can then be assigned as w_{ji}^l where l=0,1,2….l.
3. The forward network will then be propagated forward using Equations 19 and 20:

$$I_j^l = \theta_j^l + \sum_{n=1}^{i} w_{ji}^l x_i^{l-1}$$

$$y_j^l = f(I_j)$$

Where,

f(.) is the activation function (e.g. logistic sigmoid).

1. For each j^{th} node belonging to output layer ($l=l$), calculate the correction factor δ:

$$\delta_j^l = (y_t - y_j^l) \, y_j^l \, (1 - y_j^l) \qquad [65]$$

2. Update connection weights, w_{ji}^l, using the following equation:

$$\Delta w_{ji}^{l\,(current)} = \eta \, \delta_j^l \, x_l^{l-1} + \mu \Delta w_{ji}^{l\,(previous)} \qquad [66]$$

The above equation resembles the delta-rule ($\Delta w_{ji}^l = \eta \, \delta_j^l \, x_l^{l-1}$), where μ is the momentum rate ($0< \mu < 1$). This equation is also known as the generalized delta rule [97]. The update of bias can be performed as follows:

$$\Delta\theta_{ji}^{l\,(current)} = \eta \, \delta_j^l + \mu \Delta\theta_{ji}^{l\,(previous)} \qquad [67]$$

1. Similarly, for the case of hidden layers:

$$\delta_j^l = y_j^l \, (1 - y_j^l) \sum_{k=1}^{r} \left(\frac{\partial E^l}{\partial y_k^{l-1}}\right) \left(\frac{\partial y_k^{l-1}}{\partial I_k^{l-1}}\right) \left(\frac{\partial I_k^{l-1}}{\partial y_{ji}^l}\right) \qquad [68]$$

2. The weights and biases will be updated using Equations 4 and 5, respectively.

3. Finally, Steps 1-7 are iterated until the output error is within acceptable tolerance.

The number of training cycles required for a better performance of the model is determined iteratively. A long training can result in overtraining or overfitting along with a near-zero error on predicting training data. The generalization of test data degrades significantly in such situation (see Figure 38). In the beginning, for a small number of training epochs, the error of the test-sets continues to decrease like the training examples. However, as the network loses its capability to generalize on test data, the error starts to increase after each epoch. The onset of an increase in the error of the test-sets' data resembles the optimum number of training cycles. When there are a limited number of training examples available, a sufficiently large test set is usually difficult to arrange. In such a case, Hecht-Nielsen [99] suggested that the network be trained on all available data and the training process be stopped when the error in training data is at the onset of stabilization.

Figure 38. Evolution of error for training and test data as a function of network size and number of training cycles [98]

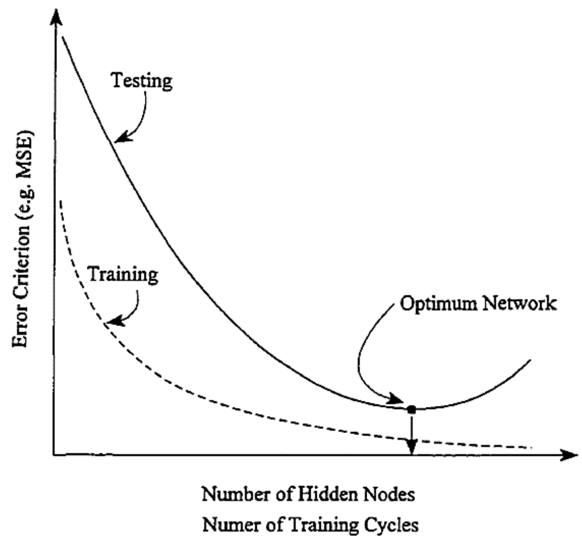

Develop ANN Models

The number of nodes in the input and output layers is usually determined by the number of model input and output parameters, respectively. There is hardly any explicit approach to quantify the optimum number of nodes in a certain hidden layer. A trial-and-error procedure is usually conducted to estimate the number of nodes in each hidden layer. It is important to remember that ANNs comprised of large numbers of hidden layer nodes are susceptible to overfitting and poor generalization. To obtain satisfactory performance of the model, the number of hidden nodes should be kept to a minimum. Initially, the number of hidden nodes can be considered at 75% of the number of input units. Also, a number between the average and the sum of the nodes in both input and output layers can be considered as the number of hidden nodes. In this case, the highest allowable number of hidden nodes in a single layer network can be considered as (2I+ 1), where I is the number of input parameters. However, it is better to start with a small number of nodes and gradually increase the number until no significant improvement in the performance of the model is obtained. For networks with two hidden layers, the geometric pyramid rule can be used, where the number of nodes in each layer decreases from the input layer toward the output layer. Considering all the facts, starting from one, up to three hidden layers with different combinations of nodes were explored in this study. For a single hidden layer, the maximum number of nodes was (2I+ 1), while for double and triple hidden layers the geometric pyramid rule was followed. The input layer consisted of nodes varying in number from one to five, depending on the ANN type. However, for all of the ANN types, the number of nodes in the output layer was only one (the ϕ). During this study, seven different ANN types with different combinations of input parameters, number of nodes, and number of hidden layers, were tried as described in Table 36. The ANN input parameters included N_{60}, overburden pressure (σ_0), water content (W%), silt content (silt%), fine sand content (fine sand%), combination of silt and fine sand content (Si+FS%), and particle roundness (R).

Table 36. Input parameters for ANN models

ANN Type	ANN Model	Parameters used as inputs
Type 1	2-5-1	(N_{60}) , (σ_0)
	2-4-3-1	
Type 2	5-4-3-2-1	(N_{60}), (σ_0) , (W%), (Silt%), (R)
	5-4-3-1	
Type 3	5-4-3-2-1	(N_{60}), (σ_0) , (W%), (Si+FS%), (R)
	5-4-3-1	
Type 4	6-4-3-2-1	(N_{60}), (σ_0) , (W%), (Silt%), (Fine sand%), (R)
	6-5-3-1	
Type 5	4-3-3-1	(N_{60}), (σ_0), (W%), (Silt%)
	4-3-2-1	
Type 6	4-3-3-1	(N_{60}), (σ_0), (W%), (Si+FS%)
	4-3-2-1	
Type 7	5-4-3-2-1	(N_{60}), (σ_0), (W%), (Silt%), (Fine sand%)
	5-4-3-1	

The performance of ANN models for training, testing, and validation steps in terms of RMSE and R^2 values are summarized in Table 37. Based on the results of the analysis, the value of R^2 ranged from 0.039 to 0.99, which implies that the input parameters have a direct influence on the overall performance and accuracy of the ANN models. Based on the results, the ANN Type 4 models (6-5-3-1 and 6-4-3-2-1) that considered silt and fine sand contents separately are considered the most accurate of the ANN models and included R. This was followed by the ANN Type 7 models (5-4-3-1, 5-4-3-2-1), which also considered silt and fine sand contents separately but did not include R. Type 6 models (4-3-3-1, 4-3-2-1) and Type 5 models (4-3-3-1, 4-3-2-1) also provided reasonable accuracy in terms of RMSE and R^2. Type 5 models used only silt content, while Type 6 models used combined silt and fine sand contents. Neither Type 5 nor Type 6 ANN models included R.

Table 37. Performance of ANN models

ANN Type	ANN Model	Phase	R^2	RMSE	ANN Type	ANN Model	Phase	R^2	RMSE
Type 1	2--5--1	Training	0.039	5.2	Type 5	4-3-3-1	Training	0.99	0.46
		Testing	0.032	5.2			Testing	0.94	1.27
		Validation	0.13	3.6			Validation	0.91	1.13
	2-4-3-1	Training	0.27	4.4		4-3-2-1	Training	0.9	1.65
		Testing	0.3	3.42			Testing	0.93	1.29
		Validation	0.25	3.69			Validation	0.94	1.1
Type 2	5-4-3-2-1	Training	0.96	1.06	Type 6	4-3-3-1	Training	0.95	1.18
		Testing	0.87	0.14			Testing	0.97	1.24
		Validation	0.9	1.38			Validation	0.94	0.97
	5-4-3-1	Training	0.98	0.71		4-3-2-1	Training	0.96	1.08
		Testing	0.91	1.42			Testing	0.9	1.4
		Validation	0.94	1.18			Validation	0.98	1
Type 3	5-4-3-2-1	Training	0.95	1.06	Type 7	5-4-3-2-1	Training	0.97	0.92
		Testing	0.87	1.58			Testing	0.94	1.24
		Validation	0.97	0.8			Validation	0.96	1.3
	5-4-3-1	Training	0.97	0.87		5-4-3-1	Training	0.98	0.73
		Testing	0.89	1.95			Testing	0.96	0.97
		Validation	0.9	1.59			Validation	0.98	0.93
Type 4	6-4-3-2-1	Training	0.98	0.65					
		Testing	0.97	0.87					
		Validation	0.96	0.92					
	6-5-3-1	Training	0.99	0.46					
		Testing	0.97	0.95					
		Validation	0.99	0.73					

The comparisons between the measured friction angles (ϕ) from the direct shear tests and those predicted using the ANN Type 4 (6-5-3-1) model for the training, validation, testing and all data are presented in Figure 39. The complete comparisons between the measured ϕ from direct shear tests and those predicted using the seven types of ANN models for training, testing, validation, and all of the sand-fines mixtures are presented in Appendix D.

Figure 39. Measured friction angle from direct shear vs predicted friction angle from ANN Type 4 (6-5-3-1) model: a) training; b) validation; c) testing; d) all

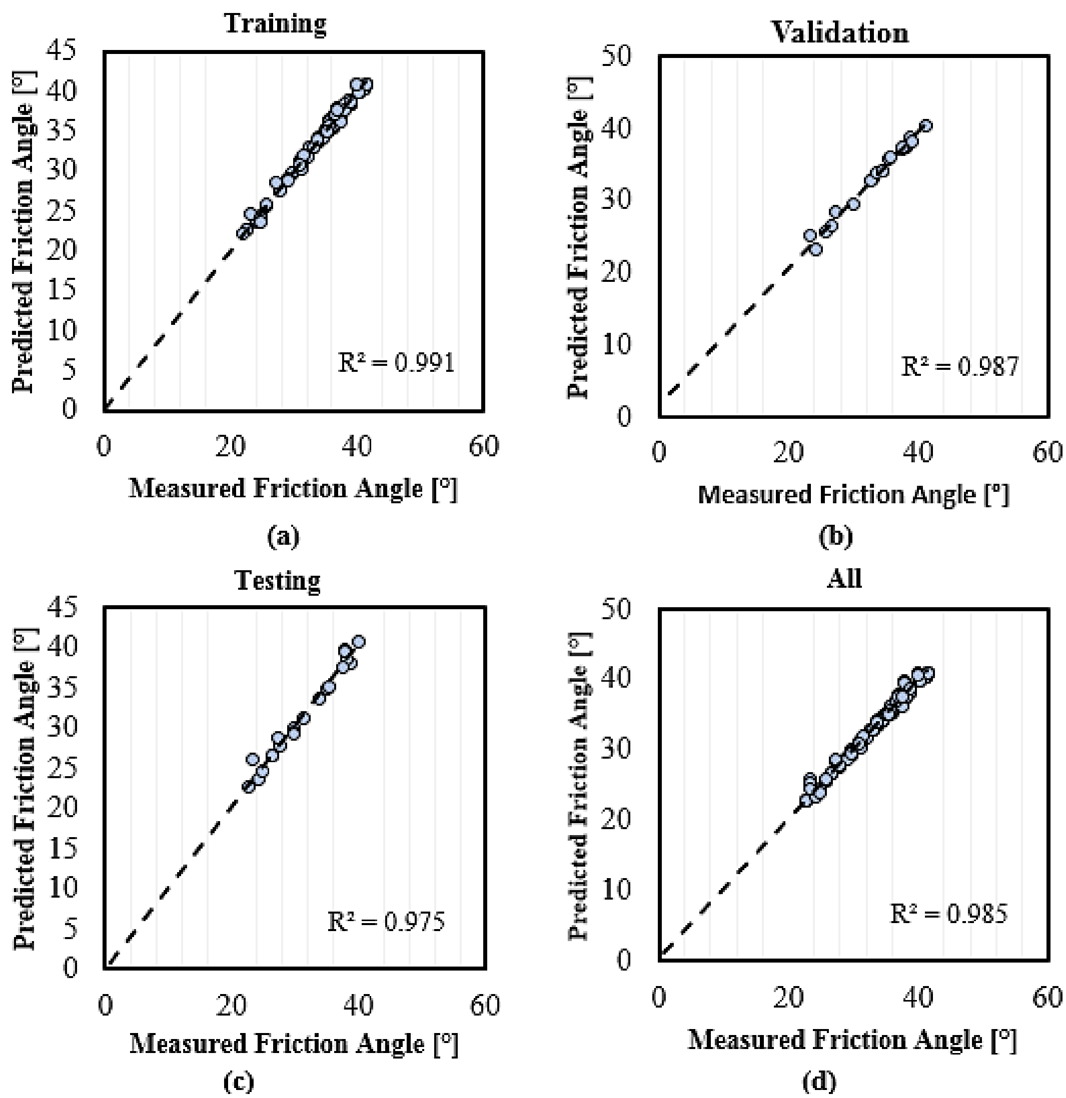

Verification of Modified ϕ-N_{60} Models using Case Studies

Two problematic project sites with sand soil mixed with fines (primarily silts) were used for the verification of the developed ϕ-N_{60} models. These two sites were the Boeuf River Bridge replacement site (H.014454) and the Tangipahoa River Bridge replacement site (H.013052).

Boeuf River Bridge Replacement Site

The Boeuf River Bridge replacement site is located at LA 15 over the Boeuf River approximately 2 miles west of Alto, southeast of Monroe, Louisiana (see Figure 40). Two soil borings were drilled to a depth of 110 ft. for this study. Standard penetration tests (SPT) were performed every 3 ft. from depths of 28 ft. to 85 ft. in the first boring (B-1) in order to retrieve enough soil samples for laboratory direct shear tests. In the second boring (B-2), SPTs were performed every 3 ft. from depths of 20 ft. to 40 ft. and every 5 ft. from depths of 40 ft. to 105 ft. One cone penetration test (CPT) was also performed in the site and used to classify the subsurface soil layers. The results of CPT tests and corresponding soil behavior classification according to the Zhang and Tumay [100] method are presented in Figure 41. The results of the SPT and CPT tests showed that the subsurface soil primarily consists of silty clay soil down to approximately 15 ft., followed by medium dense to dense sand and silty sand down to the bottom of the boring. The ground water table in the site was measured at 15.4 ft. and 16.5 ft. below the surface for soil borings B-1 and B-2, respectively.

Figure 40. Location of Boeuf River Bridge

Figure 41. Results of CPT test and soil behavior classification at Boeuf River Bridge site

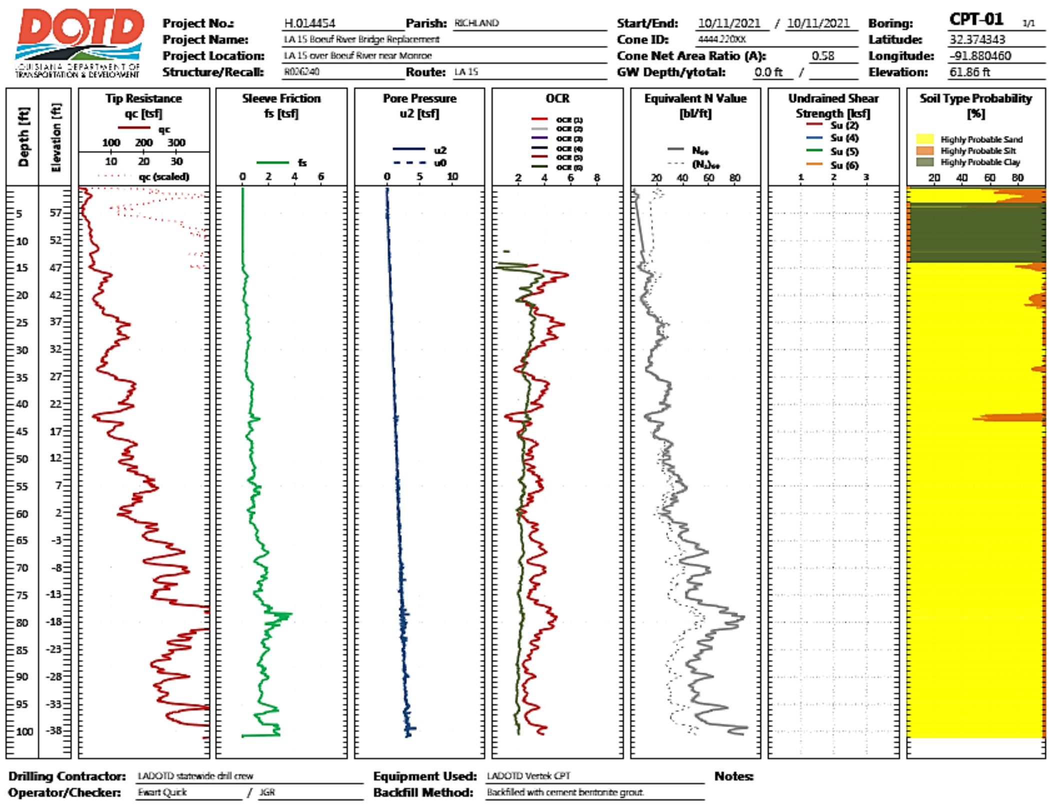

Direct Shear Tests

Sandy samples were collected from the SPTs down to 85 ft. depth in B-1 and down to 105 ft. depth in B-2. The subsurface soil was grouped into five layers in B-1 and six layers in B-2 depending on the color, density, and number of blows. This ensured that researchers had enough samples for the direct shear test. The wet unit weight of sand ranged from 112 lb/ft^3 to 124 lb/ft^3, and the moisture content ranged from 15% to 28%. Sieve analysis tests were performed to determine the percent of fine sand, silt, and clay for each soil layer. The water content was also determined for each soil layer. The average SPT numbers were taken to represent the entire soil layer. A total of 15 drained shear tests (DSTs) were conducted on collected soil samples from B-1 (three tests per soil layer), and 18 DSTs were conducted on collected soil samples from B-2. The DSTs were performed at the same moisture content and relative densities that were calculated from the field. The average corrected SPT number N_{60}, moisture content, percent fine sand, and percent silt for each soil layer of B-1 and B-2 are presented in Table 38. The table also includes the results of drained direct shear tests in terms of internal friction angle (ϕ). The soil samples for direct shear tests were prepared at the corresponding relative density calculated from the average

N_{60} for each soil layer. Due to a lack of enough soil samples per layer, the minimum and maximum void ratios (e_{min}, e_{max}) were evaluated using soil samples collected from several layers.

Table 38. Average N_{60}, moisture content, percent fine sand, percent silt, and measured friction angles for each soil layer at Boeuf River Bridge site

Layer	Depth (ft.)	Average N	N_{60}	Water content (%)	Fine sand (%)	Silt (%)	Friction angle (ϕ)(º)
B-1							
1	28 - 40	17	16.3	13.86	52	14	28.5
2	40 - 52	20	19.2	17.26	47	18	29.2
3	52 - 58	26	24.9	13.18	55	13	29.7
4	58 – 73	15	14.4	16.73	51	21	26.7
5	73 - 85	23	22.0	12.53	57	19	28.8
B-2							
1	20 - 29	7	6.4	14.14	61	12	26.7
2	29 - 40	15	14.4	16.73	56	11.5	28.3
3	40 - 60	20	19.2	14.22	58	10.5	29.4
4	60 - 80	25	24.0	15.47	54	12.7	28.8
5	80 – 92	32	30.7	12.53	57	11.5	30.2
6	92 - 104	36	34.5	13.24	54	13.5	30.7

The internal friction angle (ϕ) for all soil layers in B-1 and B-2 borings were calculated using the original Schmertmann model based on N_{60} and effective overburden pressure (σ'_{vo}); original Japan Road Association based on $(N_1)_{60}$; modified Schmertmann equation for Type 6 of Category 1 and Category 2; and modified Japan Road Association for Type 6 of Category 3 and Category 4. The results are presented and compared with the measured ϕ values in Table 39. The results show that the original Schmertmann and Japan Road Association models overestimated the results of direct shear tests. However, the modified Schmertmann and Japan Road Association models gave a good estimate of the ϕ for sand-silt mixtures with an error of < |±6|%.

Table 39. Friction angle from Schmertmann and Japan Road Association correlations and direct shear test at Boeuf River Bridge site

Layer	Direct Shear ϕ (°)	Original Shmert. ϕ (°)	Original JRA ϕ (°)	Modified Shmert. ϕ (°) Type 6 – Cat. 1	Modified Shmert. ϕ (°) Type 6 – Cat. 2	Modified JRA ϕ (°) Type 6 – Cat. 3	Modified JRA ϕ (°) Type 6 – Cat. 4
B-1							
1	28.5	36.7	36.7	27.9	28.1	28.2	27.8
2	29.2	36.9	37.2	27.6	27.3	27.9	27.9
3	29.7	38.4	38.9	28.6	28.2	30.4	29.8
4	26.7	32.4	33.9	25.8	25.0	23.8	23.7
5	28.8	35.2	36.6	27.0	25.9	26.8	26.0
B-2							
1	26.7	29.4	30.9	25.1	24.3	22.3	22.7
2	28.3	35.3	35.5	27.2	27.1	27.0	26.8
3	29.4	36.3	36.8	28.0	27.6	28.5	28.0
4	28.8	36.6	37.7	28.1	27.8	29.1	28.8
5	30.2	37.7	39.2	28.8	28.3	30.8	30.2
6	30.7	38.0	39.8	28.8	28.3	31.2	30.6

Tangipahoa River Bridge Replacement Site

The Tangipahoa River Bridge replacement site is located on LA 442 over the Tangipahoa River approximately 3.5 miles east of US 51 and 2.5 miles west of LA 443 in Louisiana (see Figure 42). One soil boring was drilled down to 95 ft. depth at the site for this study. Standard penetration tests (SPT) were performed every 5 ft. from the surface down to 95 ft. One cone penetration test (CPT) was also performed in the site and used to classify the subsurface soil layers. The results of the CPT test and corresponding soil behavior classification according to the Zhang and Tumay [100] method are presented in Figure 43. The results of the SPT and CPT tests showed that the subsurface soil consists of stiff sandy clay down to approximately 15 ft., followed by medium dense to dense sand and silty sand down to the bottom of the boring. Sand and gravel was encountered between 40 ft. to 50 ft. depth. The ground water table in the site was measured at 11.5 ft. below the ground surface.

Figure 42. Location of Tangipahoa River Bridge

Direct Shear Tests

Sandy soil samples were collected from SPT samplers from 10 ft. depth down to 95 ft. depth from the surface. The subsurface soil was grouped into seven layers depending on the color, density, and number of blows. This ensured that researchers had enough samples to perform the direct shear test. The wet unit weight of sand was estimated to be 115 lb/ft^3, and the moisture content ranged from 10% to 25%. Sieve analysis tests were performed to determine the percentage of fine sand, silt, and clay for each soil layer. The water content was also determined for each soil layer. The average SPT numbers were taken to represent the entire soil layer. A total of 21 drained shear tests (DSTs) were conducted on collected soil samples. The DSTs were performed at the same moisture content and relative densities that were calculated from the field. The average corrected SPT number N_{60}, moisture content, percent fine sand, and percent silt are presented in Table 38. The table also includes the internal friction angles (ϕ) obtained from drained direct shear tests. The soil samples for direct shear tests were prepared at the corresponding relative density calculated from the average N_{60} for each soil layer. Due to a lack of enough soil samples per layer, the values of e_{min} and e_{max} were evaluated using soil samples collected from several layers.

Figure 43. Results of CPT test and soil behavior classification at Tangipahoa River Bridge site

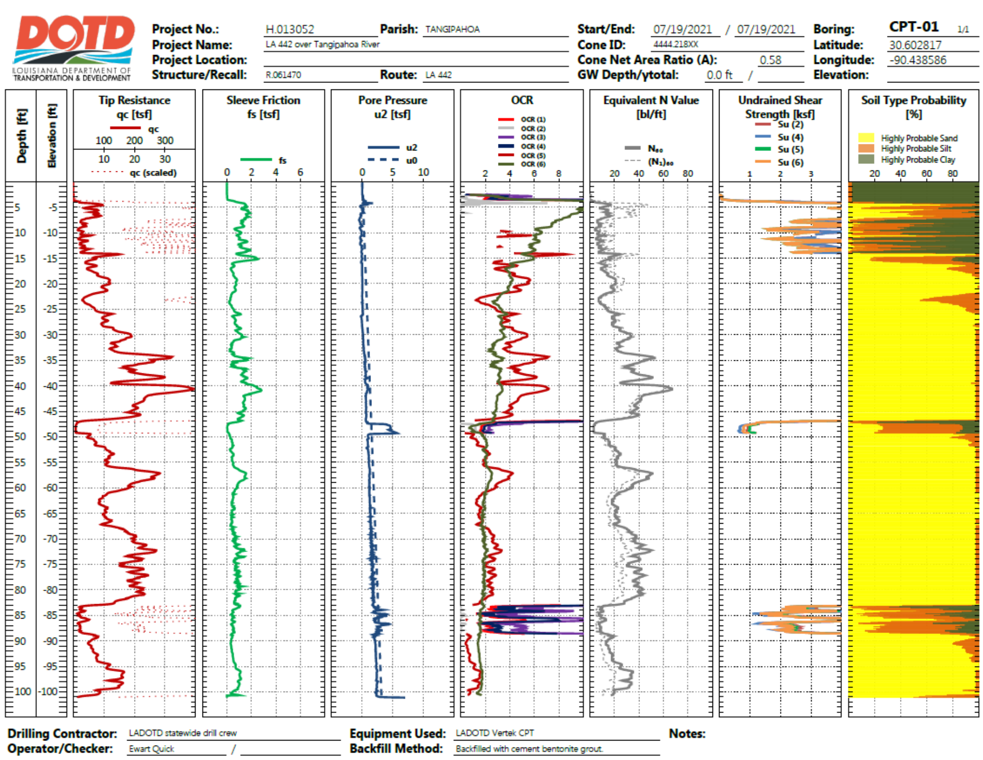

Table 40. Average N_{60}, moisture content, percent fine sand, percent silt, and measured friction angles for each soil layer at Tangipahoa River Bridge site

Layer	Depth (ft.)	Average N	N_{60}	Water content (%)	Fine sand (%)	Silt (%)	Friction angle (ϕ)(º)
1	10 – 20	10	9.6	17	38	24	29.8
2	20 - 30	19.5	18.7	20	64	11	31.2
3	30 – 40	18.5	17.7	18	61	11	28.7
4	50 - 55	20	19.2	16	62	10	30.2
5	55 – 65	23.5	22.5	23	56	11	30.5
6	65 – 80	22	21.1	21	51	10	31.1
7	80 - 95	31.5	30.2	16	39	12	32.4

The internal friction angles (ϕ) for the seven sandy soil layers were calculated using the original Schmertmann model based on N_{60} and effective overburden pressure (σ'_{vo}); the original Japan Road Association equation based on $(N_1)_{60}$; the modified Schmertmann equation for Type 6 of Category 1 and Category 2; and the modified Japan Road Association for Type 6 of Category 3 and Category 4. The results are presented in Table 41. The comparison with the measured ϕ values from direct shear tests shows that the original Schmertmann and Japan Road Association models overestimated the results of direct shear tests by 15-30%. However, the modified Schmertmann and Japan Road Association models gave a good estimate of the ϕ for sand-silt mixtures with an error of $<|\pm10|\%$.

Table 41. Friction angle from Schmertmann and Japan Road Association correlations and direct shear test at Tangipahoa River Bridge site

Layer	Direct Shear ϕ (°)	Original Shmert. ϕ (°)	Original JRA ϕ (°)	Modified Shmert. ϕ (°) Type 6 – Cat. 1	Modified Shmert. ϕ (°) Type 6 – Cat. 2	Modified JRA ϕ (°) Type 6 – Cat. 3	Modified JRA ϕ (°) Type 6 – Cat. 4
1	29.8	35.2	34.9	27.2	26.4	32.2	32.4
2	31.2	39.9	39.3	26.4	25.9	25.1	25.4
3	28.7	38.0	37.7	27.3	27.6	29.7	29.6
4	30.2	36.7	37.0	27.4	27.5	28.6	28.4
5	30.5	37.4	38.0	27.6	27.4	28.3	27.9

Layer	Direct Shear ϕ (°)	Original Shmert. ϕ (°)	Original JRA ϕ (°)	Modified Shmert. ϕ (°) Type 6 – Cat. 1	Modified Shmert. ϕ (°) Type 6 – Cat. 2	Modified JRA ϕ (°) Type 6 – Cat. 3	Modified JRA ϕ (°) Type 6 – Cat. 4
6	31.1	35.7	36.7	27.4	28.1	28.8	29.2
7	32.4	37.9	39.2	27.7	28.4	28.4	28.8

Threshold of Cohesive and Cohesion-less Soils with Fines Content

The results of this study (for Sand Soil 1 mixed with Soil 2, Soil 3, Soil 4, and Soil 5) and the results in the literature show that the behavior of sand soil changes when increasing the fines content (silt, clay, or both). The threshold percentage of fines content (FC) that defines the boundary between the cohesion-less soil behavior and cohesive soil behavior of sand-fines mixtures (in addition to the fines content) depends on many factors, including the particle shape, surface roughness, effective stress, and the density/void ratio of the soil mixtures. The Unified Soil Classification System (USCS) classifies the soils as fine-grained soils when > 50% of particles are finer than sieve No. 200, although soil mixtures with 20-50% fines content can exhibit some cohesive behavior that will significantly affect shear strength parameters. There is no distinct fines content percentage in the literature beyond which the sand soil mixtures begin to behave as cohesive soils and the fines content begins to influence the shear strength of the cohesion-less soil. The boundary between these two values is referred to as the transition zone. Lupini et.al. [41] describes the effect of fines content on the behavior of sand soil mixtures through three modes of shear behavior: a turbulent mode, transitional mode, and sliding mode (see Figure 44). The turbulent, or rolling, mode occurs when the soil behavior is dominated by rotund particles and the coefficient of inter-particle friction is high. The sliding mode occurs when the soil behavior is dominated by platy and low-friction particles. A low strength shear surface of strongly orientated platy particles then develops. The transitional mode occurs when there is no dominant particle shape which involves turbulence and sliding behavior in different parts of the shear zone. The value of inter-granular void ratio (e_g) is an important factor contributing to the type of sand soil behavior.

The clay fraction (CF) at the condition when the e_g of the mixture becomes equal to the maximum void ratio (e_{max-s}) of the sand (i.e., $e_g = e_{max-s}$) can be defined as the “transition clay content” or “threshold clay content” (CF_{th}). When the clay content is higher than the threshold clay content ($CF > CF_{th}$), the grains of sand are expected to be fully separated by clay particles. When $e_g < 1.0$, the turbulent, or rolling, behavior occurs. When $e_g > 7.0$, the sliding behavior occurs. However, when $1.0 < e_g < 7.0$, both transposal and sliding behavior occurs. The value of e_g increases when increasing the clay content in the sand soil mixture.

Skempton and Brogan [101] identified the following two fines contents (FC) that describe the evolution of soil fabric with the increase of fines content:

- S∗ is the critical fines content at which the fines just fill the voids between the coarse particles. S∗ was estimated to range from FC = 24% to 29% for dense and loose sands, respectively.
- Smax is the fines content at which the fines begin to separate the coarse particles from one another, which is no more than FC = 35% [101].

According to Skempton and Brogan [101], when FC < S^{*}, the soil has an underfilled fabric; when $S^{*} < FC < S_{max}$, the fabric is filled; and when $FC > S_{max}$, the fabric is overfilled, as shown in Figure 45.

Figure 44. Possible interface shear by sliding in low-plasticity clays [41]

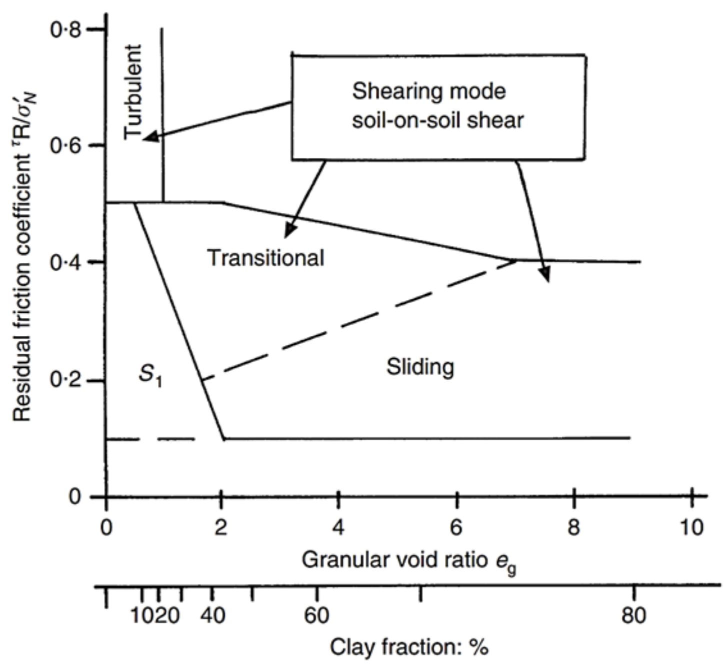

Figure 45. Evolution of fabric with fines content: a) underfilled with large size ratio; b) filled; c) overfilled; d) underfilled with small size ratio [101]

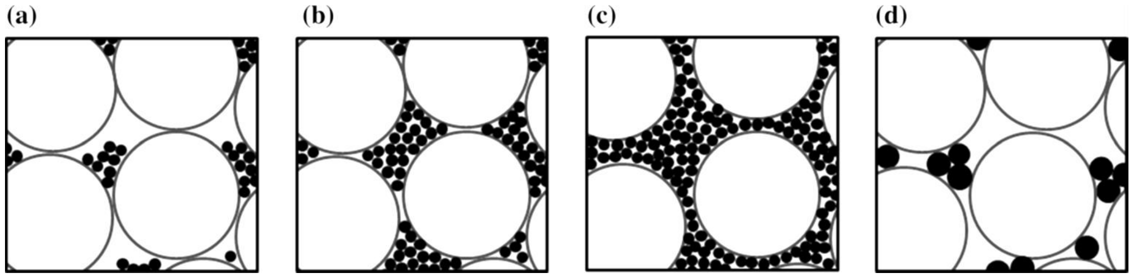

The threshold fines content (F_{thr}) is a key parameter to describe the behavior of sand-fines mixtures to distinguish between the “fines-in-sand” or “sand-in-fines” structure below or above the F_{thr}, respectively. Studies on the dynamic characteristics of sand-silt mixtures show that in mixtures with $FC < F_{thr}$, the host sand controls the overall behavior of the mixture (fines-in-sand), while for $FC > F_{thr}$, the fines becomes dominant (sand-in-fines) (e.g., [102]). Therefore, it is very important to evaluate F_{thr} in order to predict the behavior of sand-fines mixtures. Typical values of F_{thr} range between 20% and 40% of fines content [31].

Several researchers in the literature developed models to estimate the F_{thr} of sand-fines mixtures using analytical, empirical, or semi-empirical methods based on experimental results. Two approaches were used to determine the threshold fines content (F_{thr}) based on the e_{min} and e_{max} from experiments:

- Approach 1: F_{thr} is taken as the minimum limit of fines content (FC) versus void ratio curve through visual observation (M1 in Figure 46).
- Approach 2: Uses the Lade et al. [44] procedure, which is based on the theory of binary packing. In this procedure, F_{thr} is the point of intersection of the two tangent lines of the e_{max} versus fine content (or e_{min} versus fine content) curve near FC = 0 and FC = 100% (M2 in Figure 46).

Figure 46. Schematic of determining the threshold fine content (F_{thr}) at the minimum of the e-F_{fine} curve (method M1), or using the Lade et al. [44] procedure (dashed linear curves, method M2) [103]

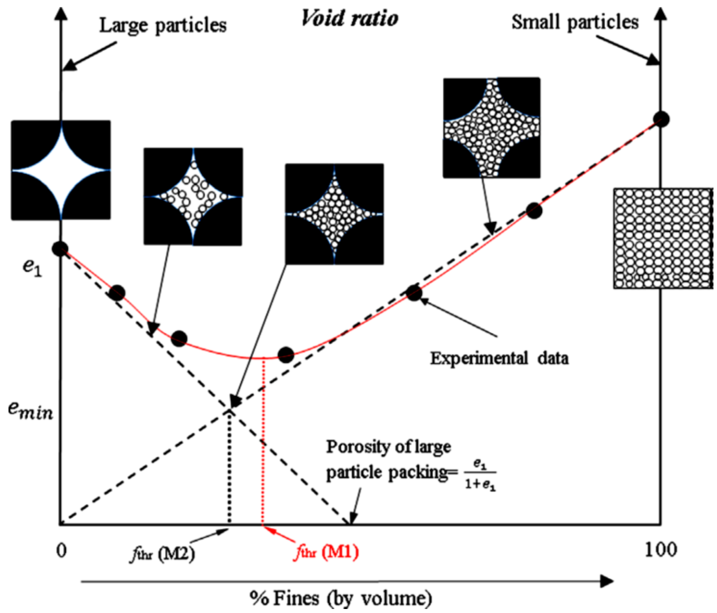

Hazirbaba [104] proposed the following analytical equation to determine F_{thr} based on the ratio of the weight of fines to the total weight of the sand and fines:

$$f_{thr} = \frac{G_f e_s}{G_f e_s + G_s(1 + e_f)} \tag{69}$$

Where,

G_s and G_f are the specific gravities of the sand and fine material, and
e_s and e_f are the void ratios of the pure sand and the pure fines, respectively.

Zuo and Baudet [105] adapted Equation 69 by substituting the values of maximum and minimum void ratios of sand ($e_{max,s}$ and $e_{min,s}$) and fines ($e_{max,f}$ and $e_{min,f}$) as follows:

$$\begin{gathered} f_{thr,emax} = \frac{G_f e_{max,s}}{G_f e_{max,s} + G_s(1 + e_{max,f})} \\ f_{thr,emin} = \frac{G_f e_{min,s}}{G_f e_{min,s} + G_s(1 + e_{min,f})} \end{gathered} \tag{70}$$

Kaothon et al. [106] studied the effect of fines content on the compressional behavior of sand-kaolinite mixtures. Using the minimum void ratios of sand and kaolinite clay ($e_{min,s}$ and $e_{min,f}$), they found F_{thr} to be equal to 21.67%, which is within the range of transition zone (i.e., 21–26% of fines content) obtained from experimental observation, as shown in Figure 47.

Figure 47. Overall behavior of sand-kaolinite [106]

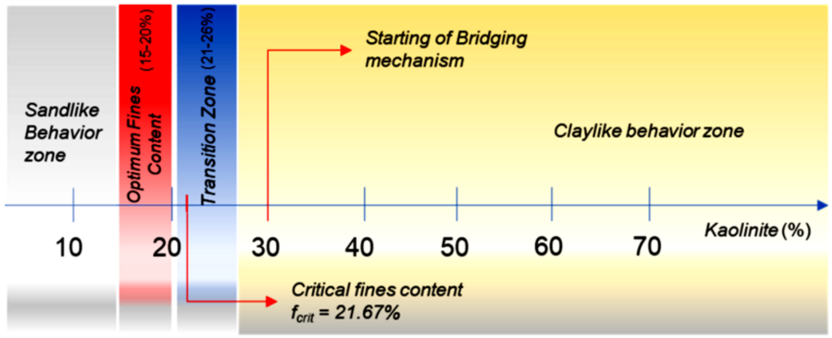

Belkhatir et al. [107] studied the effect of fines content and void ratio on the saturated hydraulic conductivity and undrained shear strength of sand-silt mixtures. They plotted the variation of e_{max} and e_{min} versus the fines content F_{fine} to determine F_{thr} as shown in Figure 48. The values from the two indices showed that F_{thr} = 30 %.

Figure 48. Maximum and minimum void ratios of sand-silt mixtures versus fines content [107]

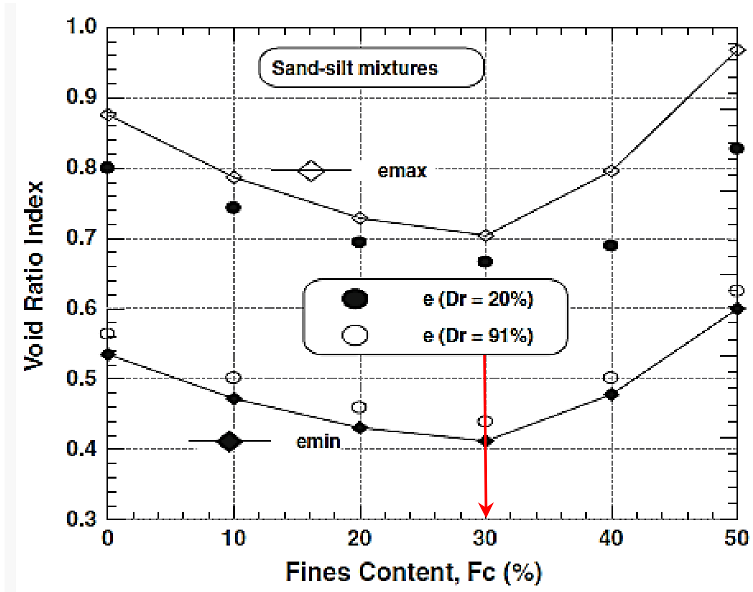

A recent study was performed by Abdi et al. [108] to investigate the effect of fines content and matric suction on the behavior of silty sand soil in terms of net and effective stresses. The plots of both the e_{max} and e_{min} of sand-silt mixtures versus the fines content in their study gave the same value of the threshold fines content (F_{thr}), which is approximately 35%, as shown in Figure 49.

Figure 49. Variation of e_{max} and e_{min} of sand-silt mixtures versus fines content [108]

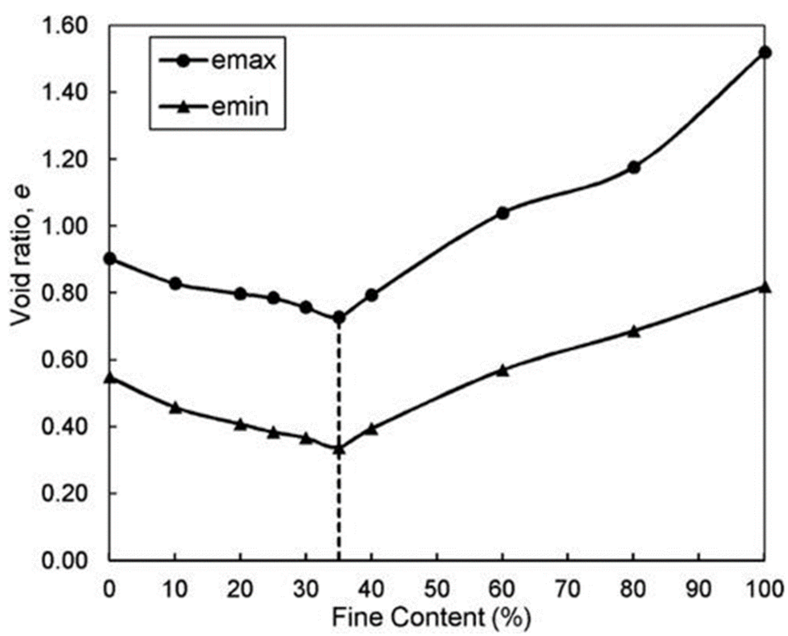

A study by Thevanayagam [109] on the effect of fines and confining stresses on the undrained shear strength (S_u) of silty sands showed that the inter-granular void ratio, e_s, plays an important role on the value of S_u of sand-silt mixtures. The value of e_s is calculated as:

$$e_s = \frac{e + F_{fine}}{1 - F_{fine}} \qquad [71]$$

Where,
e is the void ratio of silty sand, and
F_{fine} is the fines content.

Their results showed that for the same e value, the silty sand had low S_u compared to the sand alone. However, when compared at the same e_s, both the silty sand and sand alone had similar S_u values, which is independent of the initial confining stress. When the fines content, FC > 30%, the silty sand mixture starts behaving like a silt at an interfine void ratio, e_f, defined as the void ratio of the silt-matrix (given by e/FC).

Polito and Sibley [110] evaluated the threshold fines content and behavior of sand mixed with silt. They identified the lower- and upper-bounds of threshold fines content (F_{thr}) of the sand-silt mixture as 21% and 30%, respectively. They found out that the soils above the upper-bound F_{thr} had lower friction angles than the soils below the lower-bound F_{thr}, as described in Figure 50. This represents the transitions from being a “sand-like” soil, with silt particles are entirely contained in the voids between the sands, to being a “silt-like” soil that contains isolated sand particles.

Figure 50. Variation of friction angle and cyclic resistance with silt content [110]

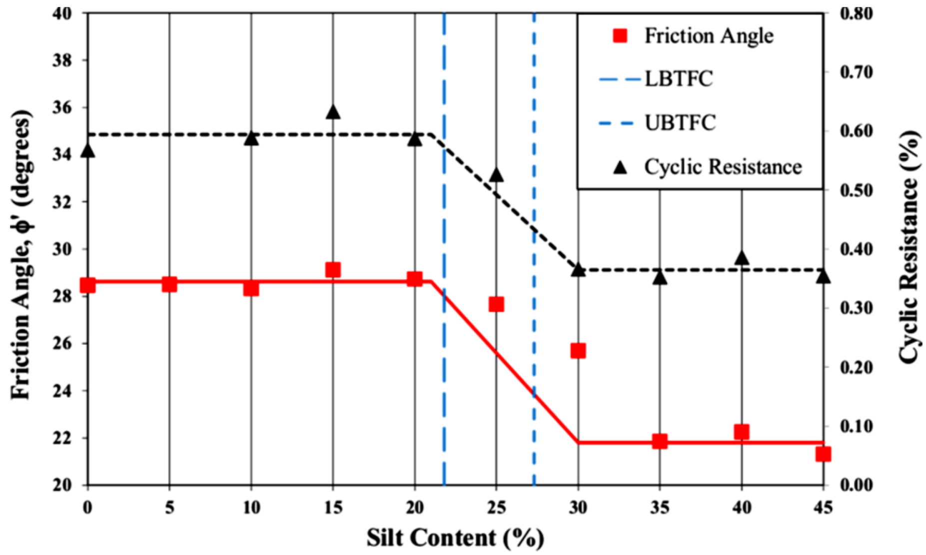

Stark et al. [111] studied the effect of clay fraction (CF), plasticity limit (LL), and liquid limit (LL) on the drained residual and fully softened shear strengths of soil mixtures. They found out that the friction angle correlates better by using the liquid limit instead of activity, and that the plastic limit does not correlate well with the friction angle. Stark et al. (2005) divided the soils into three groups based on clay fractions (CF) [CF < 25%, 25% < CF < 45%, and CF > 50%] to account for three different shearing behaviors [rolling (or turbulent), transitional, and sliding, respectively], as suggested by Lupini et al. [41] (see Figure 51 and Figure 52). Accordingly, they proposed empirical equations for each CF group based on LL and confining pressure.

Figure 51. Results of ring shear tests on sand-bentonite mixtures [41]

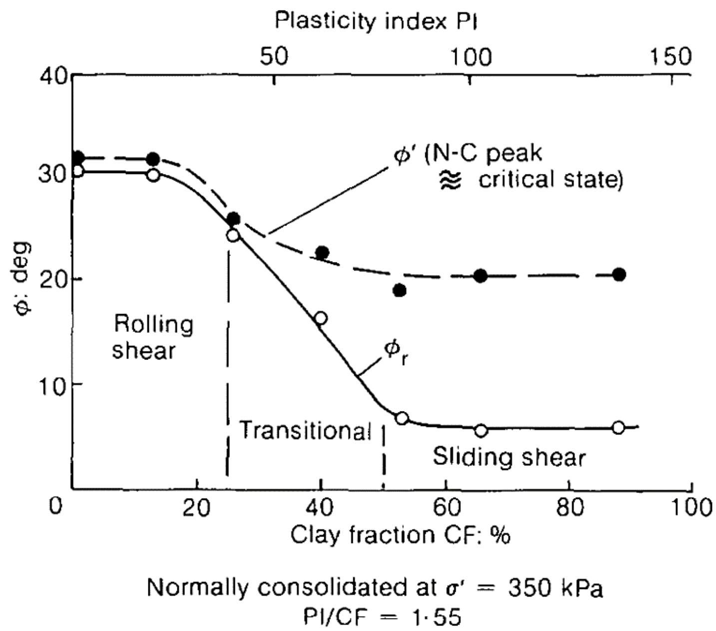

Figure 52. Shear strength of soils with different clay size fractions (a) residual (b) fully softened [41]

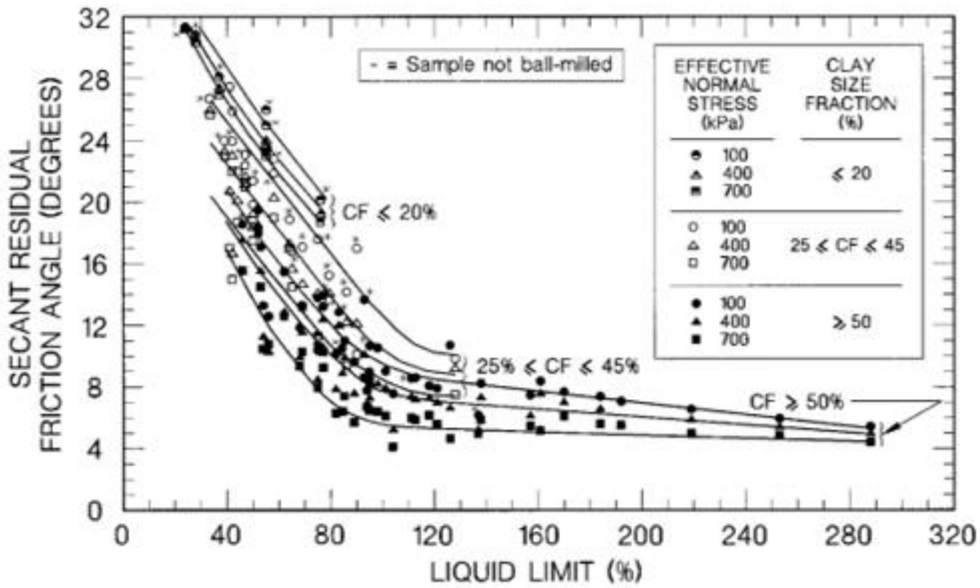

(a)

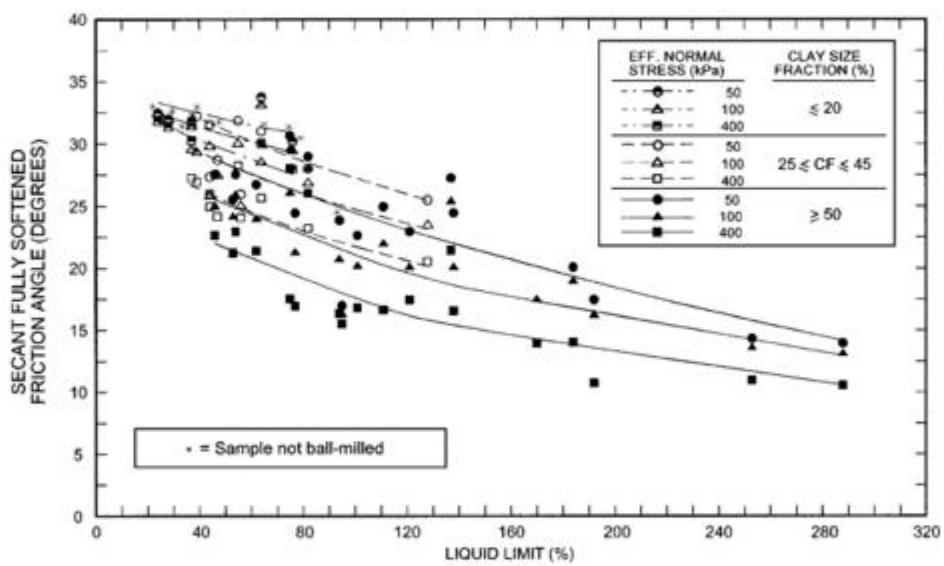

(b)

Based on a review of several research studies in the literature and the results of this study, the researchers can propose the following on the behavior of sand-fines soil mixtures:

1. The threshold of fines content (F_{thr}) beyond which the sand soils mixed with fines properly behave as fine-grained soils with sliding shearing mode is 35%. When the fines content is dominated by clay fraction, the sand-fines mixture will behave as clay-like cohesive soils, and when the fines content is dominated by silt soil, the sand-fines mixtures will behave as silt-like soil.
2. For sand soils mixed with less than 25% of fines content, the sand-fines mixture will properly behave as sand soil with turbulent shearing mode.
3. For sand soils with 25% < fines content < 35%, the sand soil behavior will be within transitional shearing mode, which contains both sliding and turbulent shearing simultaneity that occurs at mixtures with no dominant particles.

Summary and Conclusions

- This study was performed to evaluate the effect of fines content on the internal friction angle (ϕ) of sand soils mixed with fines typically encountered in Louisiana; evaluate the effect of fines content on the interface friction angle (δ) between sand soils mixed with fines and the concrete pile face; and try to determine the threshold percentage of fines content beyond which the sand soils mixed with fines will behave as cohesive soils, rather than cohesion-less soils.
- The study also focused on enhancing the Schmertmann SPT-ϕ correlation equation and chart to estimate the ϕ considering fines content and other soil parameters. To achieve these objectives, a comprehensive laboratory testing program, including both small and large direct shear tests, was performed on sand mixed with different percentages of fines content. Small direct shear tests were performed to evaluate the internal friction angle (ϕ) for sand soils mixed with different fines contents (10%, 20%, 30%, 40%, 50%, and 70%), different relative densities, and different moisture contents (omc, omc+2%, omc+4%, omc+6%), while large direct shear tests were conducted to investigate the interface friction angle (δ) between sand soil mixed with fines and the concrete pile surface. Four different soils (Soil 2 to Soil 5) were employed to mix the original sand soil (Soil 1) with fines at different specified fines content. Different fines contents, relative densities, moisture contents, soil mixtures/gradations, and confining stresses were considered to determine the effect of fines content on both the ϕ and δ. Additionally, the study involved advanced techniques, such as the Scanning Electron Microscope (SEM), to examine the particle shapes and measure the roundness within the experimental soil mixtures. The results of these tests were used to develop non-linear regression equations between the fines (silt) content, fine sand content, relative density, moisture content, roundness, and ϕ. Artificial Neural Network (ANN) models were also developed to estimate the ϕ of the sand-fines mixtures. Two problematic sites in Louisiana (Boeuf River Bridge and Tangipahoa River Bridge replacement sites) with a high percentage of fines (primarily silts) were used to verify the developed regression equations. Results from the literature and this study were also explored to provide insight into the factors governing the critical threshold of fines content and guidelines to evaluate the threshold percentage of fines content (silt or clay) beyond which sand soils mixed with fines will behave as silty or cohesive clayey soils. Based on these findings, the following conclusions can be made:

- The results of this study showed that the internal friction angle (ϕ) of sand mixtures and the interface friction angle (δ) between sand mixtures and the concrete pile face for all sand-fines mixtures decreased when increasing the fines content (mainly silt content), decreased when increasing the fine sand content, decreased when increasing the moisture content, and decreased when decreasing the relative density.
- The coefficient of interface friction [$\tan(\delta)/\tan(\phi)$] between the sand soil mixtures and concrete surface range from 0.7 to 0.76 (average = 0.73) for Soil 1 and Soil 2 mixtures, from 0.65 to 0.77 (average = 0.69) for Soil 1 and Soil 3 mixtures, from 0.66 to 0.70 (average = 0.68) for Soil 1 and Soil 4 mixtures, and from 0.66 to 0.70 (average = 0.68) for Soil 1 and Soil 5 mixtures.
- The results showed that the internal friction angle (ϕ) corresponding to the SPT values for the different soil mixtures are lower than the values obtained from the original Schmertmann SPT-ϕ chart; thus, the chart lines are shifted toward the right to capture the effect of fines content (mainly silt content) on SPT(N_{60})-ϕ correlations. The SPT-ϕ charts were modified to include the effect of different fines content on various sand-fines soil mixtures.
- A weighted average roundness to describe the shape of particles was introduced and calculated for the various sand-fines mixtures.
- The results of the ϕ from small direct shear tests were first used to modify the Schmertmann ϕ-N_{60} equation for different fines contents (10%, 20%, 30%, 40%, 50%, 60%, and 70%) without including other variables. Bivariate correlation analysis using SPSS Software was performed to measure the correlation and the significance of the resulting parameters.
- The general ϕ-N_{60} equation for the Schmertmann equation was then modified to include the effect of four input parameters: silt content, fine sand content, water content, and roundness. Several non-linear regression models were generated to develop the most accurate model for estimating the friction angle (ϕ) of the sand-fines mixtures. Two category input sets were explored to develop the regression models of the ϕ. One set included water content, and the other set did not. The results clearly demonstrated that using the silt content, fine sand content, and water content in the modified Schmertmann equation for Category 1 models, or using only the silt content and fine sand content parameters in the modified Schmertmann equation for Category 2 models, will give a better prediction of the ϕ for the sand-fines mixtures.

- The Japan Road Association (JRA) ϕ-N_{60} model was also modified to include the effect of fine contents by adding the same parameters used in the modified Schmertmann models for the two category input sets. One set included water content, and the other set did not. Again, the results showed that separating the input parameters of silt content and fine sand content (in both Category 3 and Category 4 models), rather than combining them together, would give the most accurate ϕ prediction of the sand-fines mixtures.

- Several Artificial Neural Network (ANN) models were developed to enhance the accuracy of estimating the internal friction angle (ϕ) of the sand-fines mixtures using seven input parameters. The results show that the ANN Type 4 models that considered silt and fine sand contents separately and included roundness (R) are considered the most accurate, followed by the ANN Type 7 models, which also considered silt and fine sand contents separately, but did not include R.

- A reduction factor (ψ) was introduced and calculated to account for the effect of silt and fine sand contents, which represent the ratio between the interface coefficient of friction [$\tan(\delta)/\tan(\phi)$] for clean coarse/medium sand and sand with fines content. Two equations for calculating ψ were introduced. The results suggested that a sand mixture with approximately 60% silt or approximately 20% fine sand will reduce the interface coefficient of friction to approximately 80% of the value for clean sand [$\tan(\delta)/\tan(\phi)$]$_{(\text{Clean sand})}$.

- Two problematic project sites with sand soil mixed with a high percentage of fines (primarily silts) were used to verify the developed ϕ-N_{60} models. The results show that the modified Schmertmann and JRA ϕ-N_{60} models gave good estimates of the ϕ for sand-silt mixtures, with an error of $\leq$ 5% for the Boeuf River Bridge replacement site and an error of $<\pm$ 10% for the Tangipahoa River Bridge replacement site.

- General guidelines were provided to assess the behavior of sand soils mixed with fines content (FC). The critical threshold of fines contents (F_{thr}) beyond which the sand soils mixed with fines will properly behave as fine-grained soils is 35%. When the FC is dominated by clay fraction, the sand-fines mixture will behave as a clay-like cohesive soil, and when the fines content is dominated by silt soil, the sand-fines mixtures will behave as silt-like soil. For sand soils with FC < 25%, the sand-fines mixture will properly behave as sand soil. However, for sand soils with 25% < FC < 35%, the sand soil will behave within a transitional shearing mode that contains both sliding and turbulent shearing simultaneity.

Recommendations

Based on the results of this research study, the following recommendations are offered to DOTD engineers:

- It is highly recommended that DOTD geotechnical design engineers utilize the modified Schmertmann and Japan Road Association (JRA) of ϕ-N_{60} correlation equations developed in this study based on non-linear regression analysis. Both can be used to estimate the internal friction angle (ϕ) for sand mixed with fines content in Louisiana soils for subsurface soil characterization, as well as for the analysis and design of different geotechnical engineering problems and infrastructures, such as shallow and deep foundations.
- It is recommended that DOTD geotechnical design engineers utilize the developed ANN prediction models to estimate the ϕ for sand mixed with fines content in Louisiana soils for subsurface soil characterization, as well as for the analysis and design of different geotechnical engineering problems and infrastructures, such as shallow and deep foundations.
- In order to be able to use the developed ϕ-N_{60} correlation equations to estimate the internal friction angle (ϕ) from SPT tests for problematic sites, it is necessary to include sieve #40 (425µm) and sieve #200 (75 µm) in the sieve analysis to establish the grain size distribution and evaluate the fine sand content. It is also recommended to perform the hydrometer tests to evaluate the silt content. These two parameters (fine sand content and silt content) are needed as inputs for the developed ϕ-N_{60} equations.
- It is recommended that DOTD design engineers use the values of internal friction angles (ϕ) and interface friction angles (δ) estimated using the modified Schmertmann, modified JRA, and ANN ϕ-N_{60} correlations. It is also recommended that they utilize the coefficient of interface friction for the design of piles in problematic sites with high fines content, and that they compare the estimated pile capacities with the measured capacities from pile load tests.
- It is recommended to perform additional experimental work on sand-fines mixtures to more accurately evaluate the threshold of fines content (clay, silt, or both) beyond which the sand soils mixed with fines will behave differently than clean sand with fines content <5%. This evaluation should include three criteria, one each for sand mixed with clay fines, sand mixed with silty fines, and sand mixes with clay + silt fines.

Acronyms, Abbreviations, and Symbols

Term	Description
ANN	Artificial Neural Network
C	Cohesion
c'	Effective cohesion
CF	Clay Fraction
CON	Convexity
CPT	Cone Penetration Test
CRF	Coarse fraction
C_u	Coefficient of uniformity
DOTD	Department of Transportation and Development
D_r	Relative density
DST	Direct shear test
D_{50}	Mean grain size
e_{eq}	Equivalent void ratio
e_g	Inter-granular void ratio
EL	Elongation
e_{max}	Maximum void ratio
e_{max-f}	Maximum void ratio for pure fines
e_{max-s}	Maximum void ratio for pure sand
e_{min}	Minimum void ratio
e_{min-f}	Minimum void ratio for pure fines
e_{min-s}	Minimum void ratio for pure sand
e_o	Initial void ratio
e_f	Void ratio for pure fines
e_s	Void ratio for pure sand

Term	Description
FC	Fines Content
F_{fine}	fines content
FHWA	Federal Highway Administration
f_s	Skin resistance
F_{thr}	Threshold fines content
G_s	Specific Gravity
kPa	Kilopascal
ICP	Inductively Coupled Plasma
$(I_D)_s$	Relative density of sand in mixture
LL	Liquid limit
LTRC	Louisiana Transportation Research Center
N	SPT number
N_{60}	Corrected SPT number for 60% efficiency
N_{70}	Corrected SPT number for 70% efficiency
$(N_1)_{60}$	Corrected SPT number for overburden pressure
Omc	Optimum moisture contents
p_a	Atmospheric pressure
PI	Plasticity index
PL	Plastic limit
Pcf	Pounds per cubic foot
Psi	Pounds per square inch
q_c	Cone tip resistance
R	Roundness
R^2	Coefficient of determination
R_{avg}	Weighted average roundness
R_f	Friction ratio

Term	Description
$R_{Fines,}$	Roundness of fines
$R_{Fine\ sand}$	Roundness of fine sand
$R_{m\&c}$	Roundness of medium and course sand
RMSE	Root mean square of error
S^{*}	Critical fines content
SEM	Scanning Electron Microscope
Si+FS	Silt + fine sand
SM	Silty sand
S_{max}	Fines content at which fines begin to separate coarse particles from one another
SP	Poor sand
SPT	Standard Penetration Test
S_u	Undrained shear strength
USCS	Unified Soil Classification System
V	Volume
W	Water content
W_s	Solid weight
ϕ	Internal friction angle
ϕ'	Effective friction angle
ϕ_{cr}	Critical friction angle
ϕ'_p	Peak friction angle
ϕ_R	Residual friction angle
δ	Interface friction angle
γ_{dmax}	Maximum dry unit weight
ψ	Reduction factor
$\sigma h'$	Effective horizontal overburden pressure

Term	Description
σ_{vo}'	Effective overburden pressure

References

[1] J. W. Dunhanm, "Dunhanm, J.W. (1954). Pile foundation for buildings," *Journal of the Soil Mechanics and Foundation Division, ASCE,* vol. 80, no. 1, pp. 1-21, 1954.

[2] R. B. Peck, W. E. Hanson and T. H. Thornburn, Foundation Engineering, New York: John Wiley & Sons. Inc, 1974.

[3] G. G. Meyerhof, "Discussion on research on determining the density of sands by spoon penetration testing," in *4th International Conference on Soil Mechanics and Foundation Engineering*, London, 1957.

[4] J. H. Schmertmann, "Measurement of in situ shear strength, SOA Report," in *ASCE Conference on In Situ Measurement of Soil Properties*, Raleigh, NC, 1975.

[5] Y. Shioi and J. Fukui, "Application of N-Value to Design of Foundation in Japan. 2nd ESOPT," in *2nd European Symposium on Penetration Testing (ESOPT II)*, Amsterdam, 1982.

[6] T. F. Wolff, "Pile capacity prediction using parameter functions," in *Predicted and observed axial behavior of piles: results of a pile prediction symposium*, Evanston, IL, 1989.

[7] Japan Road Association, Specifications for highway bridges, Part IV. Seismic design, 1990.

[8] F. H. Kulhawy and P. W. Mayne, "Manual on estimating soil properties for foundation design," Geotechnical Engineering Group, Ithaca, NY, 1990.

[9] M. Hatanaka and A. Uchida, "Empirical correlation between penetration resistance and internal friction angle of sandy soils," *Soils and foundations,* vol. 36, no. 5, pp. 1-9, 1996.

[10] W. C. Villet and J. K. Mitchell, "October. Cone resistance, relative density and friction angle," *In Cone penetration testing and experience ,* pp. 178-208, 1981.

[11] P. K. Robertson and R. G. Campanella, "Interpretation of cone penetration tests," *Canadian Geotechnical Journal,* vol. 20, no. 4, pp. 718-733, 1983.

[12] G. Ricceri, P. Simonini and S. Cola, "Applicability of piezocone and dilatometer to characterize the soils of the Venice Lagoon," *Geotechnical & Geological Engineering,* vol. 20, no. 2, pp. 89-121, 2002.

[13] J. Lee, R. Salgado and J. A. H. Carraro, "Stiffness degradation and shear strength of silty sands," *Canadian Geotechnical Journal,* vol. 41, no. 5, pp. 831-843, 2004.

[14] I. W. Searle, "September. The interpretation of Begemann friction jacket cone results to give soil types and design parameters," in *7th European Conference on Soil Mechanics and Foundation Engineering (ECSMFE)*, Brighton, England, 1979.

[15] S. C. Murley and H. Hettiarachchi, "Predicting shear strength properties for low-sensitivity granular-cohesive soils from SPT results," in *Geo-Frontiers 2011: Advances in Geotechnical Engineering*, Dallas, Texas, 2011.

[16] W. N. Houston and J. Mitchell, "Property interrelationships in sensitive clays," *Journal of the soil Mechanics and Foundations Division,* vol. 95, no. 4, pp. 1037-1062, 1969.

[17] H. Hettiarachchi and T. Brown, "Use of SPT blow counts to estimate shear strength properties of soils: energy balance approach," *Journal of Geotechnical and Geoenvironmental Engineering,* vol. 135, no. 6, pp. 830-834, 2009.

[18] J. Lee, M. Kim and D. Kyung, "Estimation of lateral load capacity of rigid short piles in sands using CPT results," *Journal of Geotechnical and Geoenvironmental Engineering,* vol. 136, no. 1, pp. 48-56, 2010.

[19] M. D. Bolton, "The strength and dilatancy of sands," *Geotechnique,* vol. 36, no. 1, p. 65–78, 1986.

[20] C. R. Wener, Standard penetration test correlations for Las Vegas soils (Doctoral dissertation), Las Vegas, Nevada: University of Nevada, 1995.

[21] Z. C. Moh, C. T. Chin, C. J. Liu and S. M. Woo, "Engineering correlations for soil deposits in Taipei," *Journal of the Chinese Institute of Engineers,* vol. 12, no. 3, pp. 273-283, 1989.

[22] P. Salari, G. Lashkaripour and M. Ghafoori, "Presentation of Empirical Equations for Estimating Internal Friction Angle of SP and SC Soils in Mashhad, Iran Using Standard Penetration and Direct Shear Tests and Comparison with Previous Equations," *International Journal of Geography and Geology,* vol. 4, no. 5, pp. 89-95, 2015.

[23] H. Mujtaba, K. Farooq, N. Sivakugan and B. M. Das, "Evaluation of relative density and friction angle based on SPT-N values," *KSCE Journal of Civil Engineering,* vol. 22, no. 2, pp. 572-581, 2018.

[24] M. Cubrinovski and K. Ishihara, "Empirical correlation between SPT N-value and relative density for sandy soils," *Soils and Foundations,* vol. 39, no. 5, pp. 61-71, 1999.

[25] M. Jamiolkowski, "Penetration resistance and liquefaction of sands," in *11th International Conference of Soil Mechanics and Foundation Engineering*, San Francisco, CA, 1985.

[26] H. J. Gibbs and W. G. Holtz, "Research on Determining the Density of Sands by Spoon Penetration Testing," in *4th ICOSOMEF*, London, 1957.

[27] A. Haldar and W. H. Tang, "Uncertainity Analysis of Relative Density," *Journal of the Geotechnical Engineering Division,* vol. 105, no. 7, pp. 899-904, 1979.

[28] R. B. Peck and A. R. Bazaraa, "Discussion of settlement of spread-footings on sand," *Soil Mechanics and Foundations Division,* vol. 95, no. SM3, pp. 305-309, 1969.

[29] A. Skempton, "Standard penetration test procedures and the effects in sands of overburden pressure, relative density, particle size, ageing and overconsolidation," *Geotechnique,* vol. 36, no. 3, pp. 425-447, 1987.

[30] K. Tokimatsu and Y. Yoshimi, "Empirical correlation of soil liquefaction based on SPT N-value and fines content," *Soils and Foundations,* vol. 23, no. 4, pp. 56-74, 1983.

[31] M. Cubrinovski and K. Ishihara, "Correlation between penetration resistance and relative density of sandy soils," in *5th International Conference on Soil Mechanics and Geotechnical Engineering*, Leiden, 2001.

[32] G. Baldi, "Interpretation of CPT's and CPTU's. 2nd Part: Drained penetration of sands," in *The IV International Geotechnical Seminar*, Singapore, 1986.

[33] R. Lancellotta, "Analisi di adidabilita in ingegneria geotecnica," in *Atti Instituto Scienza Costruzioni*, Politecnico di Torino, 1983.

[34] M. Jamiolkowski, C. C. Ladd, J. T. Germaine and R. Lancelotta, "New developments in field and laboratory testing of soils," in *11th International Conference on Soil Mechanics and Foundation Engineering*, San Francisco, CA, 1985.

[35] M. Jamiolkowski, D. C. Presti and M. Manassero, "Evaluation of Relative Density and Shear Strength of Sands from CPT and DMT," in *Symposium on Soil Behavior and Soft Ground Construction Honoring Charles C. "Chuck" Ladd*, Cambridge, MA, 2001.

[36] M. Ghali, M. Chekired and M. Karray, "Framework to improve the correlation of SPT-N and geotechnical parameters in sand," *Acta Geotechnica,* vol. 15, no. 3, pp. 735-75, 2020.

[37] J. A. Carraro, M. Prezzi and R. Salgado, "Shear strength and stiffness of sands containing plastic or nonplastic fines," *Journal of Geotechnical and Geoenvironmental Engineering,* vol. 135, no. 9, pp. 1167-1178, 2009.

[38] J. A. Yamamuro and F. M. Wood, "Effect of depositional method on the undrained behavior and microstructure of sand with silt," *Soil Dynamics and Earthquake Engineering,* vol. 24, no. 9-10, pp. 751-760, 2004.

[39] S. S. Vinayagam, Entrepreneurial behaviour of agri-business operators in Kerla. Ph.D. Thesis, Kerala, India: Kerala Agricultural University, 1998.

[40] T. C. Kenny, "Residual strength of mineral mixtures," in *International Conference on Soil Mechanics*, Vienna, Austria, 1977.

[41] J. F. Lupini, A. E. Skinner and P. R. Vaughan, "The drained residual strength of cohesive soils," *Geotechnique,* vol. 31, no. 2, pp. 181-213, 1981.

[42] V. N. Georgiannou, J. B. Burland and D. W. Hight, "The undrained behaviour of clayey sands in triaxial compression and extension," *Geotechnique,* vol. 40, no. 3, pp. 431-449, 1990.

[43] T. D. Pitman, P. K. Robertson and D. C. Sego, "Influence of fines on the collapse of loose sands," *Canadian Geotechnical Journal,* vol. 31, no. 5, pp. 728-739, 1994.

[44] P. V. Lade, C. D. Liggio and J. A. Yamamuro, "Effects of non-plastic fines on minimum and maximum void ratios of sand," *Geotechnical Testing Journal,* vol. 21, no. 1, pp. 336-347, 1998.

[45] R. Salgado, P. Bandini and A. Karim, "Shear strength and stiffness of silty sand," *Journal of Geotechnical and Geoenvironmental Engineering,* vol. 126, no. 5, pp. 451-462, 2000.

[46] M. M. Monkul and G. Ozden, "Compressional behavior of clayey sand and transition fines content," *Engineering Geology,* vol. 89, no. 3-4, pp. 195-205, 2007.

[47] Q. T. Ni, T. S. Tan, G. R. Dasari and D. W. Hight, "Contribution of fines to the compressive strength of mixed soils," *Géotechnique,* vol. 54, no. 9, pp. 561-569, 2004.

[48] U. G. Kim, M. Hyodo, C. Koga and R. P. Orense, "Effect of fines content on the monotonic shear behavior of sand-clay mixtures," *Geomechanics and Geotechnics of Particulate Media,* pp. 133-138, 2017.

[49] N. Ismael, "Influence of Fines on the Properties of Arid Climate Sand Deposits," in *Unsaturated Soils 2006*, Carefree, AZ, 2006.

[50] Y. Xiao, H. Liu, Y. Chen and J. Chu, "Strength and dilatancy of silty sand," *Journal of Geotechnical and Geoenvironmental Engineering,* vol. 140, no. 7, 2014.

[51] J. H. Yin, "Properties and behaviour of Hong Kong marine deposits with different clay contents," *Canadian Geotechnical Journal,* vol. 36, no. 6, pp. 1085-1095, 1999.

[52] L. H. Mollins, D. I. Stewart and T. W. Cousens, "Drained strength of bentonite-enhanced sand," *Geotechnique,* vol. 49, no. 4, pp. 523-528, 19999.

[53] D. I. Stewart, T. W. Cousens, P. G. Studds and Y. Y. Tay, "Design parameters for bentonite-enhanced sand as a landfill liner," *Proceedings of the Institution of Civil Engineers-Geotechnical Engineering,* vol. 137, no. 4, pp. 189-195, 1999.

[54] M. M. Haider, B. B. Huat and M. A. Malek, "Effect of mixing fine sand on the drained shear strength of completely decomposed granite soil," *GEOMATE Journal,* vol. 1, no. 1, pp. 10-18, 2011.

[55] Y. Mahmoudi, A. Cherif Taiba, M. Belkhatir, A. Arab and T. Schanz, "Influence of the equivalent intergranular void ratio on shear strength of sand-silt mixtures," in *In Colloque International sur la Caratérisation des Matériaux et Structures*, Tizi Ouzou, Algérie, 2014.

[56] Y. Li, A. Aydin, Q. Xu and J. Chen, "Constitutive behavior of binary mixtures of kaolin and glass beads in direct shear," *KSCE Journal of Civil Engineering,* vol. 16, no. 7, pp. 1152-1159, 2012.

[57] Y. Li, "Effects of particle shape and size distribution on the shear strength behavior of composite soils," *Bulletin of Engineering Geology and the Environment,* vol. 72, no. 3, pp. 371-381, 2013.

[58] C. A. Bareither, T. B. Edil, C. H. Benson and D. M. Mickelson, "Geological and physical factors affecting the friction angle of compacted sands," *Journal of Geotechnical and Geoenvironmental Engineering,* vol. 134, no. 10, pp. 1476-148, 2008.

[59] T. Ueda, T. Matsushima and Y. Yamada, "Effect of particle size ratio and volume fraction on shear strength of binary granular mixture," *Granular Matter,* vol. 13, no. 6, pp. 731-742, 2011.

[60] S. Arasan, S. Akbulut and A. S. Hasiloglu, "The relationship between the fractal dimension and shape properties of particles," *KSCE Journal of Civil Engineering,* vol. 15, no. 7, pp. 1219-1225, 2011.

[61] N. Stark, A. E. Hay, R. Cheel and C. B. Lake, "The impact of particle shape on the angle of internal friction and the implications for sediment dynamics at a steep, mixed sand–gravel beach," *Earth Surface Dynamics,* vol. 2, no. 2, pp. 469-480, 2014.

[62] L. E. Vallejo and R. Mawby, "Porosity influence on the shear strength of granular material–clay mixtures," *Engineering Geology,* vol. 58, no. 2, pp. 125-136, 2000.

[63] A. B. Abderrahim and J. P. Tisot, "Friction at the cohesionless soil-structure interface: effect of various parameters according to a classic study and a new approach," *Geotechnical Testing Journal,* vol. 16, no. 1, pp. 122-130, 1993.

[64] T. D. O'Rourke, S. J. Druschel and A. N. Netravali, "Shear strength characteristics of sand-polymer interfaces," *Journal of Geotechnical Engineering,* vol. 116, no. 3, pp. 451-469, 1990.

[65] W. F. Brumund and G. A. Leonards, "Experimental study of static and dynamic friction between sand and typical construction materials," *Journal of Testing and Evaluation,* vol. 1, no. 2, pp. 162-165, 1973.

[66] M. Uesugi and H. Kishida, "Frictional resistance at yield between dry sand and mild steel," *Soils and Foundations,* vol. 26, no. 4, pp. 139-149, 1986.

[67] Y. B. Acar, H. T. Durgunoglu and M. T. Tumay, "Interface properties of sands," *Journal of the Geotechnical Engineering Division,* vol. 108, no. 4, pp. 648-654, 1982.

[68] M. Uesugi, H. Kishida and Y. Uchikawa, "Friction between dry sand and concrete under monotonic and repeated loading," *Soils and Foundations,* vol. 30, no. 1, pp. 115-128, 1990.

[69] D. R. Levacher and J. G. Sieffert, "Tests on model tension piles," *Journal of Geotechnical Engineering,* vol. 110, no. 2, pp. 1735-1748, 1984.

[70] C. S. Desai, E. C. Drumm and M. M. Zaman, "Cyclic testing and modeling of interfaces," *Journal of Geotechnical Engineering,* vol. 111, no. 6, pp. 793-815, 1985.

[71] Y. Yoshimi, "Friction between sand and metal surface. In Proc. of," in *10th Int. Conf. on Soil Mechanics and Foundation Engineering*, Stockholm, 1981.

[72] I. Noorany, "Side Friction of Piles in Calcareous Sands," in *Proceedings of the Recordings of The Elev11th International Conference on Soil Mechanics And Foundation Engineering*, San Francisco, CA, 1985.

[73] R. J. Jardine, B. M. Lehane and S. J. Everton, "Friction coefficients for piles in sands and silts," in *Offshore site investigation and foundation behavior*, Springer, 1993.

[74] D. Porcino, V. Fioravante, V. N. Ghionna and S. Pedroni, "Interface behavior of sands from constant normal stiffness direct shear tests," *Geotechnical Testing Journal,* vol. 26, no. 3, pp. 289-301, 2003.

[75] B. Tiwari and A. R. Al-Adhadh, " Influence of relative density on static soil–structure frictional resistance of dry and saturated sand," *Geotechnical and Geological Engineering,* vol. 32, no. 2, pp. 411-427, 2014.

[76] M. Uesugi and H. Kishida, "Frictional resistance at yield between dry sand and mild steel," *Soils and Foundations,* vol. 26, no. 4, pp. 139-149, 1986.

[77] F. Han, E. Ganju, R. Salgado and M. Prezzi, "Effects of interface roughness, particle geometry, and gradation on the sand–steel interface friction angle," *Journal of Geotechnical and Geoenvironmental Engineering,* vol. 144, no. 12, p. 04018096, 2018.

[78] S. G. Paikowsky, C. M. Player and P. J. Connors, "A dual interface apparatus for testing unrestricted friction of soil along solid surfaces," *Geotechnical Testing Journal,* vol. 18, no. 2, pp. 168-193, 1995.

[79] K. S. Subba Rao, K. S. Rao, M. M. Allam and R. G. Robinson, "Interfacial friction between sands and solid surfaces," *Institution of Civil Engineers-Geotechnical Engineering,* vol. 131, no. 2, pp. 75-82, 1998.

[80] J. G. Potyondy, "Skin friction between various soils and construction materials," *Geotechnique,* vol. 11, no. 4, pp. 339-353, 1961.

[81] V. S. Quinteros, R. Dyvik and N. Mortensen, "Interface friction angle soil-on-steel from ring shear tests on offshore North Sea sands," in *Geotechnical Frontiers 2017*, Orlando, Florida, 2017.

[82] T. Y. Ho, R. J. Jardine and N. Anh-Minh, "Large-displacement interface shear between steel and granular media," *Géotechnique,* vol. 61, no. 3, pp. 221-234, 2011.

[83] J. T. Tabucanon, D. W. Airey and H. G. Poulos, "Pile skin friction in sands from constant normal stiffness tests," *Geotechnical Testing Journal,* vol. 18, no. 3, pp. 350-364, 1995.

[84] G. Castro, J. L. Enos, J. W. France and S. J. Poulos, "Liquefaction induced by cyclic loading," National Science Foundation, Washington, D. C., 1982.

[85] J. A. Sladen, R. D. D'hollander and J. Krahn, "The liquefaction of sands, a collapse surface approach," *Canadian Geotechnical Journal,* vol. 22, no. 4, pp. 564-578, 1985.

[86] T. F. Liu, V. S. Quinteros, R. J. Jardine, J. A. Carraro and J. Robinson, "A unified database of ring shear steel-interface tests on sandy-silty soils," in *XVII ECSMGE-2019*, Reykjavik, 2019.

[87] F. B. Ferreira, C. S. Vieira and M. Lopes, "Direct shear behaviour of residual soil–geosynthetic interfaces–influence of soil moisture content, soil density and geosynthetic type," *Geosynthetics International,* vol. 22, no. 3, pp. 257-272, 2015.

[88] H. Canakci, M. Hamed, F. Celik, W. Sidik and F. Eviz, "Friction characteristics of organic soil with construction materials," *Soils and Foundations,* vol. 56, no. 6, pp. 965-972, 2016.

[89] Y. Yoshimi, "Friction between sand and metal surface," in *10th Int. Conf. on Soil Mechanics and Foundation Engineering*, Stockholm, 1981.

[90] L. J. Su, Z. W. H., W. B. Chen and X. Jie, "Effects of relative roughness and mean particle size on the shear strength of sand-steel interface," *Measurement,* vol. 122, pp. 339-346, 2018.

[91] Y. Tsubakihara and H. Hideaki, "Frictional Behaviour between Normally Consolidated Clay and Steel by Two Direct Shear Type Apparatuses," *Soils and Foundations,* vol. 33, no. 2, pp. 1-13, 1993.

[92] P. A. A. S. K. Ooi, "Resilient modulus models for compacted cohesive soils," *Transportation Research Record,* vol. 1874, p. 115–124, 2004.

[93] Z. Chik and L. E. Vallejo, "Characterization of the angle of repose of binary granular materials," *Canadian Geotechnical Journal,* vol. 42, no. 2, pp. 683-692, 2005.

[94] V. T. Phan, D. H. Hsiao and P. T. Nguyen, "Effects of Fines Contents on Engineering Properties of Sand-Fines Mixtures," *Procedia Engineering,* vol. 142, pp. 213-220, 2016.

[95] H. J. Gibbs and W. G. Holtz, "Research On Determining The Density of Sands by Spoon Penetration Testing," in *4th International Conference on Soil Mechanics and Foundation Engineering*, London, 1957.

[96] M. Shahin, M. Jasksa and H. Maier, "Recent Advances and Future Challenges for Artificial Neural Systems in Geotechnical Engineering Applications," *Advances in Artificial Neural Systems,* vol. Open Access, pp. 230-243, 2009.

[97] D. E. Rumelhart and J. L. McClleland, "Learning internal representation by error propagation," *MIT Press,* Cambridge, MA, vol. 1, 1986.

[98] I. A. Basheer, Neuromechanistic-Based Modeling and Simulaton of Constitutive Behavior of Fine Grained Soils. Dissertation, Manhattan, KS: Kansas State University, 1998.

[99] R. Hecht-Nielson, "Kolmogrov's mapping neural network existence theorem," in *Proceedings of the 1st IEEE International Joint Conference on Neural Networks*, San Diego, CA, 1987.

[100] Z. Zhang and M. Tumay, "Statistical to fuzzy approach toward CPT soil classification," *Journal of Geotechnical and Geoenvironmental Engineering,* vol. 125, no. 3, pp. 179-186, 1999.

[101] A. W. Skempton and J. Brogan, "Experiments on Piping in Sandy Gravels," *Géotechnique,* vol. 44, pp. 449-460, 1994.

[102] M. Goudarzy, D. König and T. Schanz, "Interpretation of small and intermediate strain characteristics of Hostun sand for various stress states," *Soils and Foundations,* vol. 58, no. 6, pp. 1526-1537, 2018.

[103] D. Sarkar, M. Goudarzy, D. Konig and T. Wichtmann, "Influence of particle shape and size on the threshold fines content," *Soils and Foundations,* vol. 60, pp. 621-633, 2020.

[104] K. Hazirbaba, Pore Pressure Generation Characteristics of Sands and Silty Sands: A Strain Approach. Ph.D. Thesis., Austin, TX: University of Texas at Austin, 2005.

[105] L. Zuo and B. A. Baudet, "Determination of the transitional fines content of sand-non plastic fines mixtures," *Soils and Foundations,* vol. 55, no. 1, pp. 213-219, 2015.

[106] P. Kaothon, S.H. Lee, Y.T. Choi and C.Y. Yune, "The Effect of Fines Content on Compressional Behavior When Using Sand–Kaolinite Mixtures as Embankment Materials," *Applied Sciences,* vol. 12, no. 6050, 2022.

[107] M. Belkhatir, T. Schanz and A. Arab, "Effect of fines content and void ratio on the saturated hydraulic conductivity and undrained shear strength of sand–silt mixtures," *Environ. Earth Sci.,* vol. 70, p. 2469–2479, 2013.

[108] M. Abadi, M. Maleki and E. Chali, "Investigation of the critical state behavior of unsaturated silty sand with different fine contents in terms of net and effective stresses," *European Journal of Environmental and Civil Engineering,* vol. 28, pp. 1332-1353, 2023.

[109] S. Thevanayagam, "Effect of Fines and Confining Stress on Undrained Shear Strength of Silty Sands," *Journal of Geotechnical and Geoenvironmental Engineering,* vol. 124, no. 6, pp. 479-491, 1998.

[110] C. Polito and E. L. Sibley, "Threshold fines content and behavior of sands with nonplastic silts," *Canadian Geotechnical Journal,* vol. 57, no. 3, pp. 462-465, 2019.

[111] T. D. Stark, H. Choi and S. McCone, "Drained shear strength parameters for analysis of landslides," *Journal of Geotechnical and Geoenvironmental Engineering,* vol. 131, no. 5, pp. 575-588, 2005.

Appendix A
Summary of Direct Shear Test Results

This section presents a comprehensive compilation of results obtained from both small and large direct shear tests performed on various soil mixtures. These tests were conducted to evaluate the mechanical and physical properties of different soil combinations, focusing on varying soil fractions for different soil mixtures. The tables contained herein encompass a range of crucial parameters including cohesion, friction angle, relative density, water content, and dry density. Notably, the tables highlight the coefficients of friction, friction angles, and interface friction angles specific to sand with distinct fine fractions at the soil's optimum moisture content.

Table 42. Coefficient of friction for Soil 1 and Soil 2 mixtures at optimum moisture content

Soil	**Interface Friction angle (δ') (degree)**	**Friction angle (ϕ') (degree)**	**Coefficient of friction Tan(δ')/tan (ϕ')**
Sand with 10% fine	38.3°	31.3°	0.76
Sand with 20% fine	41.3°	31.9°	0.7
Sand with 30% fine	41.6°	32.6°	0.72
Sand with 40% fine	40.0°	32.3°	0.75

Table 43. Large direct shear results for Soil 1 and Soil 3 mixtures

Soil	Dry Density ρ_d (pcf)	Water content (%)	Relative Density (%)	Friction angle (δ') (Degree)	Cohesion (psi)
Sand with 10% fine (Fine Sand%=4.1) (Clay%=1.96) (Silt%= 8)	113.4	10.3	81.3	31.3°	-
	111.2	12.2	69.1	30.7°	-
	107.4	15	57.9	28.9°	-
Sand with 50% fine (Fine Sand%=14.2) (Clay%=9.9) (Silt%= 40.1)	121.7	13	80.1	24.2°	1
	117.5	15.2	61	23°	0.8
	112.8	17.3	53.7	22.6°	0.43
Sand with 70% fine (Fine Sand%=15.2) (Clay%=14) (Silt%= 57)	117.3	12	78.5	21°	1.2
	113.4	14.2	63.3	20.5°	0.8
	109.1	16.2	52.7	20.1°	0.43

Table 44. Small direct shear test results for Soil 1 and Soil 4 mixtures

Soil	Dry unit weight (pcf)	Water content (%)	Relative density (%)	Friction angle (ϕ') (degree)	Cohesion (psi)
Sand with 10% fine (Fine sand%=5.1) (Clay%=2.3) (Silt%= 7.7)	103.1	9.1	87.3	41.4	1.47
	100.7	11.3	76.5	40.3	1.33
	99.8	13	62.9	38.9	1.23
	96.5	15.2	49.3	37.4	1
Sand with 20% fine (Fine sand%=21.3) (Clay%=1.9) (Silt%= 18.1)	104.2	9.6	86.9	39.5	0
	101.9	11.3	75.4	38.5	0
	99.8	13.5	63.3	37.4	0
	97.4	15.5	50.6	35.5	0
Sand with 30% fine (Fine sand%=11.1) (Clay%=6.6) (Silt%= 23.1)	105.1	10.2	86.5	38.0	2.5
	103.2	12.1	74.6	36.5	2.33
	100	14.3	64.2	35.6	1.76
	97.9	16	51.7	34.0	1.26
Sand with 40% fine (Fine sand%=19.6) (Clay%=4.5) (Silt%= 35.5)	106.4	11.3	87.6	36.1	0
	103.7	13.2	76.1	34.7	0
	100.1	15.3	63.8	33.6	0
	98.3	17.4	52.4	31.8	0
Sand with 50% fine (Fine sand%=16.2) (Clay%=11.5) (Silt%= 38.5)	107.8	12	88.3	34.6	3.26
	104	14.4	78.3	33.0	3.1
	100.1	16	63.9	31.6	2.7
	98.3	18.6	53.2	29.8	2.2
Sand with 60% fine (Fine sand%=15.4) (Clay%=6.6) (Silt%= 53.4)	108.8	13.3	89.1	30.5	0
	106.3	15.5	79.3	29.2	0
	102.5	17.5	65.2	27.7	0
	99.8	19.5	54.1	26.0	0
Sand with 70% fine (Fine sand%=19.2) (Clay%=16.1) (Silt%= 53.9)	110.2	14.5	90.5	27.7	5
	108.7	16.3	80.0	25.7	4.6
	105.2	18.6	66.7	24.2	4.1
	101.6	20.2	54.4	21.8	3.9

Table 45. Large direct shear results for Soil 1 and Soil 4 mixtures

Soil	Dry Density ρ_d (pcf)	Water content (%)	Relative Density (%)	Friction angle (ϕ') (Degree)	Cohesion (psi)
Sand with 10% fine (Fine Sand%=5.1) (Clay%=2.3) (Silt%= 7.7)	103.2	9.2	81.3	31.6°	-
	100.7	11.2	69.1	30.2°	-
	99.7	13.2	57.9	29.8°	-
Sand with 50% fine (Fine Sand%=16.2) (Clay%=11.5) (Silt%= 38.5)	107.4	12.1	80.1	27.3°	1
	104	14.2	61	26.18°	0.5
	99.8	16.3	53.7	25.8°	-
Sand with 70% fine (Fine Sand%=19.2) (Clay%=16.1) (Silt%= 53.9)	110.7	14.2	71.5	22.2°	1.3
	108.4	16.2	62.2	21.8°	1
	105	18.4	42.7	20.13°	0.3

Table 46. Coefficient of friction Soil 1 and Soil 4 mixtures at optimum moisture content

Soil	Interface Friction angle (δ') (degree)	Friction angle (ϕ') (degree)	Coefficient of friction Tan(δ')/tan(ϕ')
Sand with 10% fine	31.6°	41.4°	0.7
Sand with 50% fine	27.3°	34.6°	0.67
Sand with 70% fine	22.2°	27.7°	0.66

Table 47. Small direct shear results for Soil 1 and Soil 5 mixtures

Soil	Dry unit weight, γ_d (pcf)	Water content (%)	Relative density (%)	Friction angle (ϕ') (degree)	Cohesion (psi)
Sand with 10% fine (Fine sand%=7.2) (Clay%=2.1) (Silt%= 7.9)	113.4	10.1	81.6	40°	0.9
	111.2	12	71.9	37.7°	0.8
	107.4	15.3	60.4	36.8°	0.6
	102.1	18.1	44.7	35.3°	0.56
Sand with 20% fine (Fine sand%=14.6) (Clay%=2.1) (Silt%= 9.9)	116.2	10.6	83.9	39.6°	0
	114.0	12.8	73.0	37.7°	0
	109.3	15.4	61.2	35.8°	0.63
	105.4	17.4	47.0	34.7°	0.20
Sand with 30% fine (Fine sand%=13.1) (Clay%=6.3) (Silt%= 23.7)	119.1	11	86.7	38.9°	1.47
	116.9	14.3	76.2	37.4°	1.3
	111	16.6	63.0	35°	1
	108.5	18.9	50.7	33.3°	0.33
Sand with 40% fine (Fine sand%=17.7) (Clay%=4.2) (Silt%= 27.8)	120.4	12.2	87.3	37.4°	0.14
	117.3	14.6	77.3	35.0°	0.18
	112.1	16.7	63.4	33.3°	0.62
	108.2	18.8	52.4	32.4°	0.68
Sand with 50% fine (Fine sand%=18.2) (Clay%=10.5) (Silt%= 39.5)	121.7	13	88.4	35.3°	2.4
	117.5	15.2	76.6	33.7°	2.3
	112.8	17.3	64.2	31.3°	2
	108	19	53.4	31.0°	1.8
Sand with 60% fine (Fine sand%=21.5) (Clay%=5.8) (Silt%= 54.2)	119.9	14.7	90.2	33.4°	0.76
	115.8	16.8	76.5	30.7°	2.0
	111.4	18.6	66.5	28.3°	1.3
	107.4	20.5	53.6	26.5°	1.3
Sand with 70% fine (Fine sand%=20.2) (Clay%=14.7) (Silt%= 55.3)	117.9	16.1	90.9	30.9°	3.5
	114.3	18.2	77.4	27.3°	3.2
	110.1	20.3	65.2	24.7°	2.9
	106.6	22	53.7	21.8°	2.6

Table 48. Large direct shear results for Soil 1 and Soil 5 mixtures

Soil	Dry Density ρ_d (pcf)	Water content (%)	Relative Density (%)	Friction angle (δ') (Degree)	Cohesion (psi)
Sand with 10% fine (Fine Sand%=7.2) (Clay%=2.1) (Silt%= 7.9)	103.2	10	81.3	30.5°	-
	100.7	12	69.1	30.2°	-
	99.7	15.2	57.9	29.4°	-
Sand with 50% fine (Fine Sand%=18.2) (Clay%=10.5) (Silt%= 39.5)	107.4	11	80.1	25.4°	1.1
	104	14.2	61	24.1°	0.57
	99.8	18.3	53.7	24°	-
Sand with 70% fine (Fine Sand%=20.2) (Clay%=14.7) (Silt%= 55.3)	110.7	16.2	71.5	18.5°	1.32
	108.4	18.2	62.2	18°	0.8
	105	20.3	42.7	17.7°	0.6

Table 49. Coefficient of friction Soil 1 and Soil 5 Mixtures at optimum moisture content

Soil	Interface Friction angle (δ') (degree)	Friction angle (ϕ') (degree)	Coefficient of friction Tan(δ')/tan(ϕ')
Sand with 10% fine	30.°	40°	0.7
Sand with 50% fine	25.4°	35.3°	0.67
Sand with 70% fine	18.5°	27°	0.66

Appendix B
Small Direct Shear Test Results

This section presents a comprehensive compilation of tables showcasing the outcomes of small direct shear tests conducted on various soil mixtures with different soil fractions. The tables elucidate the intricate interplay between soil shear stress, soil displacement, soil normal stress, and soil horizontal displacement. These results provide a detailed perspective on how different soil mixtures respond under distinct conditions, offering insights into their shear behavior and displacement characteristics.

Figure 53. Small direct shear results for Soil 1 and Soil 2 mixtures at fine content = 10%, moisture content = 15.9%: (a) shear stress vs normal stress; (b) shear stress vs horizontal displacement; (c) vertical displacement vs horizontal displacement

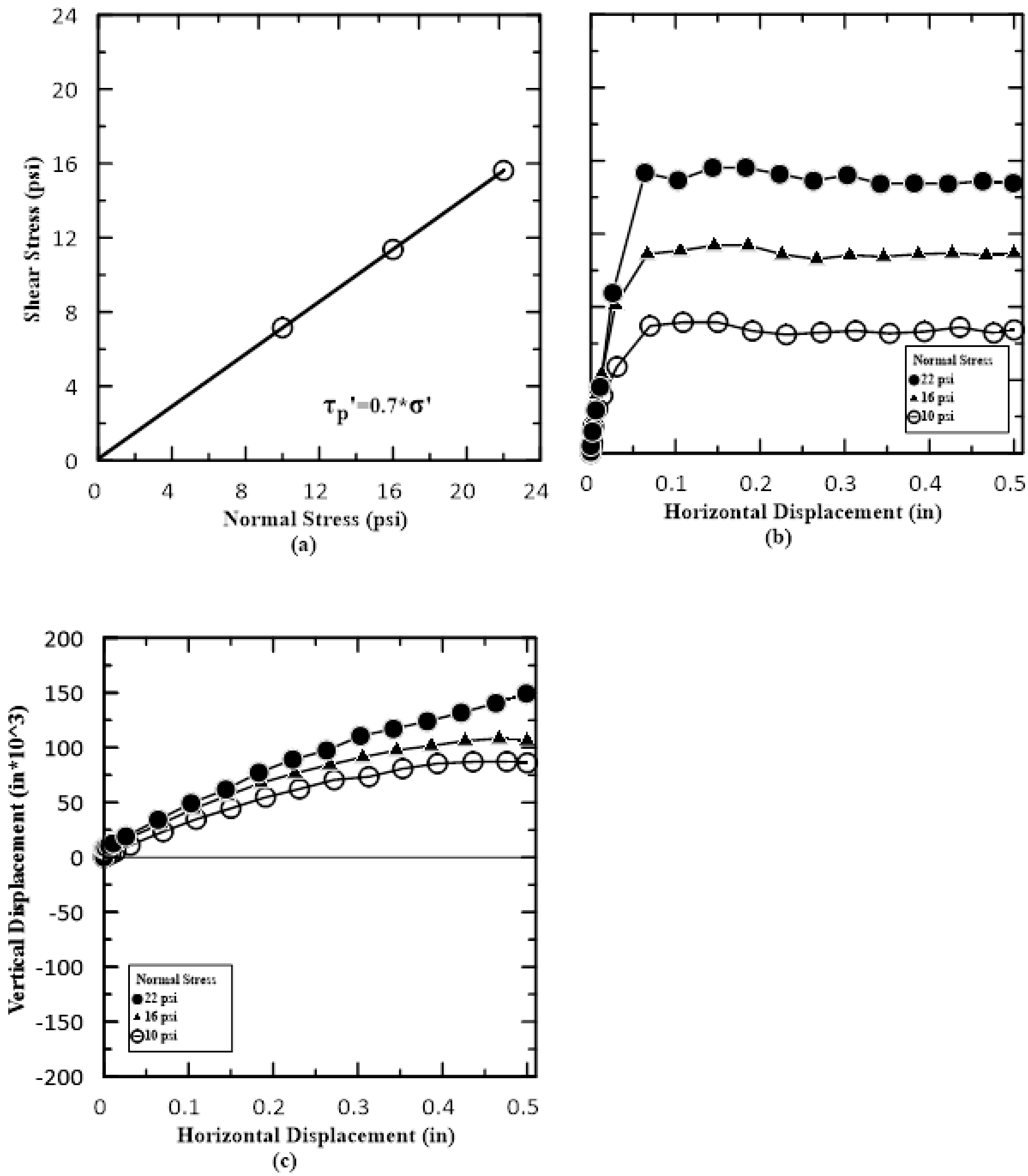

Figure 54. Small direct shear results for Soil 1 and Soil 2 mixtures at fine content = 10%, moisture content = 13%: (a) shear stress vs normal stress; (b) shear stress vs horizontal displacement; (c) vertical displacement vs horizontal displacement

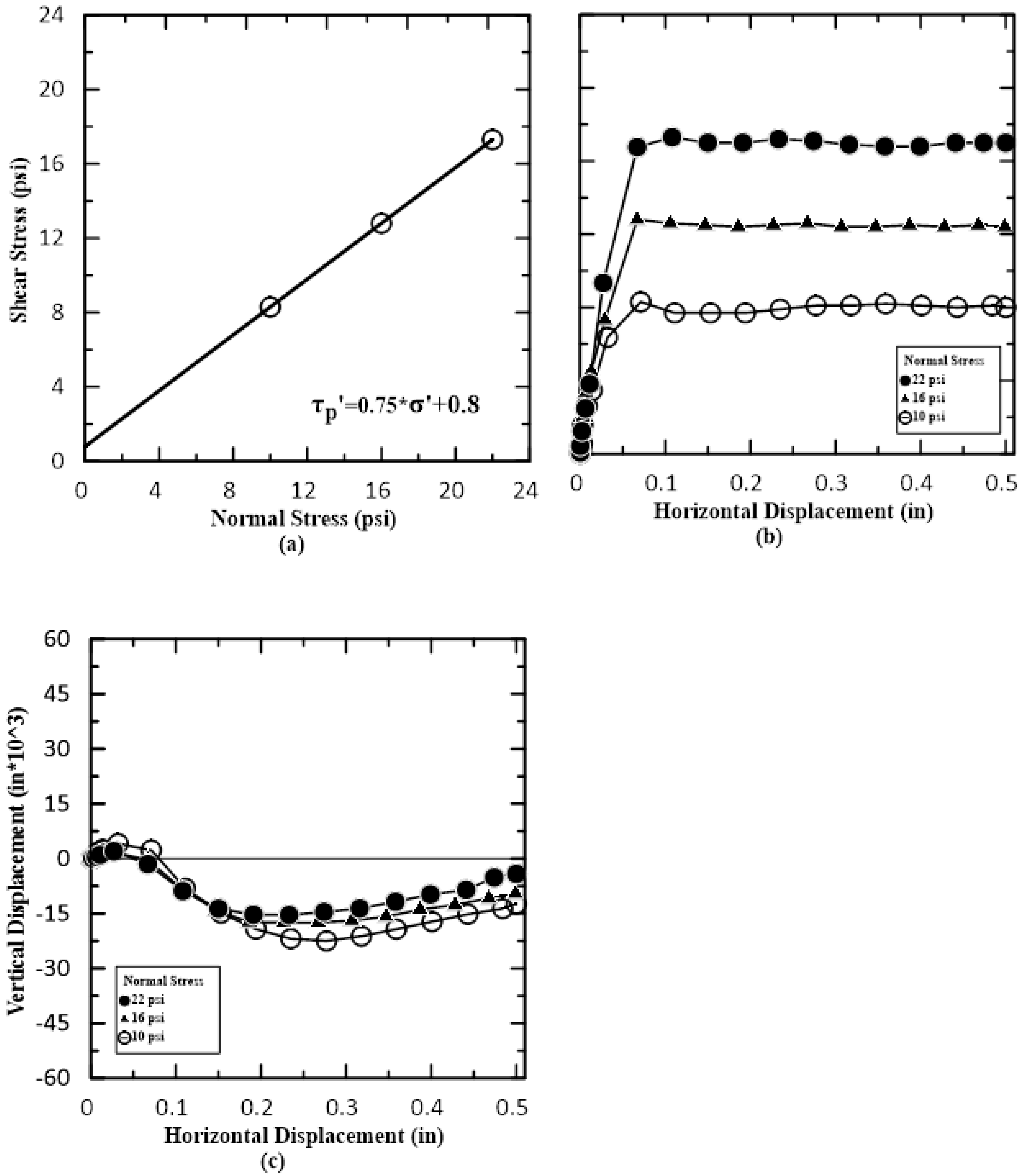

Figure 55. Small direct shear results for Soil 1 and Soil 2 mixtures at fine content = 10%, moisture content = 7.8%: (a) shear stress vs normal stress; (b) shear stress vs horizontal displacement; (c) vertical displacement vs horizontal displacement

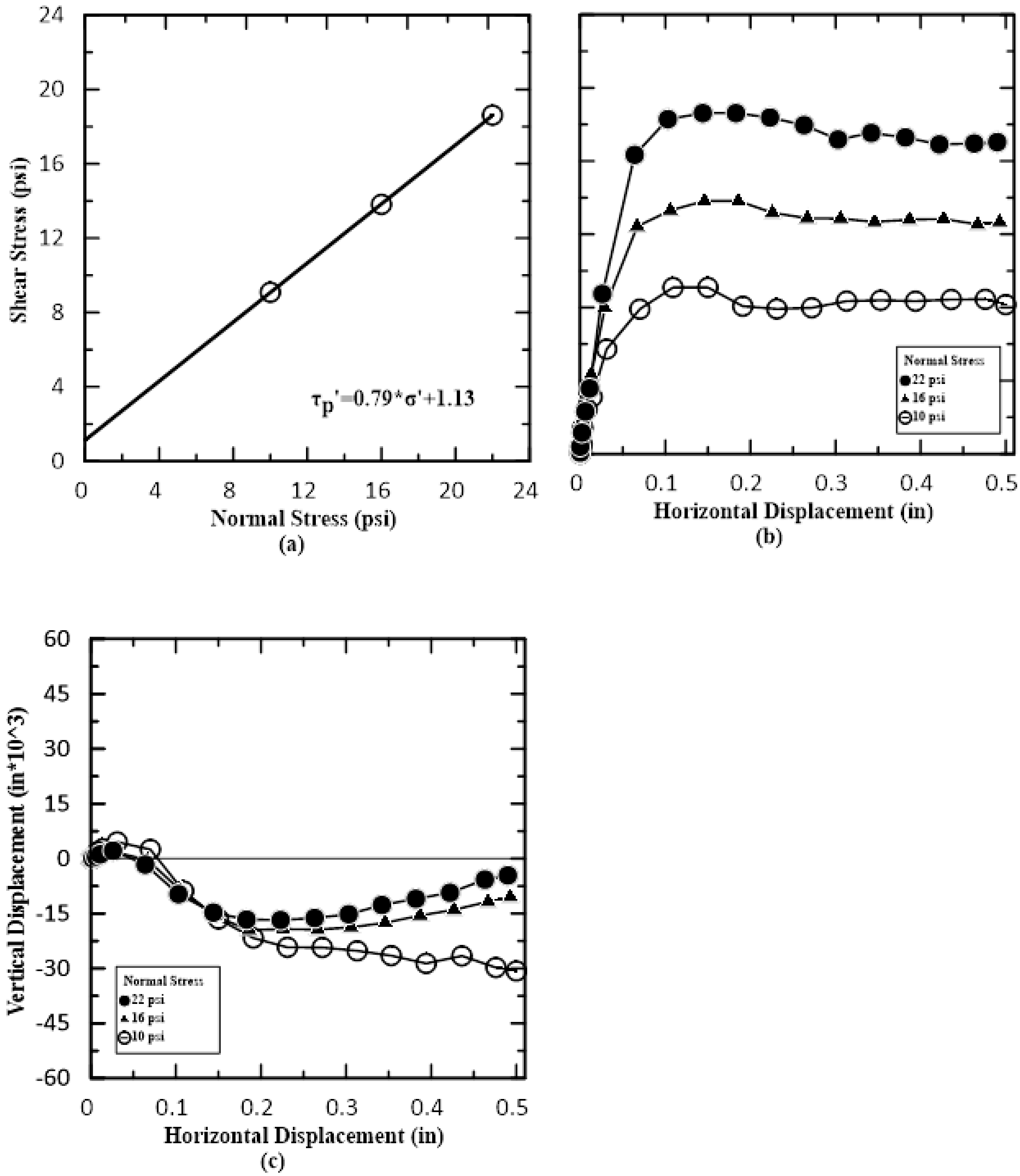

Figure 56. Small direct shear results for Soil 1 and Soil 2 mixtures at fine content = 20%, moisture content = 16.6%: (a) shear stress vs normal stress; (b) shear stress vs horizontal displacement; (c) vertical displacement vs horizontal displacement

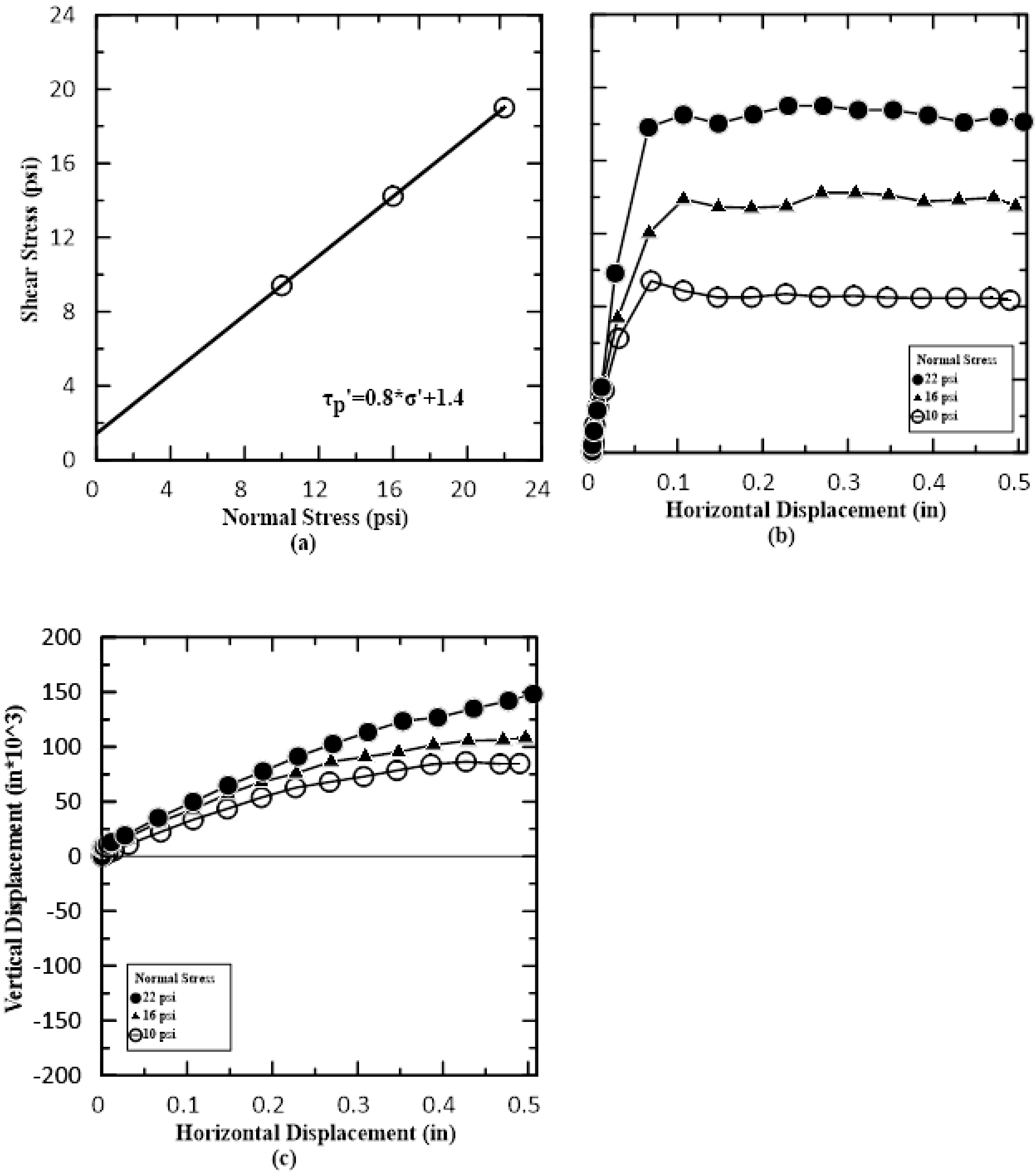

Figure 57. Small direct shear results for Soil 1 and Soil 2 mixtures at fine content = 20%, moisture content = 13.2%: (a) shear stress vs normal stress; (b) shear stress vs horizontal displacement; (c) vertical displacement vs horizontal displacement

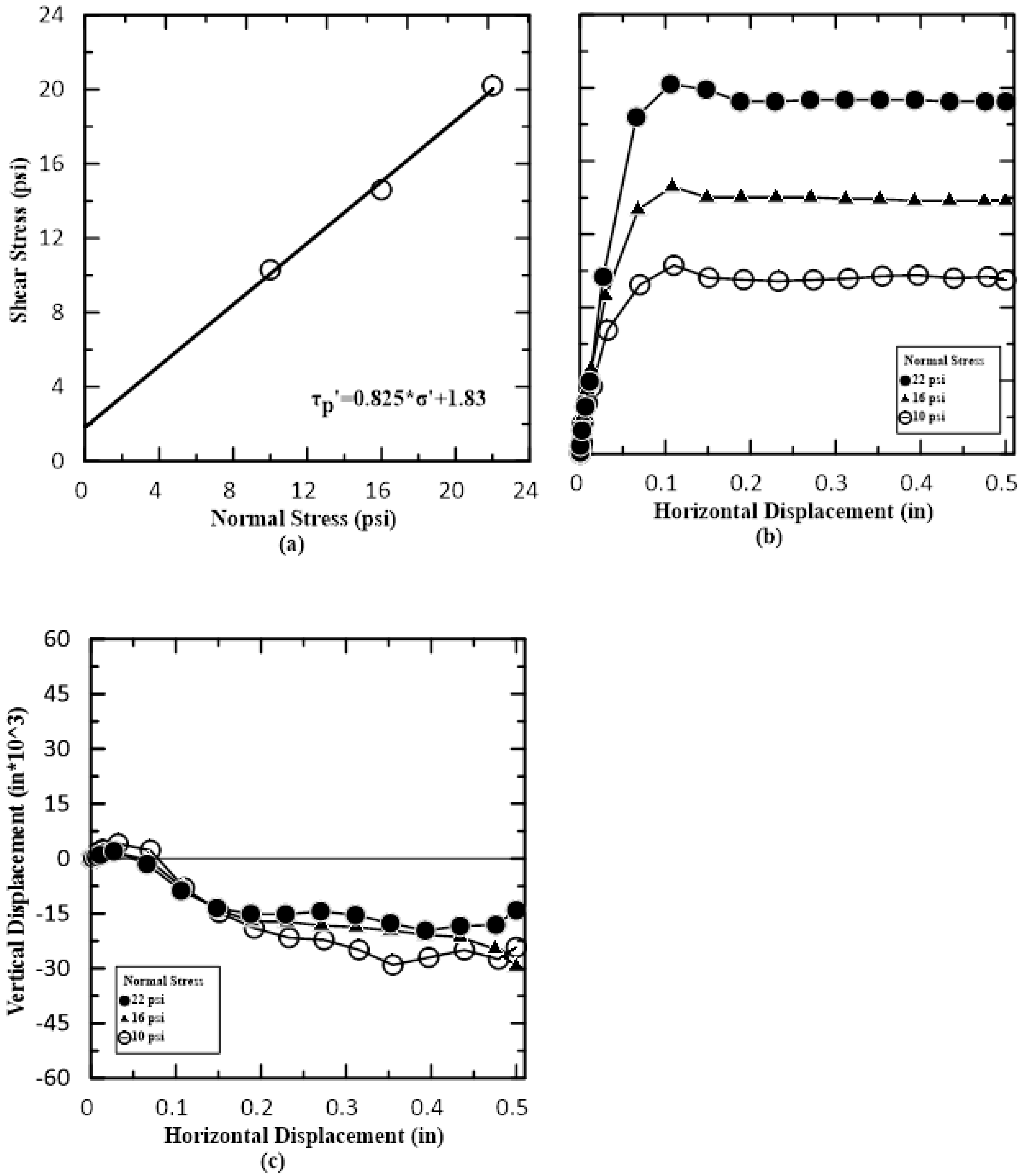

Figure 58. Small direct shear results for Soil 1 and Soil 2 mixtures at fine content = 20%, moisture content = 10.3%: (a) shear stress vs normal stress; (b) shear stress vs horizontal displacement; (c) vertical displacement vs horizontal displacement

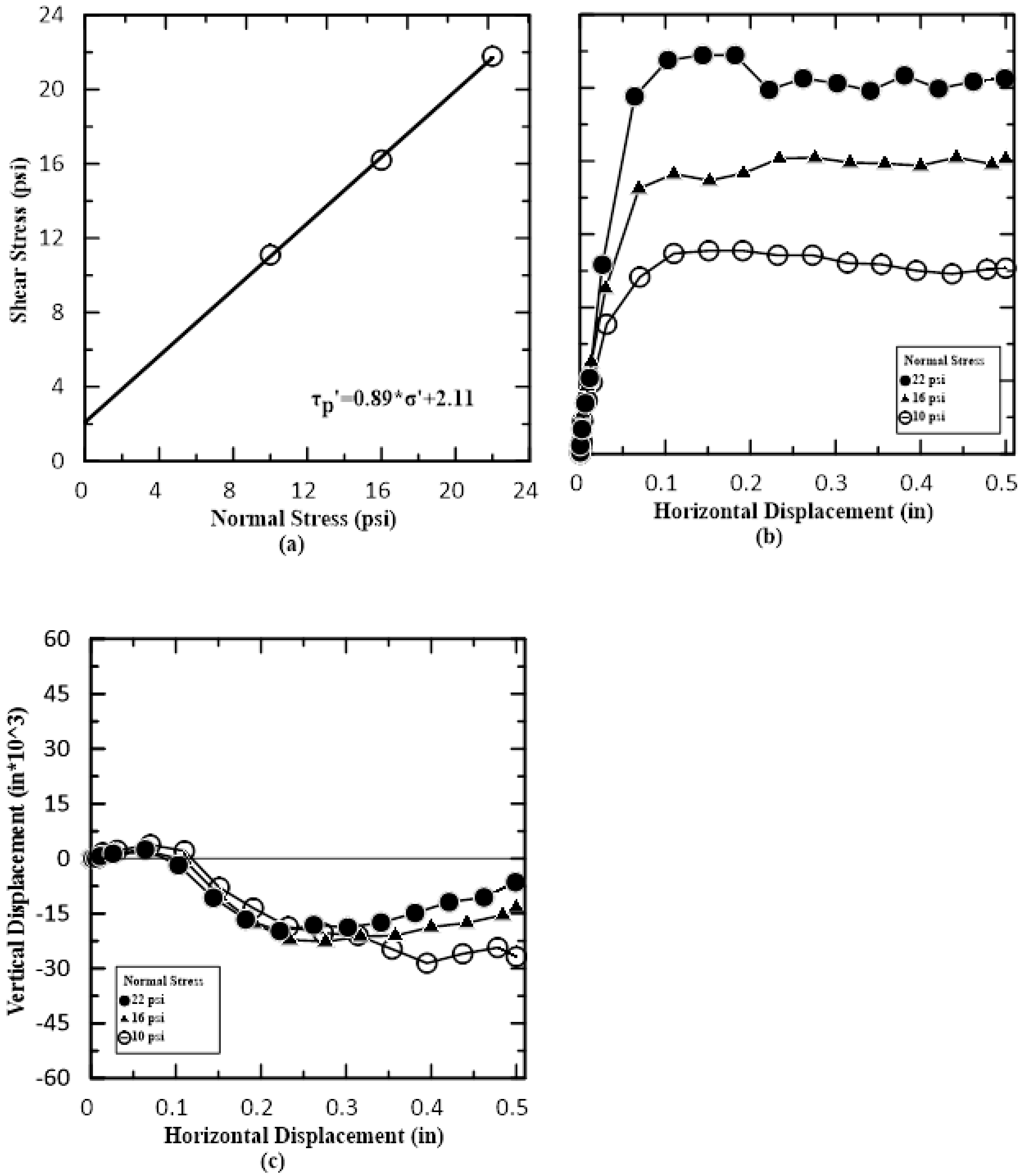

Figure 59. Small direct shear results for Soil 1 and Soil 2 mixtures at fine content = 30%, moisture content = 15.8%: (a) shear stress vs normal stress; (b) shear stress vs horizontal displacement; (c) vertical displacement vs horizontal displacement

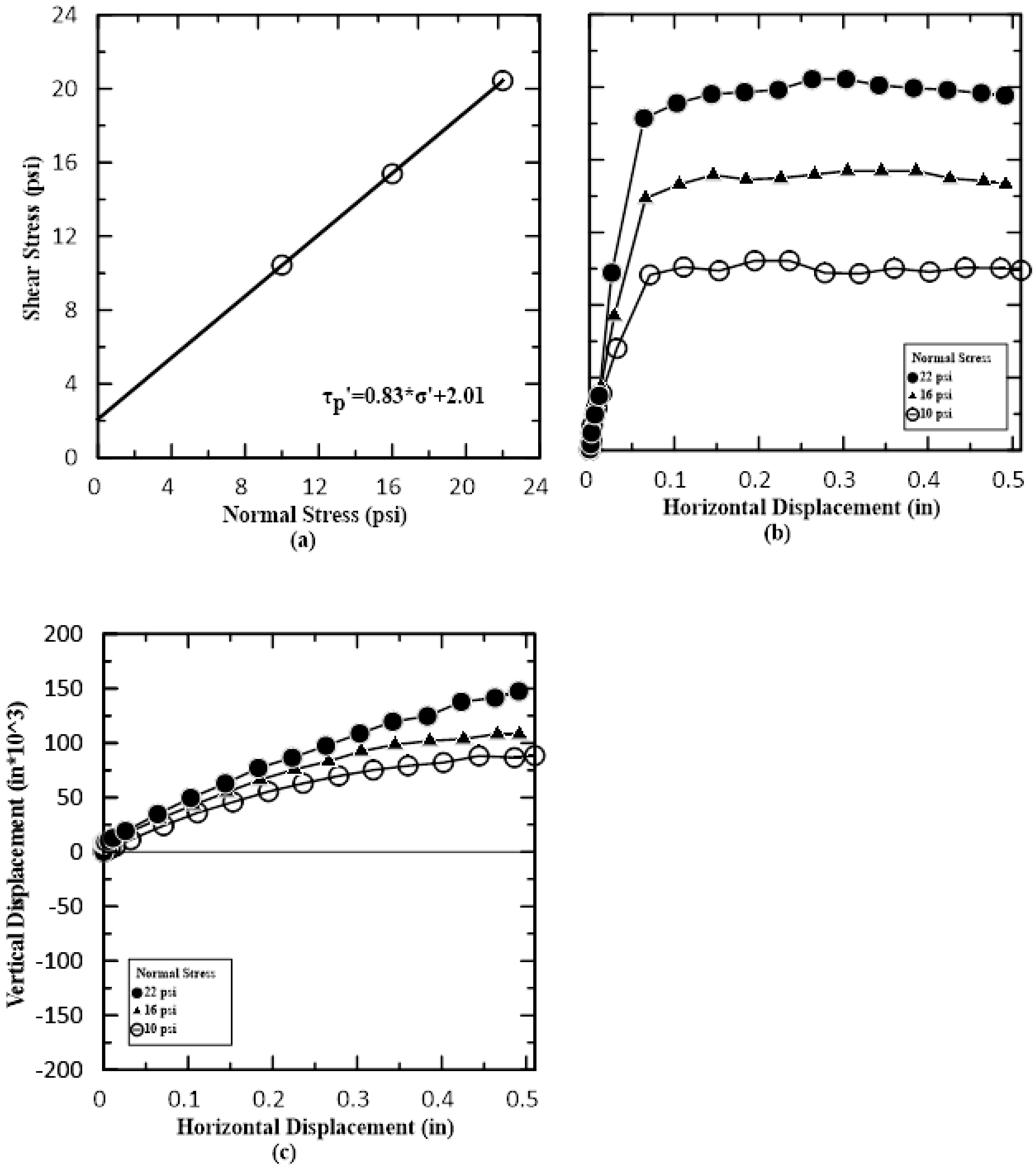

Figure 60. Small direct shear results for Soil 1 and Soil 2 mixtures at fine content = 30%, moisture content = 13.1%: (a) shear stress vs normal stress; (b) shear stress vs horizontal displacement; (c) vertical displacement vs horizontal displacement

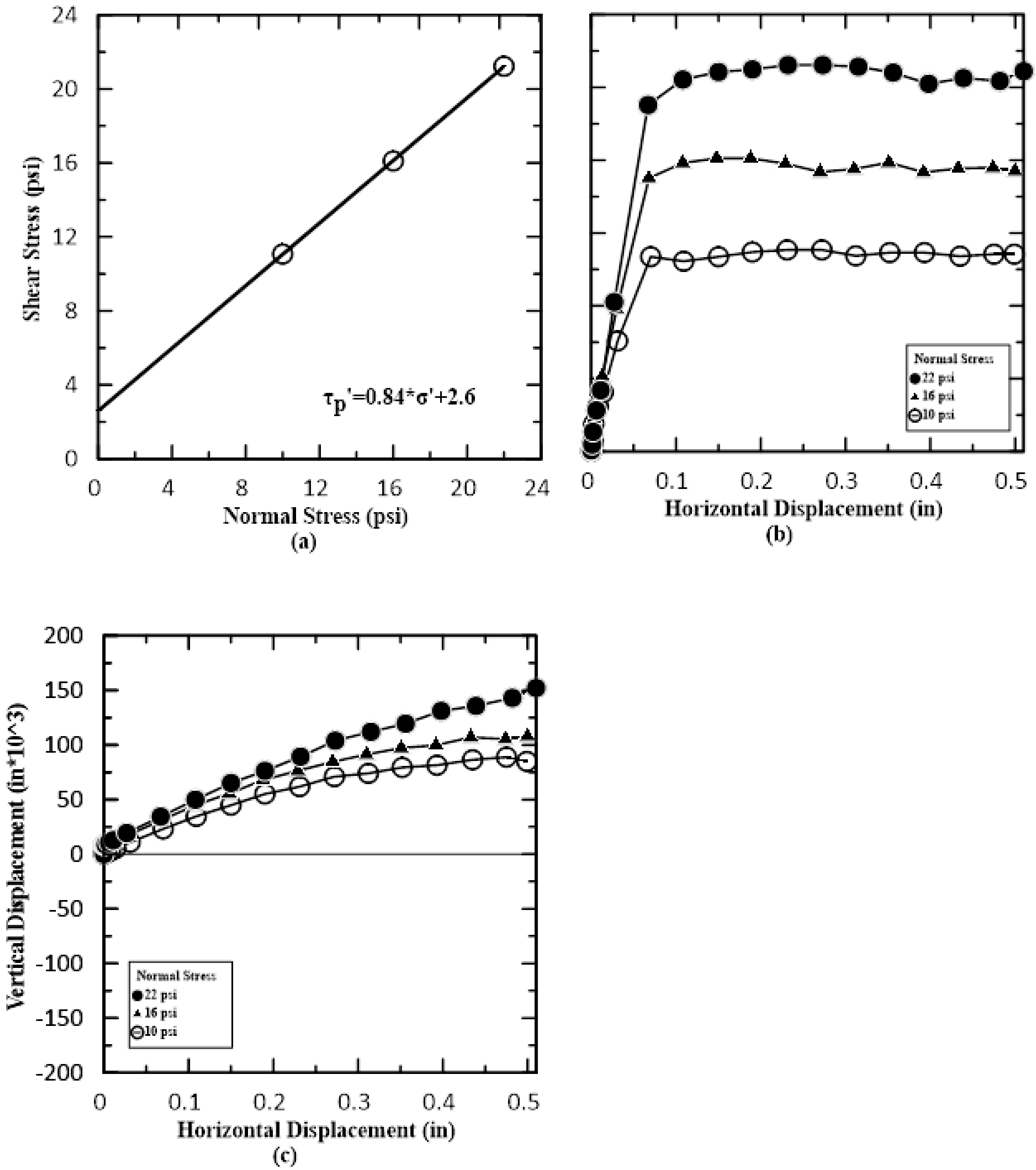

Figure 61. Small direct shear results for Soil 1 and Soil 2 mixtures at fine content = 30%, moisture content = 11.2%: (a) shear stress vs normal stress; (b) shear stress vs horizontal displacement; (c) vertical displacement vs horizontal displacement

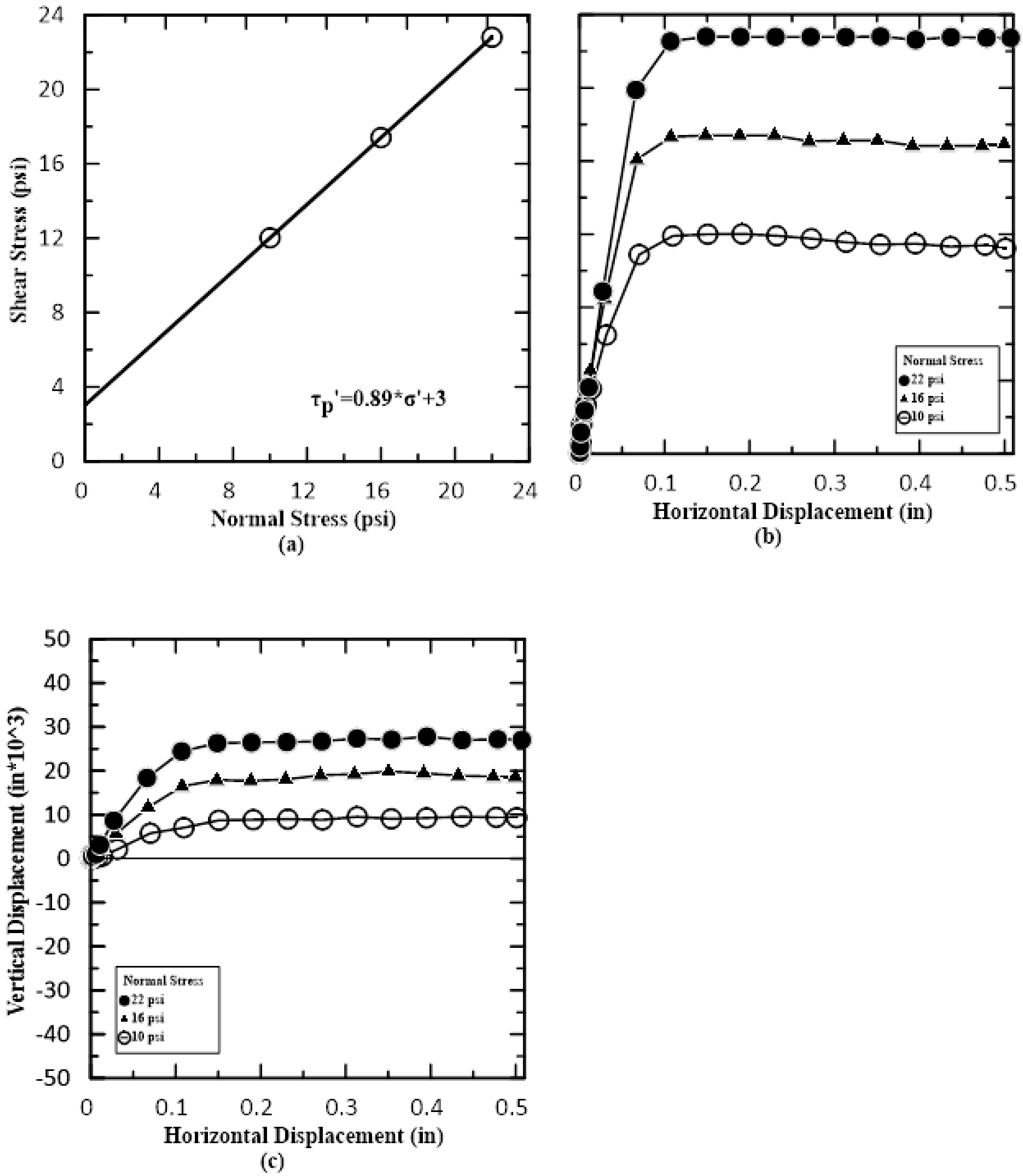

Figure 62. Small direct shear results for Soil 1 and Soil 2 mixtures at fine content = 40%, moisture content = 16.3%: (a) shear stress vs normal stress; (b) shear stress vs horizontal displacement; (c) vertical displacement vs horizontal displacement

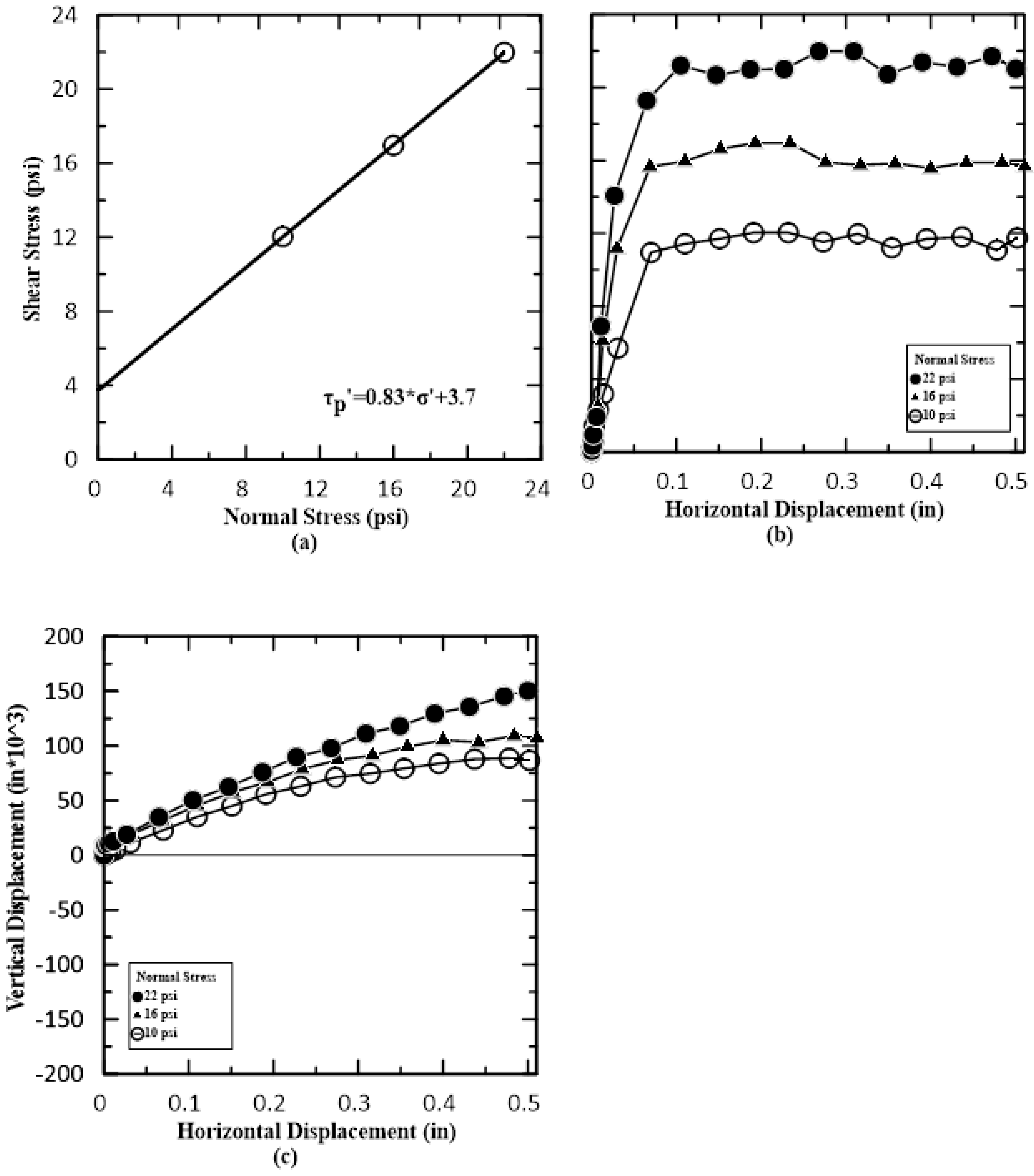

Figure 63. Small direct shear results for Soil 1 and Soil 2 mixtures at fine content = 40%, moisture content = 14.1%: (a) shear stress vs normal stress; (b) shear stress vs horizontal displacement; (c) vertical displacement vs horizontal displacement

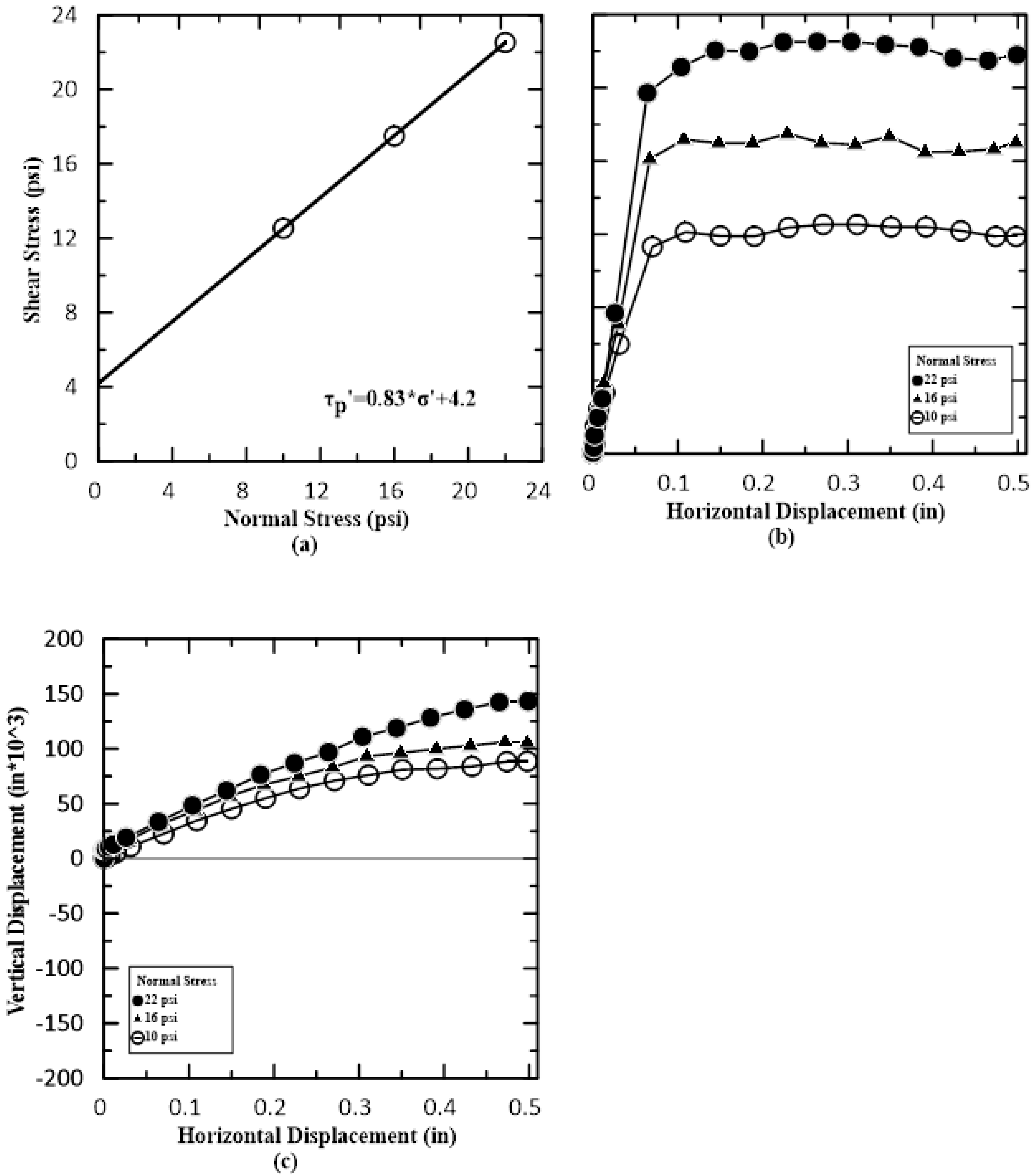

Figure 64. Small direct shear results for Soil 1 and Soil 2 mixtures at fine content = 40%, moisture content = 12.3%: (a) shear stress vs normal stress; (b) shear stress vs horizontal displacement; (c) vertical displacement vs horizontal displacement

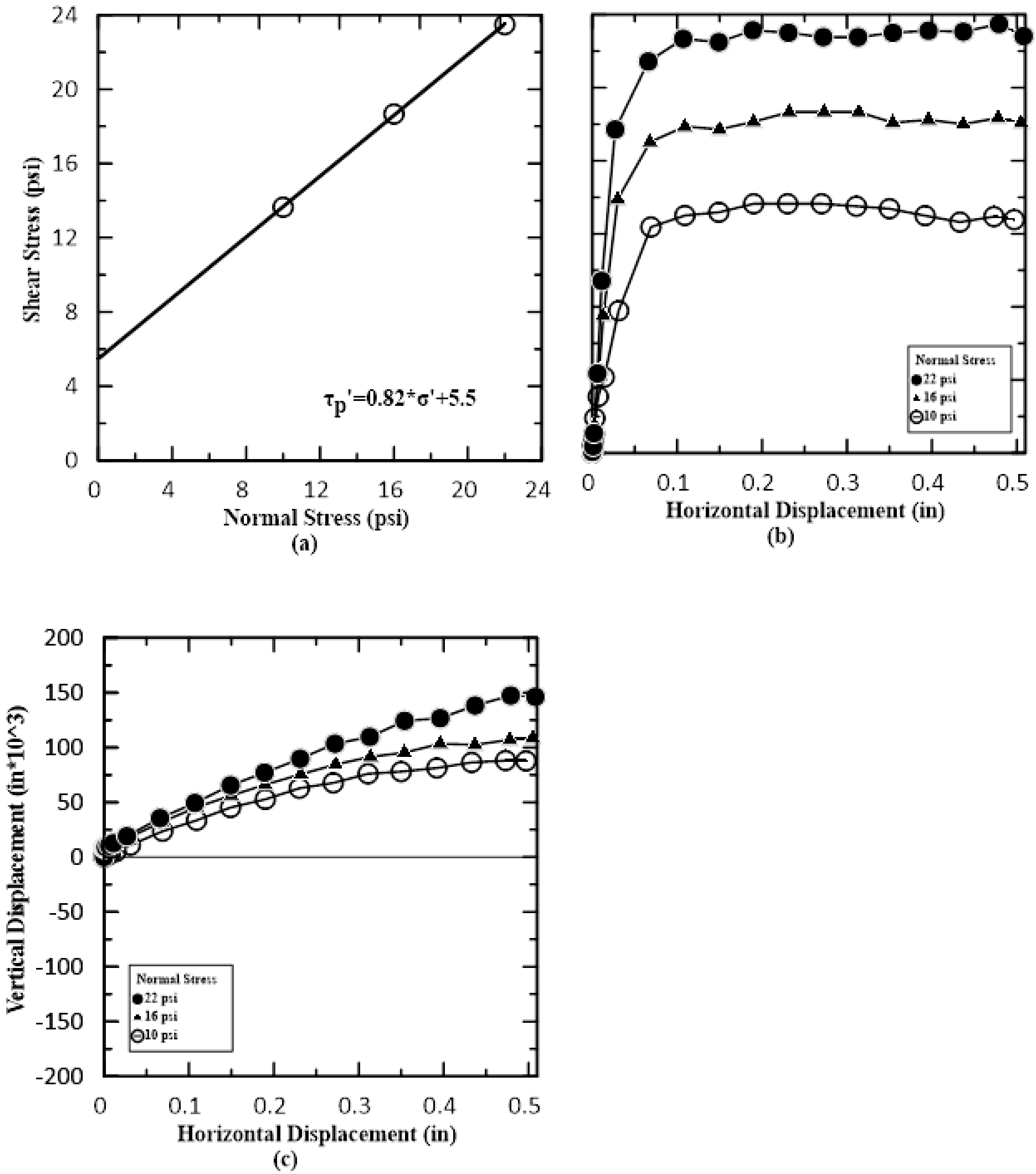

Figure 65. Small direct shear results for Soil 1 and Soil 3 mixtures at fine content = 10%, moisture content = 18.1%: (a) shear stress vs normal stress; (b) shear stress vs horizontal displacement; (c) vertical displacement vs horizontal displacement

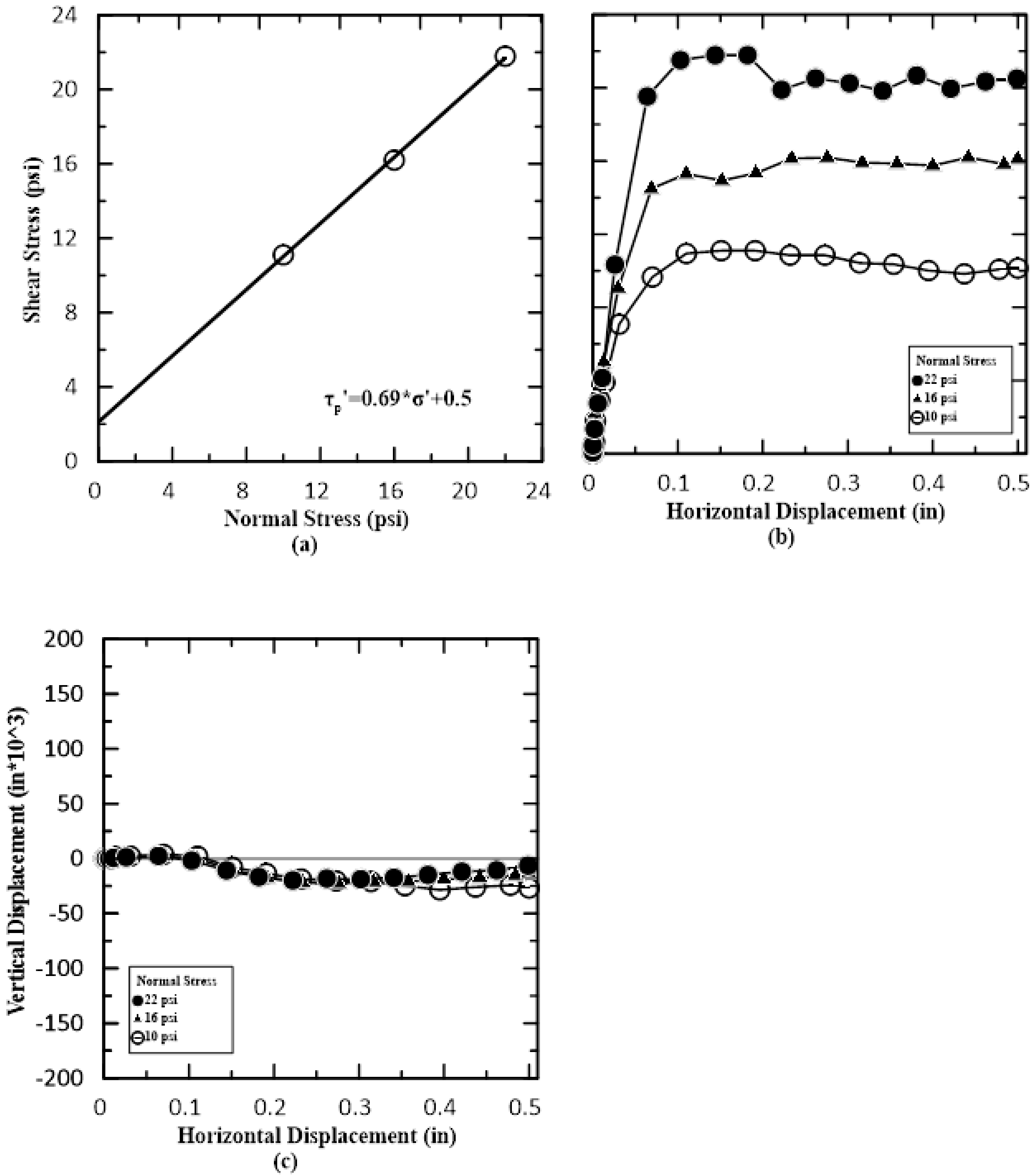

Figure 66. Small direct shear results for Soil 1 and Soil 3 mixtures at fine content = 10%, moisture content = 15.3%: (a) shear stress vs normal stress; (b) shear stress vs horizontal displacement; (c) vertical displacement vs horizontal displacement

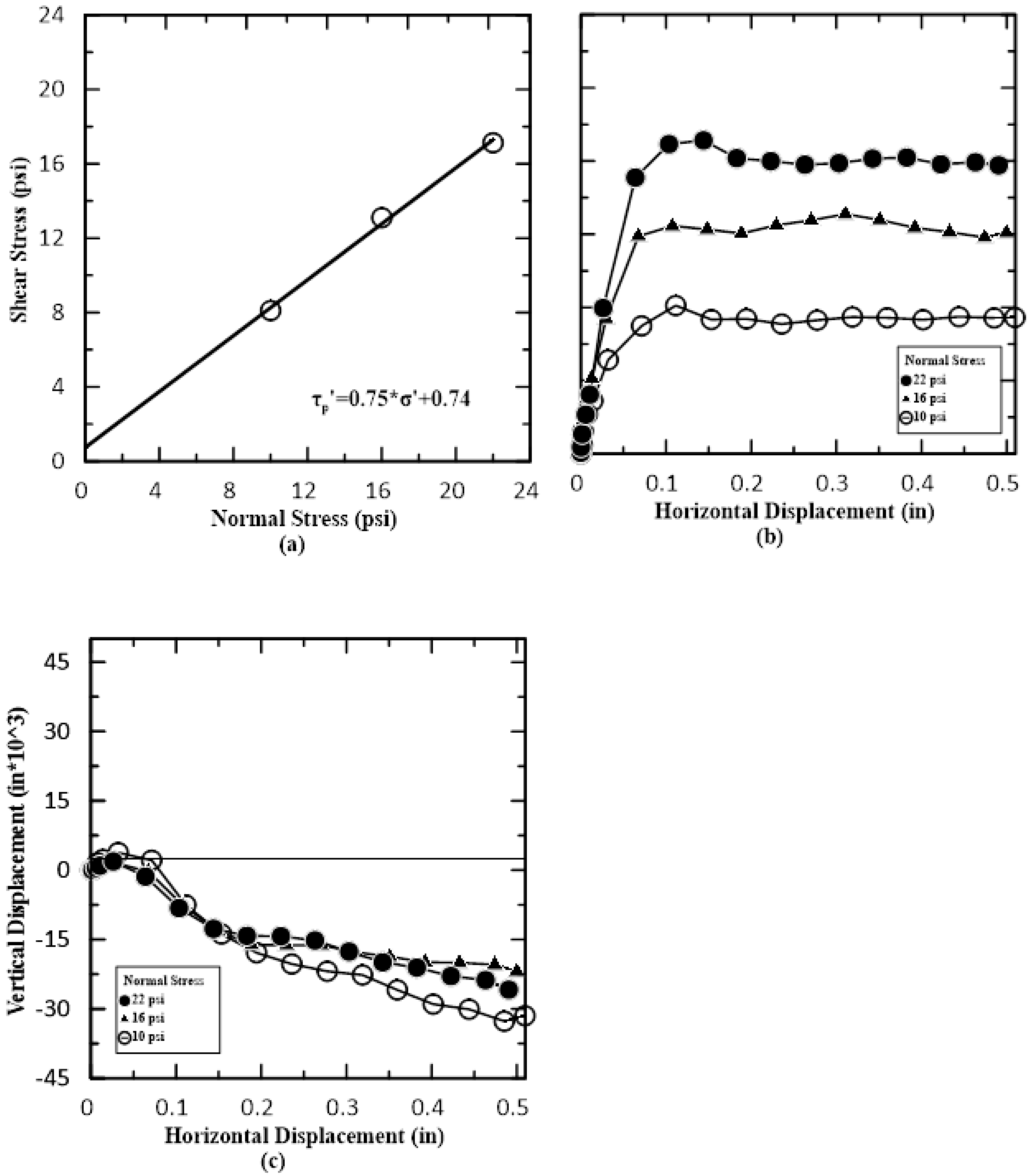

Figure 67. Small direct shear results for Soil 1 and Soil 3 mixtures at fine content = 10%, moisture content = 12%: (a) shear stress vs normal stress; (b) shear stress vs horizontal displacement; (c) vertical displacement vs horizontal displacement

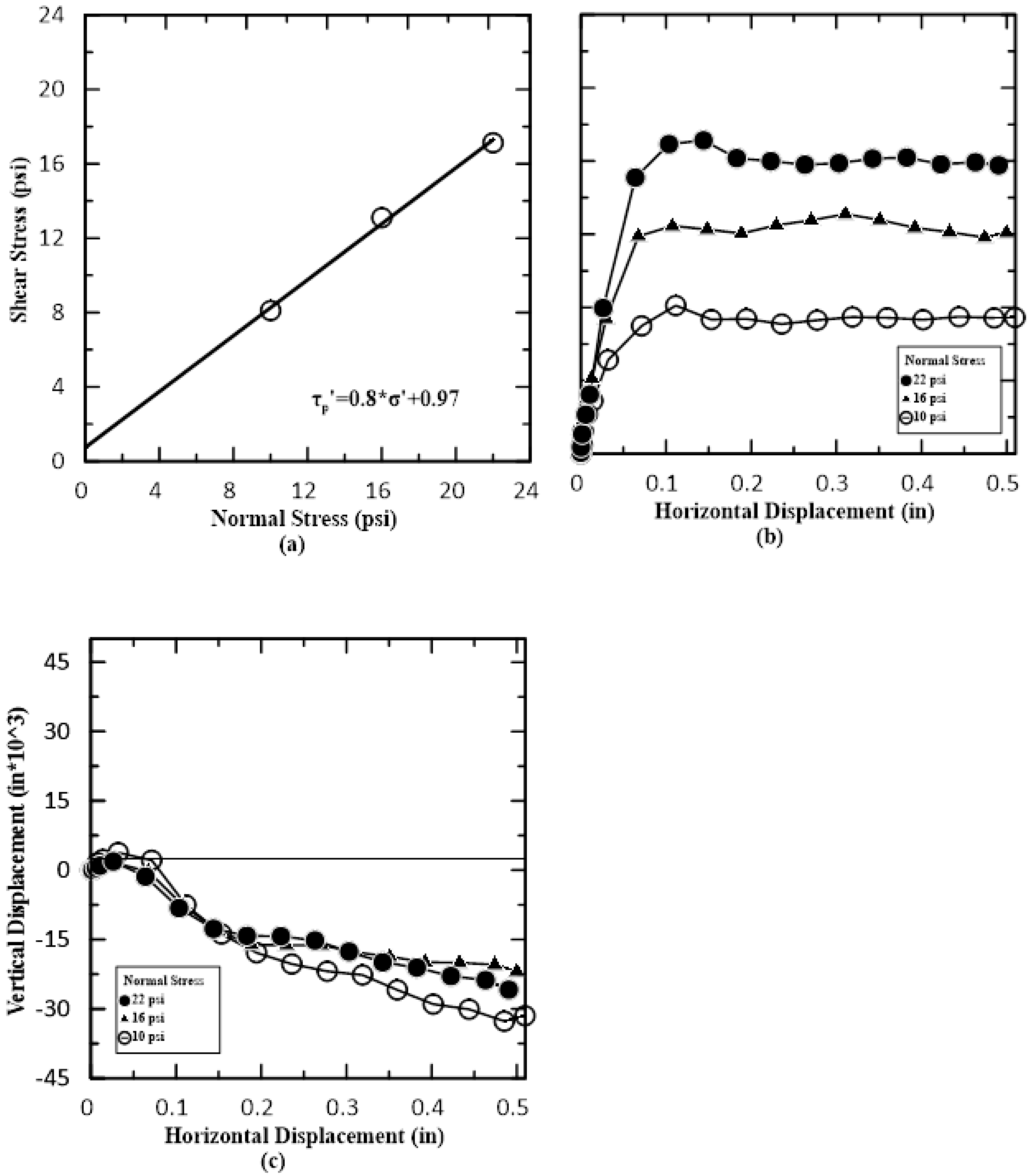

Figure 68. Small direct shear results for Soil 1 and Soil 3 mixtures at fine content = 10%, moisture content = 10.1%: (a) shear stress vs normal stress; (b) shear stress vs horizontal displacement; (c) vertical displacement vs horizontal displacement

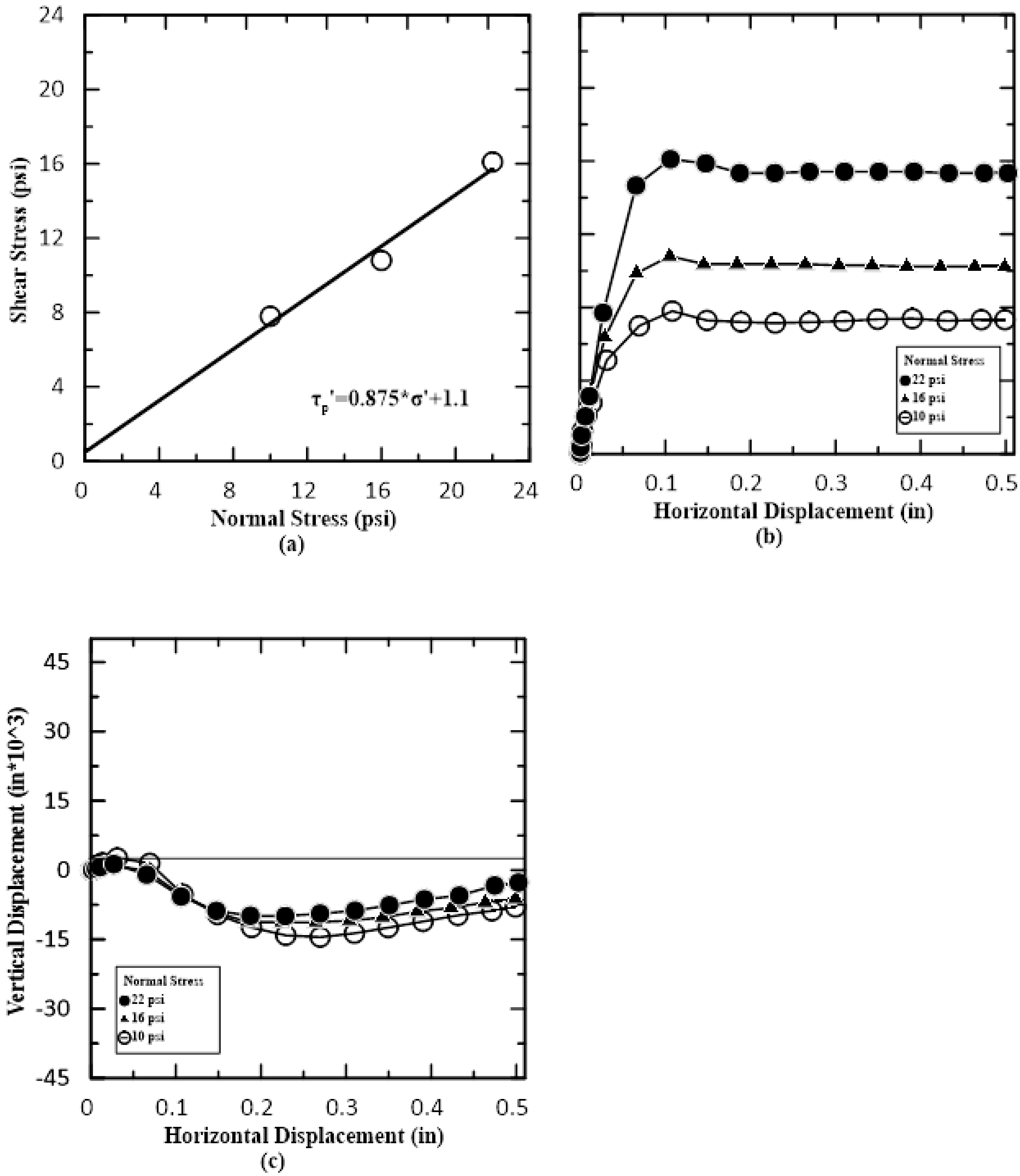

Figure 69. Small direct shear results for Soil 1 and Soil 3 mixtures at fine content = 30%, moisture content = 18.9%: (a) shear stress vs normal stress; (b) shear stress vs horizontal displacement; (c) vertical displacement vs horizontal displacement

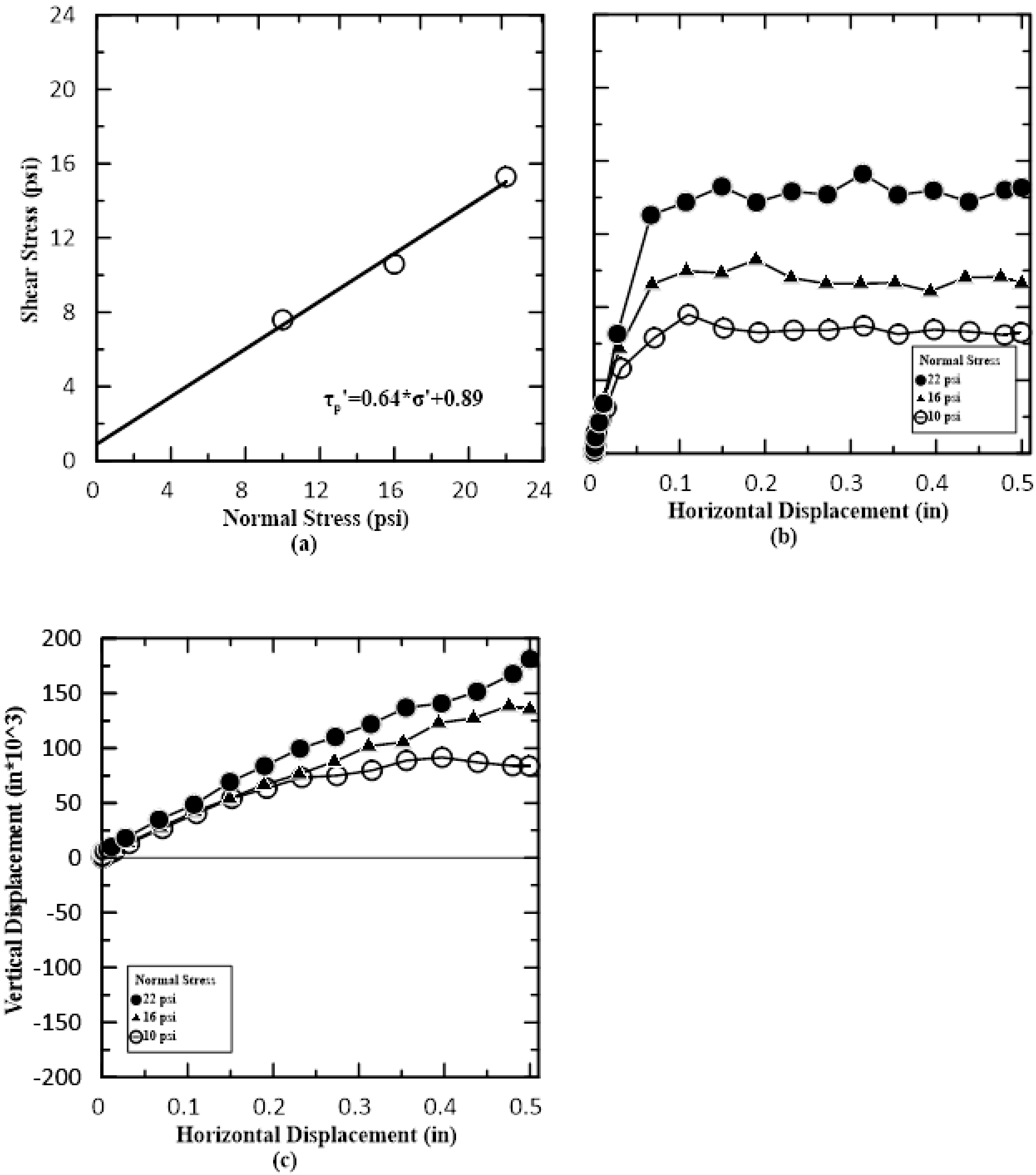

Figure 70. Small direct shear results for Soil 1 and Soil 3 mixtures at fine content = 30%, moisture content = 16.6%: (a) shear stress vs normal stress; (b) shear stress vs horizontal displacement; (c) vertical displacement vs horizontal displacement

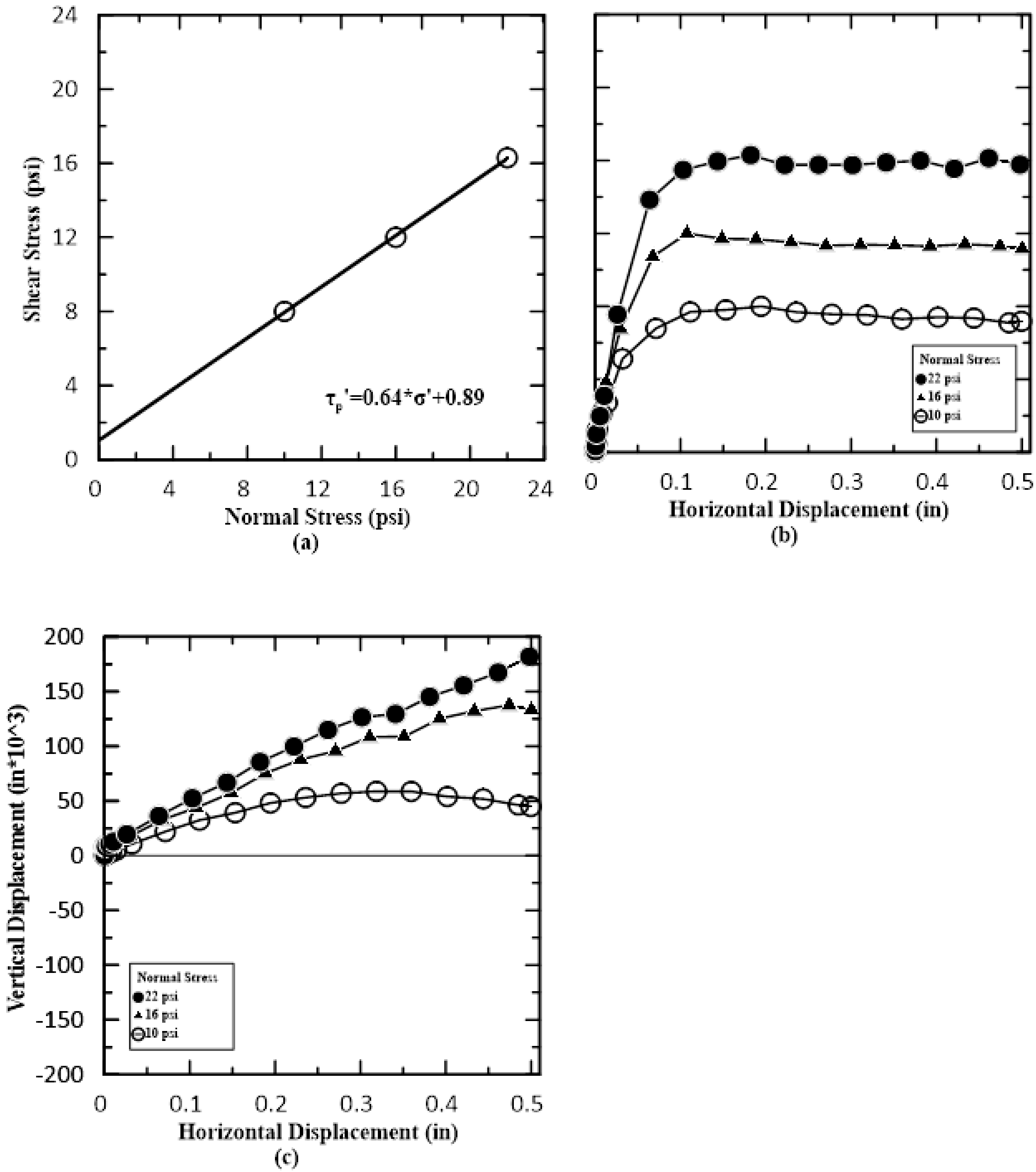

Figure 71. Small direct shear results for Soil 1 and Soil 3 mixtures at fine content = 30%, moisture content = 14.3%: (a) shear stress vs normal stress; (b) shear stress vs horizontal displacement; (c) vertical displacement vs horizontal displacement

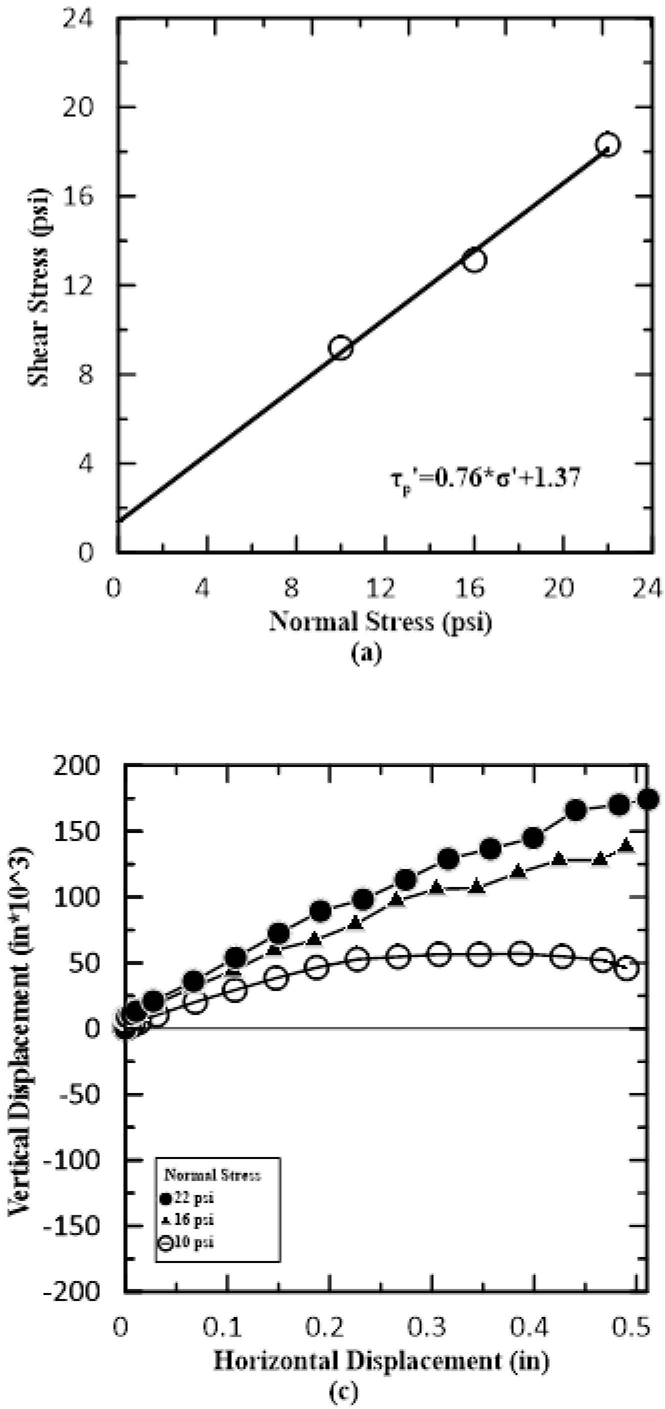

Figure 72. Small direct shear results for Soil 1 and Soil 3 mixtures at fine content = 30%, moisture content = 11%: (a) shear stress vs normal stress; (b) shear stress vs horizontal displacement; (c) vertical displacement vs horizontal displacement

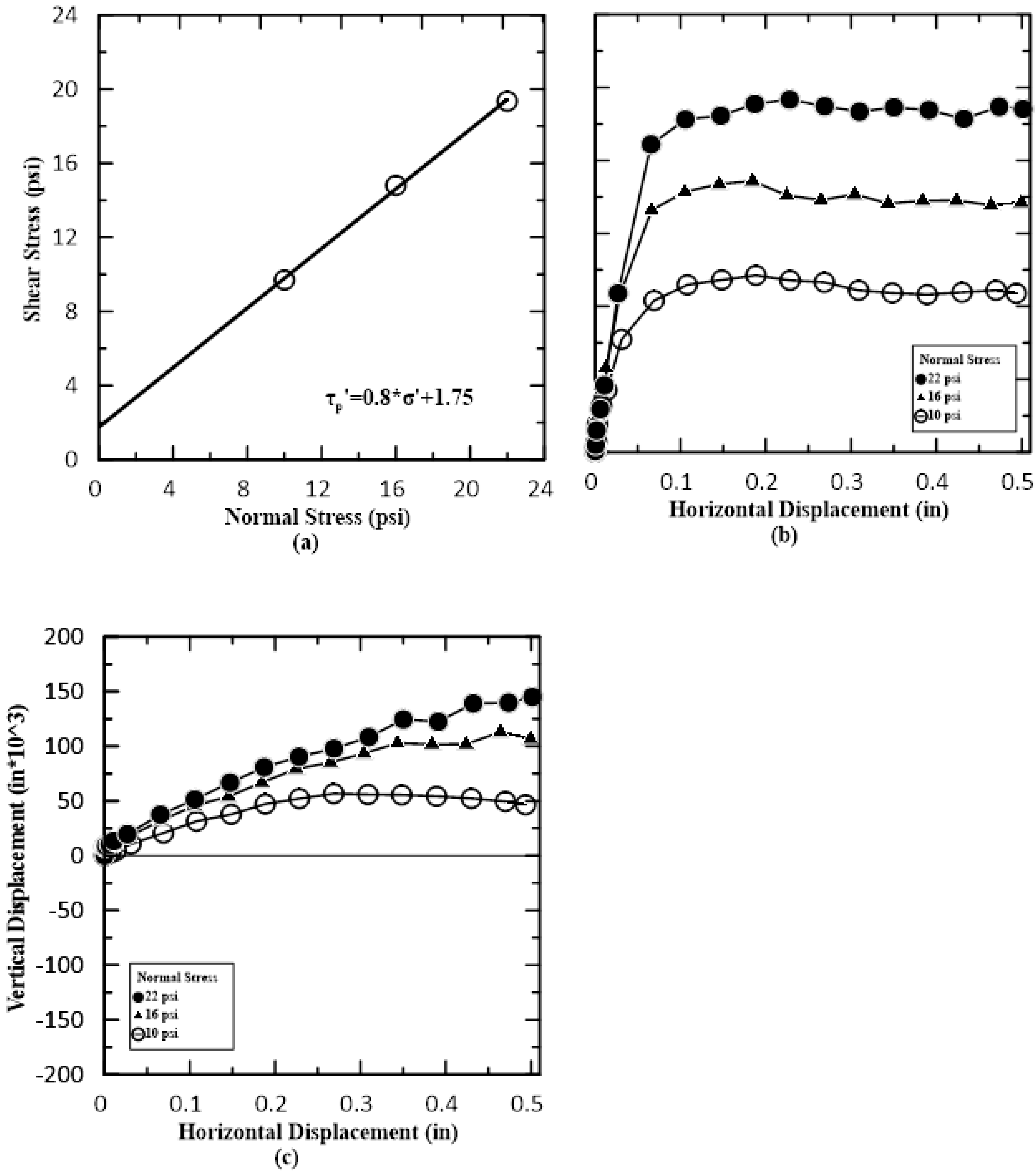

Figure 73. Small direct shear results for Soil 1 and Soil 3 mixtures at fine content = 50%, moisture content = 19%: (a) shear stress vs normal stress; (b) shear stress vs horizontal displacement; (c) vertical displacement vs horizontal displacement

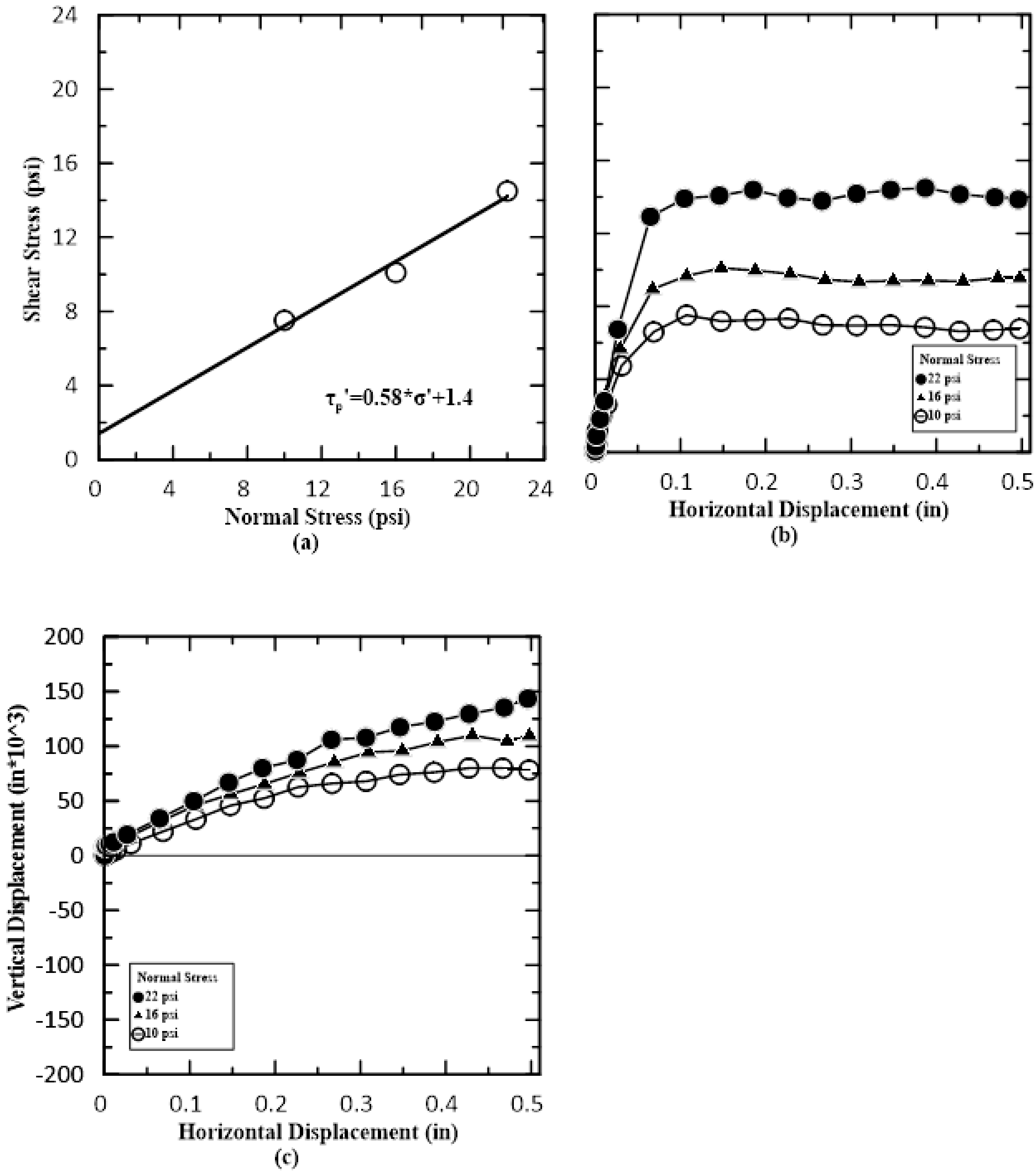

Figure 74. Small direct shear results for Soil 1 and Soil 3 mixtures at fine content = 50%, moisture content = 17.3%: (a) shear stress vs normal stress; (b) shear stress vs horizontal displacement; (c) vertical displacement vs horizontal displacement

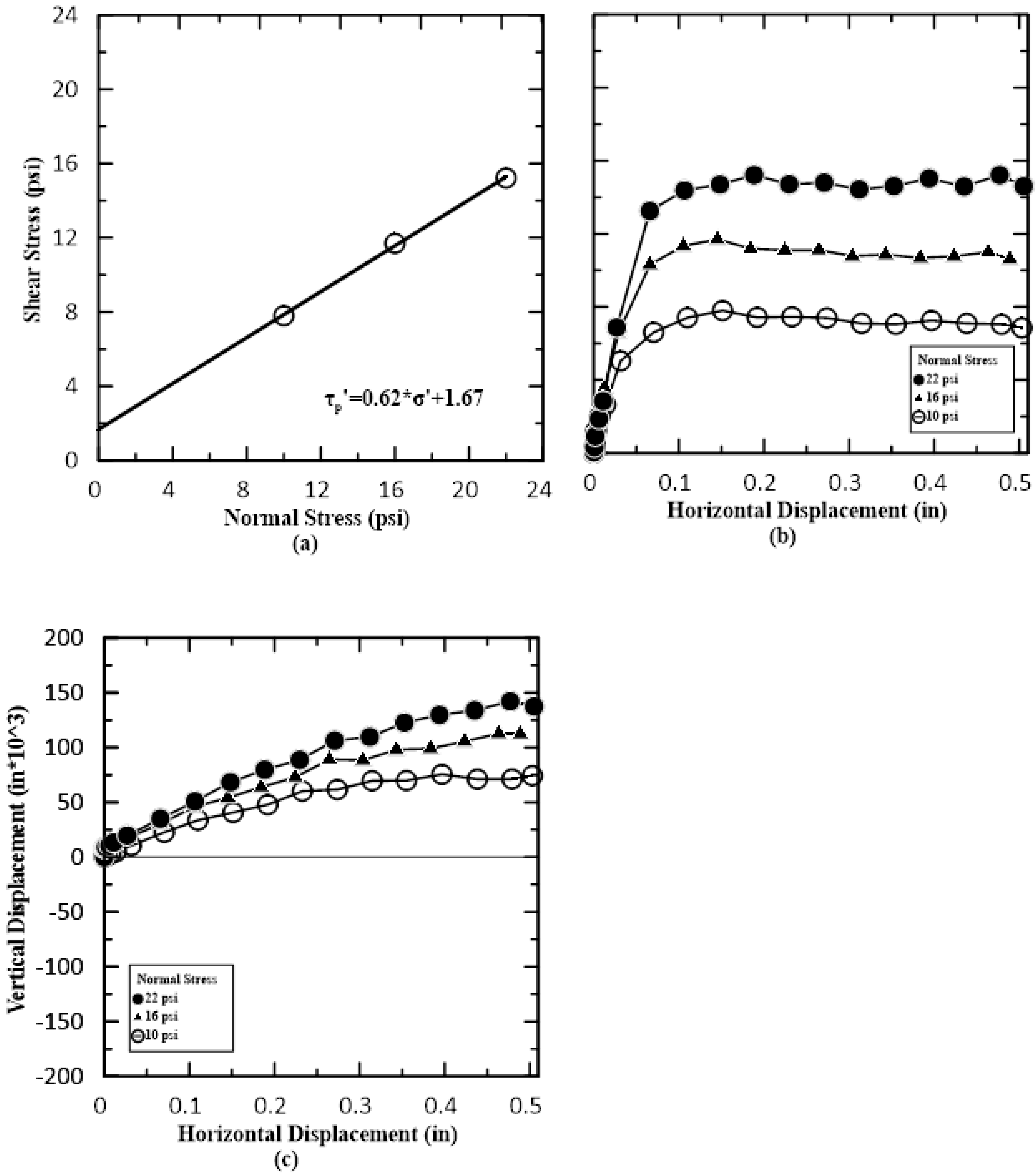

Figure 75. Small direct shear results for Soil 1 and Soil 3 mixtures at fine content = 50%, moisture content = 15.2%: (a) shear stress vs normal stress; (b) shear stress vs horizontal displacement; (c) vertical displacement vs horizontal displacement

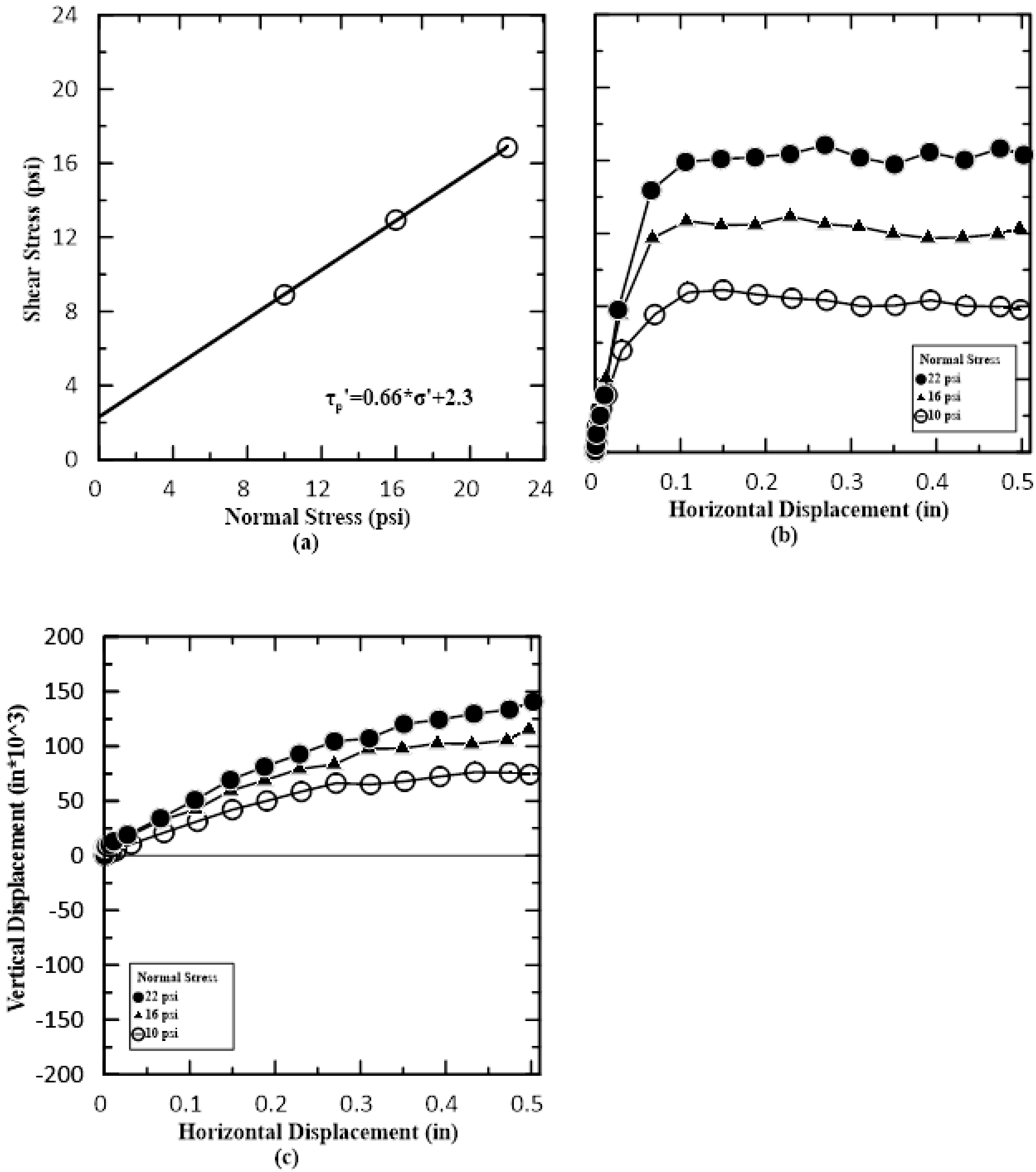

Figure 76. Small direct shear results for Soil 1 and Soil 3 mixtures at fine content = 50%, moisture content = 13%: (a) shear stress vs normal stress; (b) shear stress vs horizontal displacement; (c) vertical displacement vs horizontal displacement

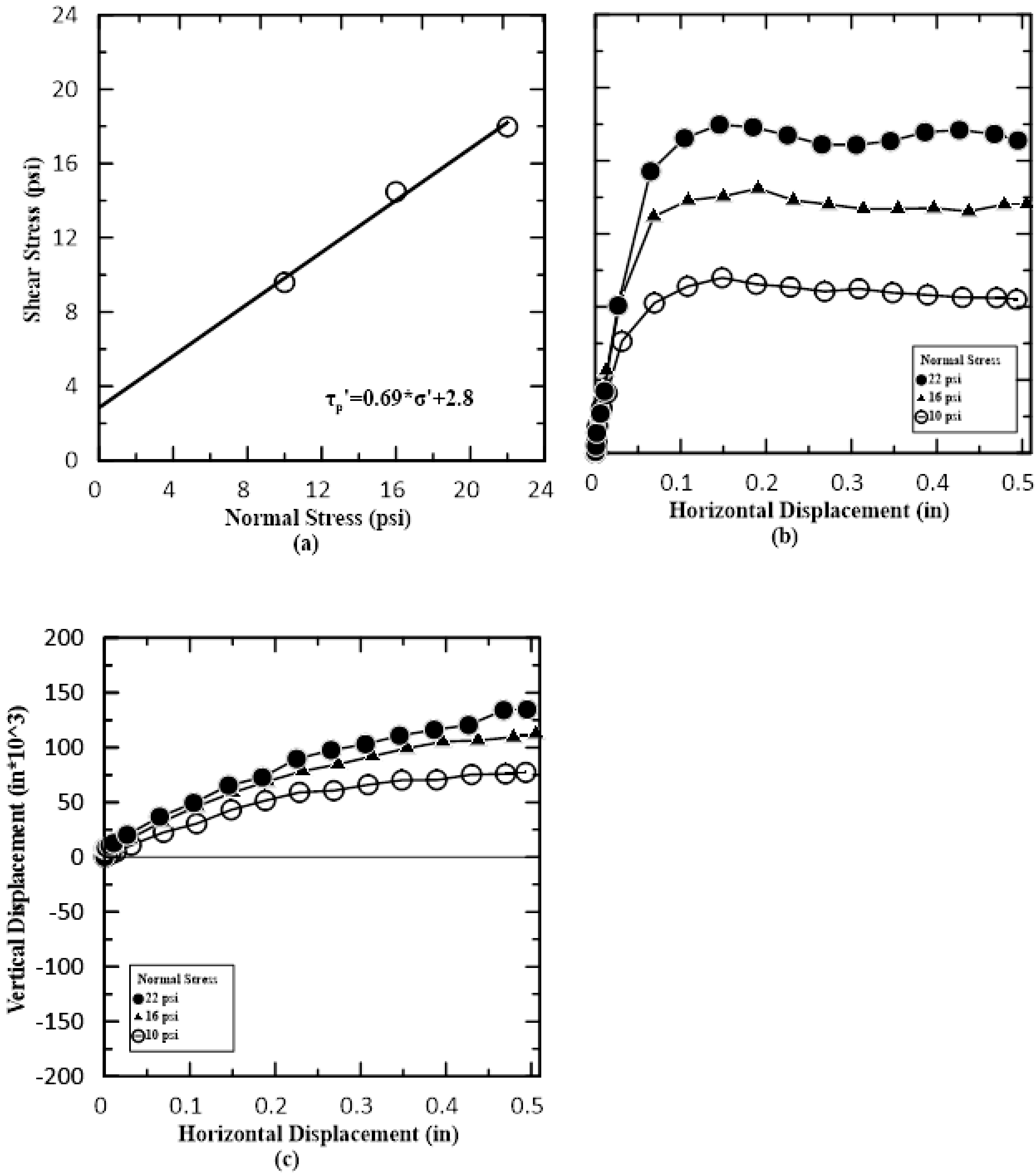

Figure 77. Small direct shear results for Soil 1 and Soil 3 mixtures at fine content = 70%, moisture content = 22%: (a) shear stress vs normal stress; (b) shear stress vs horizontal displacement; (c) vertical displacement vs horizontal displacement

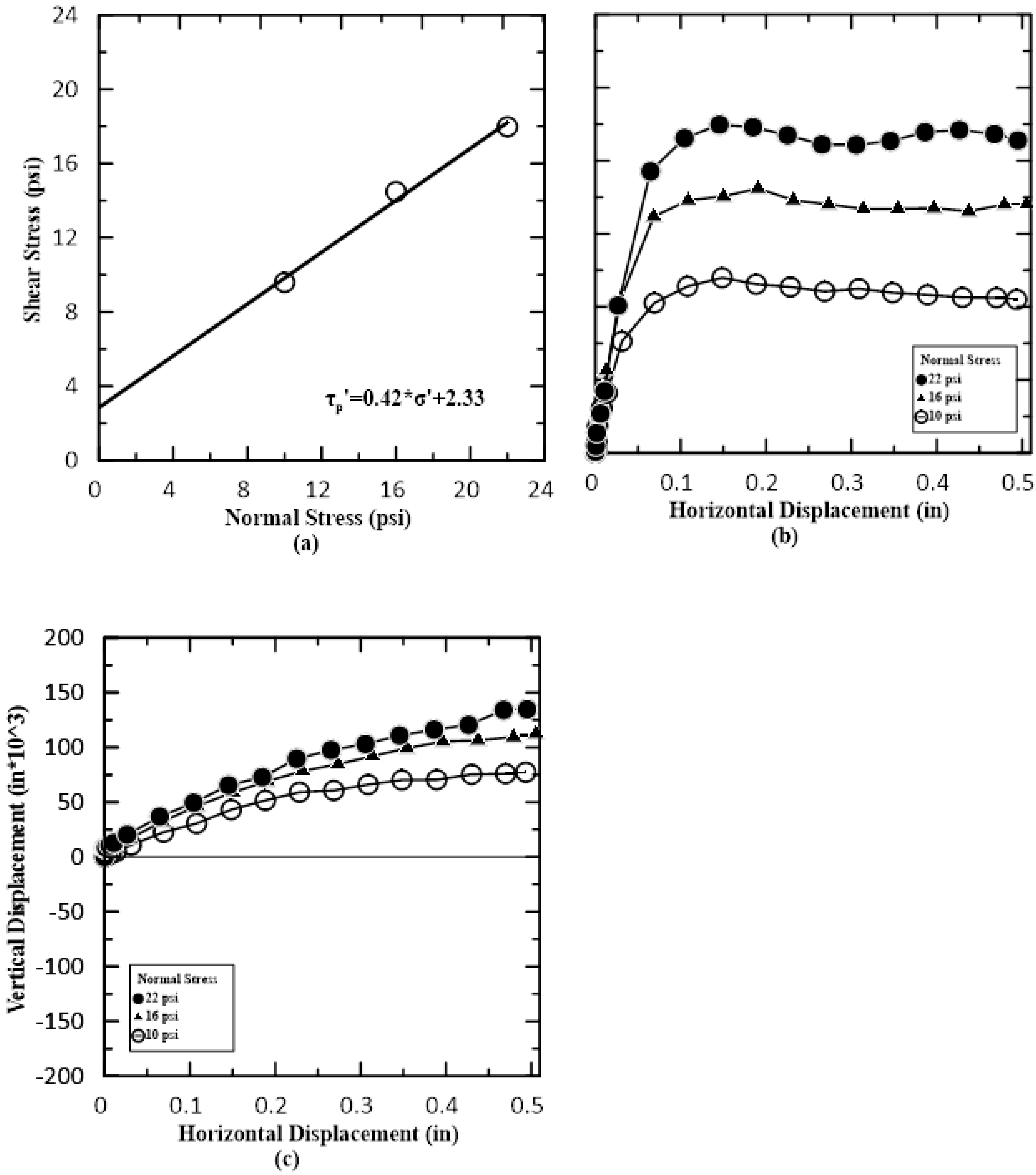

Figure 78. Small direct shear results for Soil 1 and Soil 3 mixtures at fine content = 70%, moisture content = 20.3%: (a) shear stress vs normal stress; (b) shear stress vs horizontal displacement; (c) vertical displacement vs horizontal displacement

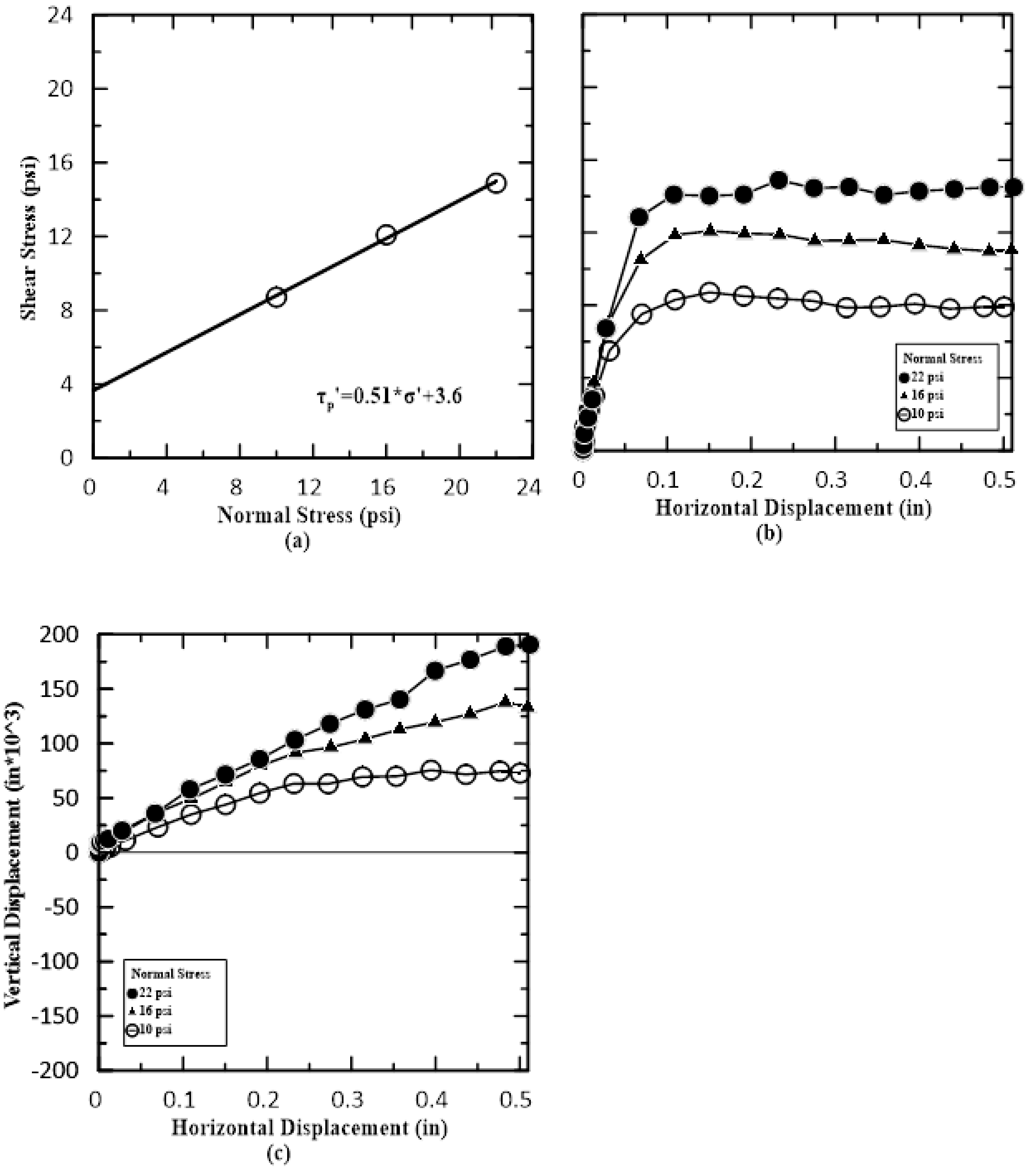

Figure 79. Small direct shear results for Soil 1 and Soil 3 mixtures at fine content = 70%, moisture content = 18.2%: (a) shear stress vs normal stress; (b) shear stress vs horizontal displacement; (c) vertical displacement vs horizontal displacement

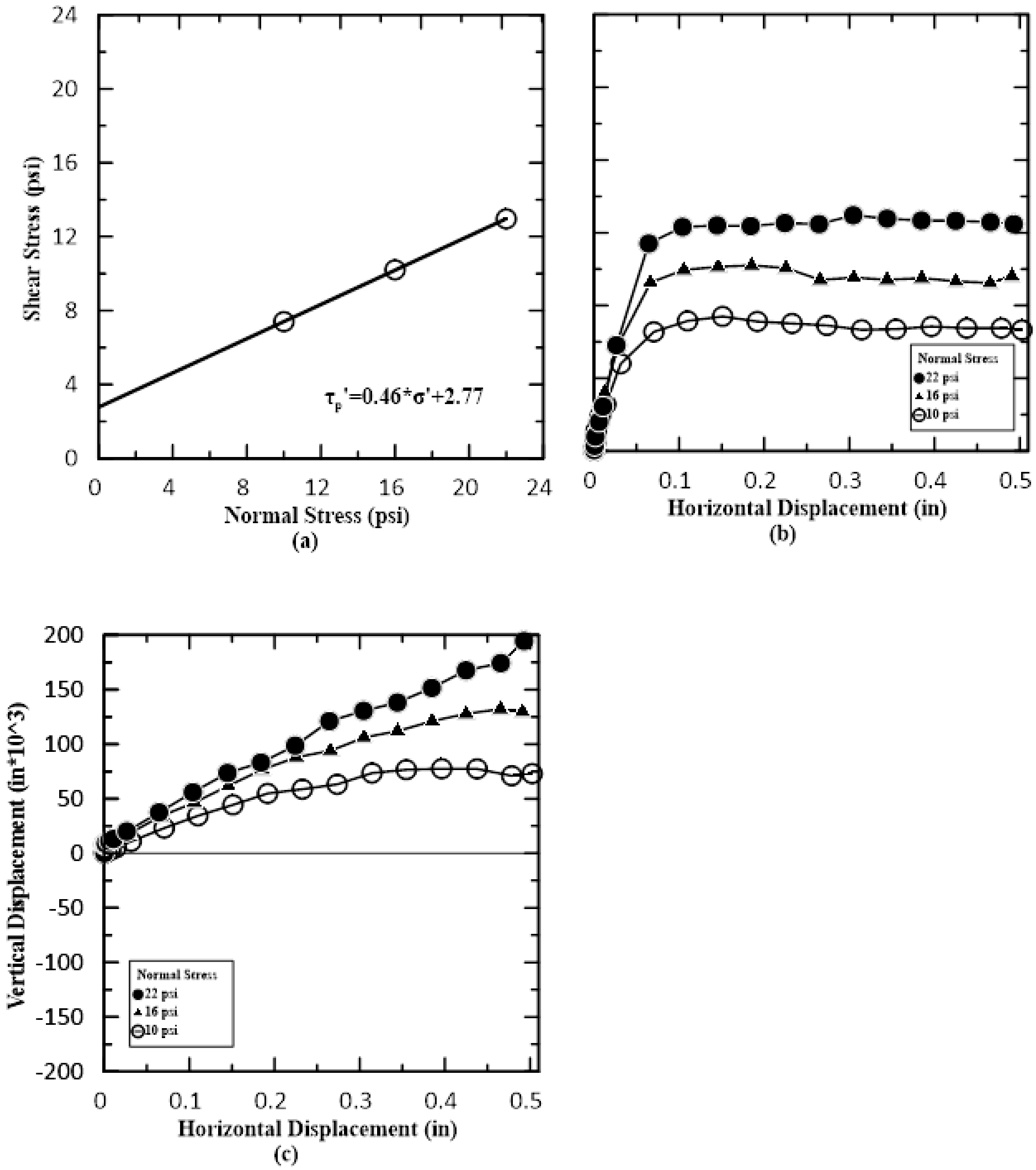

Figure 80. Small direct shear results for Soil 1 and Soil 3 mixtures at fine content = 70%, moisture content = 16.1%: (a) shear stress vs normal stress; (b) shear stress vs horizontal displacement; (c) vertical displacement vs horizontal displacement

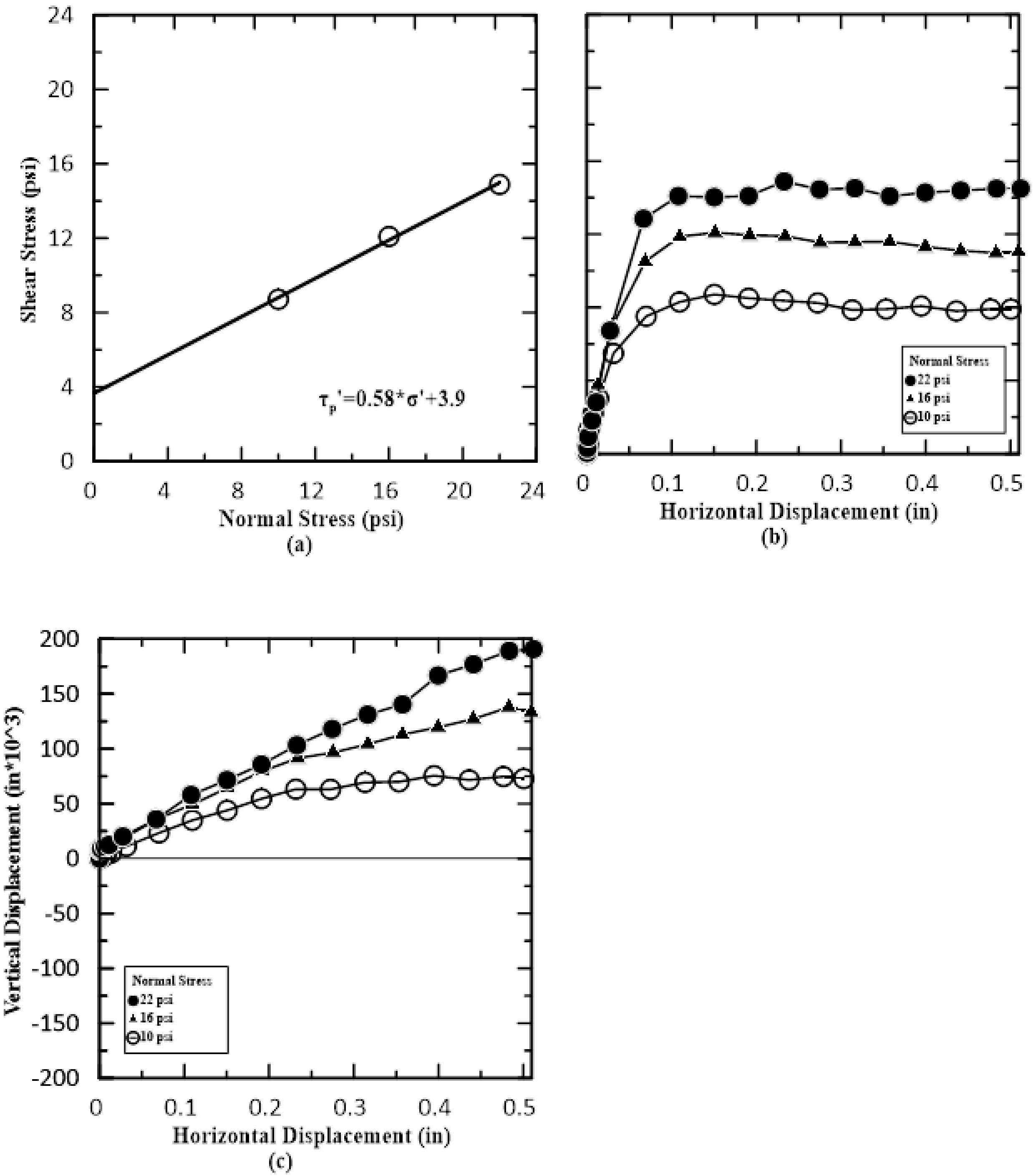

Figure 81. Small direct shear results for Soil 1 and Soil 4 mixtures at fine content = 10%, moisture content = 15.2%: (a) shear stress vs normal stress; (b) shear stress vs horizontal displacement; (c) vertical displacement vs horizontal displacement

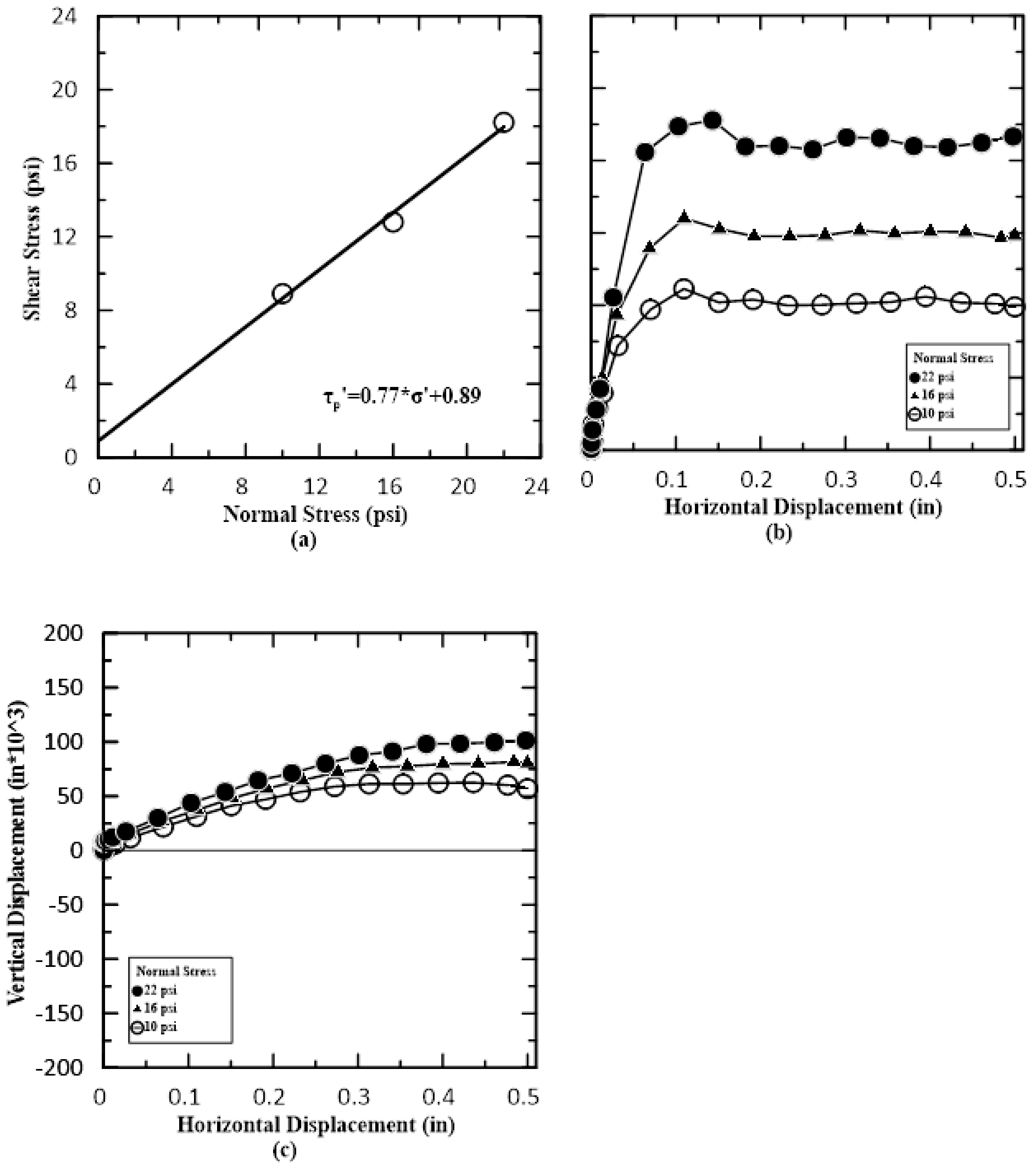

Figure 82. Small direct shear results for Soil 1 and Soil 4 mixtures at fine content = 10%, moisture content = 13%: (a) shear stress vs normal stress; (b) shear stress vs horizontal displacement; (c) vertical displacement vs horizontal displacement

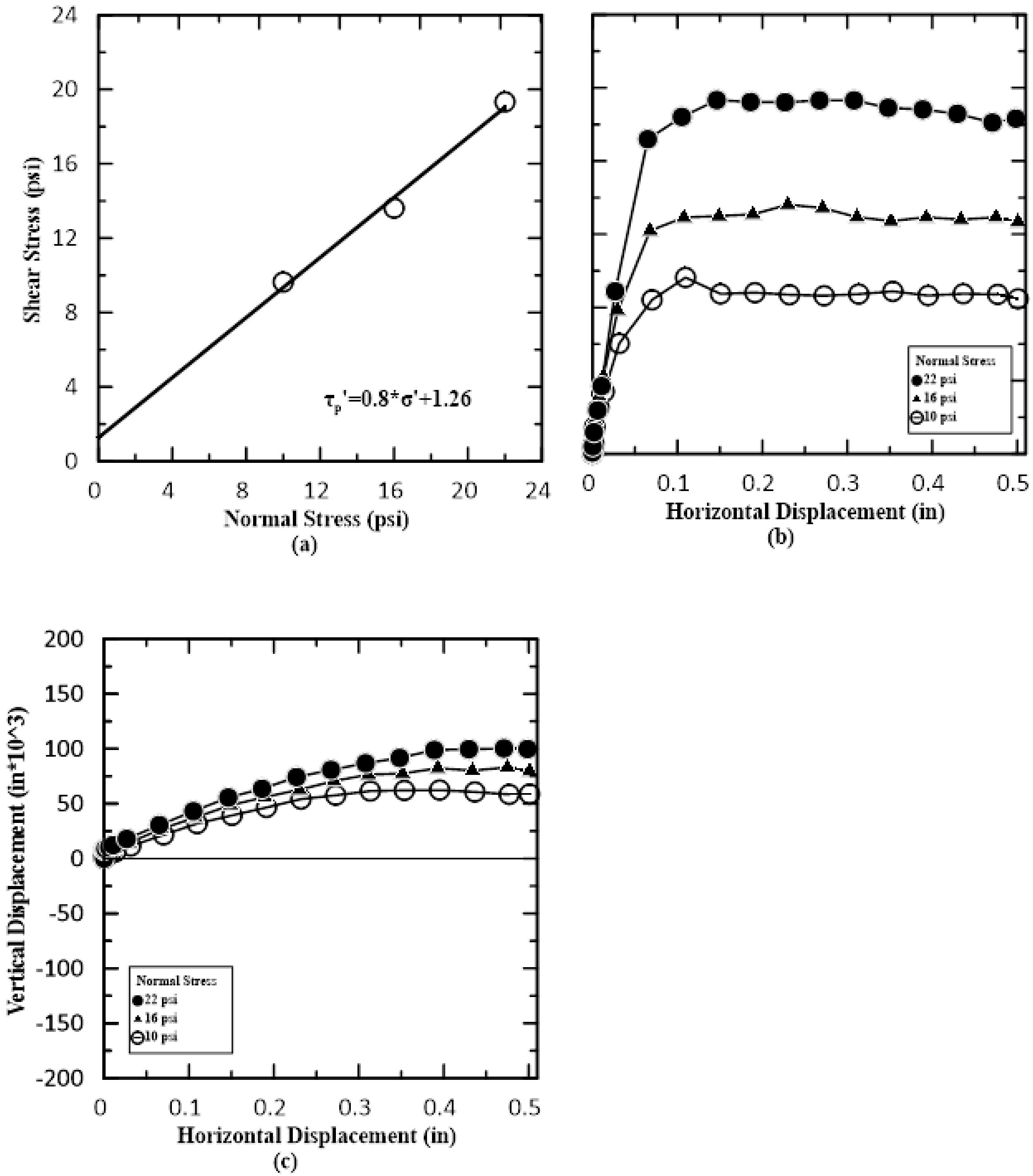

Figure 83. Small direct shear results for Soil 1 and Soil 4 mixtures at fine content = 10%, moisture content = 11.3%: (a) shear stress vs normal stress; (b) shear stress vs horizontal displacement; (c) vertical displacement vs horizontal displacement

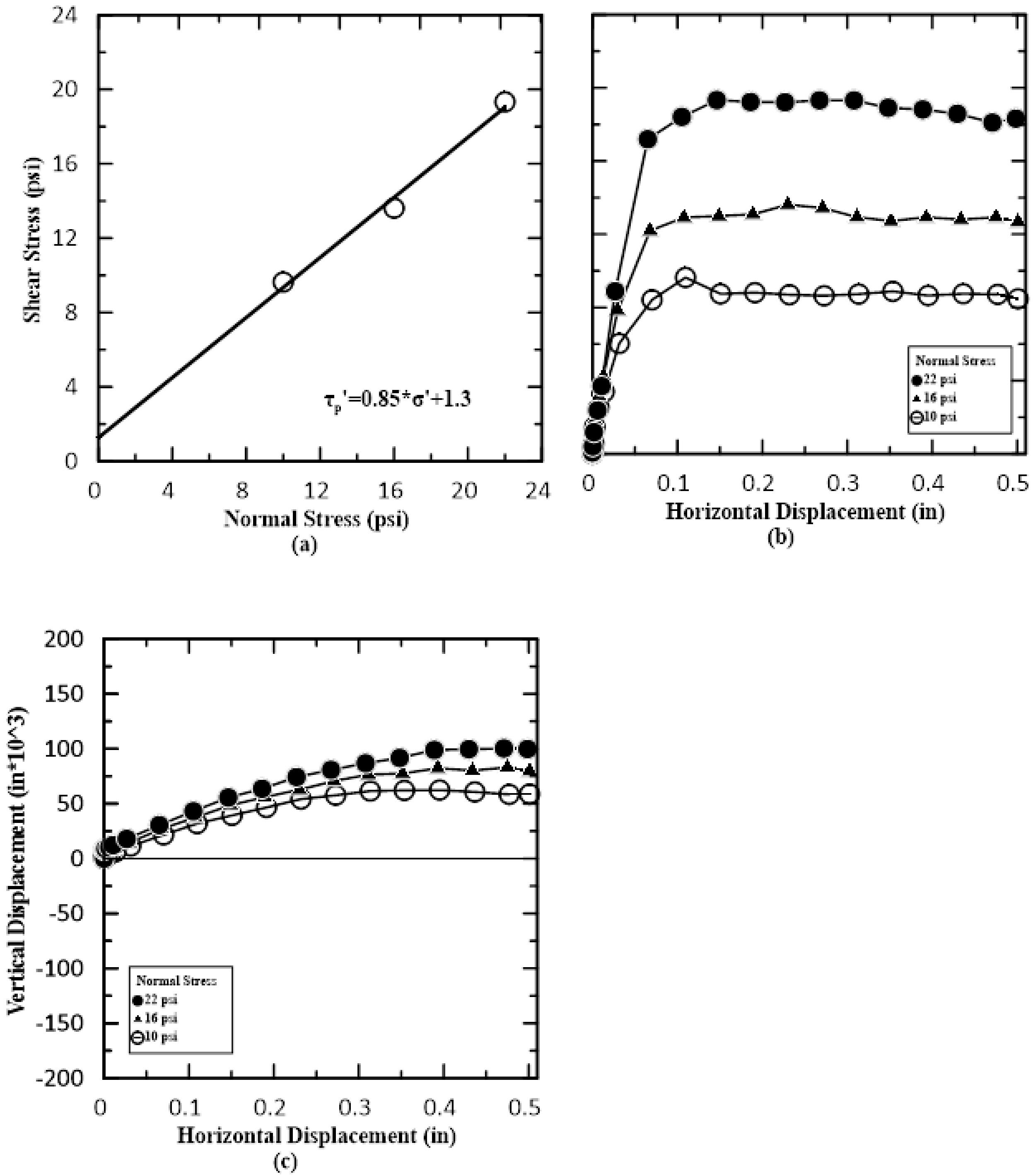

Figure 84. Small direct shear results for Soil 1 and Soil 4 mixtures at fine content = 10%, moisture content = 9.1%: (a) shear stress vs normal stress; (b) shear stress vs horizontal displacement; (c) vertical displacement vs horizontal displacement

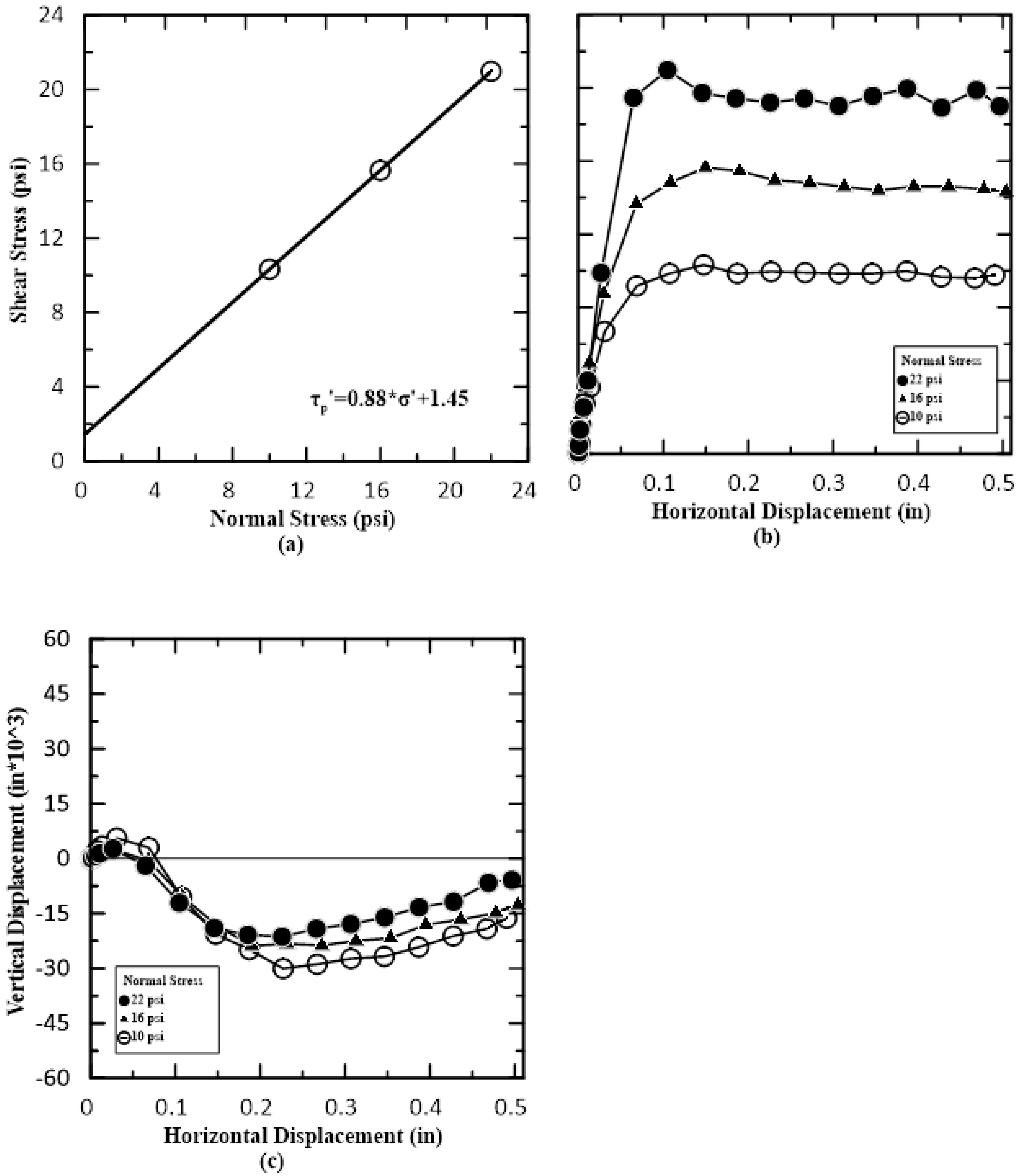

Figure 85. Small direct shear results for Soil 1 and Soil 4 mixtures at fine content = 20%, moisture content = 15.5%: (a) shear stress vs normal stress; (b) shear stress vs horizontal displacement; (c) vertical displacement vs horizontal displacement

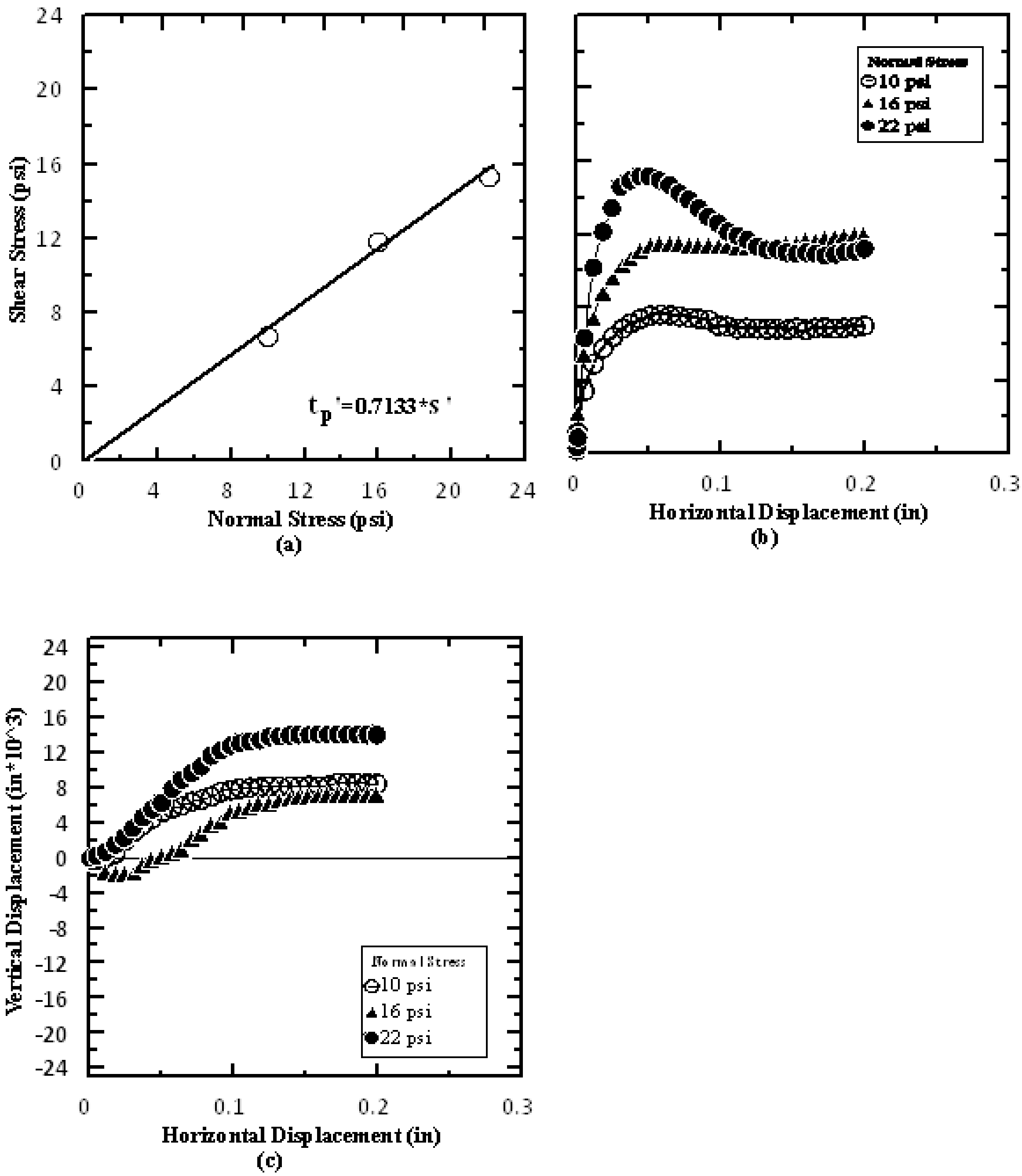

Figure 86. Small direct shear results for Soil 1 and Soil 4 mixtures at fine content = 20%, moisture content = 13.5%: (a) shear stress vs normal stress; (b) shear stress vs horizontal displacement; (c) vertical displacement vs horizontal displacement

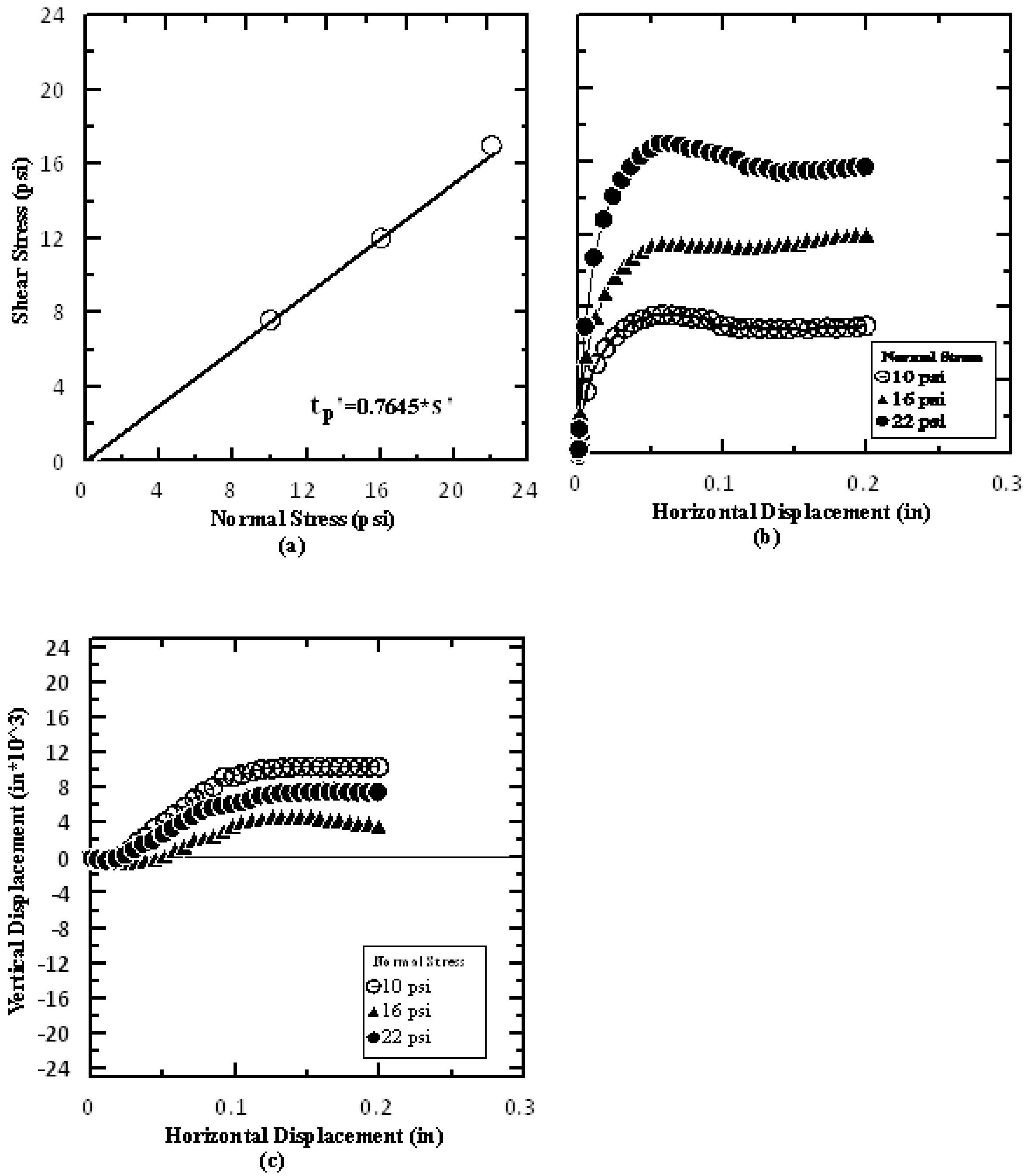

Figure 87. Small direct shear results for Soil 1 and Soil 4 mixtures at fine content = 20%, moisture content = 11.3%: (a) shear stress vs normal stress; (b) shear stress vs horizontal displacement; (c) vertical displacement vs horizontal displacement

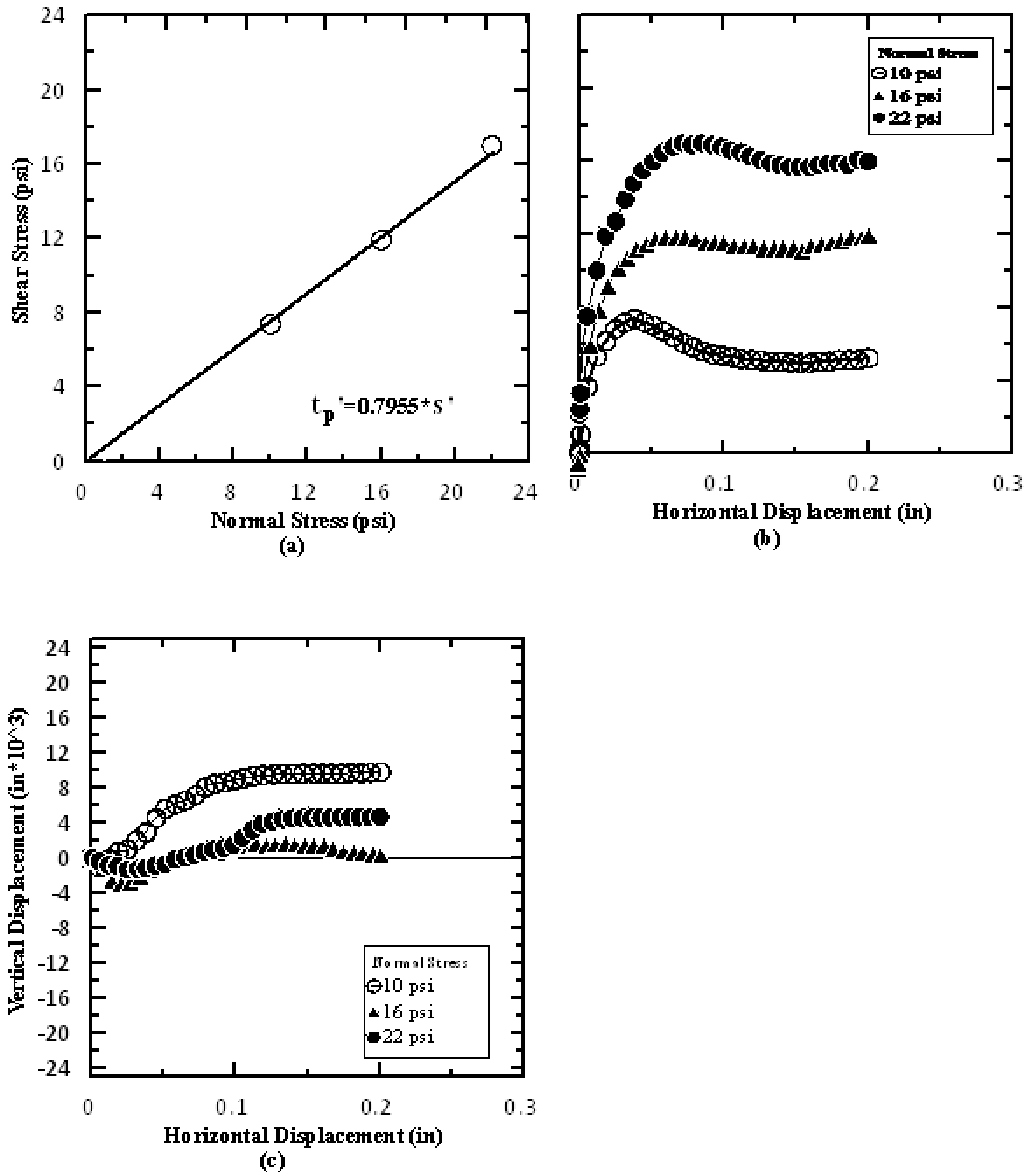

Figure 88. Small direct shear results for Soil 1 and Soil 4 mixtures at fine content = 20%, moisture content = 9.6%: (a) shear stress vs normal stress; (b) shear stress vs horizontal displacement; (c) vertical displacement vs horizontal displacement

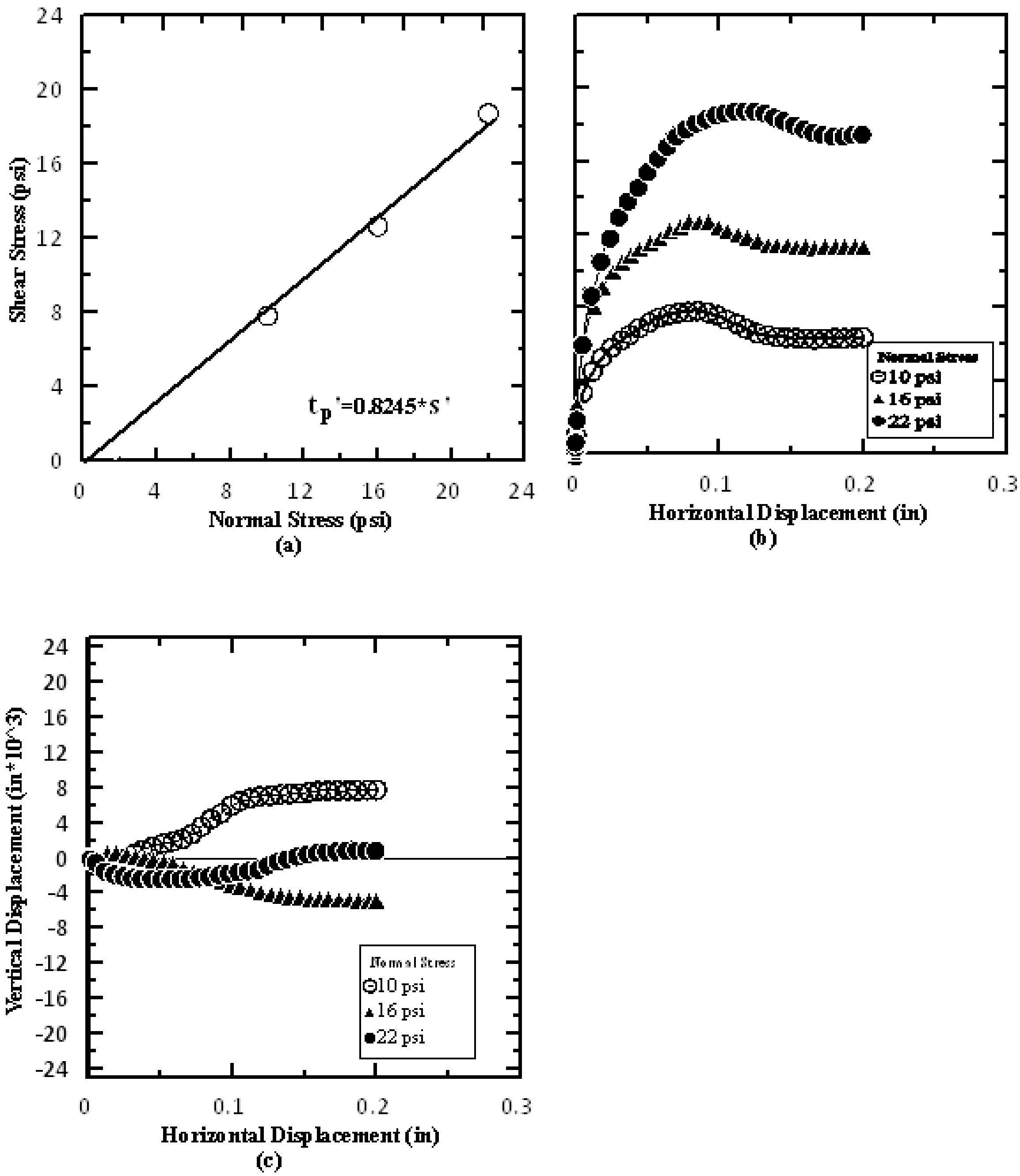

Figure 89. Small direct shear results for Soil 1 and Soil 4 mixtures at fine content = 30%, moisture content = 16%: (a) shear stress vs normal stress; (b) shear stress vs horizontal displacement; (c) vertical displacement vs horizontal displacement

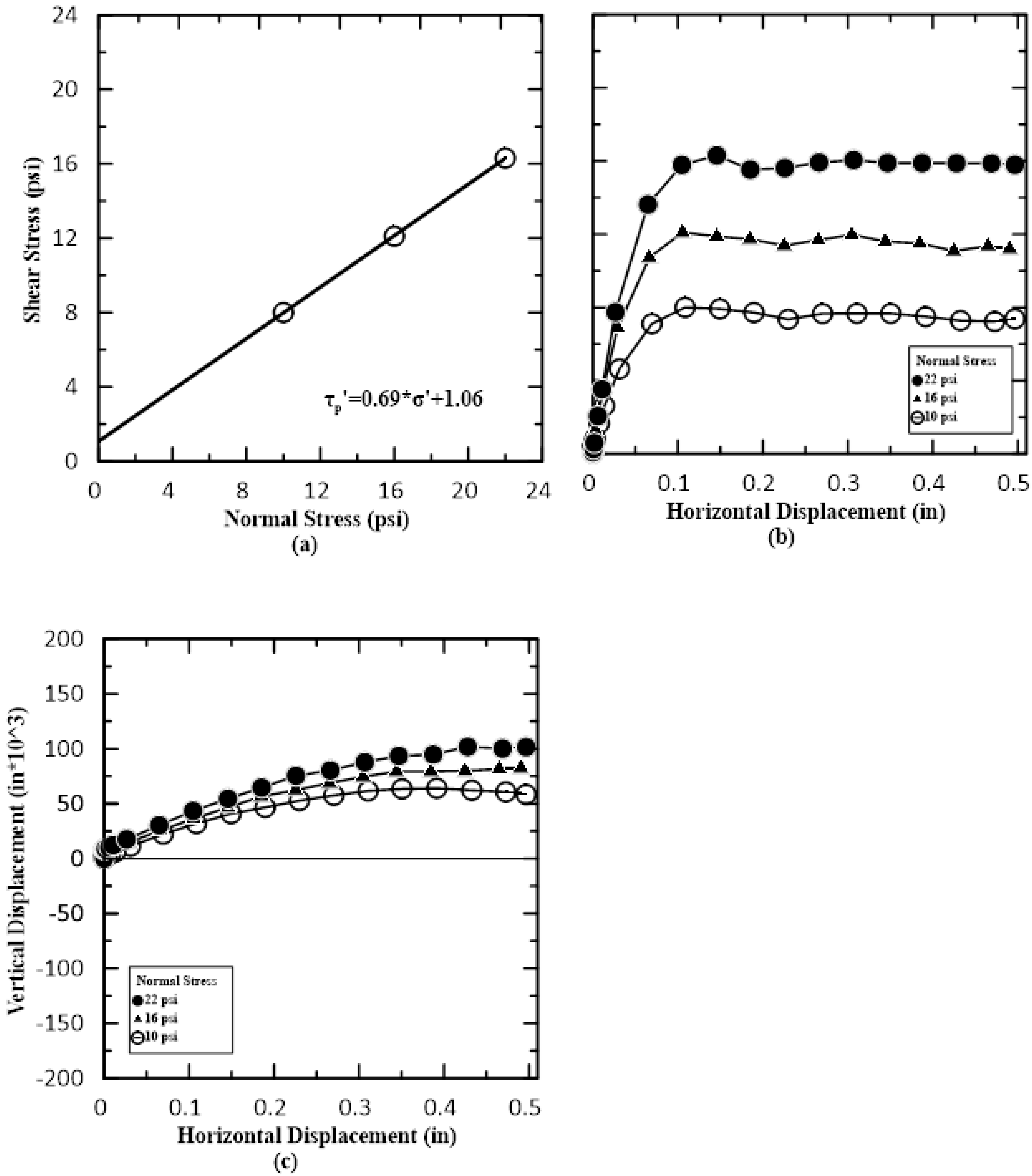

Figure 90. Small direct shear results for Soil 1 and Soil 4 mixtures at fine content = 30%, moisture content = 14.8%: (a) shear stress vs normal stress; (b) shear stress vs horizontal displacement; (c) vertical displacement vs horizontal displacement

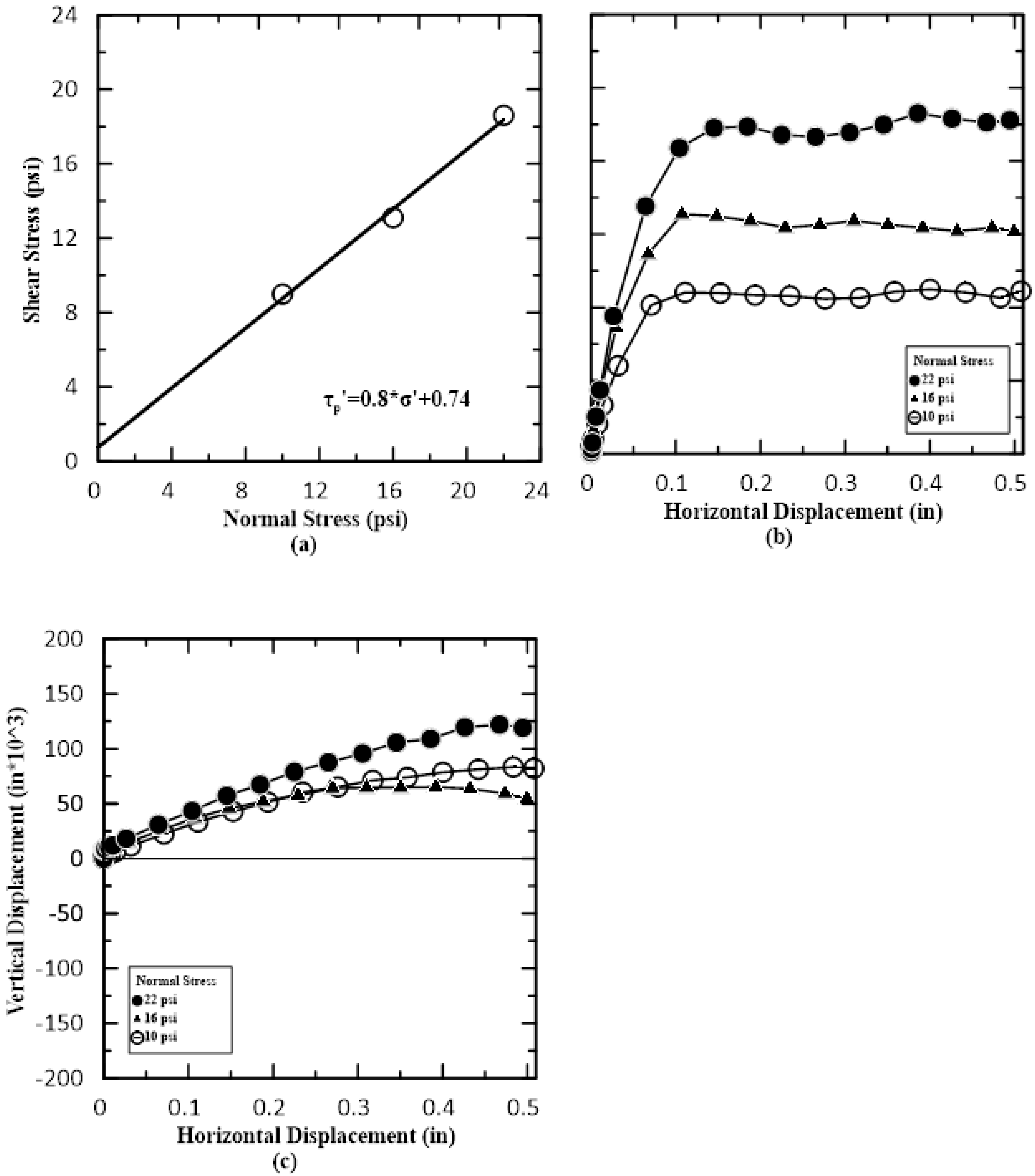

Figure 91. Small direct shear results for Soil 1 and Soil 4 mixtures at fine content = 30%, moisture content = 12.1%: (a) shear stress vs normal stress; (b) shear stress vs horizontal displacement; (c) vertical displacement vs horizontal displacement

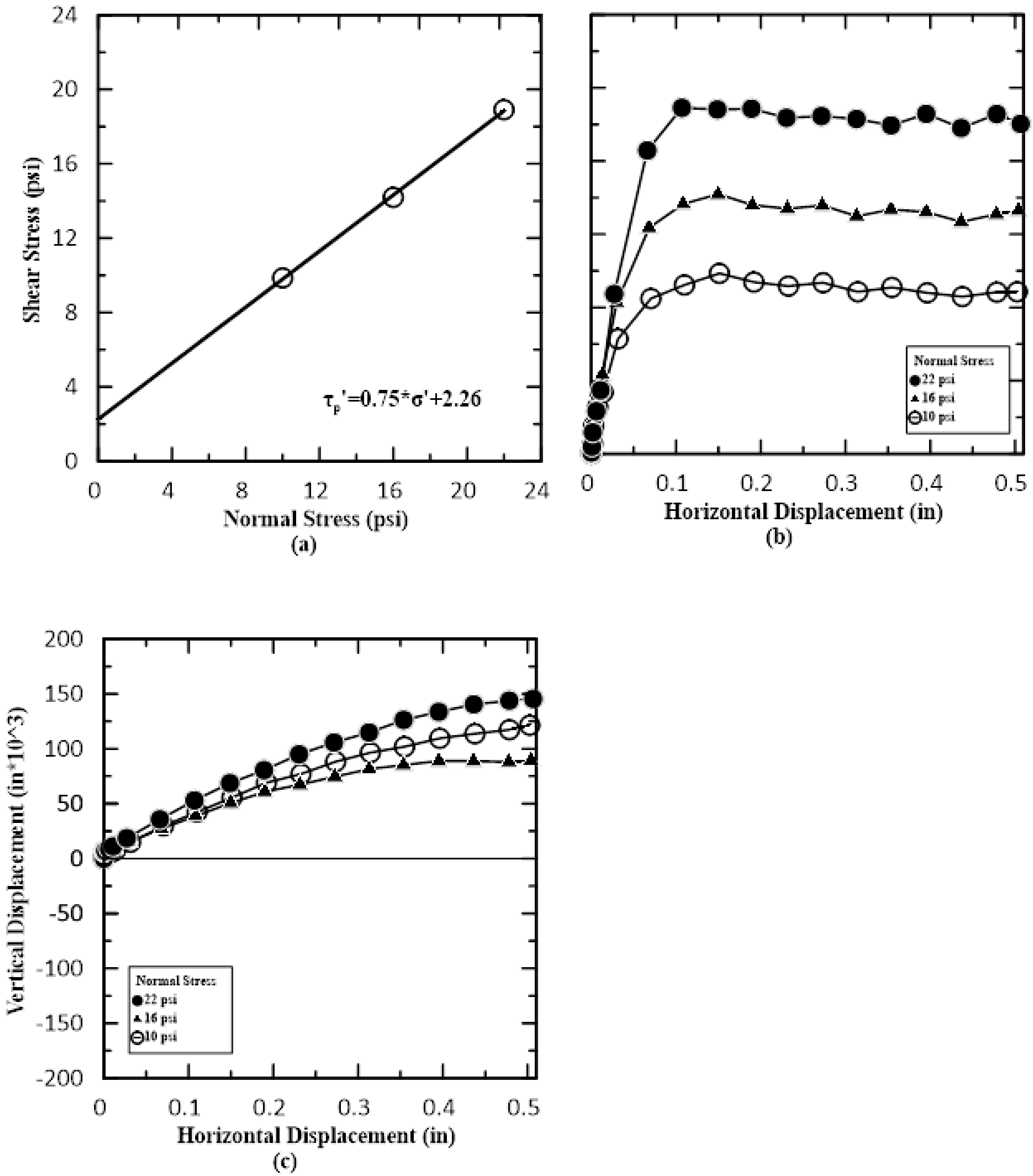

Figure 92. Small direct shear results for Soil 1 and Soil 4 mixtures at fine content = 30%, moisture content = 10.2%: (a) shear stress vs normal stress; (b) shear stress vs horizontal displacement; (c) vertical displacement vs horizontal displacement

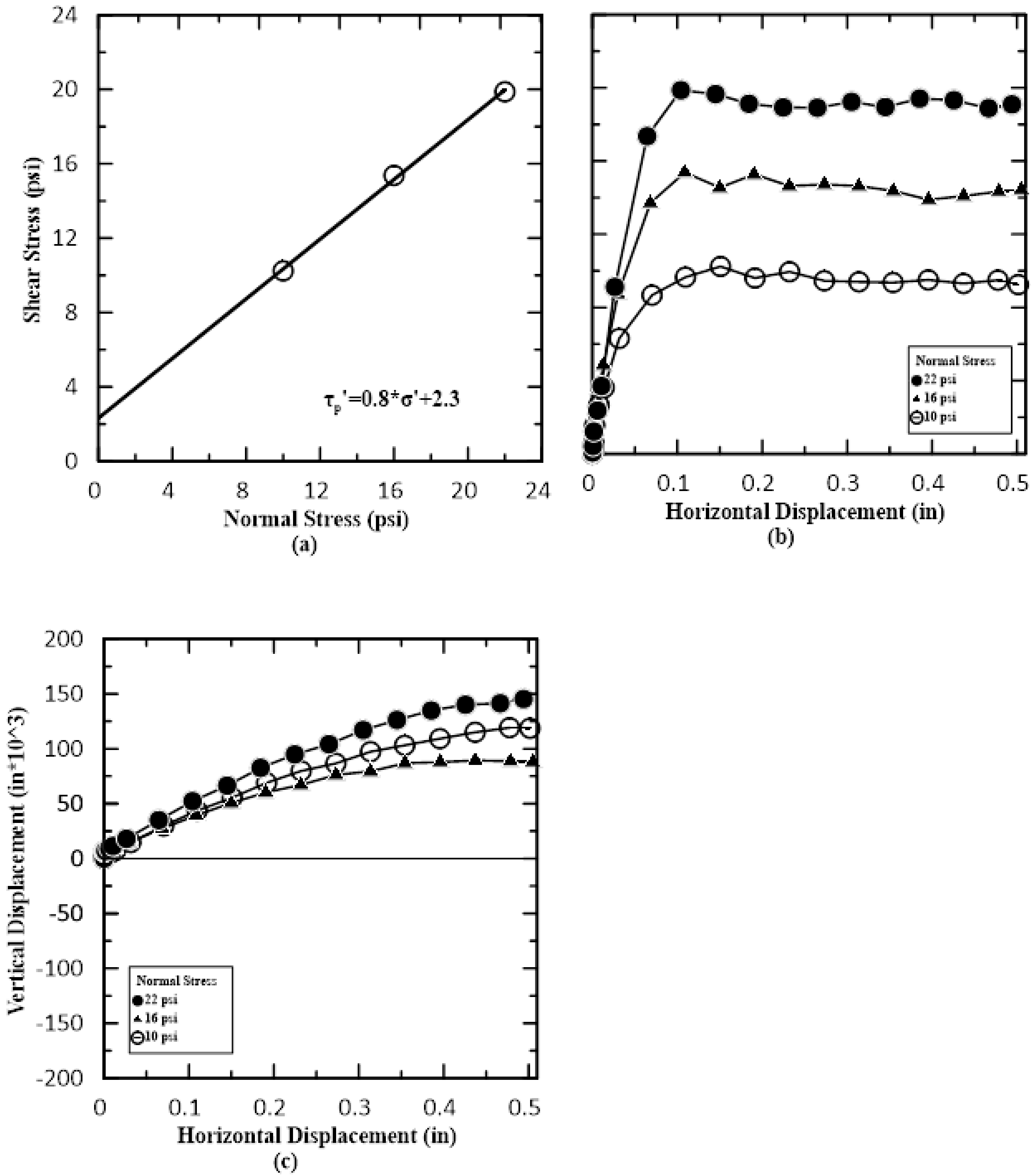

Figure 93. Small direct shear results for Soil 1 and Soil 4 mixtures at fine content = 40%, moisture content = 17.4%: (a) shear stress vs normal stress; (b) shear stress vs horizontal displacement; (c) vertical displacement vs horizontal displacement

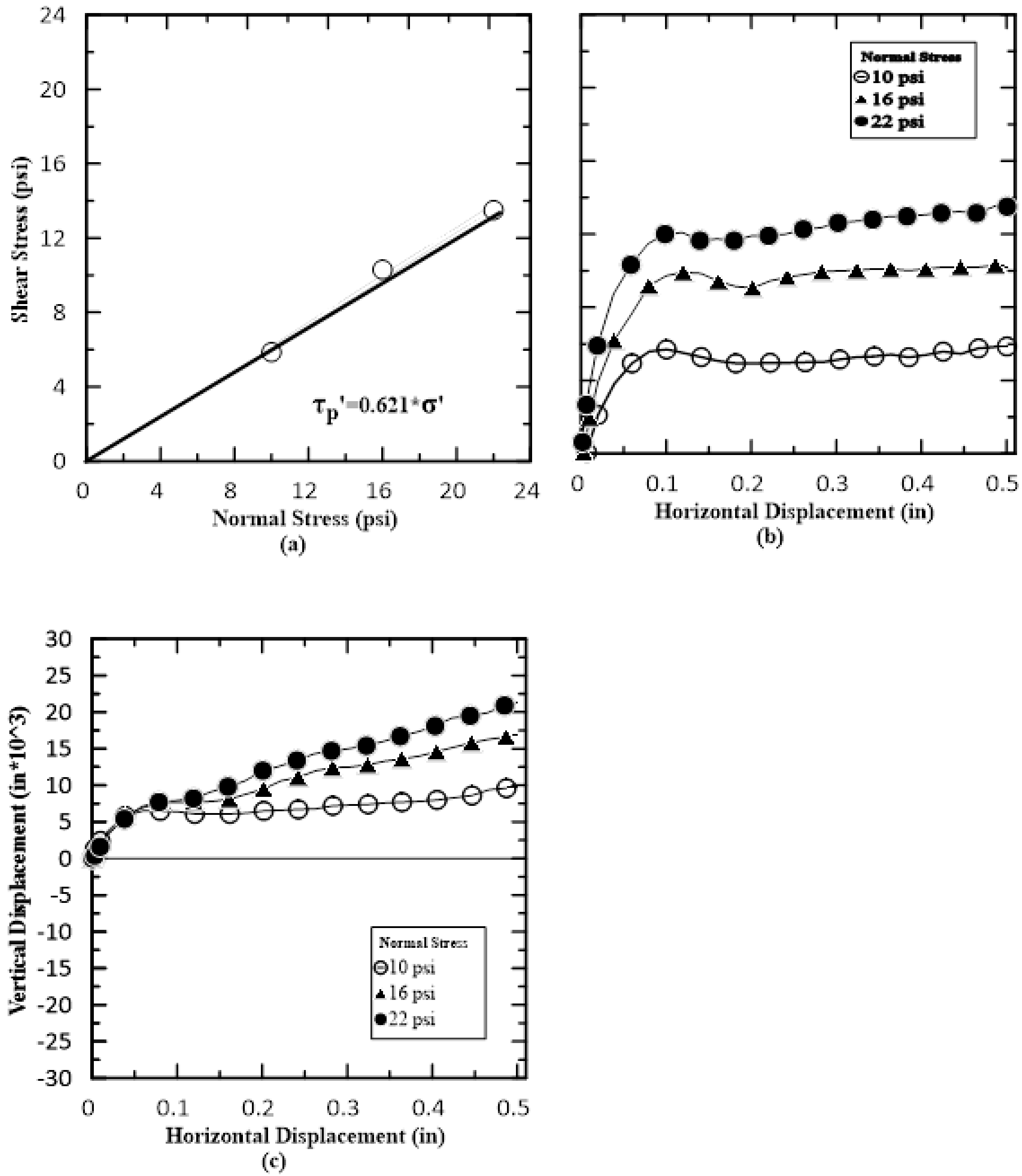

Figure 94. Small direct shear results for Soil 1 and Soil 4 mixtures at fine content = 40%, moisture content = 15.3%: (a) shear stress vs normal stress; (b) shear stress vs horizontal displacement; (c) vertical displacement vs horizontal displacement

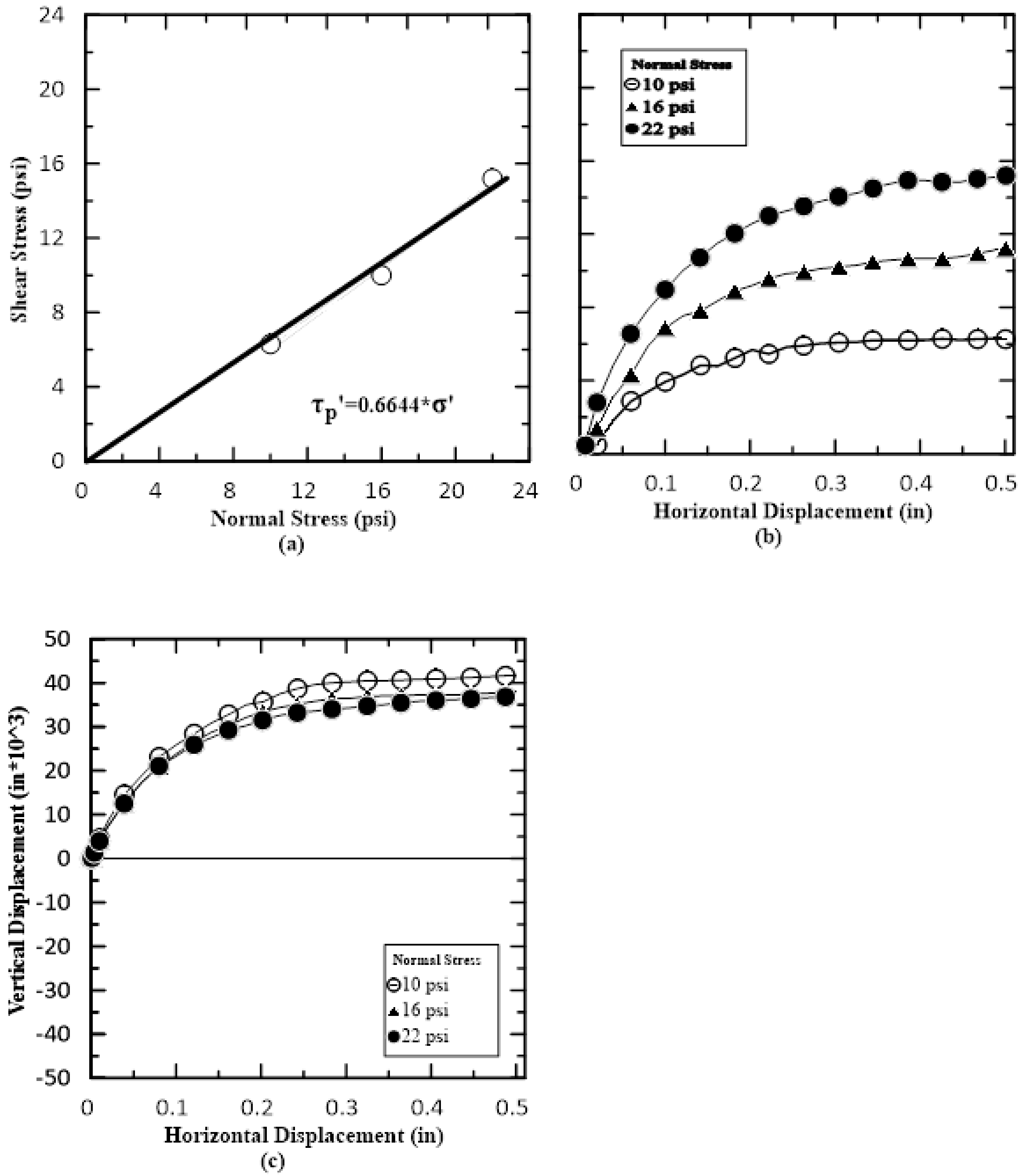

Figure 95. Small direct shear results for Soil 1 and Soil 4 mixtures at fine content = 40%, moisture content = 13.2%: (a) shear stress vs normal stress; (b) shear stress vs horizontal displacement; (c) vertical displacement vs horizontal displacement

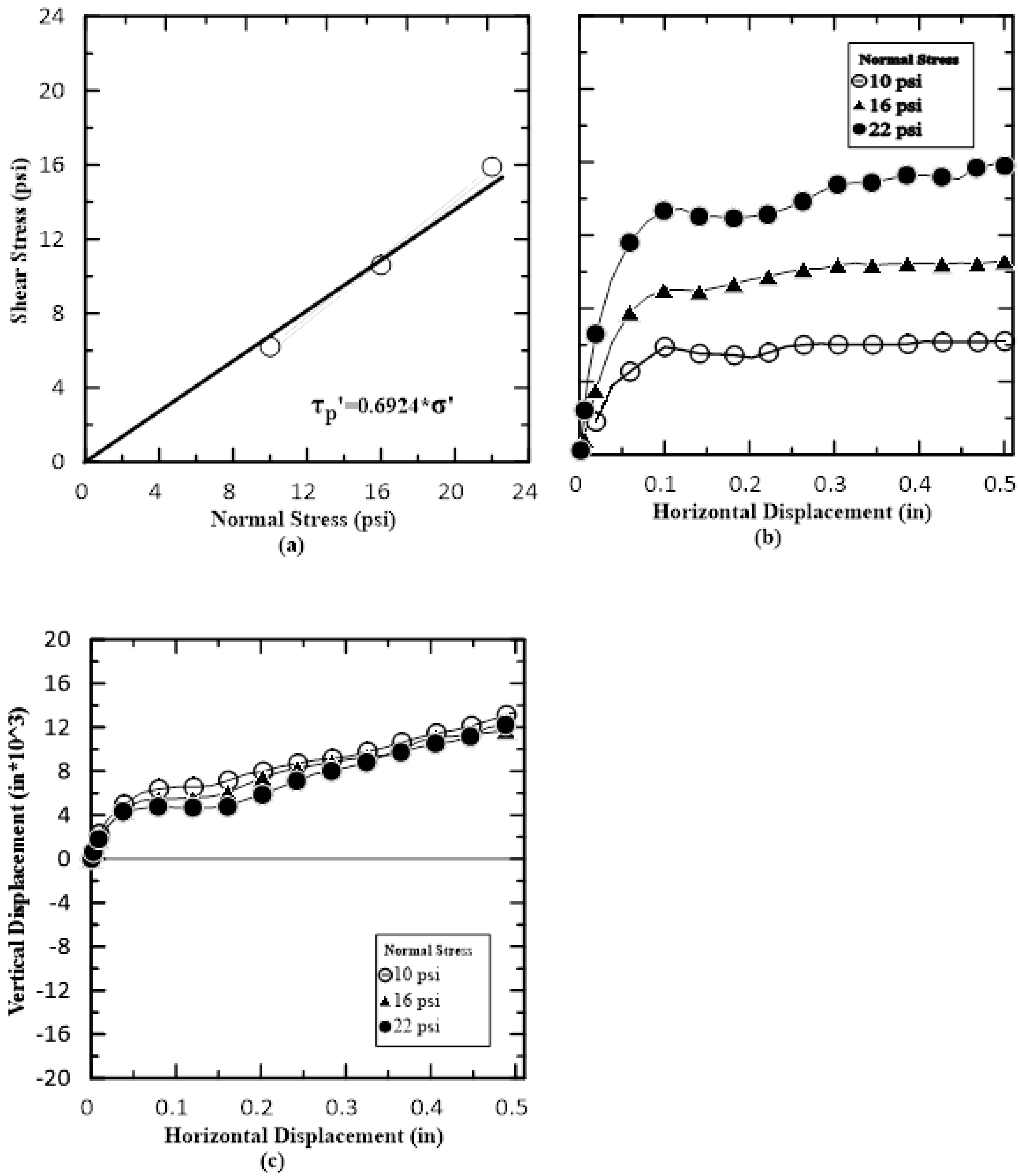

Figure 96. Small direct shear results for Soil 1 and Soil 4 mixtures at fine content = 40%, moisture content = 11.3%: (a) shear stress vs normal stress; (b) shear stress vs horizontal displacement; (c) vertical displacement vs horizontal displacement

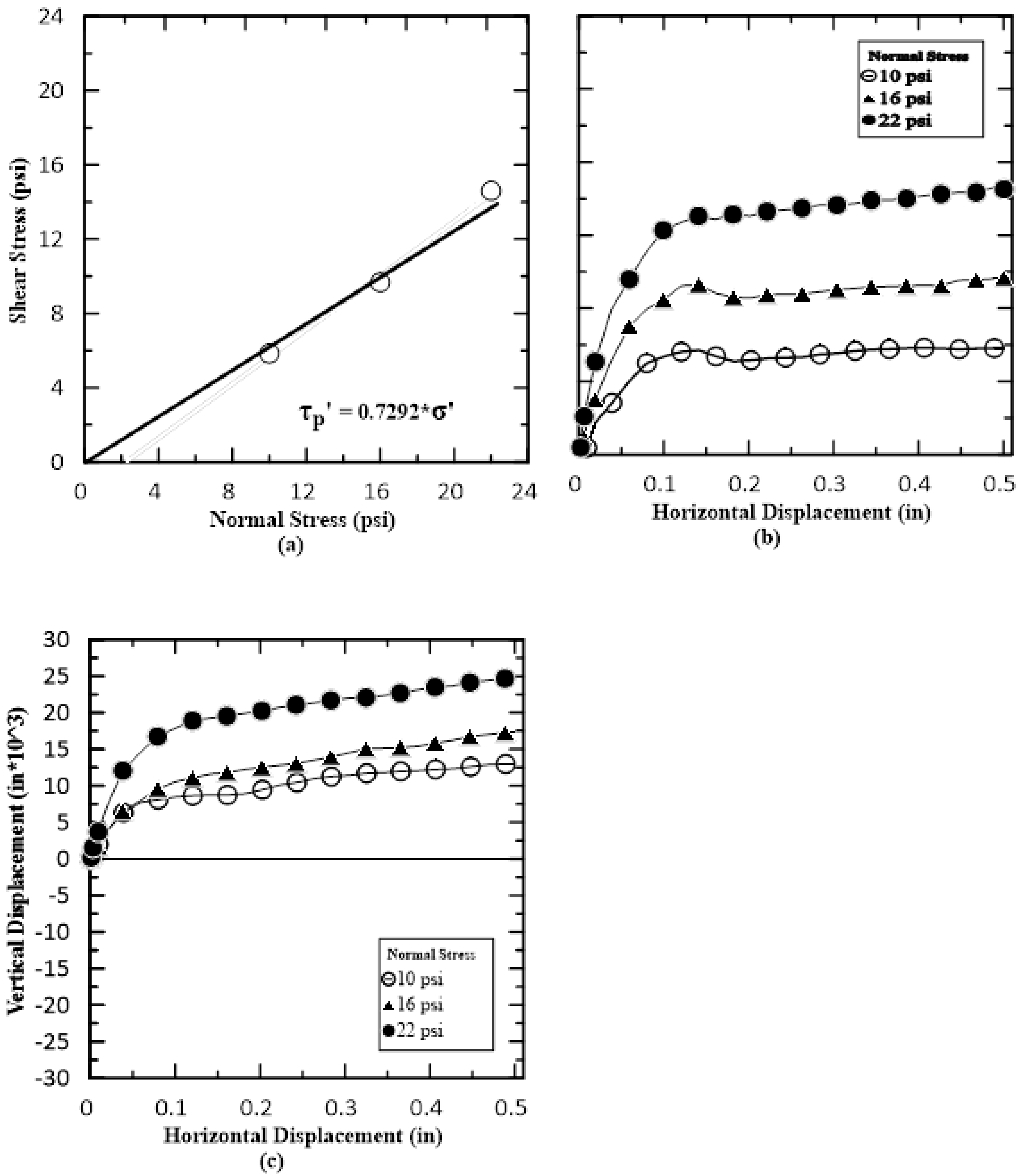

Figure 97. Small direct shear results for Soil 1 and Soil 4 mixtures at fine content = 50%, moisture content = 18.6%: (a) shear stress vs normal stress; (b) shear stress vs horizontal displacement; (c) vertical displacement vs horizontal displacement

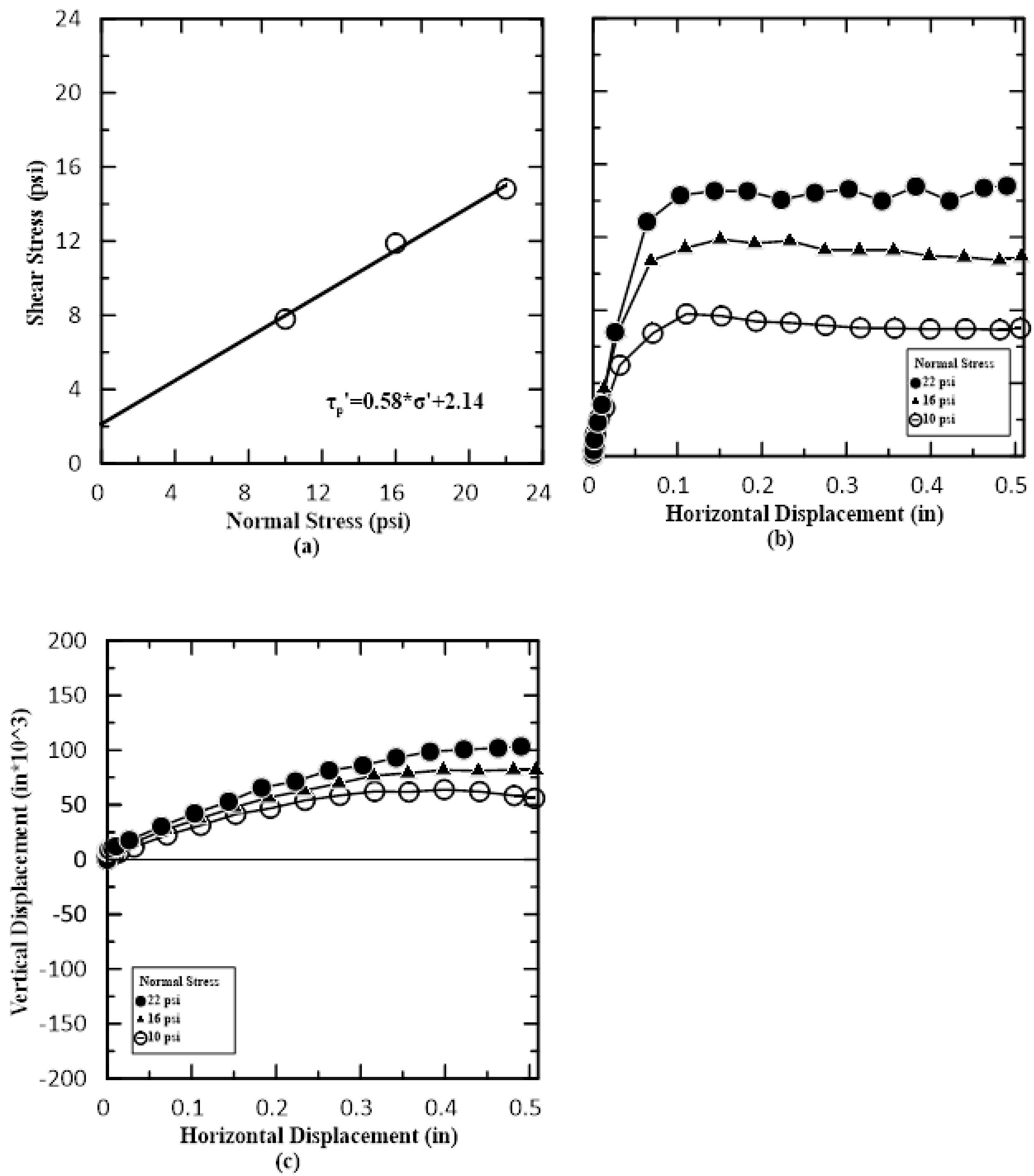

Figure 98. Small direct shear results for Soil 1 and Soil 4 mixtures at fine content = 50%, moisture content = 16%: (a) shear stress vs normal stress; (b) shear stress vs horizontal displacement; (c) vertical displacement vs horizontal displacement

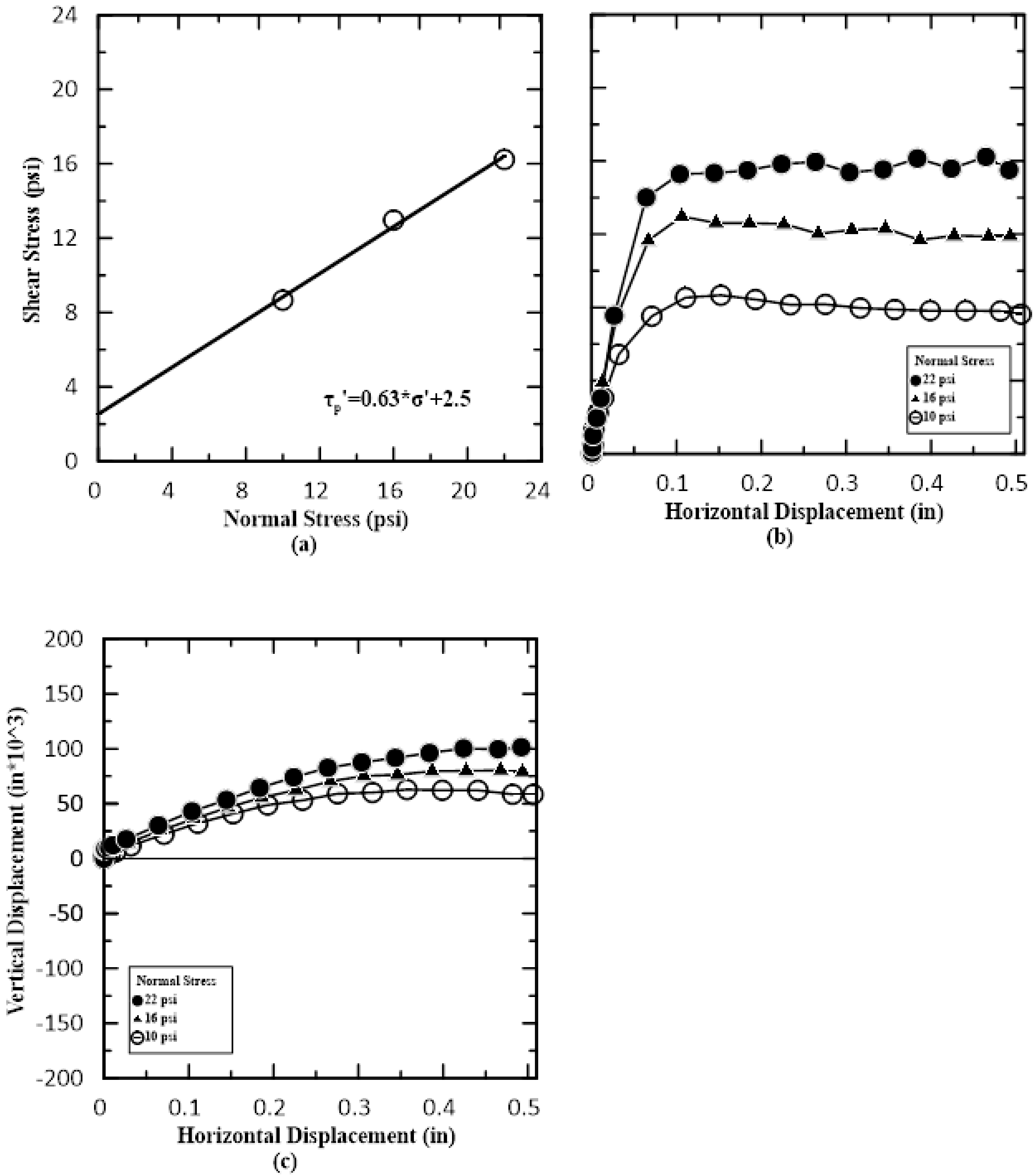

Figure 99. Small direct shear results for Soil 1 and Soil 4 mixtures at fine content = 50%, moisture content = 14.4%: (a) shear stress vs normal stress; (b) shear stress vs horizontal displacement; (c) vertical displacement vs horizontal displacement

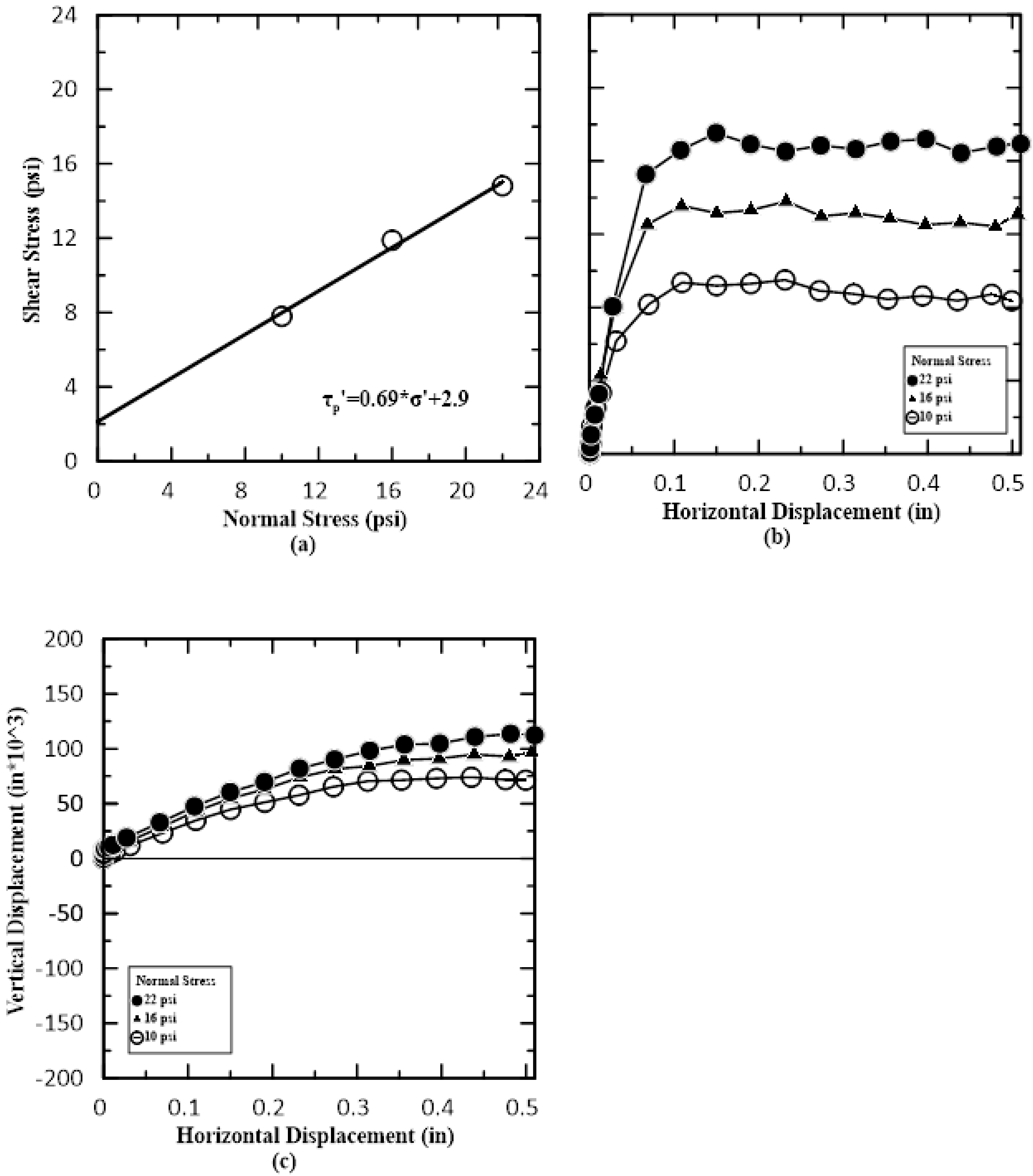

Figure 100. Small direct shear results for Soil 1 and Soil 4 mixtures at fine content = 50%, moisture content = 12%: (a) shear stress vs normal stress; (b) shear stress vs horizontal displacement; (c) vertical displacement vs horizontal displacement

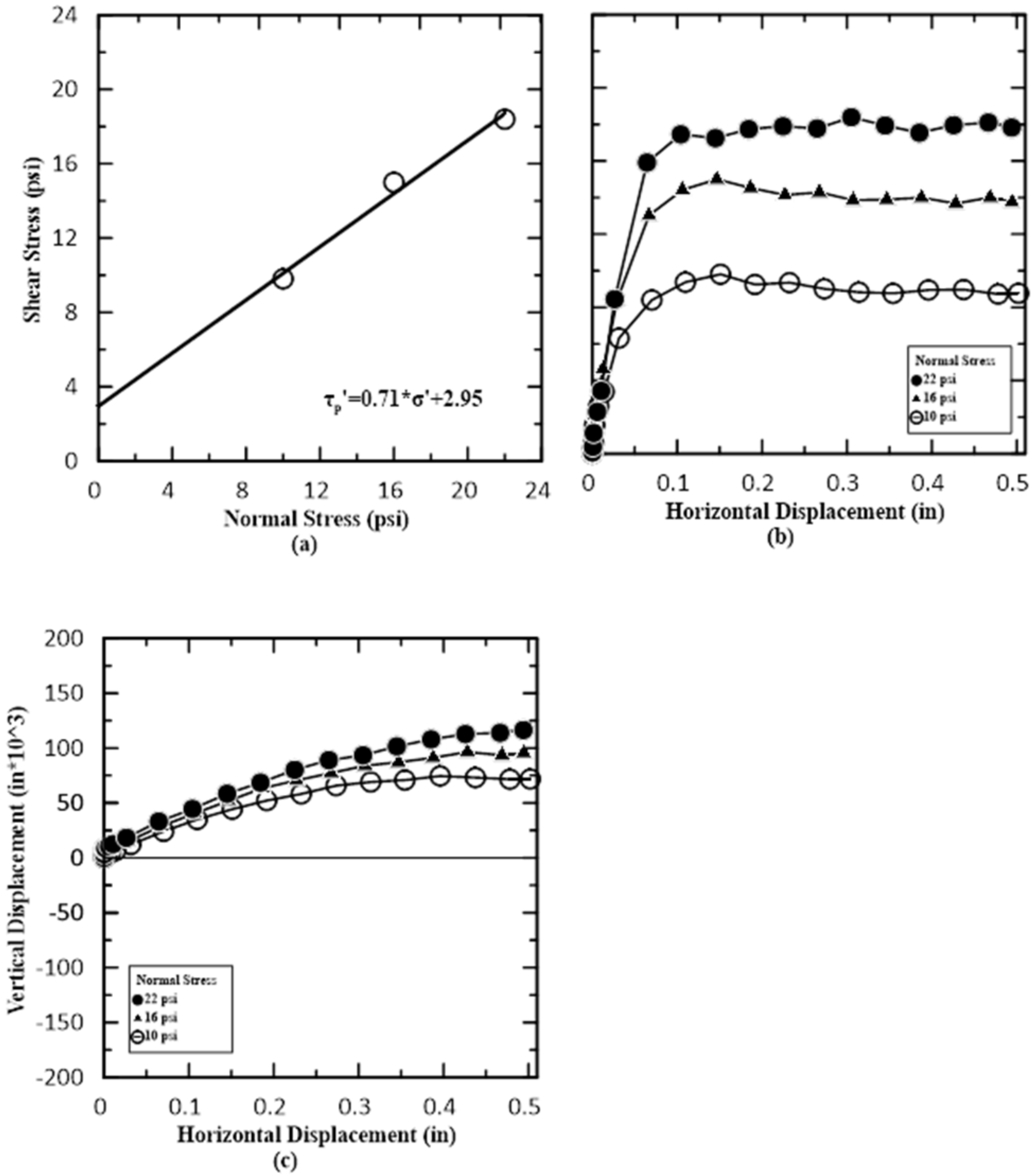

Figure 101. Small direct shear results for Soil 1 and Soil 4 mixtures at fine content = 60%, moisture content = 19.5%: (a) shear stress vs normal stress; (b) shear stress vs horizontal displacement; (c) vertical displacement vs horizontal displacement

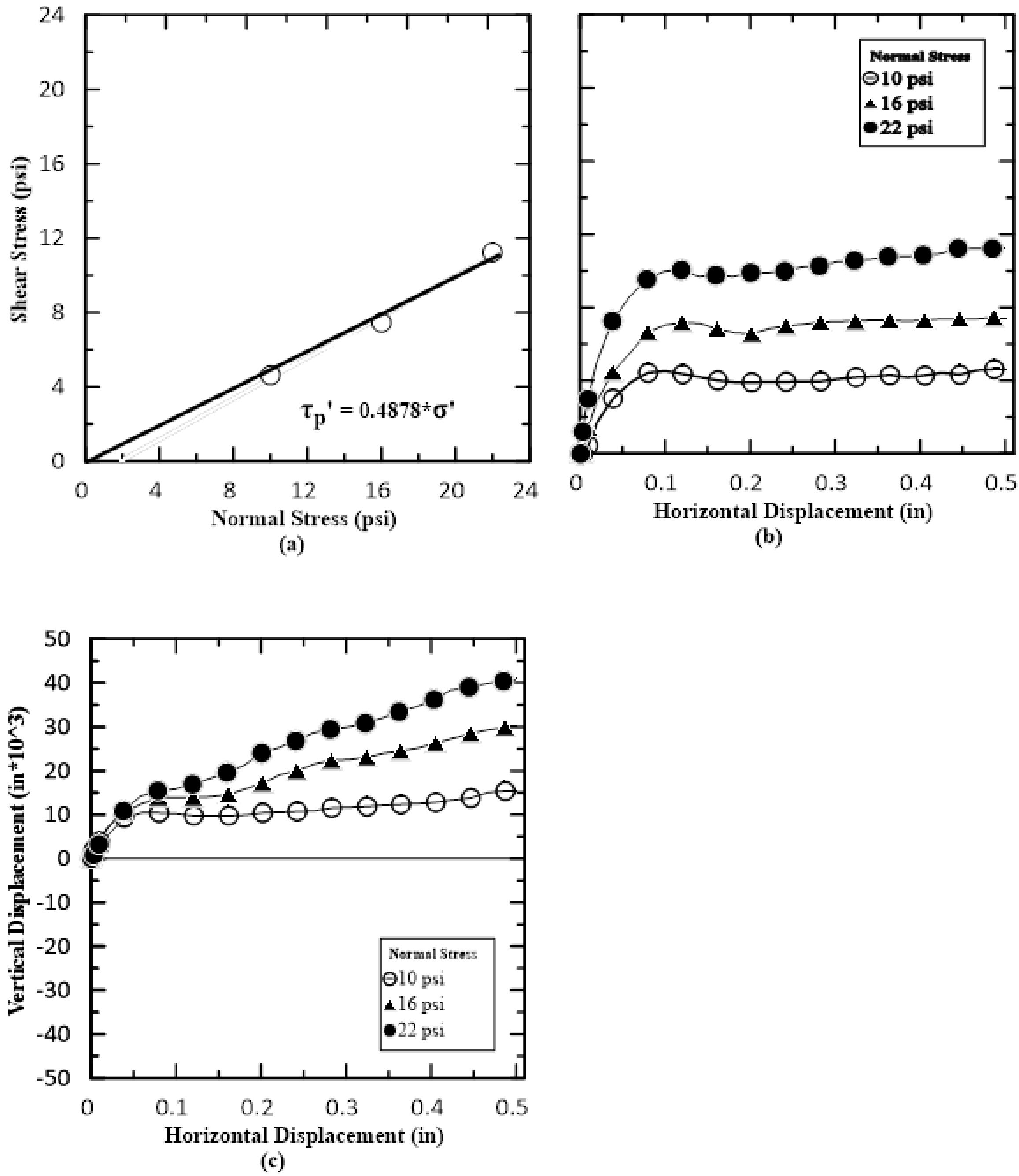

Figure 102. Small direct shear results for Soil 1 and Soil 4 mixtures at fine content = 60%, moisture content = 17.5%: (a) shear stress vs normal stress; (b) shear stress vs horizontal displacement; (c) vertical displacement vs horizontal displacement

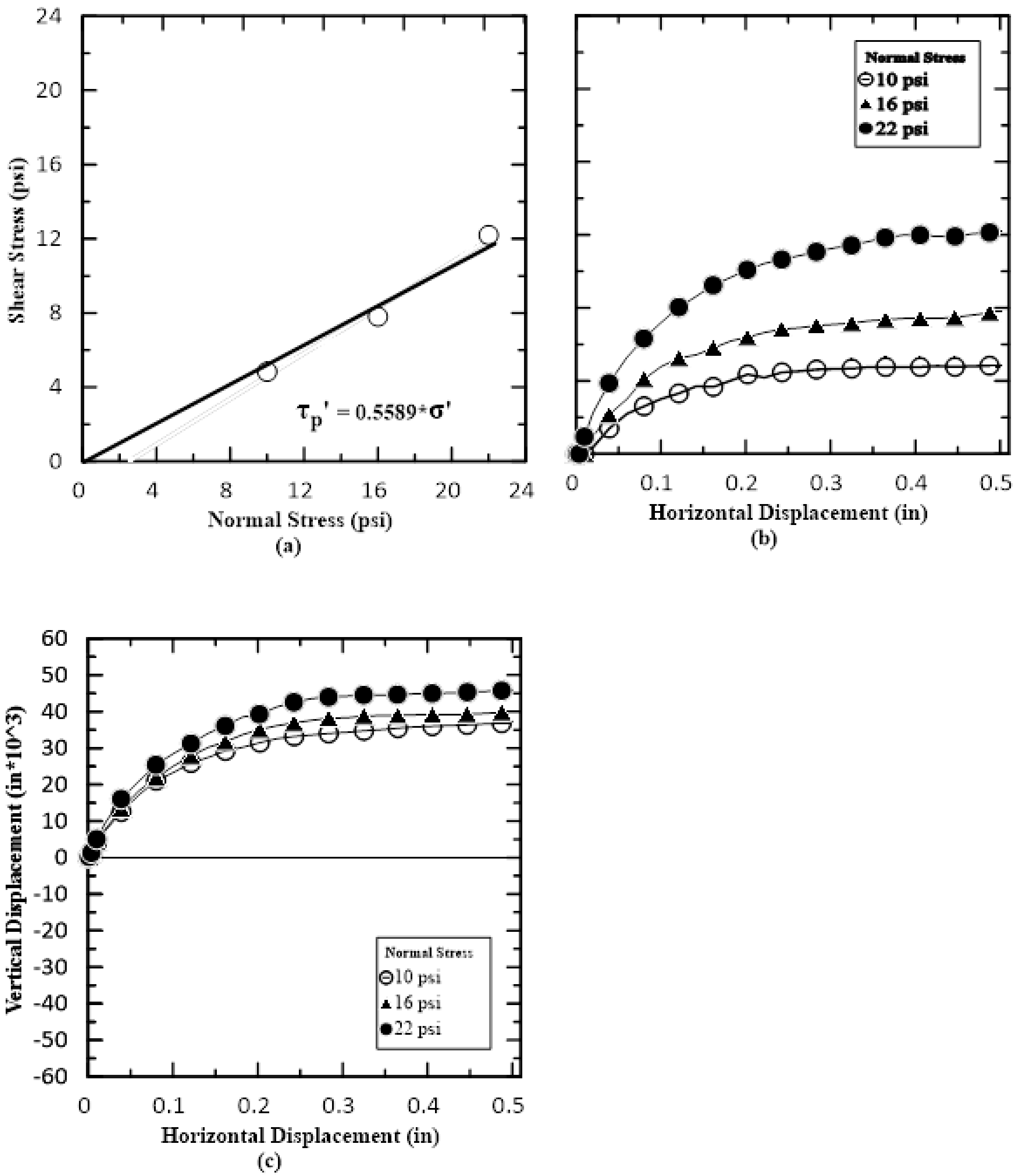

Figure 103. Small direct shear results for Soil 1 and Soil 4 mixtures at fine content = 60%, moisture content = 15.5%: (a) shear stress vs normal stress; (b) shear stress vs horizontal displacement; (c) vertical displacement vs horizontal displacement

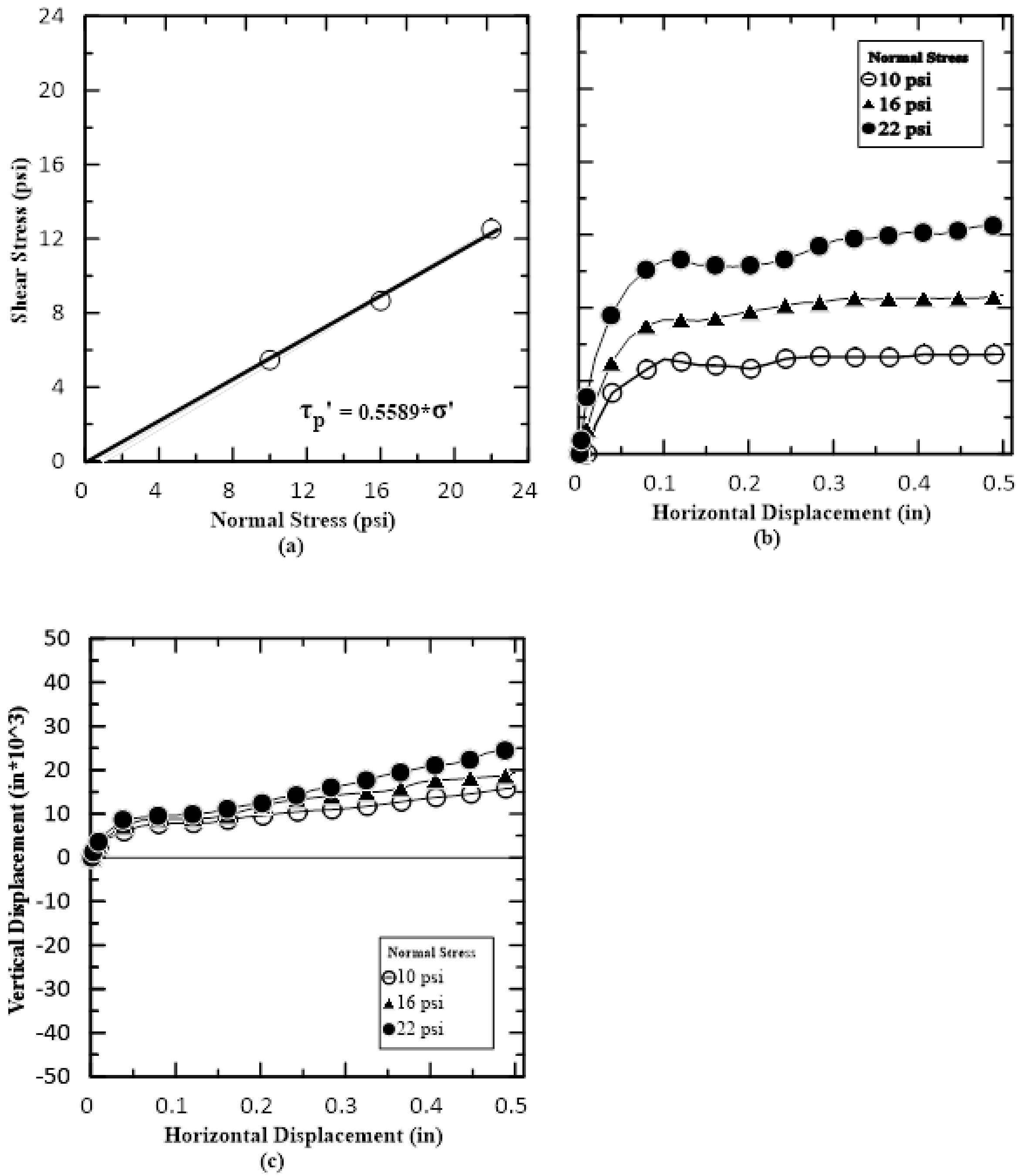

Figure 104. Small direct shear results for Soil 1 and Soil 4 mixtures at fine content = 60%, moisture content = 13.3%: (a) shear stress vs normal stress; (b) shear stress vs horizontal displacement; (c) vertical displacement vs horizontal displacement

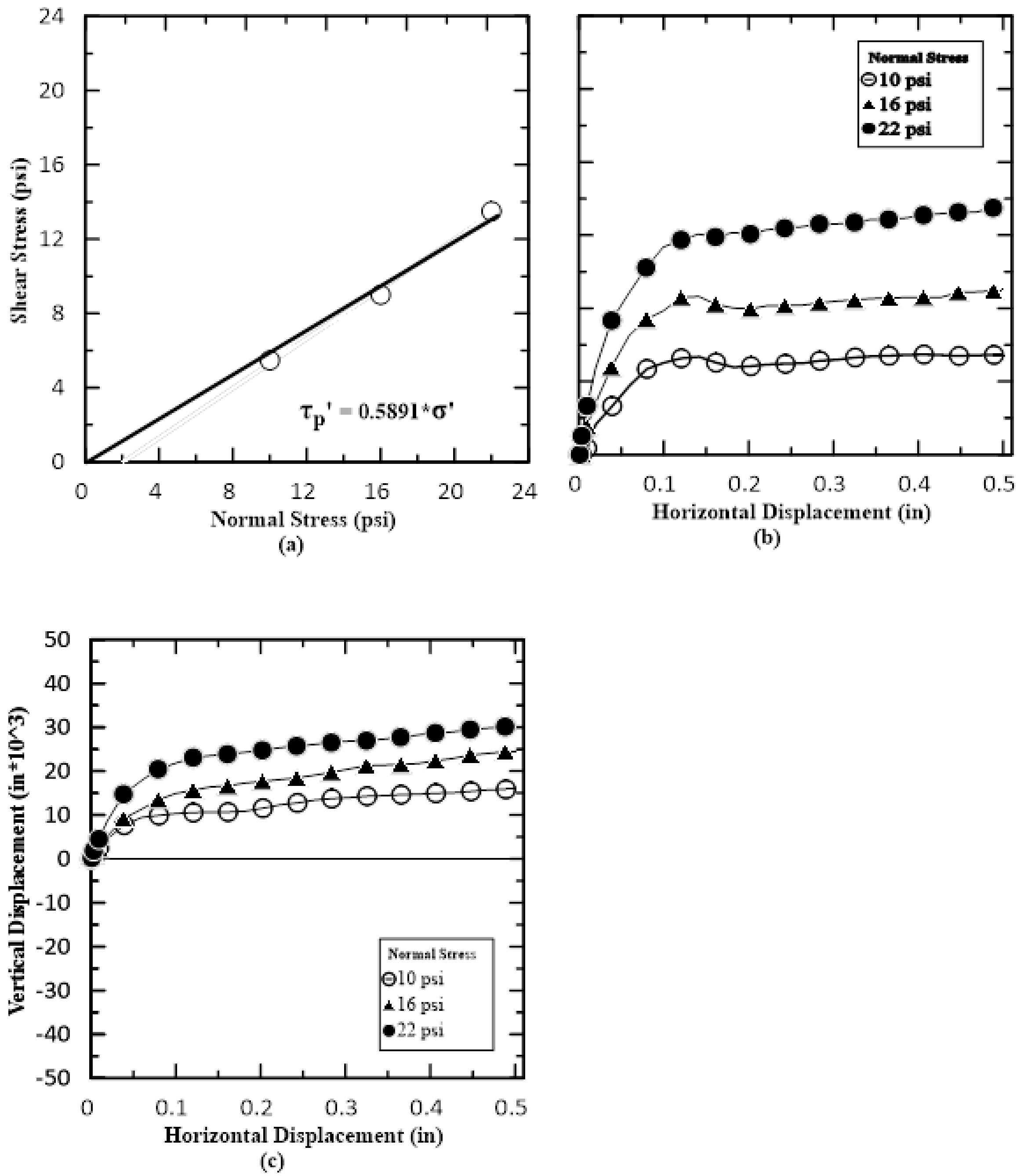

Figure 105. Small direct shear results for Soil 1 and Soil 4 mixtures at fine content = 70%, moisture content = 20.2%: (a) shear stress vs normal stress; (b) shear stress vs horizontal displacement; (c) vertical displacement vs horizontal displacement

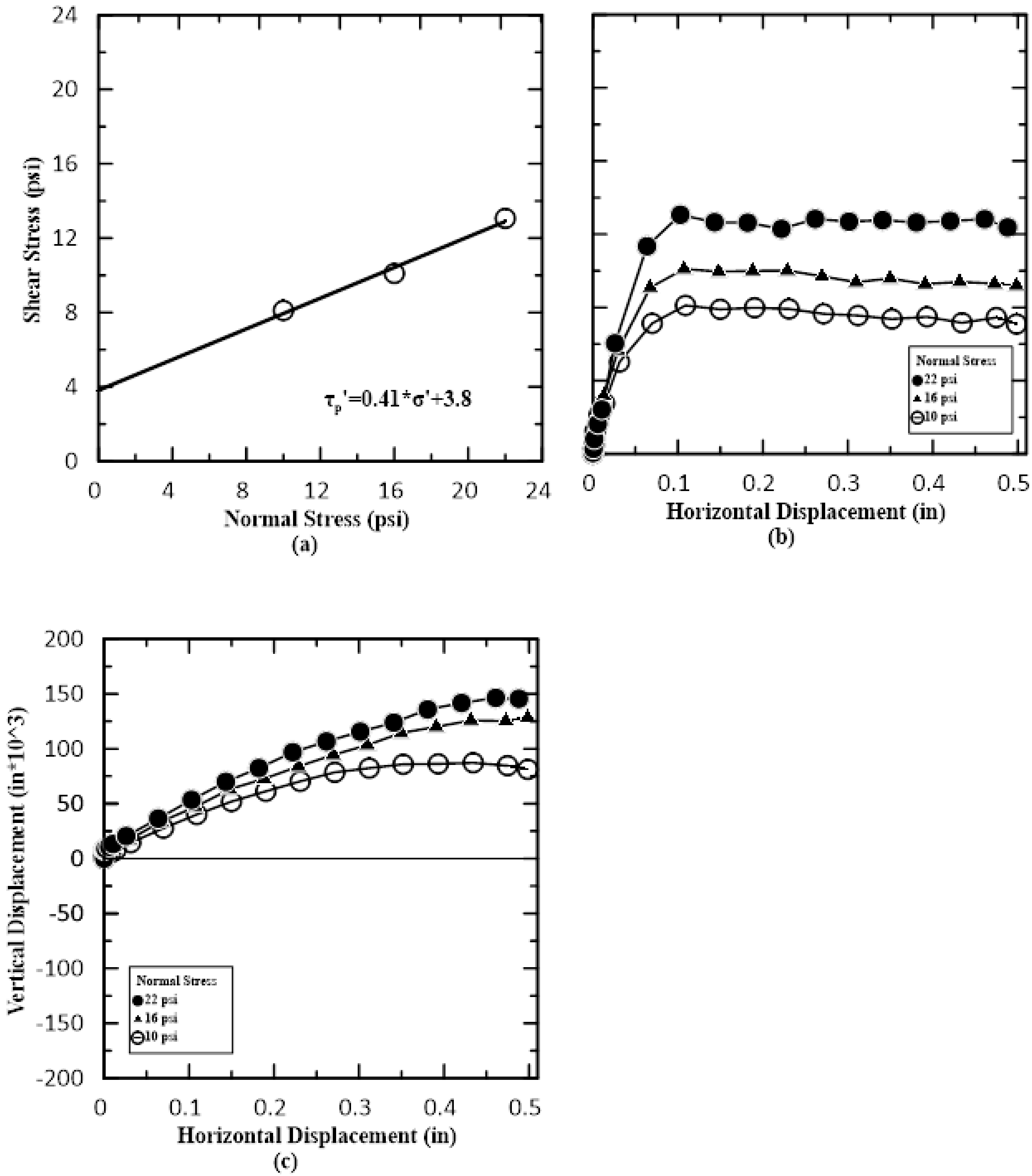

Figure 106. Small direct shear results for Soil 1 and Soil 4 mixtures at fine content = 70%, moisture content = 18.6%: (a) shear stress vs normal stress; (b) shear stress vs horizontal displacement; (c) vertical displacement vs horizontal displacement

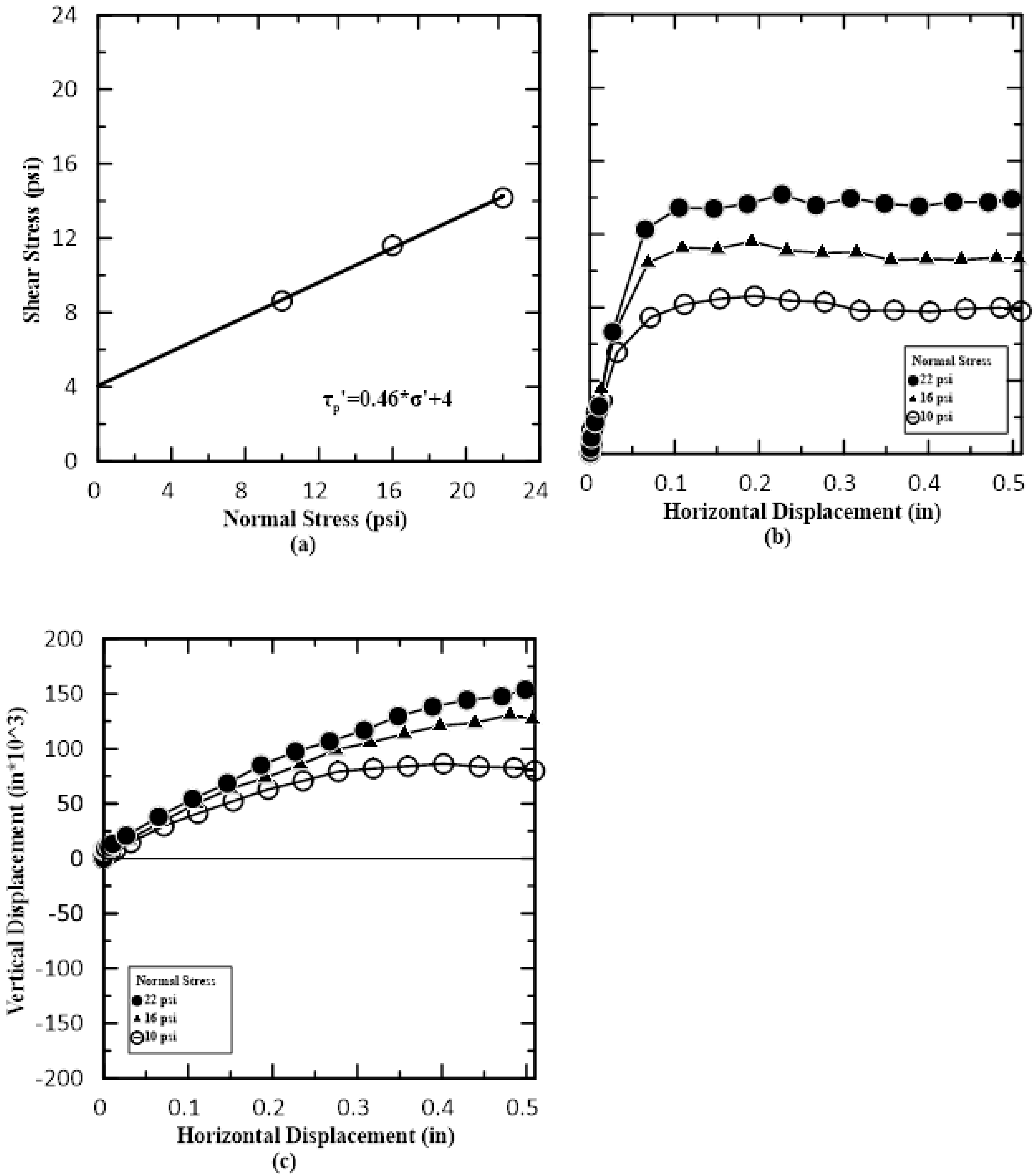

Figure 107. Small direct shear results for Soil 1 and Soil 4 mixtures at fine content = 70%, moisture content = 16.3%: (a) shear stress vs normal stress; (b) shear stress vs horizontal displacement; (c) vertical displacement vs horizontal displacement

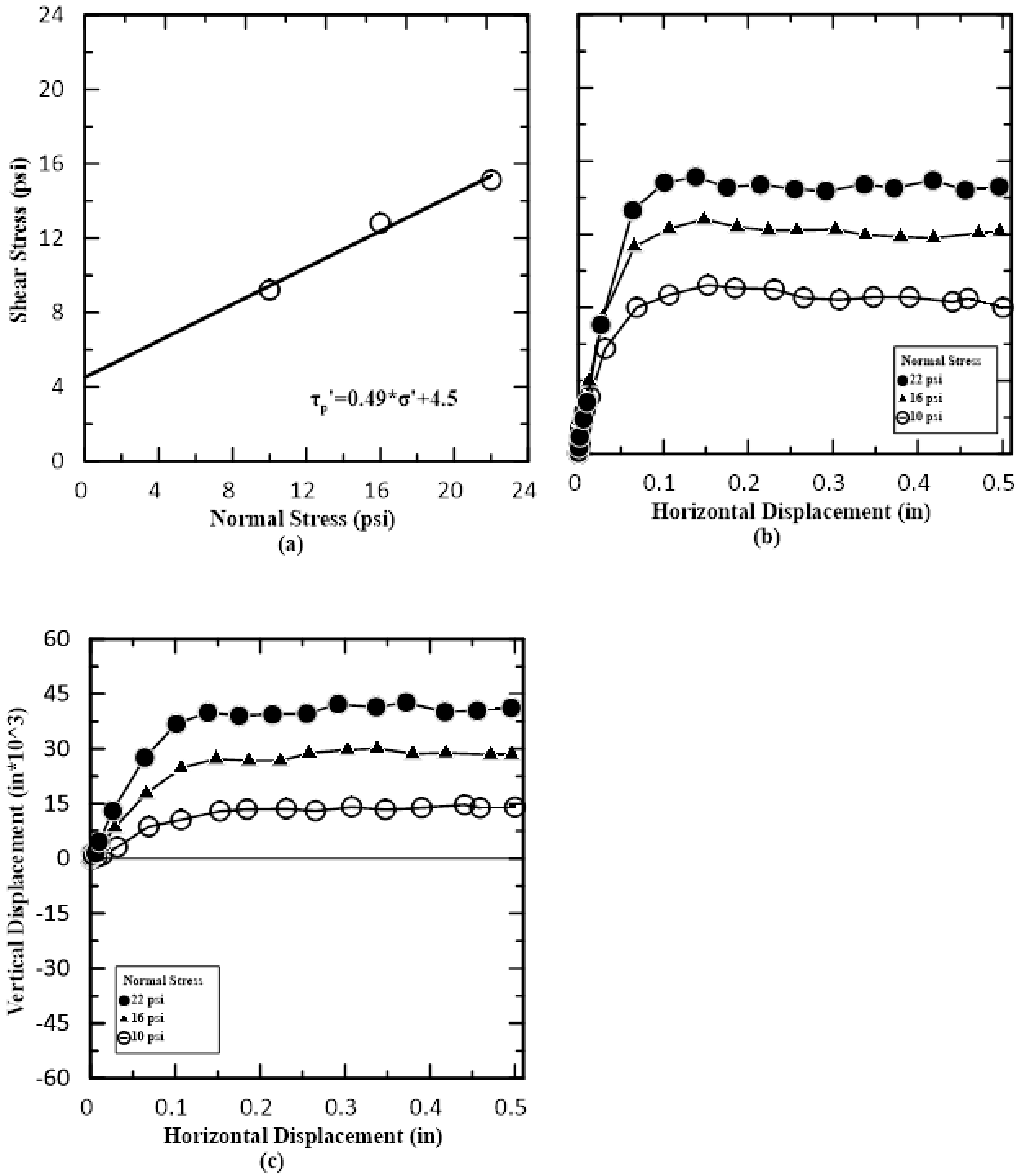

Figure 108. Small direct shear results for Soil 1 and Soil 4 mixtures at fine content = 70%, moisture content = 14.5%: (a) shear stress vs normal stress; (b) shear stress vs horizontal displacement; (c) vertical displacement vs horizontal displacement

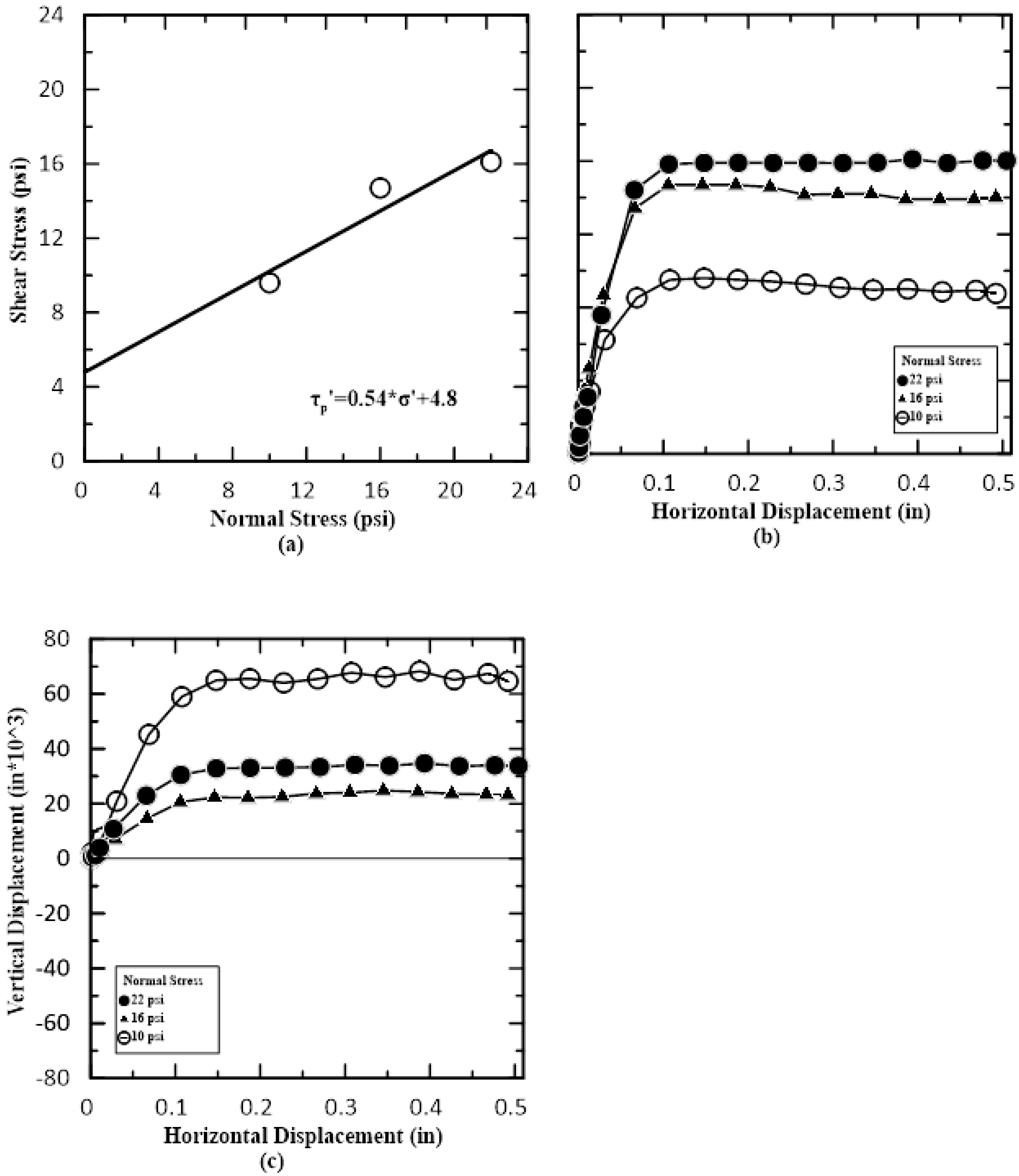

Figure 109. Small direct shear results for Soil 1 and Soil 5 mixtures at fine content = 10%, moisture content = 18.1%: (a) shear stress vs normal stress; (b) shear stress vs horizontal displacement; (c) vertical displacement vs horizontal displacement

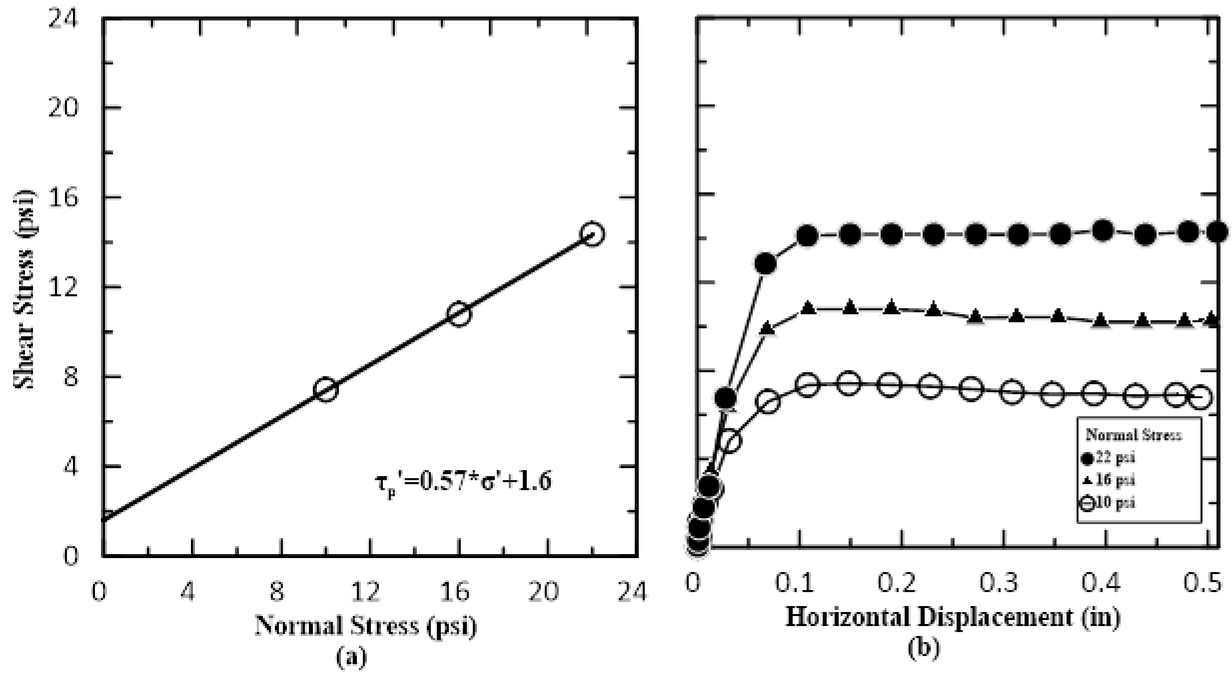

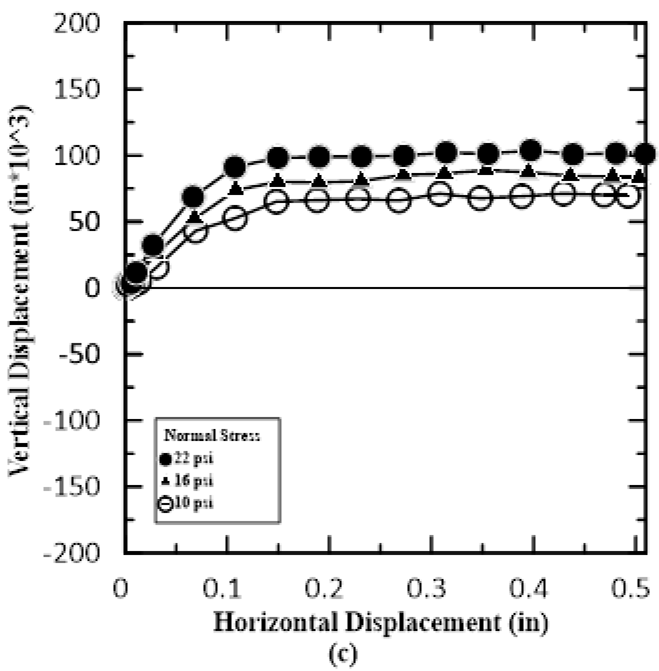

Figure 110. Small direct shear results for Soil 1 and Soil 5 mixtures at fine content = 10%, moisture content = 15.3%: (a) shear stress vs normal stress; (b) shear stress vs horizontal displacement; (c) vertical displacement vs horizontal displacement

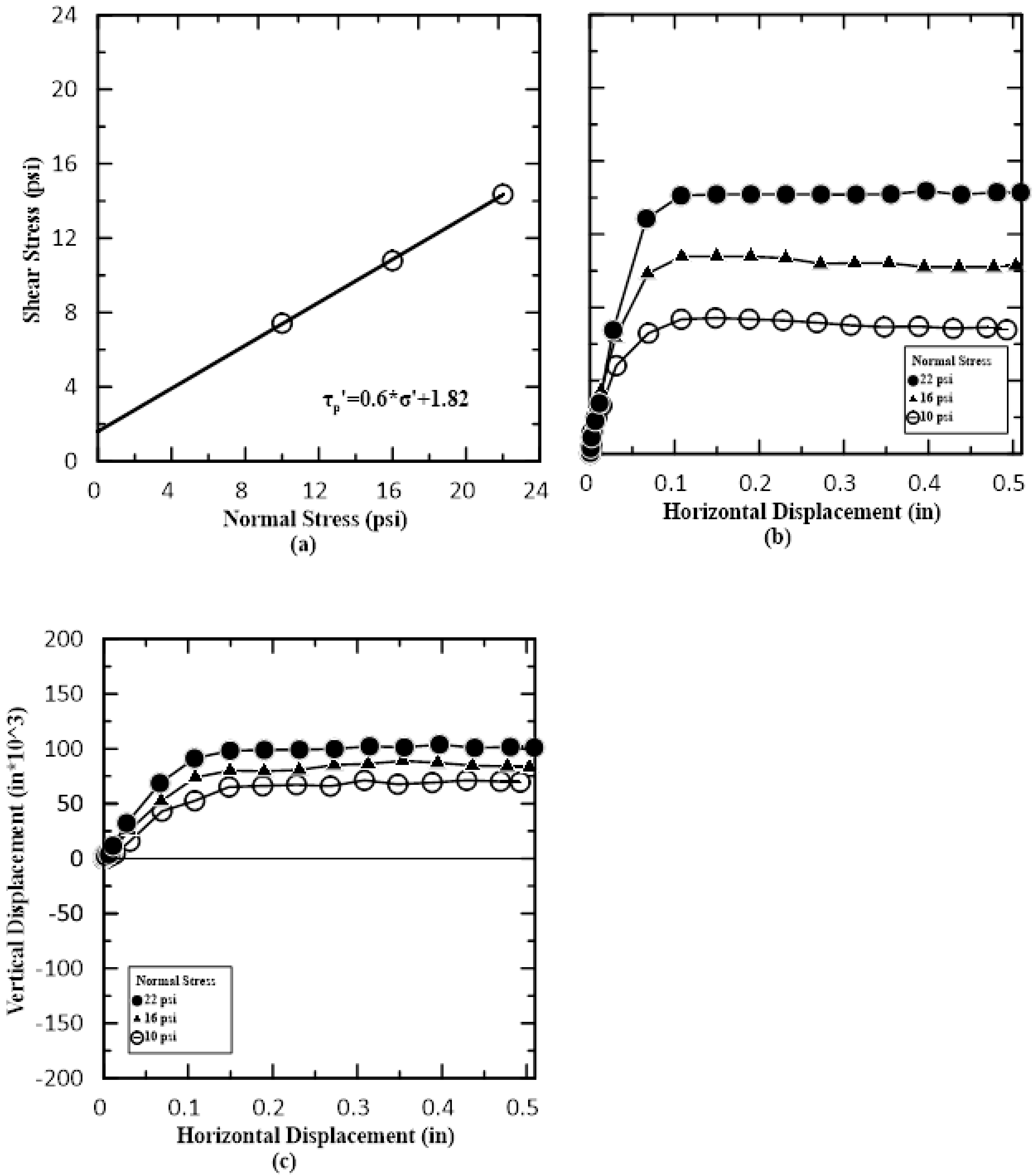

Figure 111. Small direct shear results for Soil 1 and Soil 5 mixtures at fine content = 10%, moisture content = 12%: (a) shear stress vs normal stress; (b) shear stress vs horizontal displacement; (c) vertical displacement vs horizontal displacement

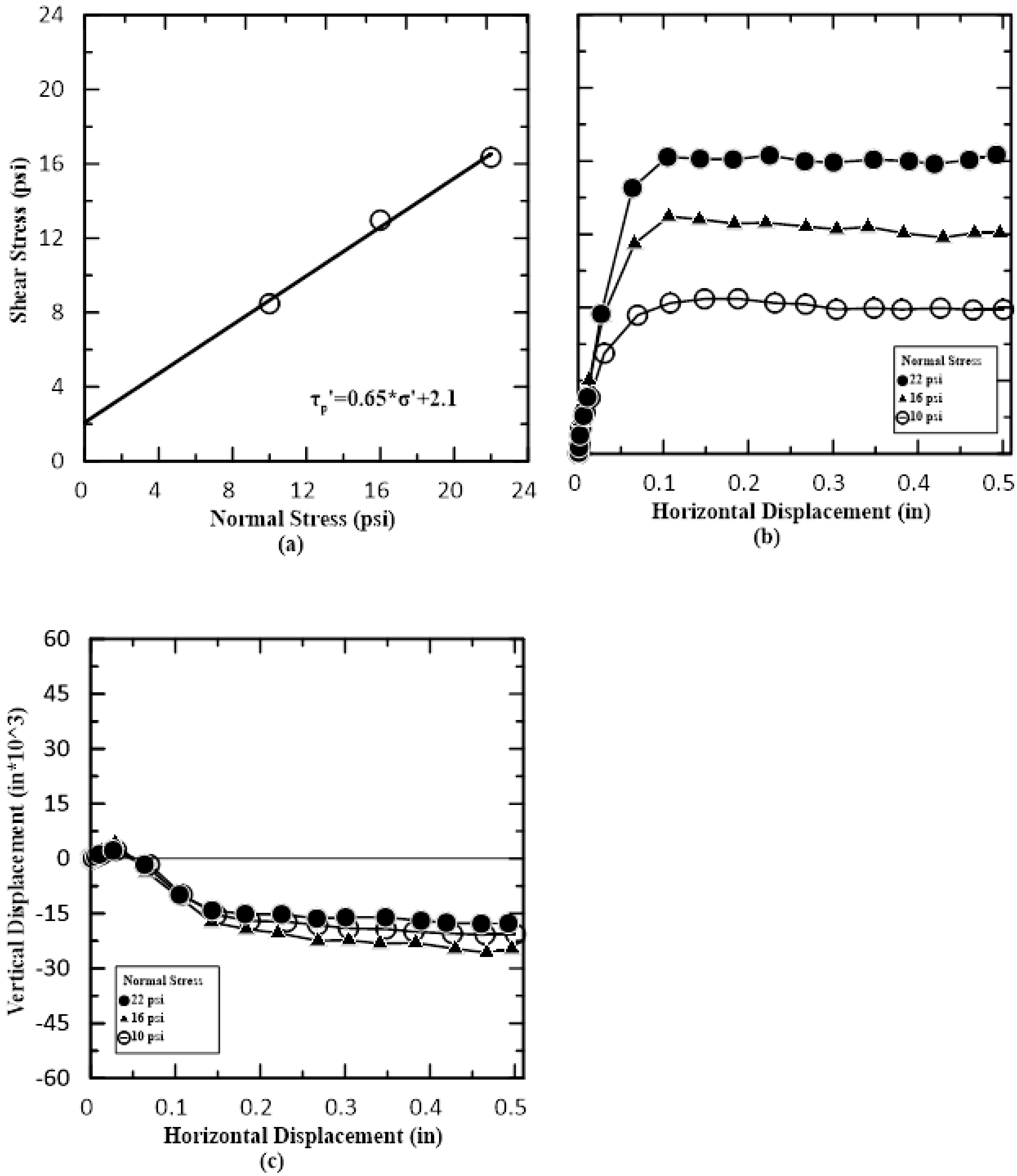

Figure 112. Small direct shear results for Soil 1 and Soil 5 mixtures at fine content = 10%, moisture content = 10.1%: (a) shear stress vs normal stress; (b) shear stress vs horizontal displacement; (c) vertical displacement vs horizontal displacement

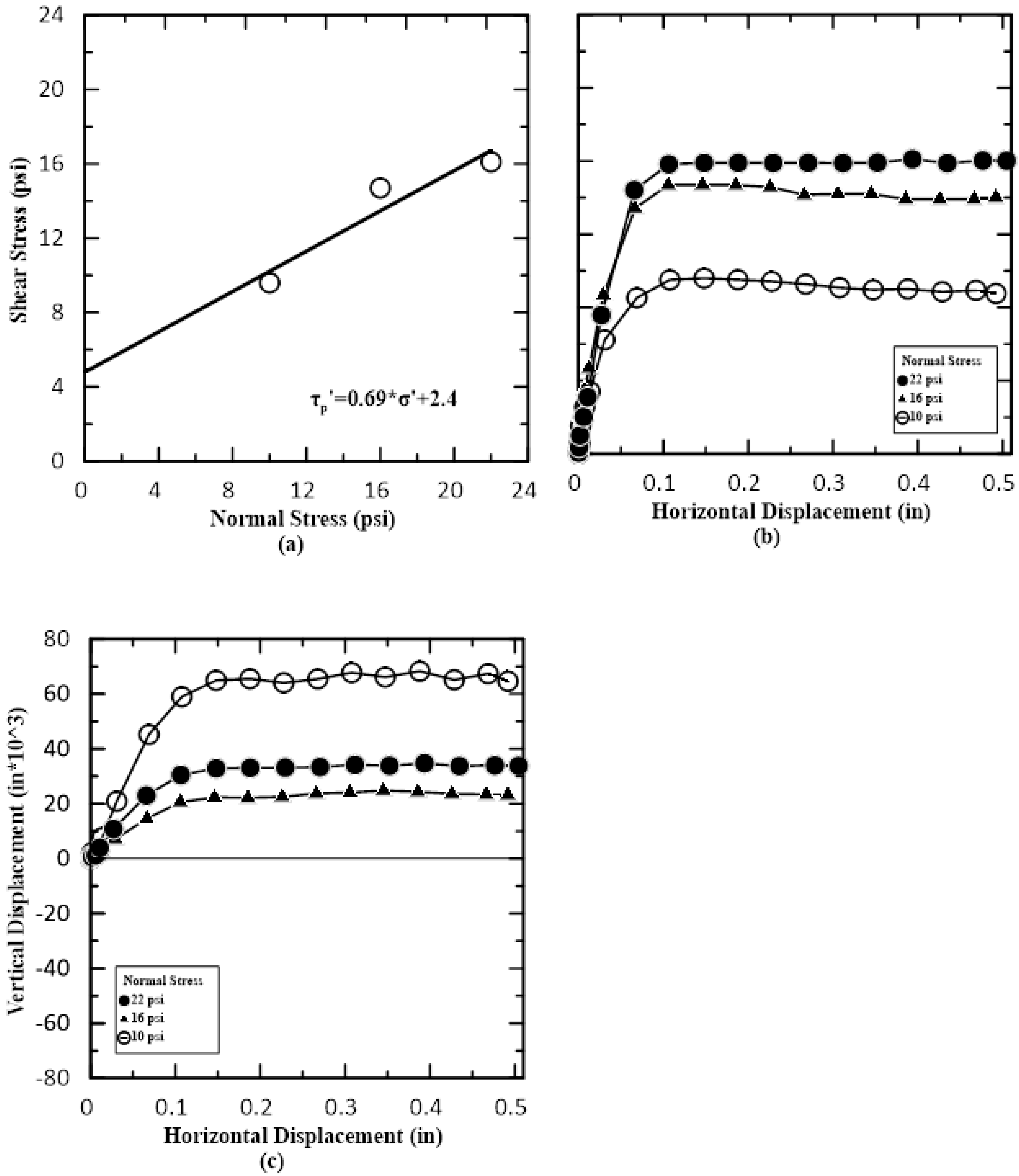

Figure 113. Small direct shear results for Soil 1 and Soil 5 mixtures at fine content = 20%, moisture content = 17.4%: (a) shear stress vs normal stress; (b) shear stress vs horizontal displacement; (c) vertical displacement vs horizontal displacement

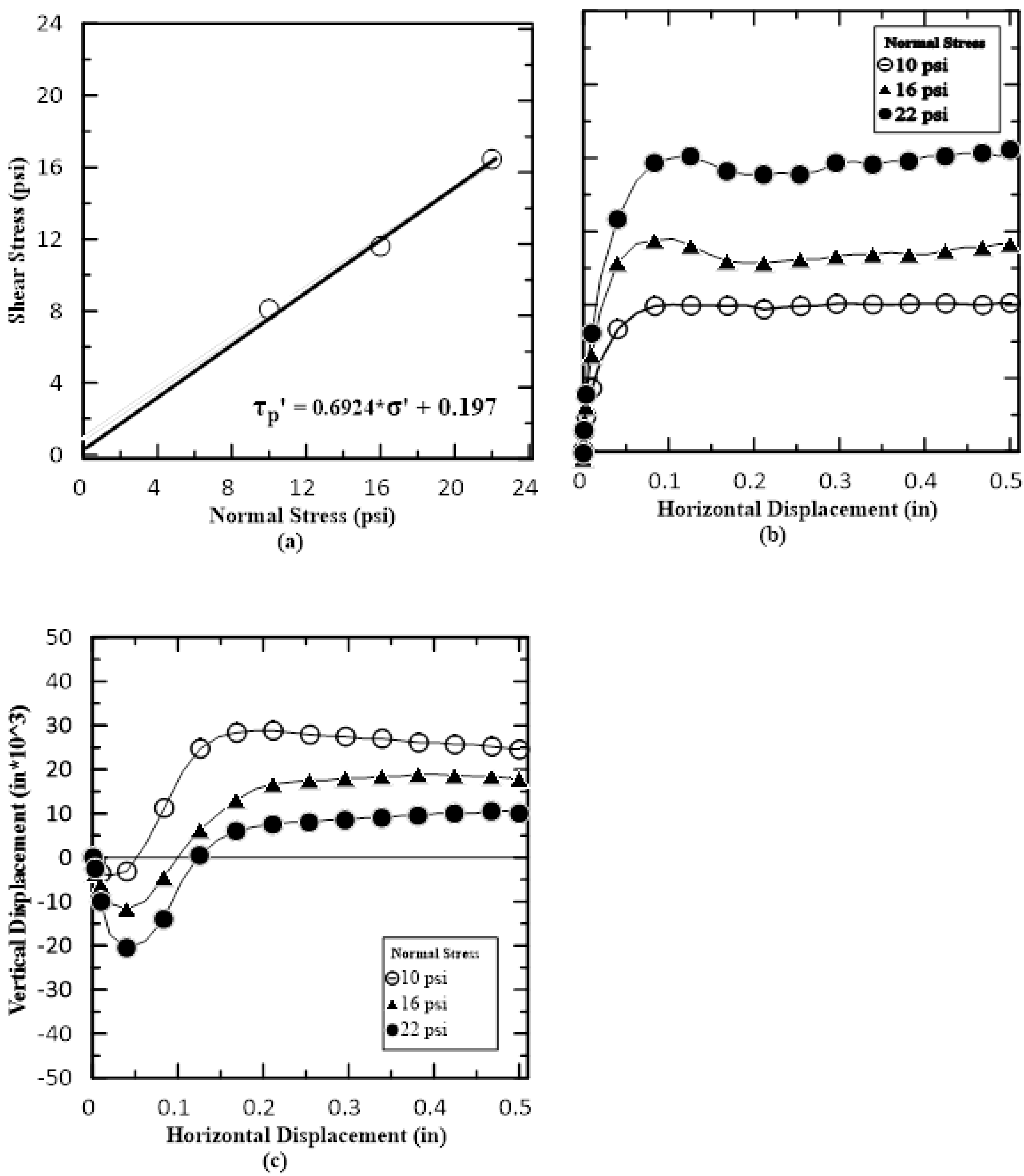

Figure 114. Small direct shear results for Soil 1 and Soil 5 mixtures at fine content = 20%, moisture content = 15.4%: (a) shear stress vs normal stress; (b) shear stress vs horizontal displacement; (c) vertical displacement vs horizontal displacement

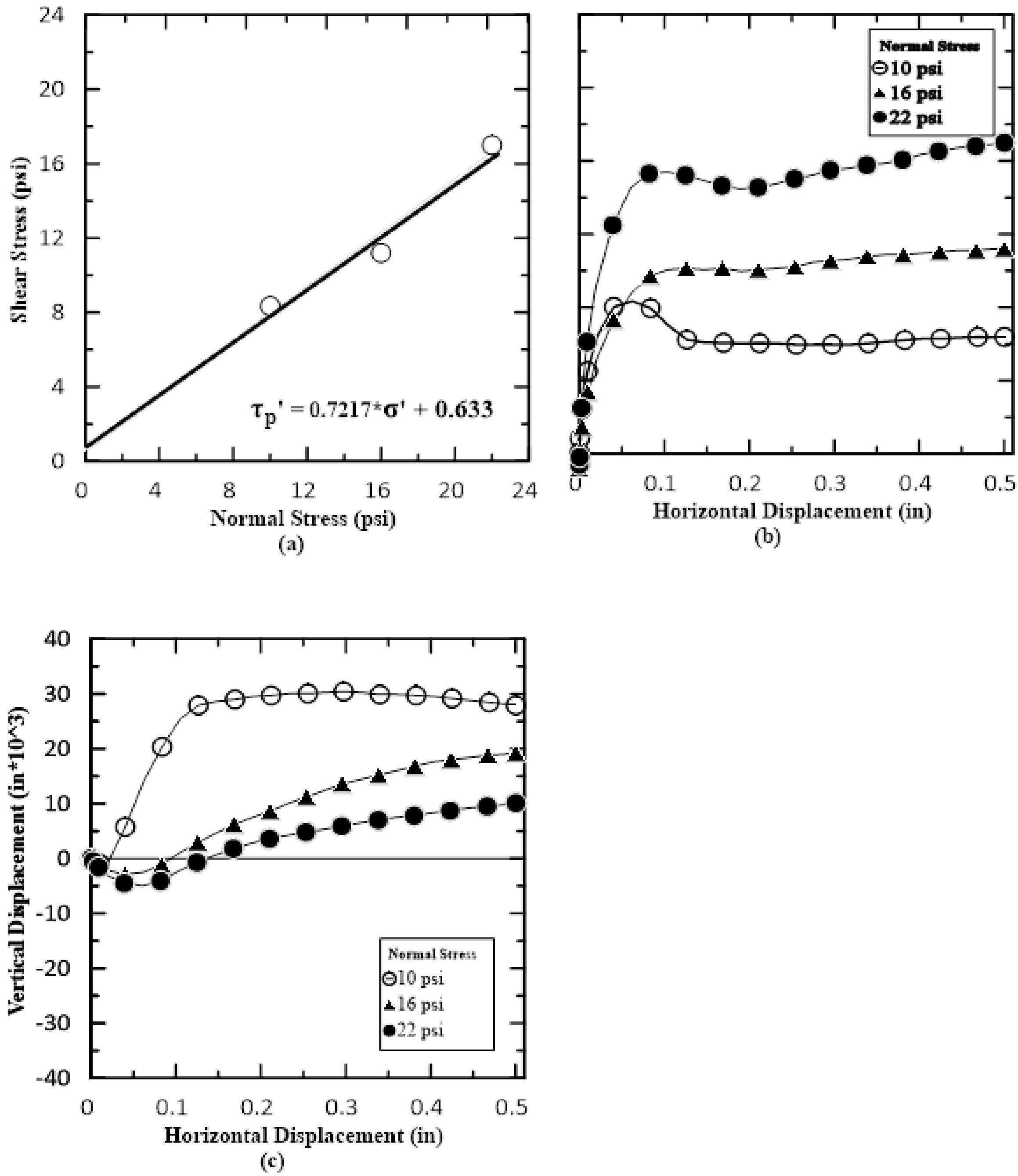

Figure 115. Small direct shear results for Soil 1 and Soil 5 mixtures at fine content = 20%, moisture content = 12.8%: (a) shear stress vs normal stress; (b) shear stress vs horizontal displacement; (c) vertical displacement vs horizontal displacement

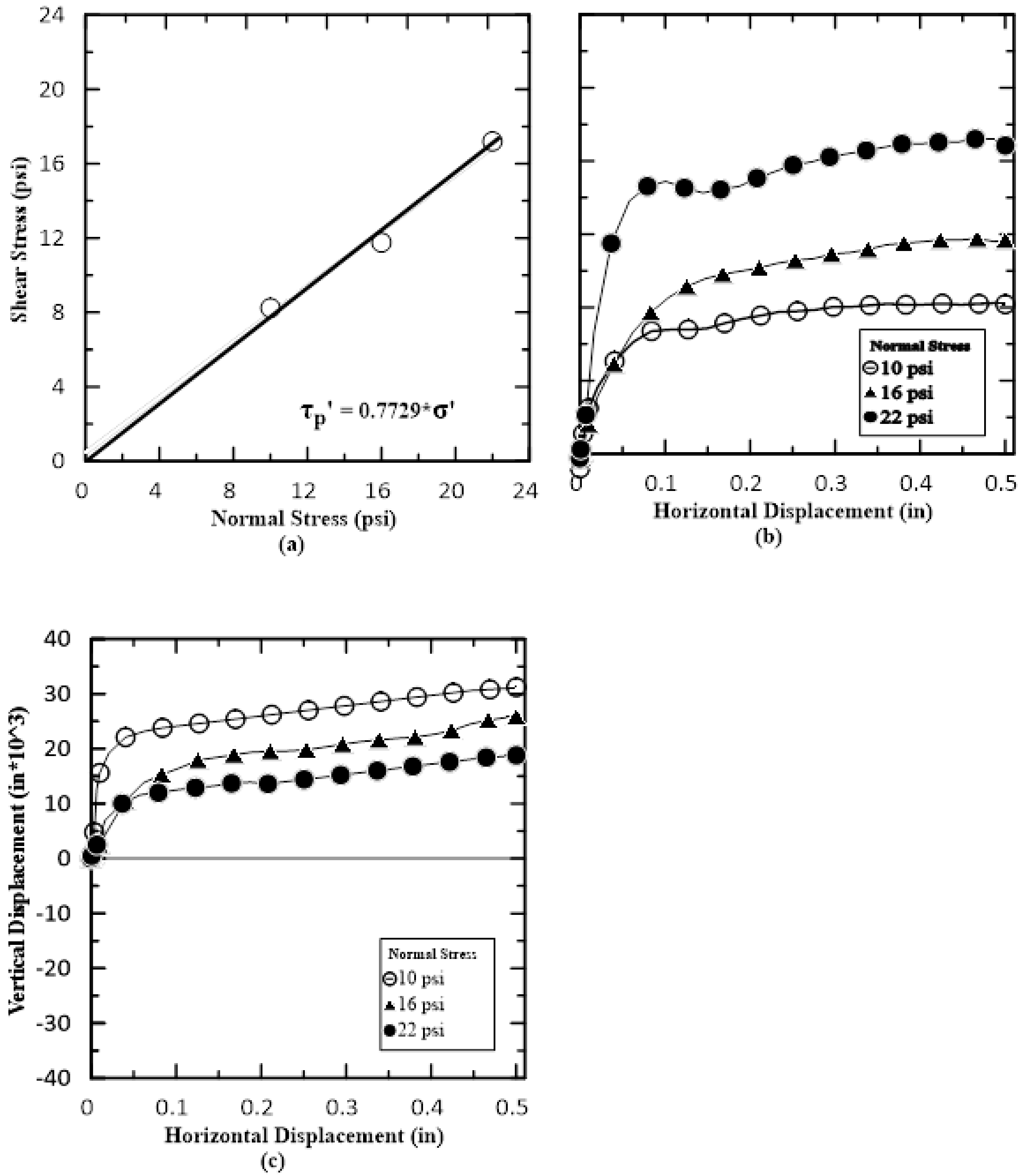

Figure 116. Small direct shear results for Soil 1 and Soil 5 mixtures at fine content = 20%, moisture content = 10.6%: (a) shear stress vs normal stress; (b) shear stress vs horizontal displacement; (c) vertical displacement vs horizontal displacement

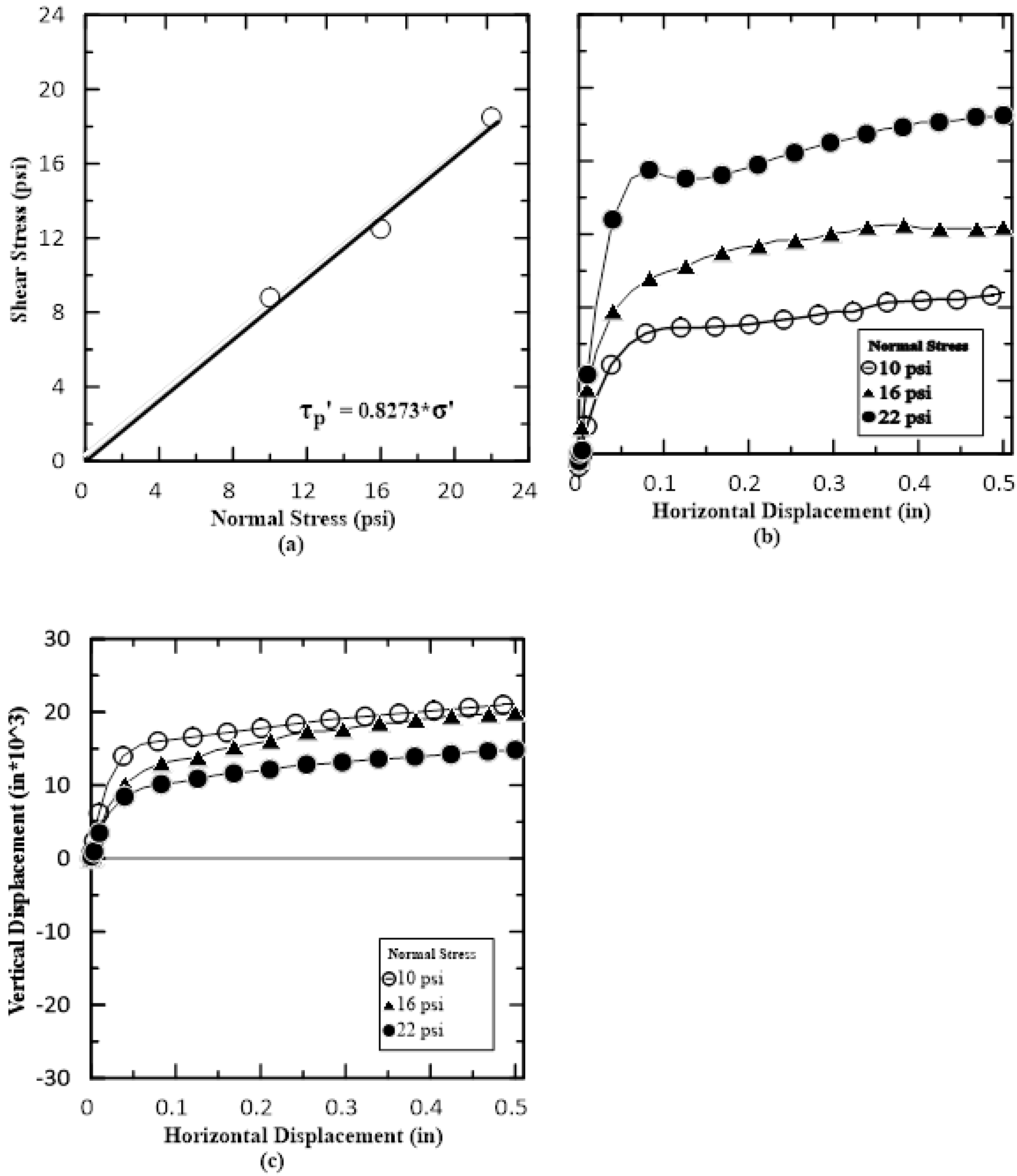

Figure 117. Small direct shear results for Soil 1 and Soil 5 mixtures at fine content = 30%, moisture content = 18.9%: (a) shear stress vs normal stress; (b) shear stress vs horizontal displacement; (c) vertical displacement vs horizontal displacement

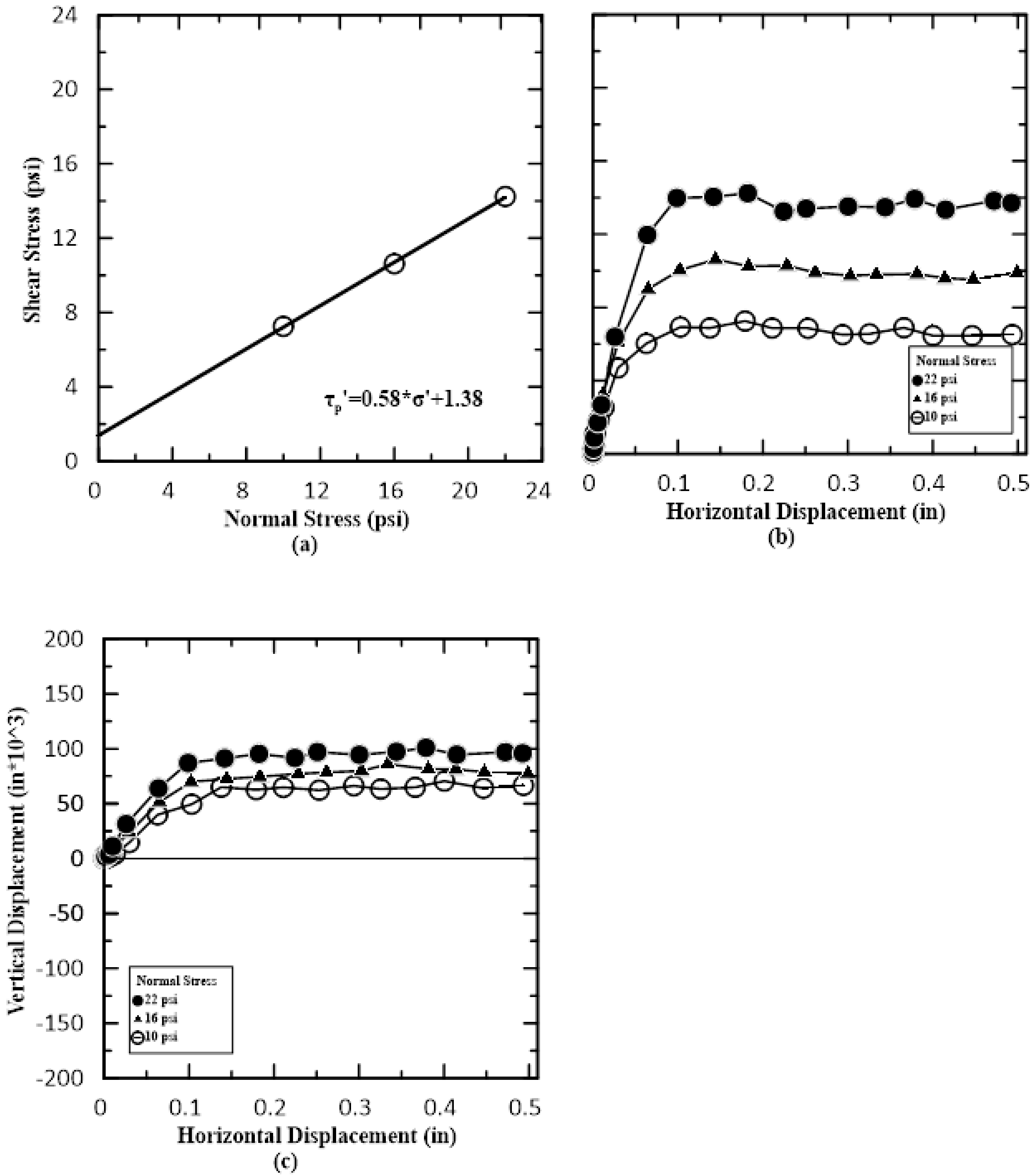

Figure 118. Small direct shear results for Soil 1 and Soil 5 mixtures at fine content = 30%, moisture content = 16.6%: (a) shear stress vs normal stress; (b) shear stress vs horizontal displacement; (c) vertical displacement vs horizontal displacement

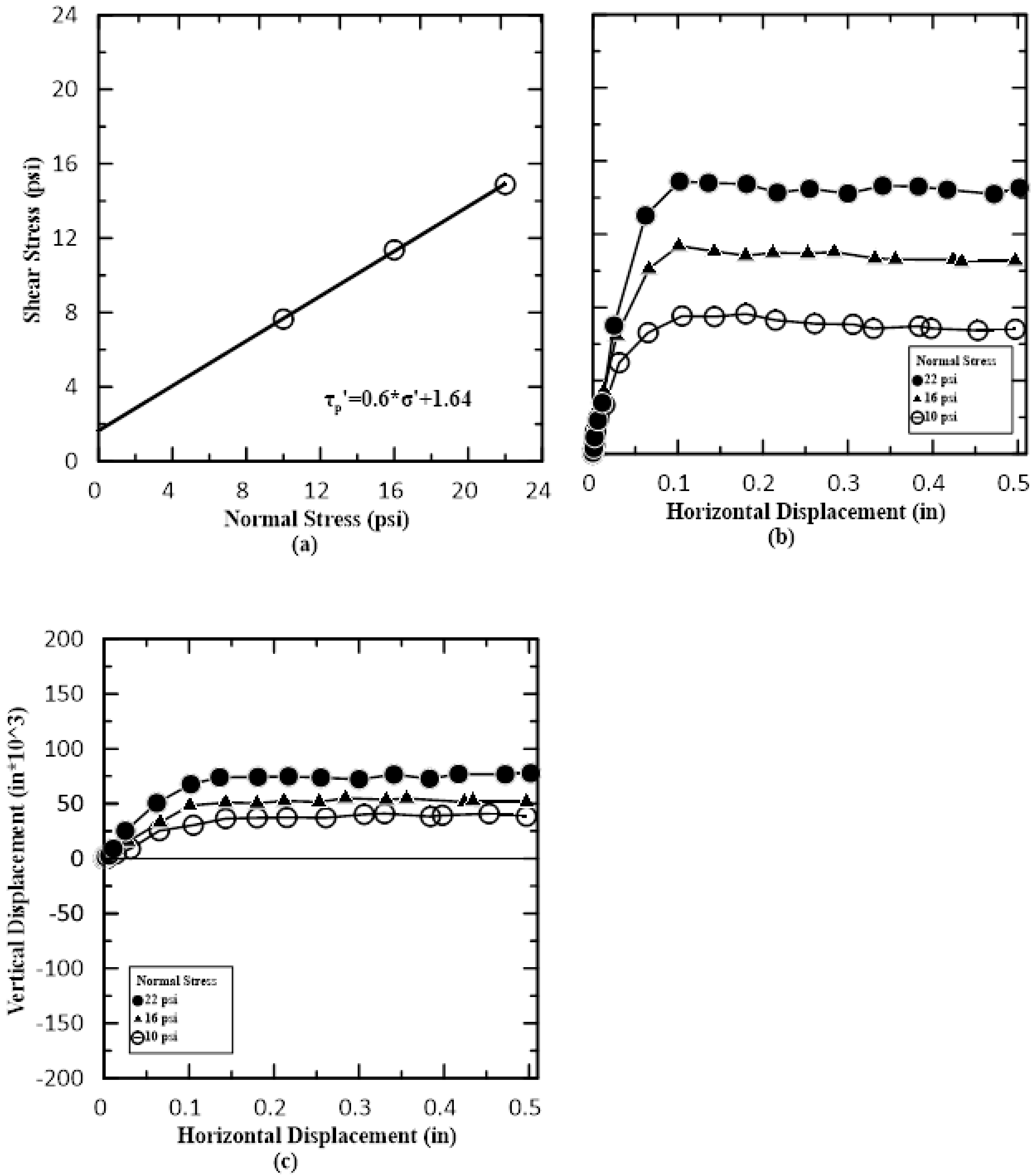

Figure 119. Small direct shear results for Soil 1 and Soil 5 mixtures at fine content = 30%, moisture content = 14.3%: (a) shear stress vs normal stress; (b) shear stress vs horizontal displacement; (c) vertical displacement vs horizontal displacement

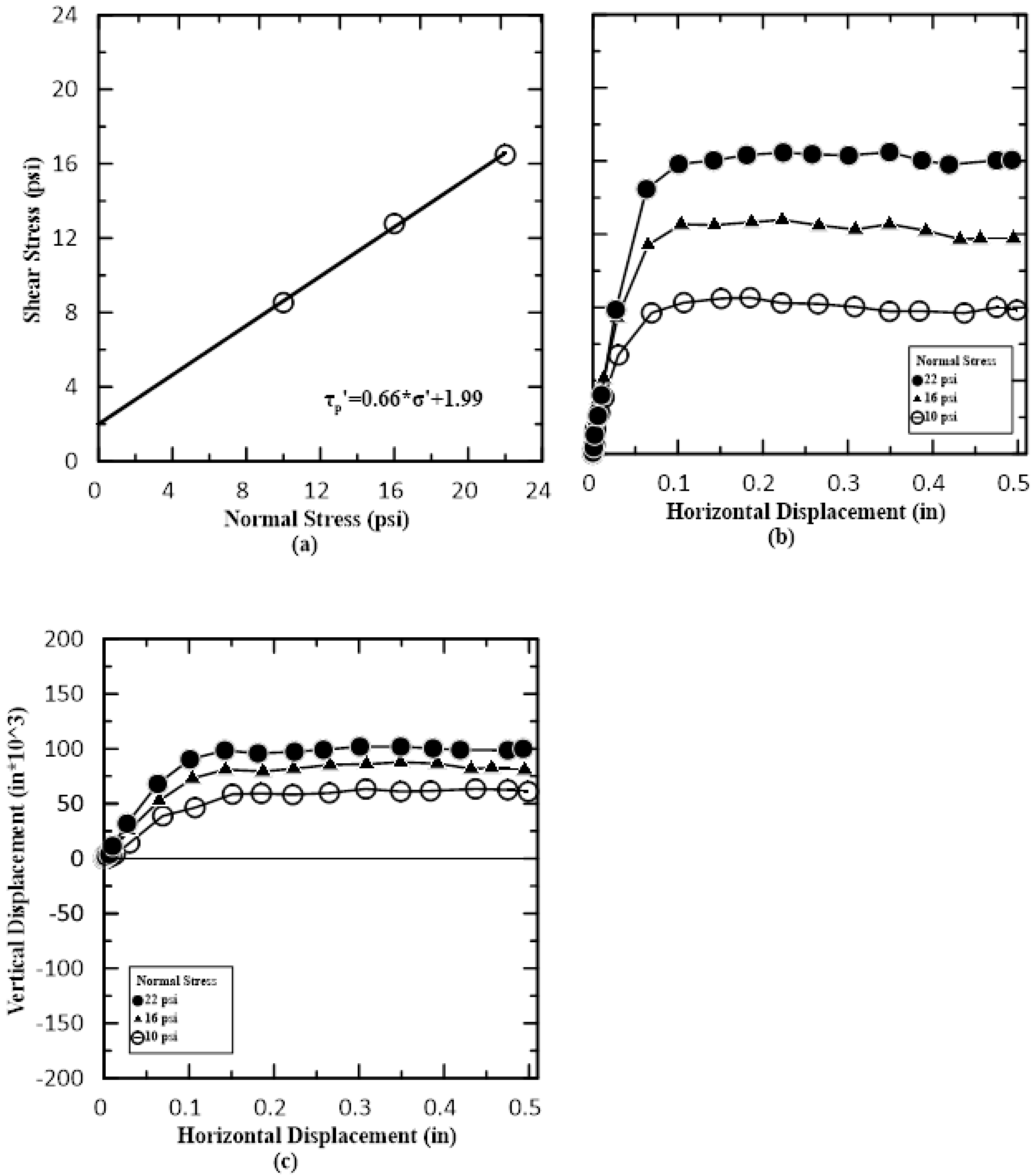

Figure 120. Small direct shear results for Soil 1 and Soil 5 mixtures at fine content = 30%, moisture content = 11%: (a) shear stress vs normal stress; (b) shear stress vs horizontal displacement; (c) vertical displacement vs horizontal displacement

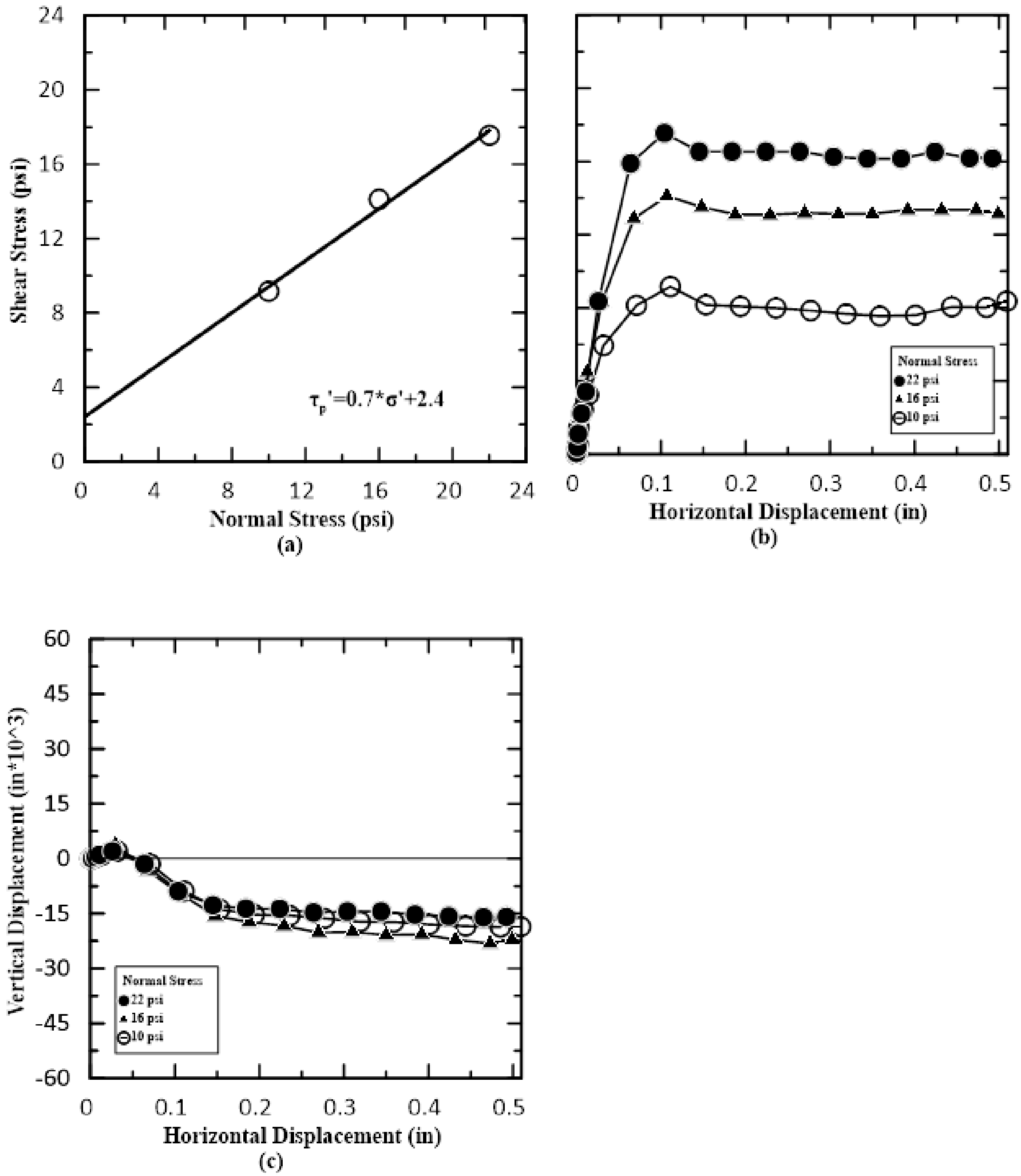

Figure 121. Small direct shear results for Soil 1 and Soil 5 mixtures at fine content = 40%, moisture content = 18.8%: (a) shear stress vs normal stress; (b) shear stress vs horizontal displacement; (c) vertical displacement vs horizontal displacement

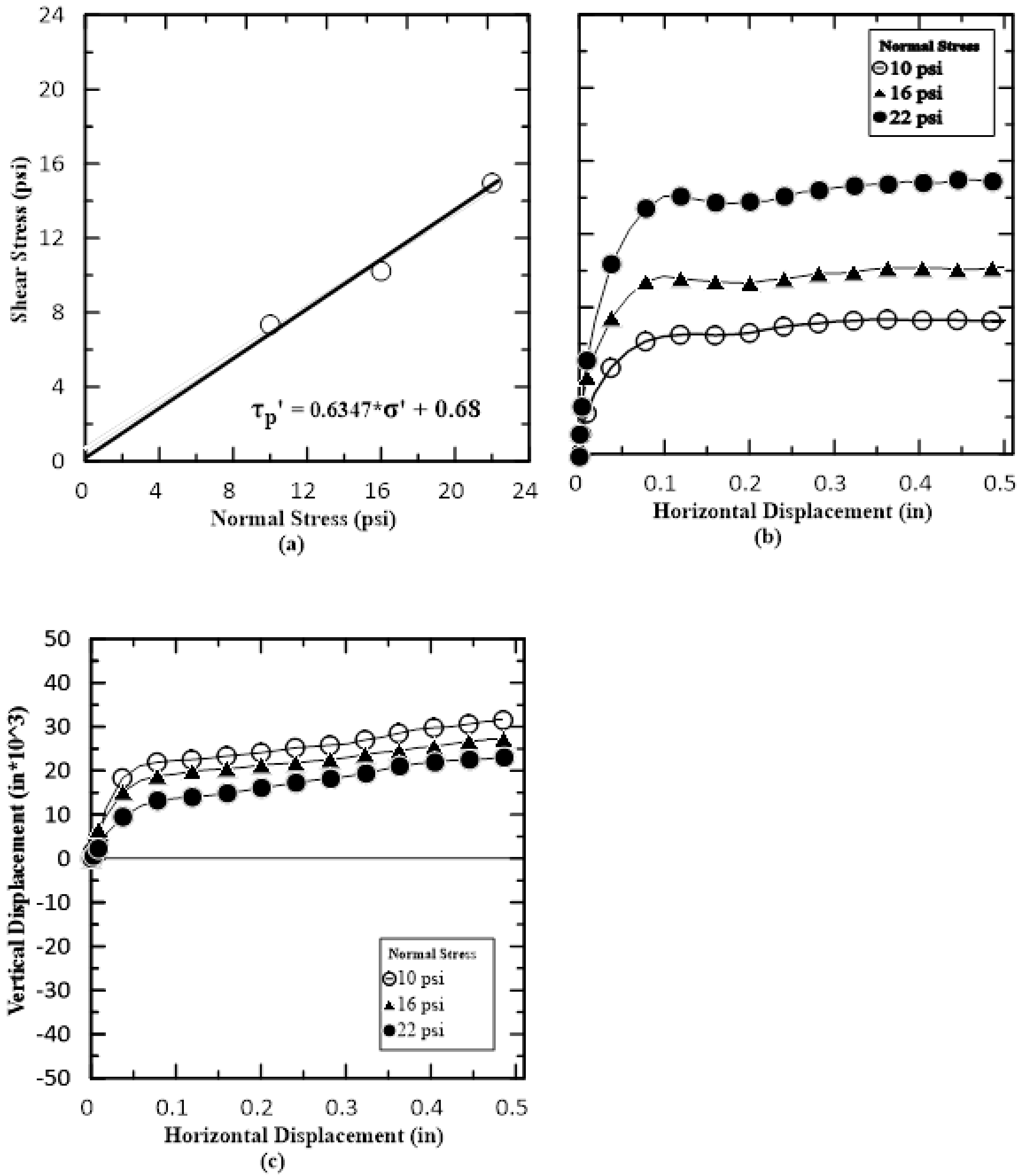

Figure 122. Small direct shear results for Soil 1 and Soil 5 mixtures at fine content = 40%, moisture content = 16.7%: (a) shear stress vs normal stress; (b) shear stress vs horizontal displacement; (c) vertical displacement vs horizontal displacement

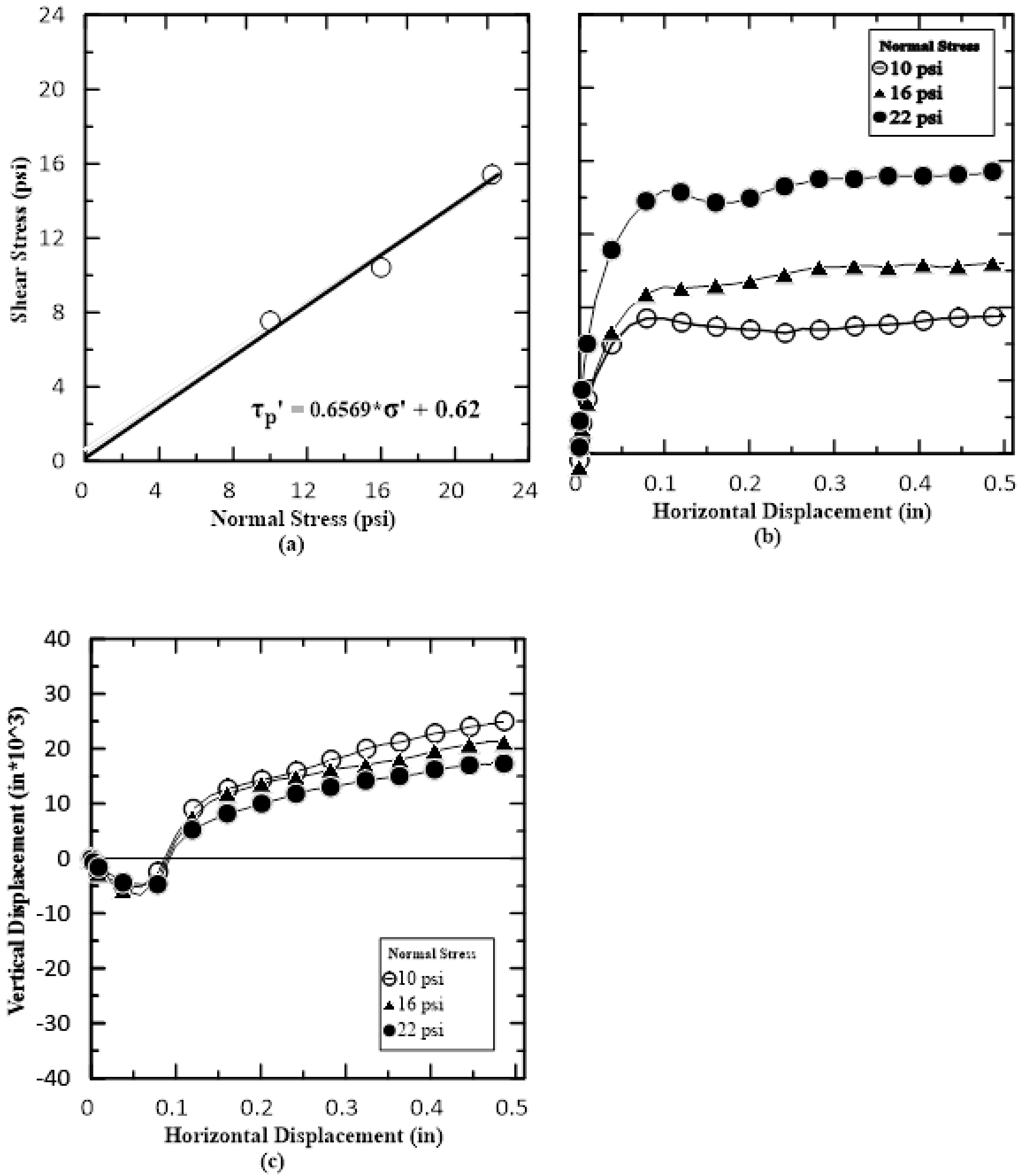

Figure 123. Small direct shear results for Soil 1 and Soil 5 mixtures at fine content = 40%, moisture content = 14.6%: (a) shear stress vs normal stress; (b) shear stress vs horizontal displacement; (c) vertical displacement vs horizontal displacement

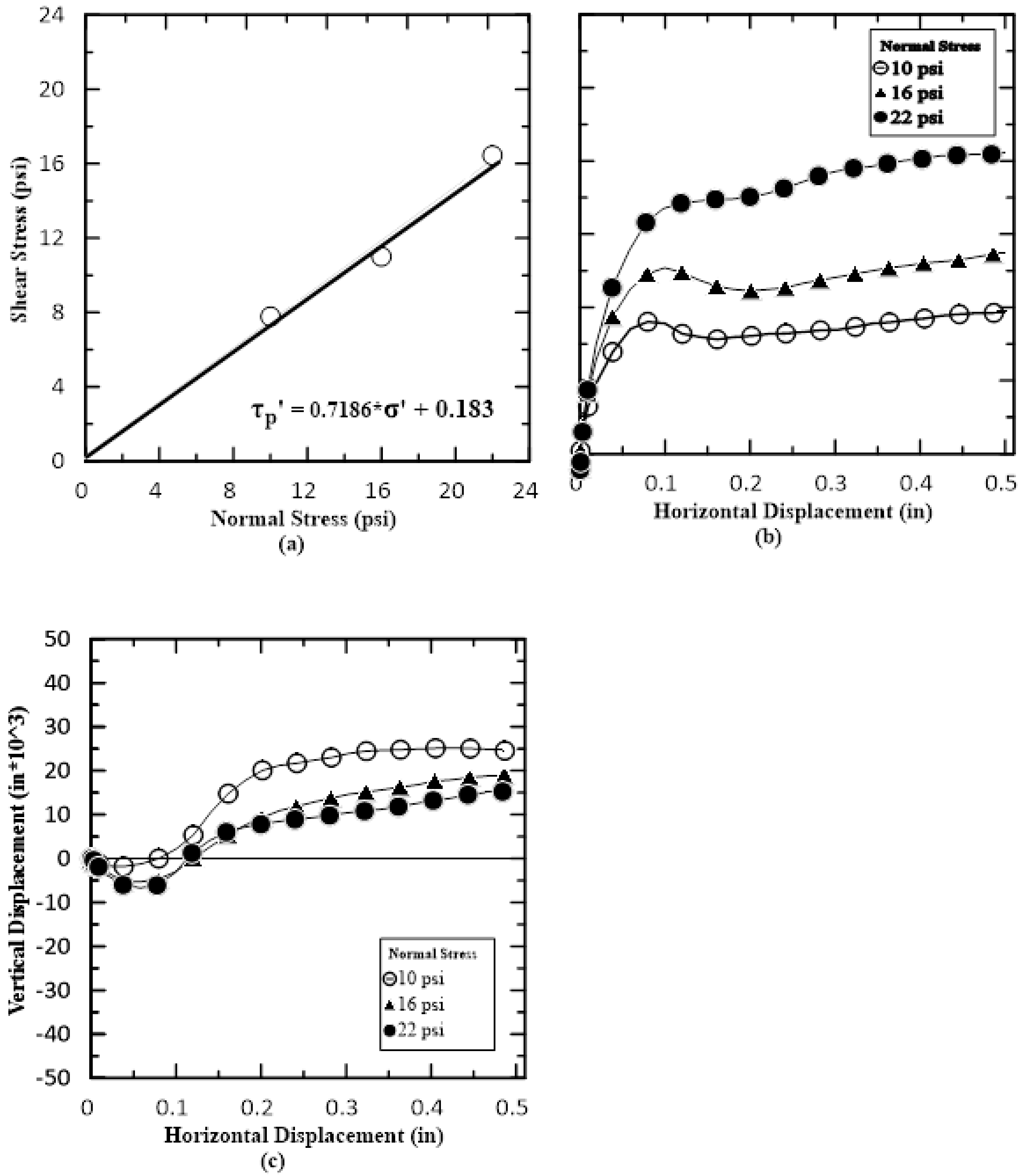

Figure 124. Small direct shear results for Soil 1 and Soil 5 mixtures at fine content = 40%, moisture content = 12.2%: (a) shear stress vs normal stress; (b) shear stress vs horizontal displacement; (c) vertical displacement vs horizontal displacement

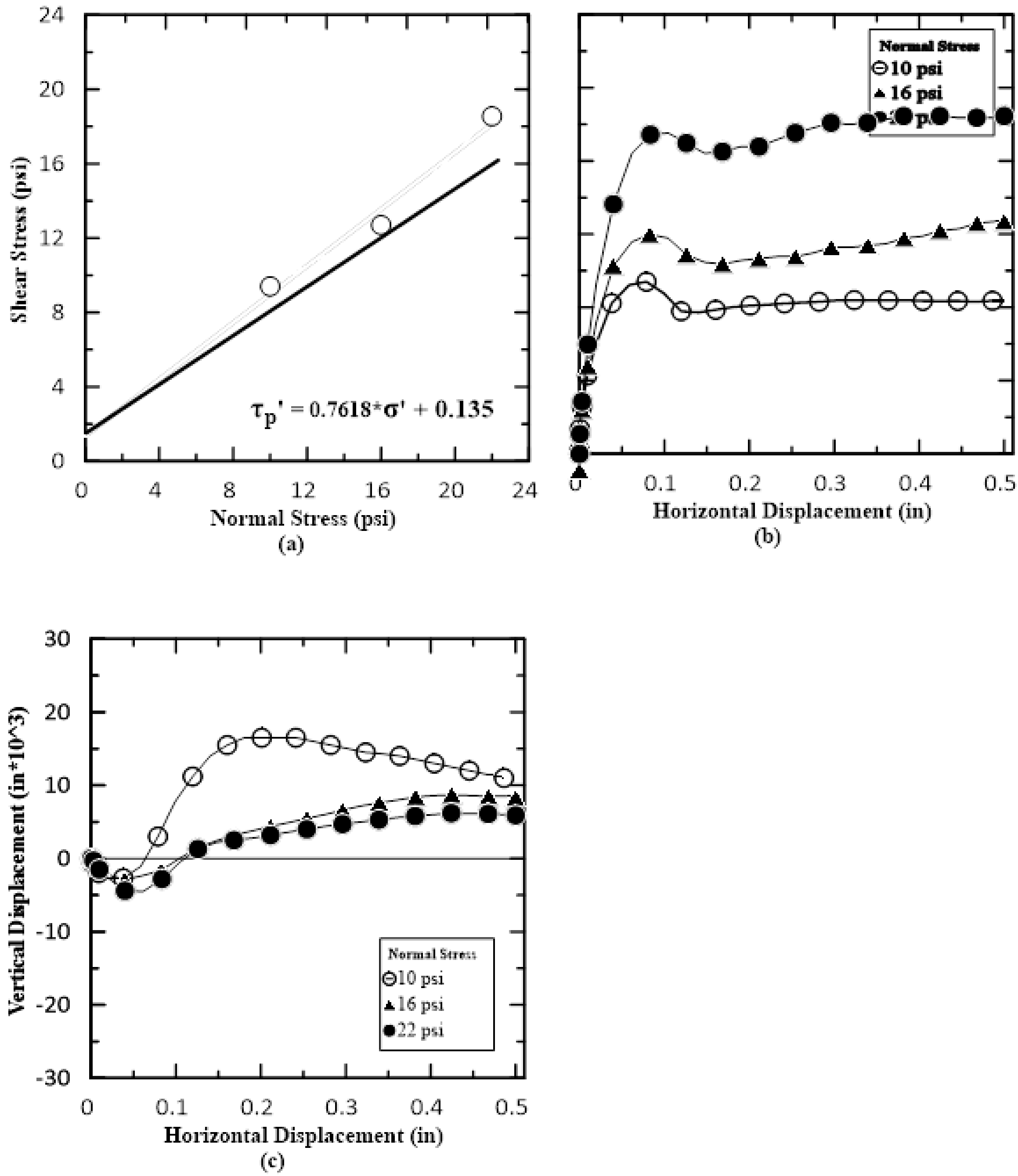

Figure 125. Small direct shear results for Soil 1 and Soil 5 mixtures at fine content = 50%, moisture content = 19%: (a) shear stress vs normal stress; (b) shear stress vs horizontal displacement; (c) vertical displacement vs horizontal displacement

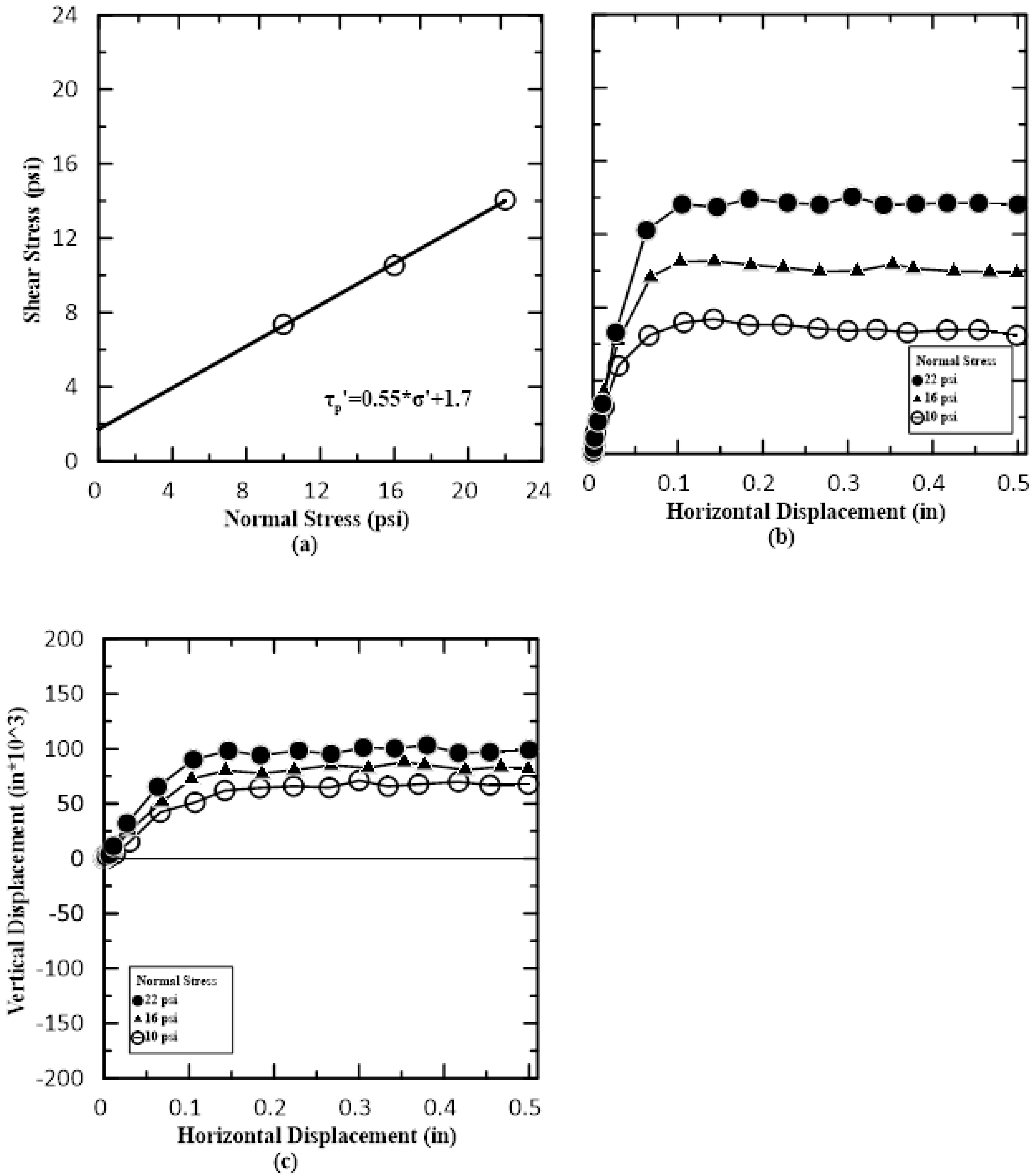

Figure 126. Small direct shear results for Soil 1 and Soil 5 mixtures at fine content = 50%, moisture content = 17.3%: (a) shear stress vs normal stress; (b) shear stress vs horizontal displacement; (c) vertical displacement vs horizontal displacement

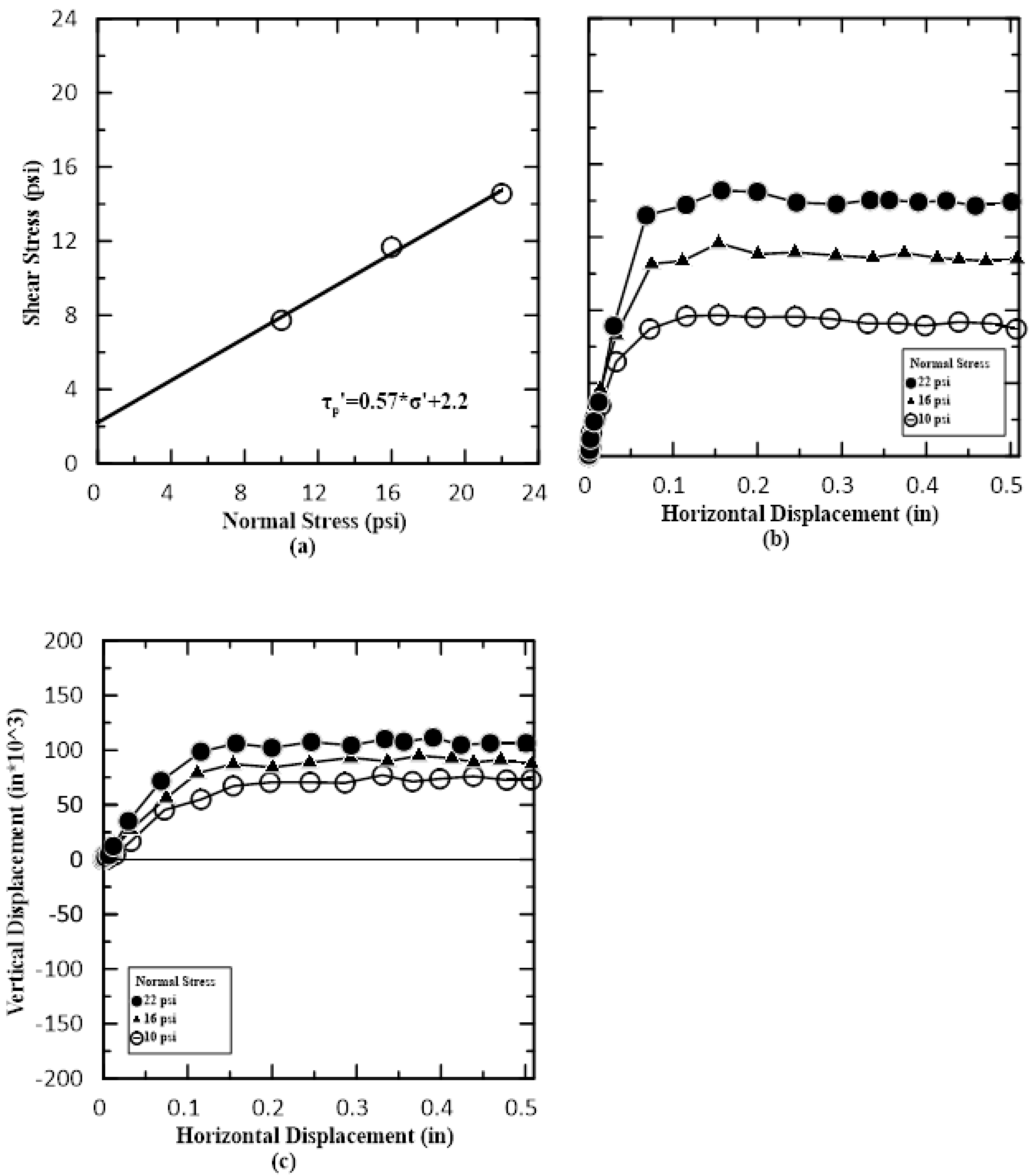

Figure 127. Small direct shear results for Soil 1 and Soil 5 mixtures at fine content = 50%, moisture content = 15.2%: (a) shear stress vs normal stress; (b) shear stress vs horizontal displacement; (c) vertical displacement vs horizontal displacement

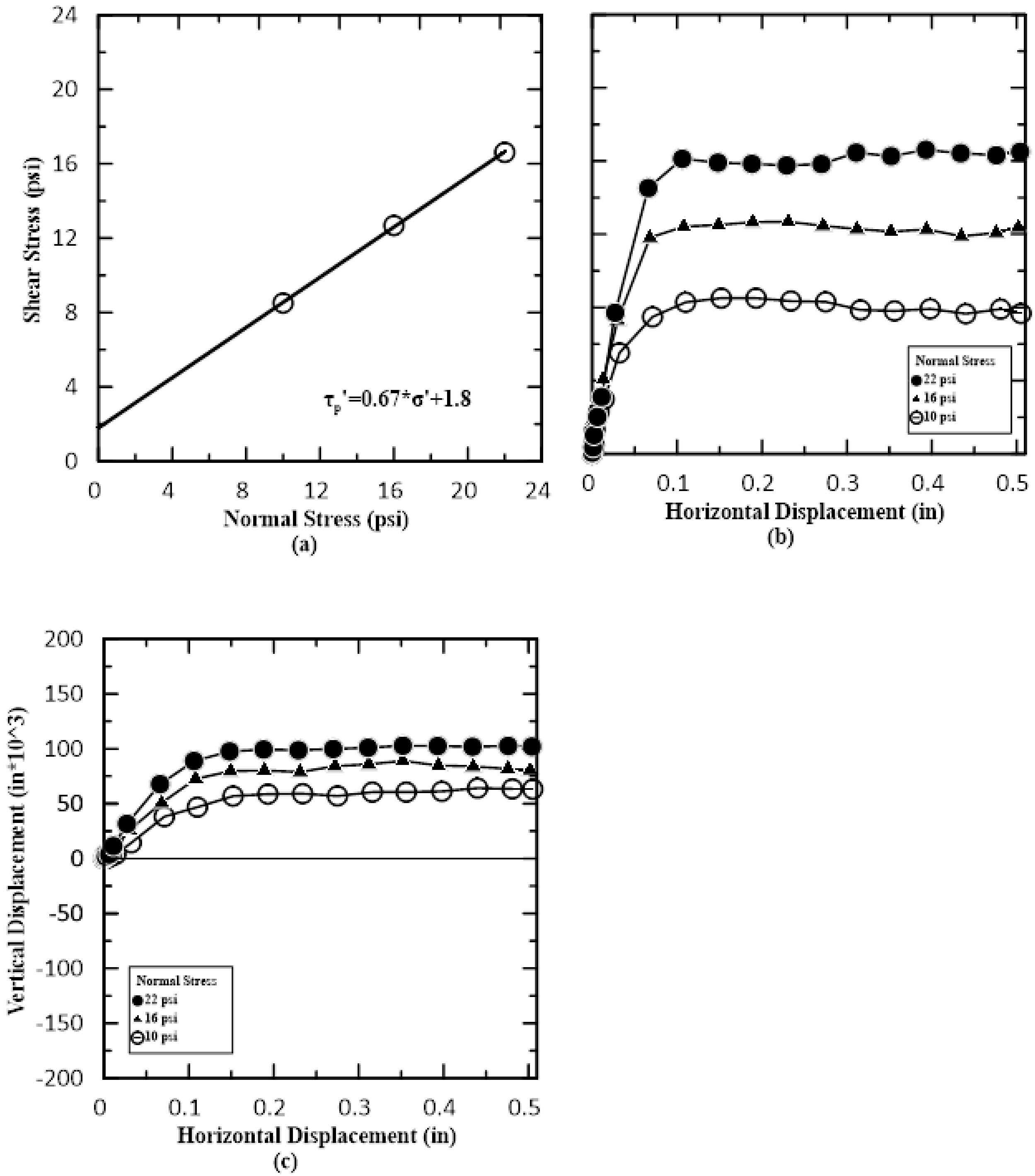

Figure 128. Small direct shear results for Soil 1 and Soil 5 mixtures at fine content = 50%, moisture content = 13%: (a) shear stress vs normal stress; (b) shear stress vs horizontal displacement; (c) vertical displacement vs horizontal displacement

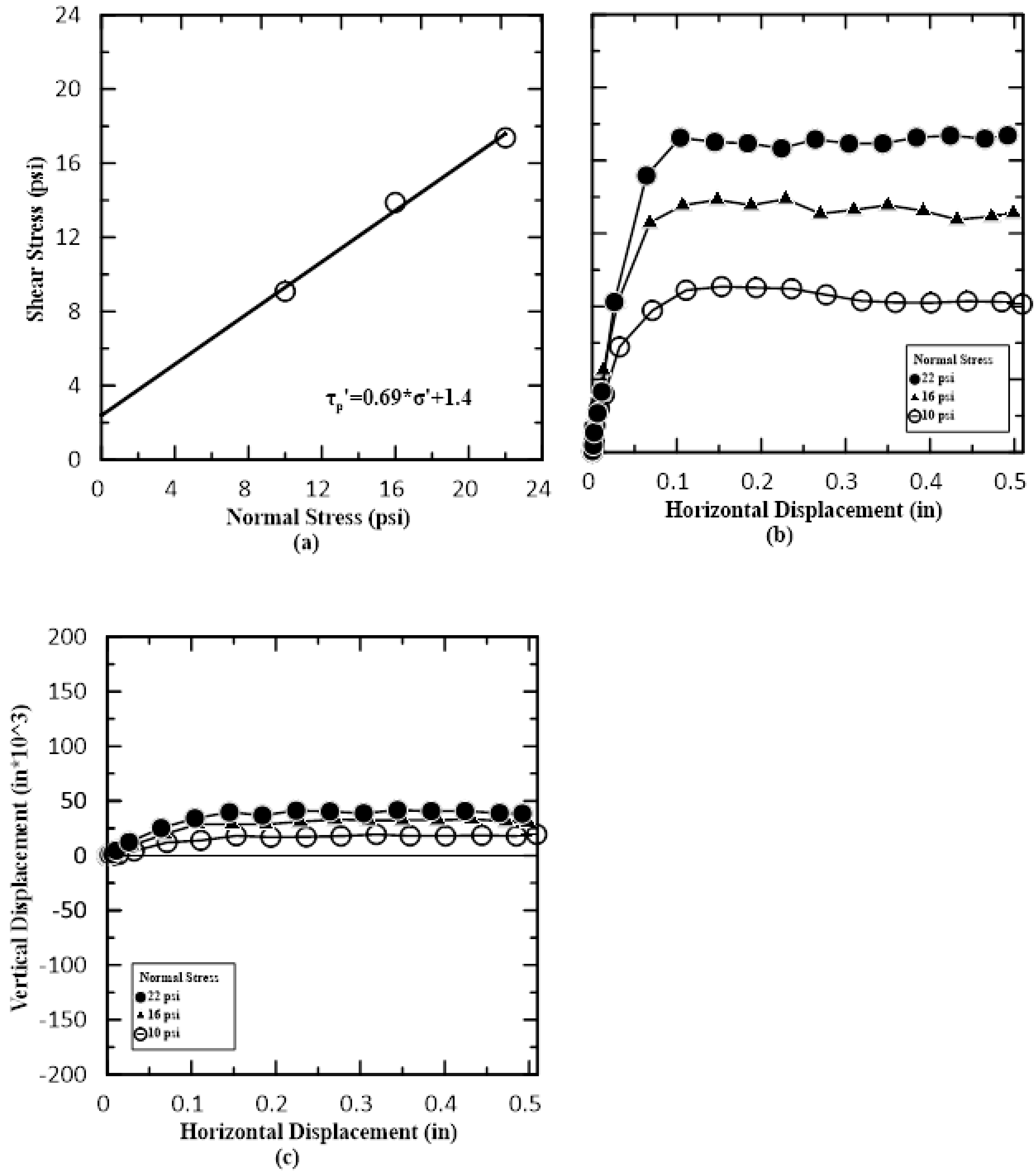

Figure 129. Small direct shear results for Soil 1 and Soil 5 mixtures at fine content = 60%, moisture content = 20.5%: (a) shear stress vs normal stress; (b) shear stress vs horizontal displacement; (c) vertical displacement vs horizontal displacement

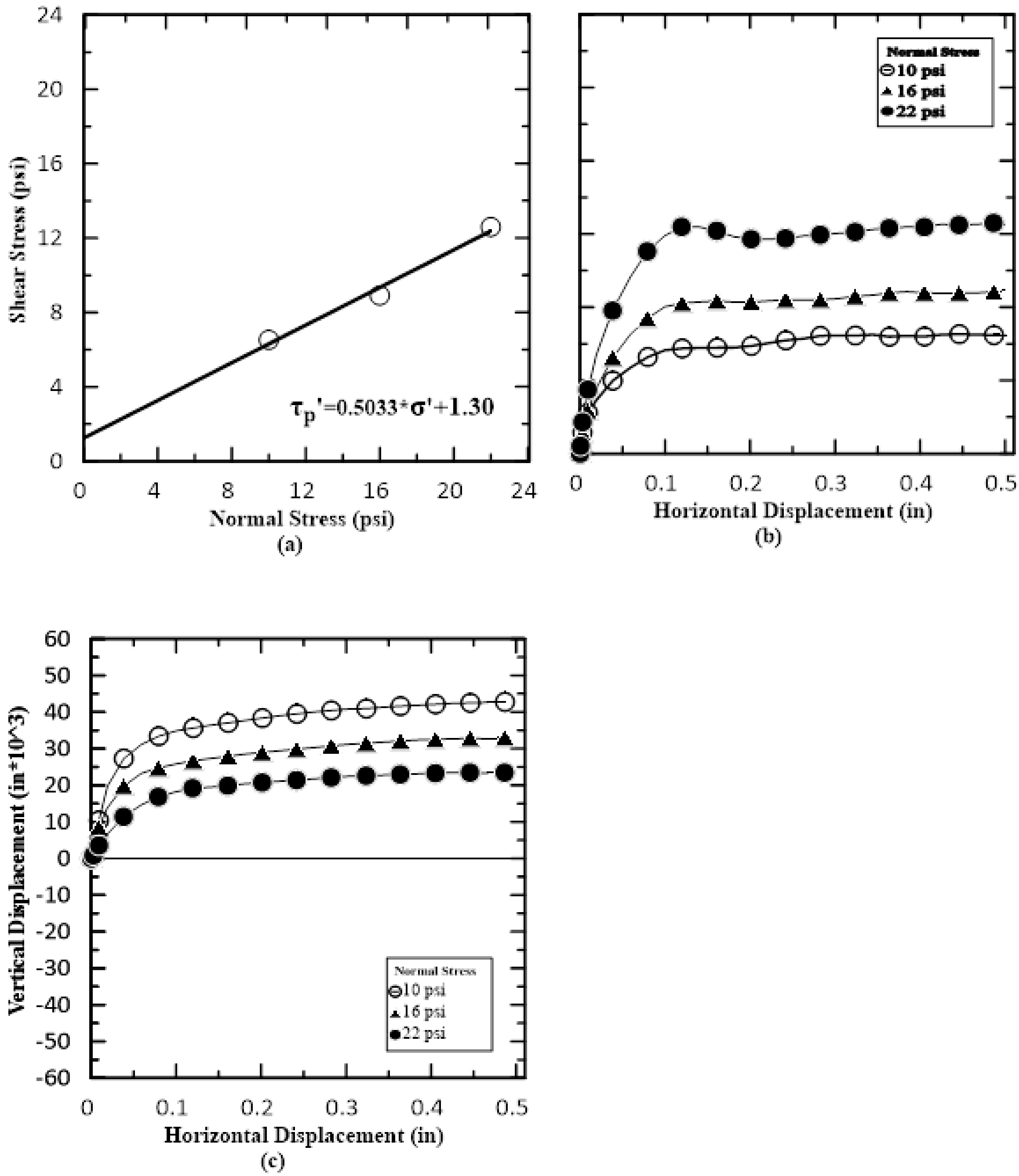

Figure 130. Small direct shear results for Soil 1 and Soil 5 mixtures at fine content = 60%, moisture content = 18.6%: (a) shear stress vs normal stress; (b) shear stress vs horizontal displacement; (c) vertical displacement vs horizontal displacement

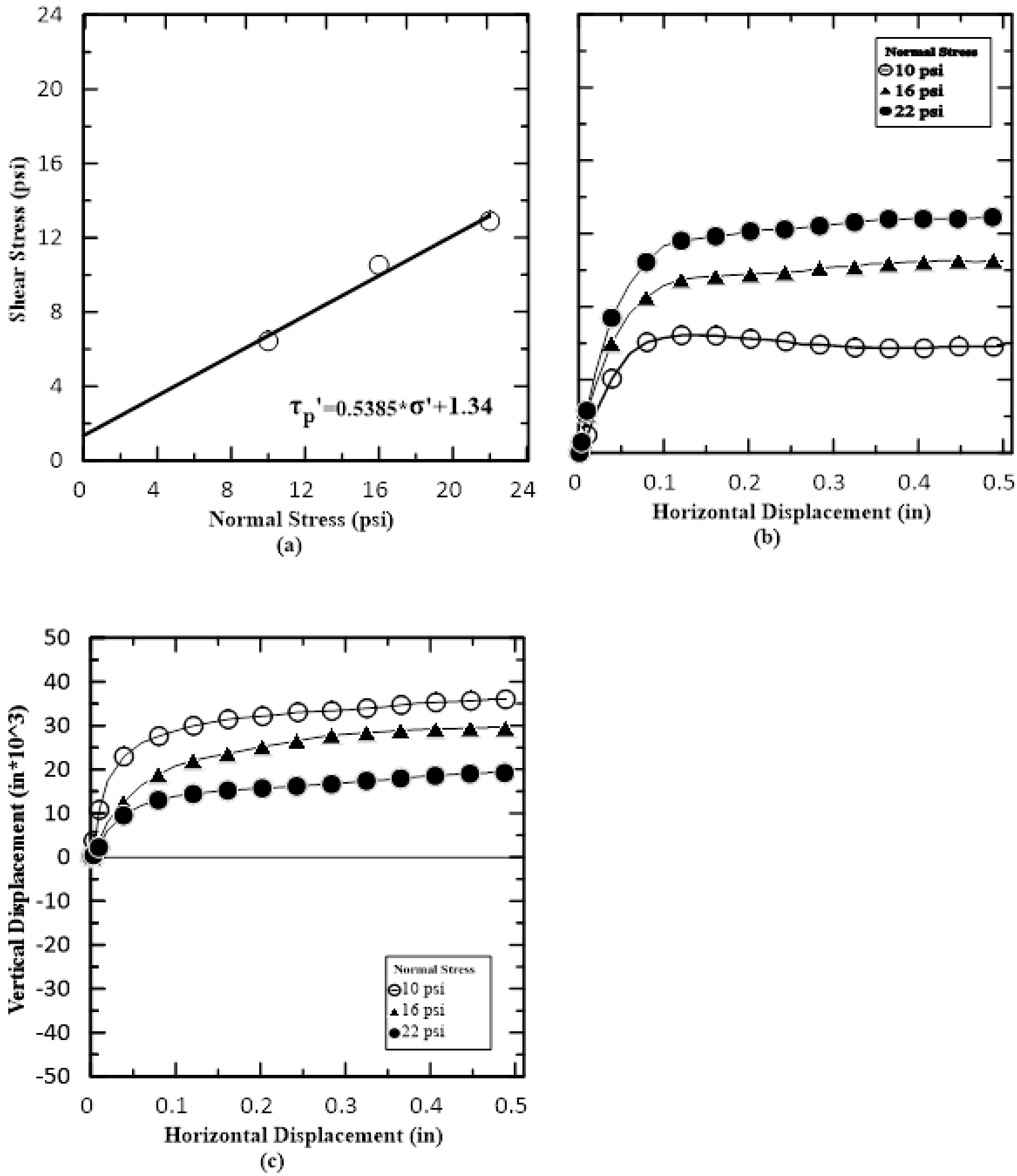

Figure 131. Small direct shear results for Soil 1 and Soil 5 mixtures at fine content = 60%, moisture content = 16.8%: (a) shear stress vs normal stress; (b) shear stress vs horizontal displacement; (c) vertical displacement vs horizontal displacement

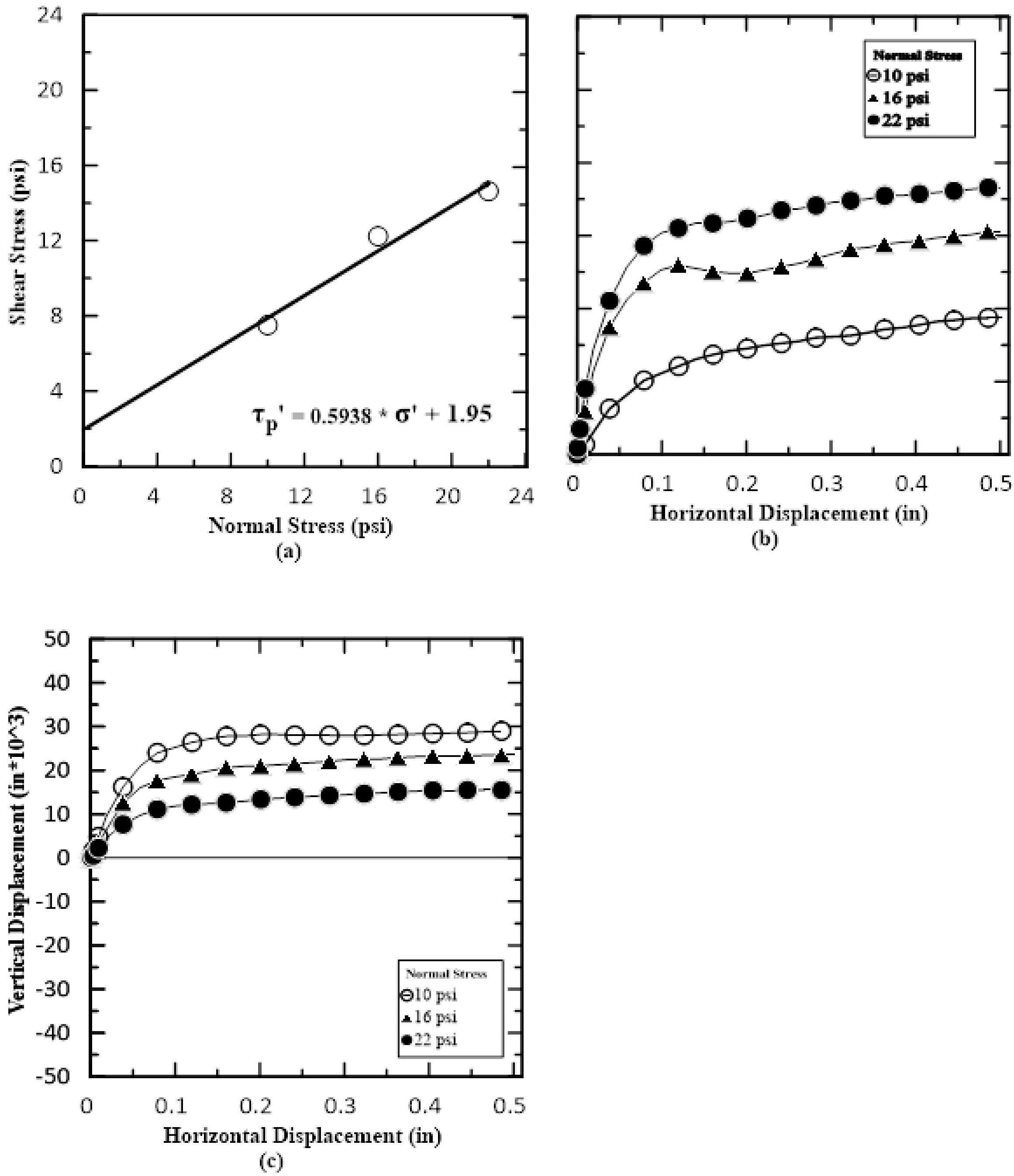

Figure 132. Small direct shear results for Soil 1 and Soil 5 mixtures at fine content = 60%, moisture content = 14.7%: (a) shear stress vs normal stress; (b) shear stress vs horizontal displacement; (c) vertical displacement vs horizontal displacement

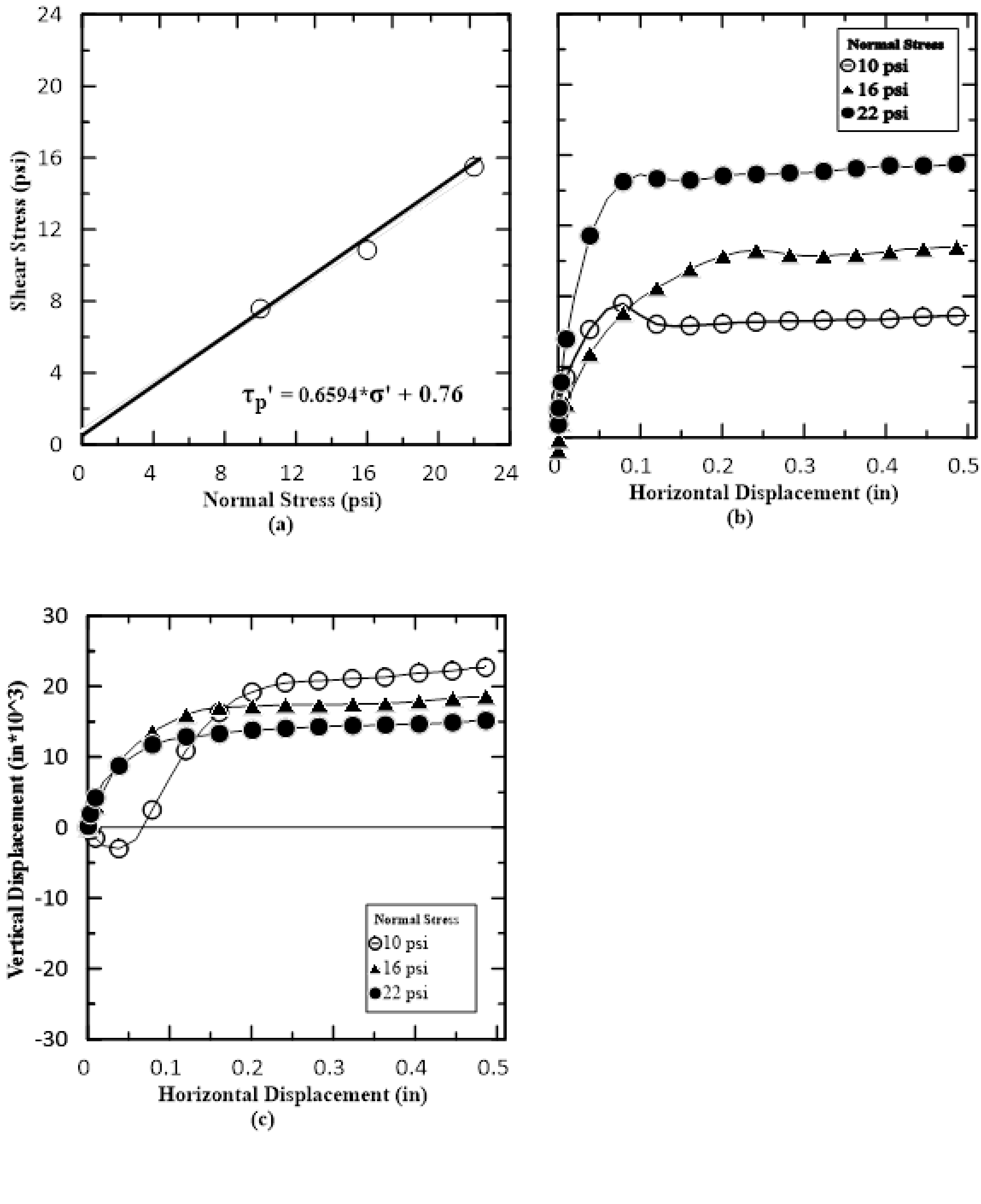

Figure 133. Small direct shear results for Soil 1 and Soil 5 mixtures at fine content = 70%, moisture content = 22%: (a) shear stress vs normal stress; (b) shear stress vs horizontal displacement; (c) vertical displacement vs horizontal displacement

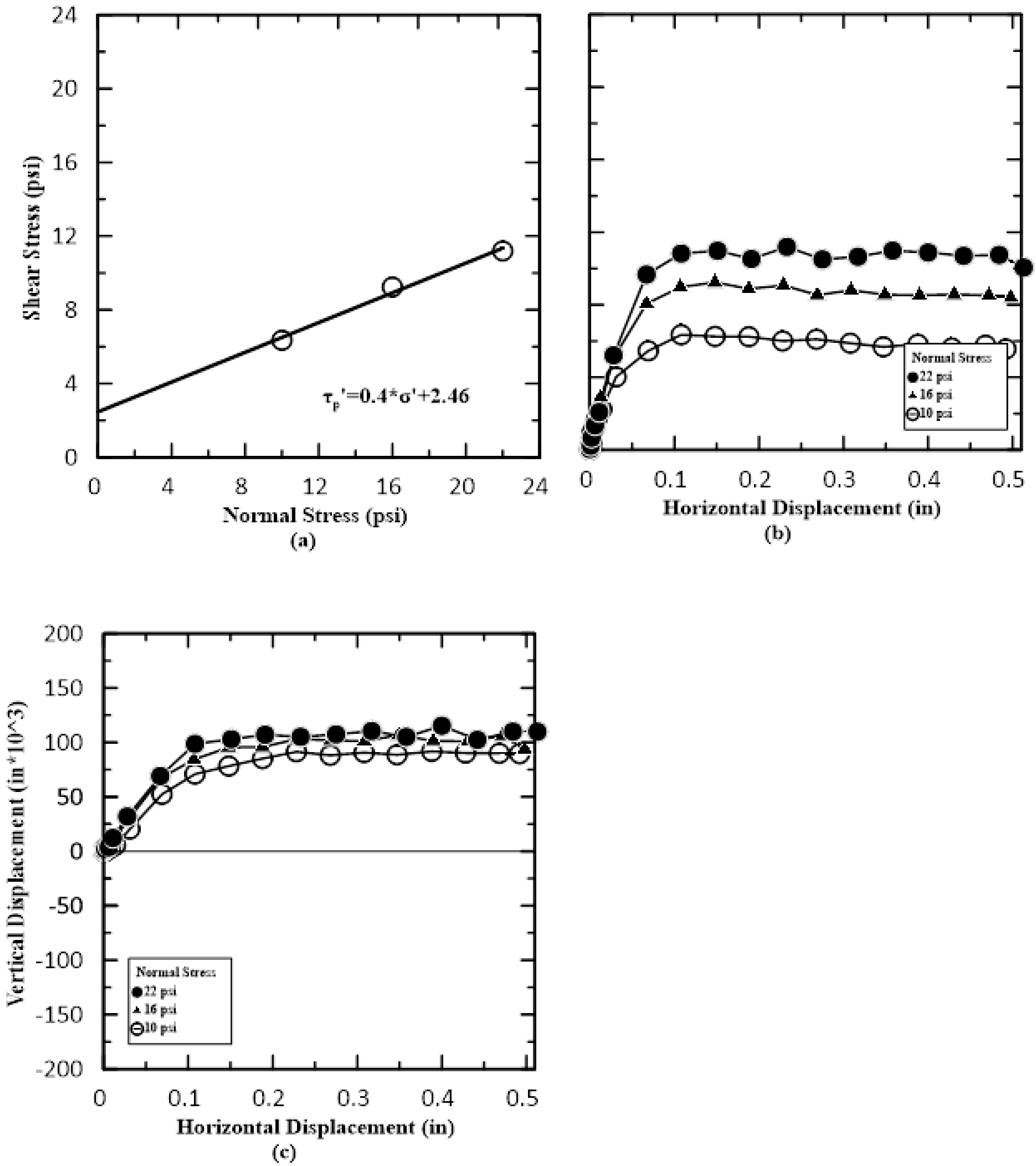

Figure 134. Small direct shear results for Soil 1 and Soil 5 mixtures at fine content = 70%, moisture content = 20.3%: (a) shear stress vs normal stress; (b) shear stress vs horizontal displacement; (c) vertical displacement vs horizontal displacement

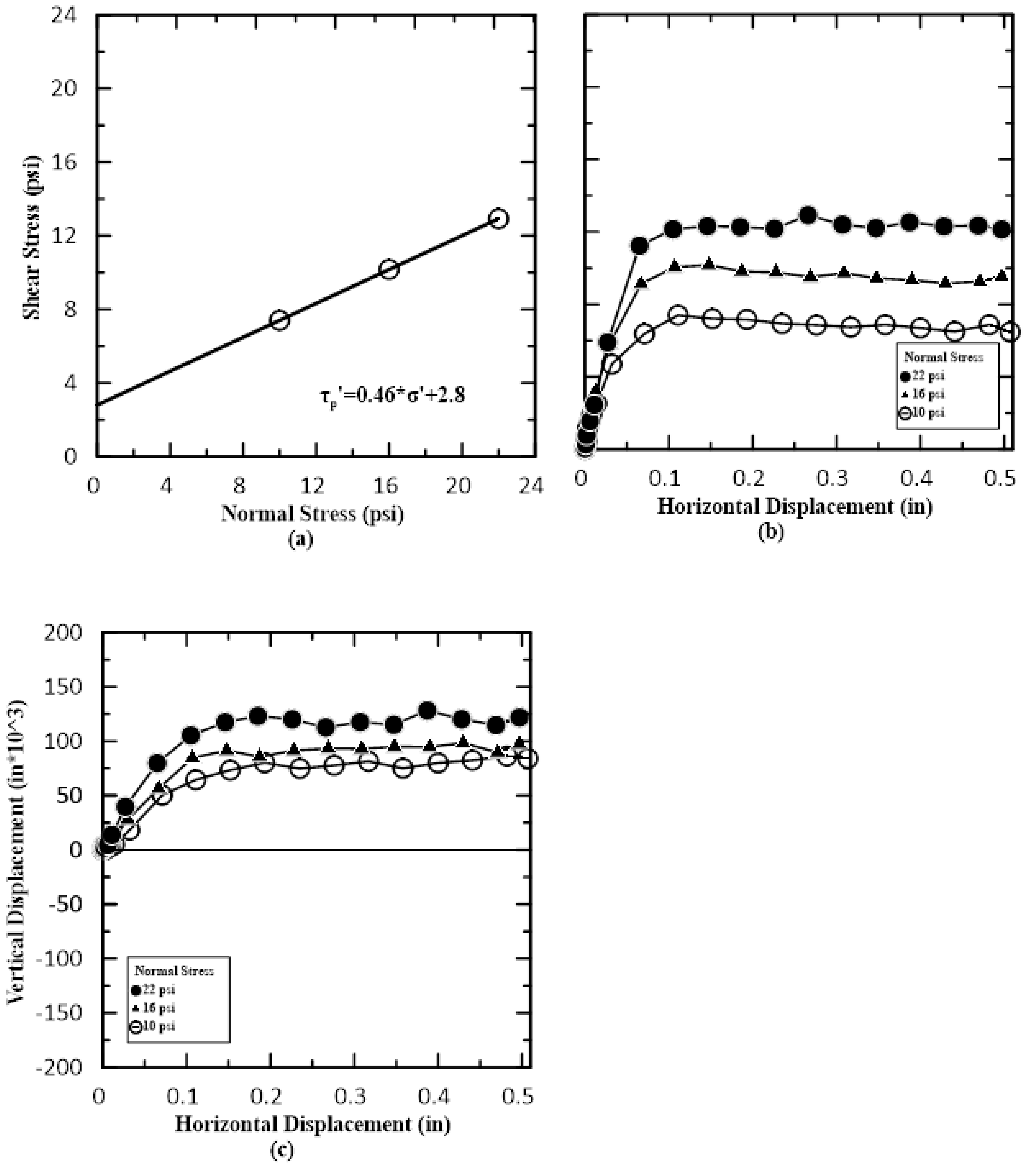

Figure 135. Small direct shear results for Soil 1 and Soil 5 mixtures at fine content = 70%, moisture content = 18.2%: (a) shear stress vs normal stress; (b) shear stress vs horizontal displacement; (c) vertical displacement vs horizontal displacement

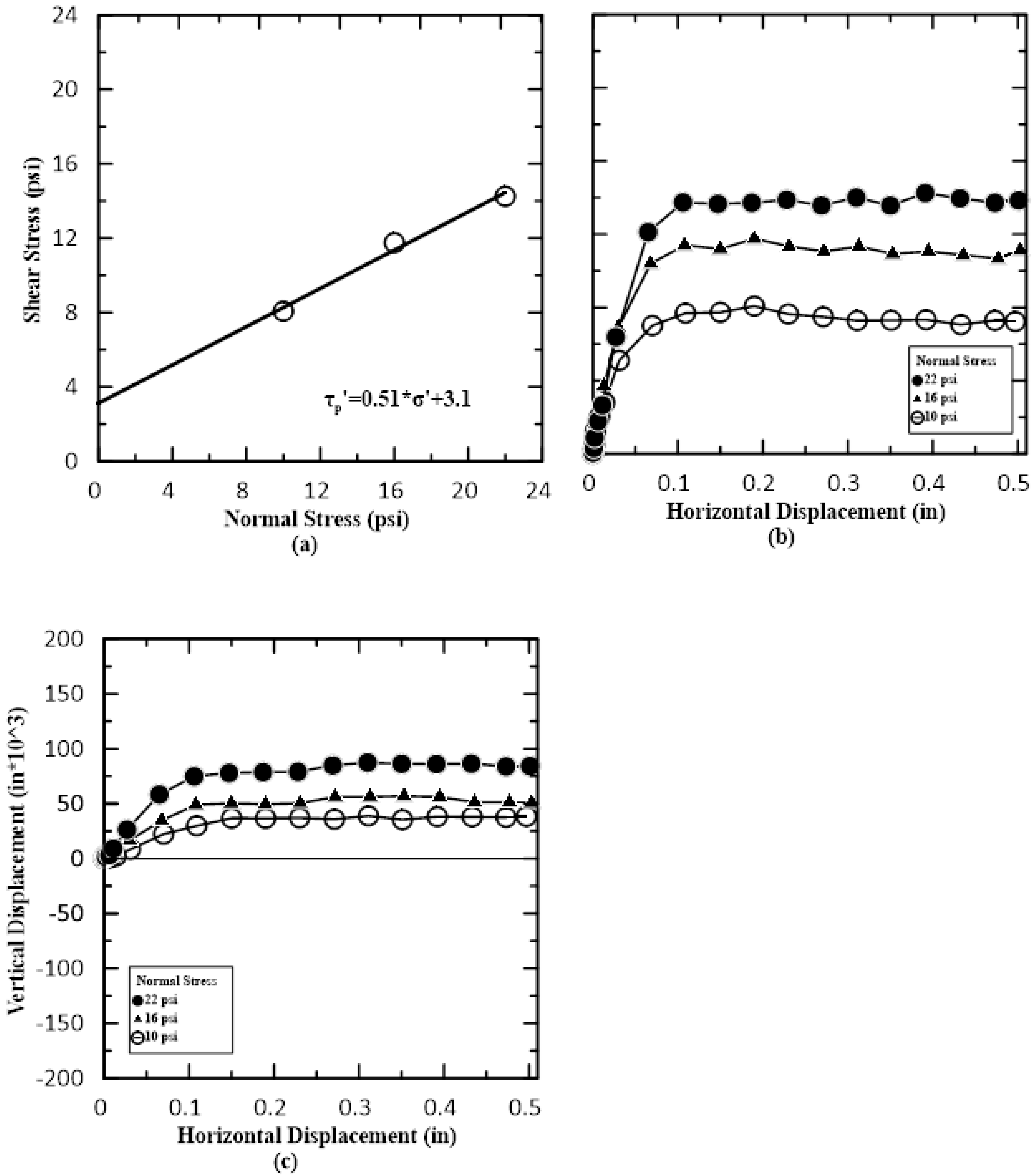

Figure 136. Small direct shear results for Soil 1 and Soil 5 mixtures at fine content = 70%, moisture content = 16.1%: (a) shear stress vs normal stress; (b) shear stress vs horizontal displacement; (c) vertical displacement vs horizontal displacement

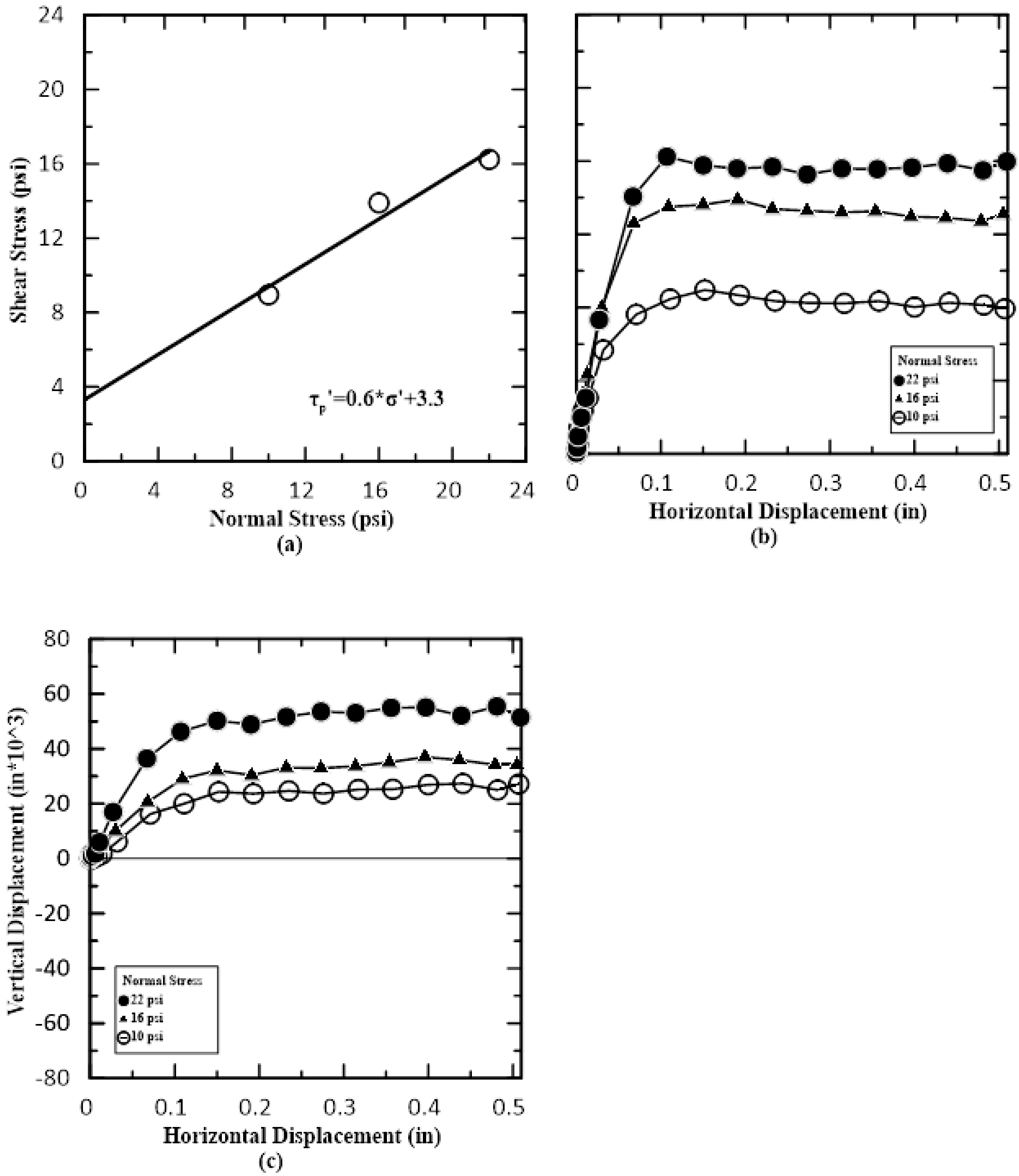

Appendix C
Large Direct Shear Test Results

This section has a thorough collection of tables that demonstrate the results of large direct shear tests carried out on a range of soil mixtures with varying soil fractions. The tables explain how the variables of soil displacement, soil shear stress, soil normal stress, and soil horizontal displacement interact in complex ways. These findings provide a thorough understanding of the shear behavior and displacement properties of various soil combinations and how they react to various environmental situations.

Figure 137. Large direct shear results for Soil 1 and Soil 2 mixtures at fine content = 10%, moisture content = 15.9%: (a) shear stress vs normal stress; (b) shear stress vs horizontal displacement; (c) vertical displacement vs horizontal displacement

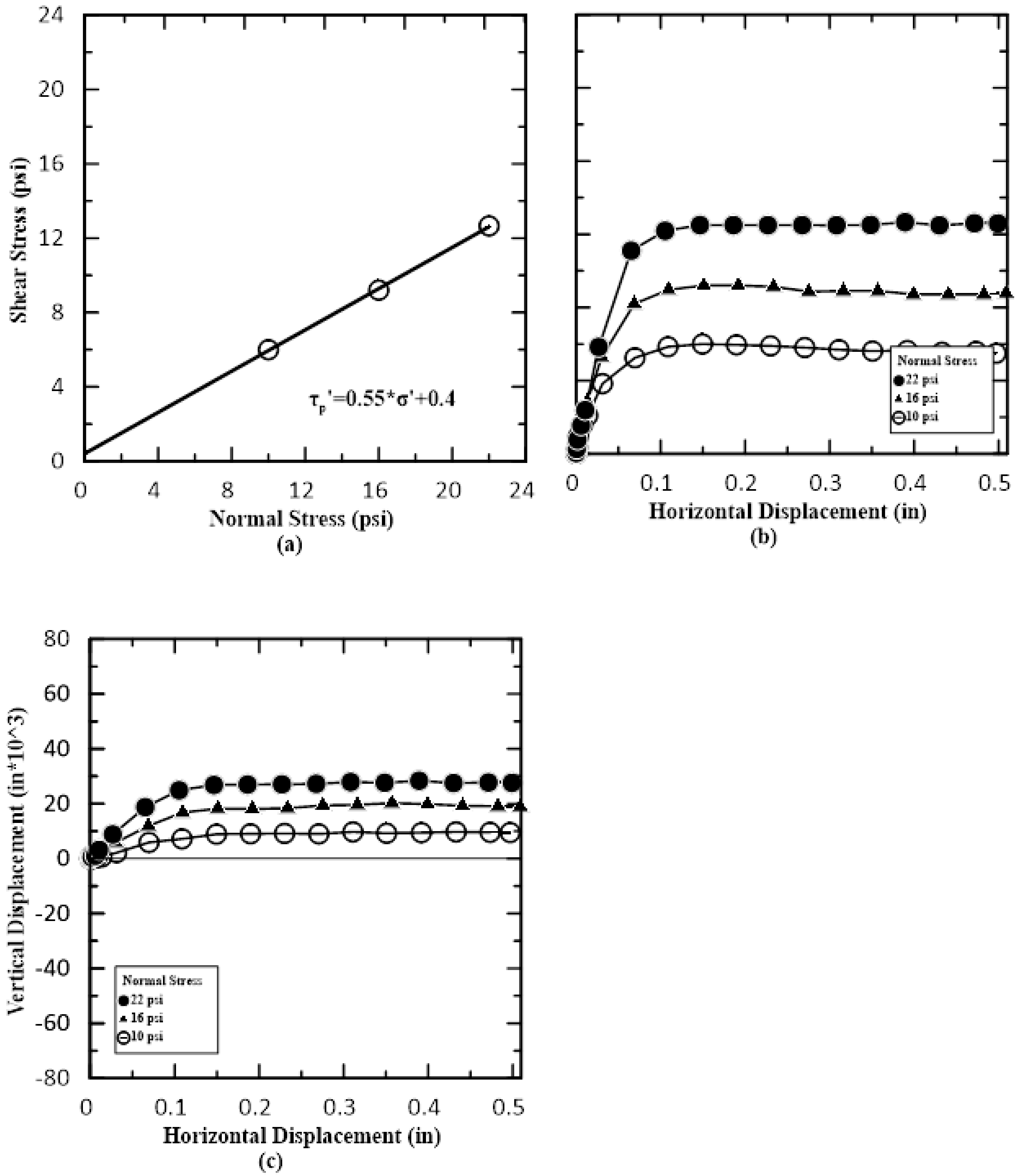

Figure 138. Large direct shear results for Soil 1 and Soil 2 mixtures at fine content = 10%, moisture content = 7.8%: (a) shear stress vs normal stress; (b) shear stress vs horizontal displacement; (c) vertical displacement vs horizontal displacement

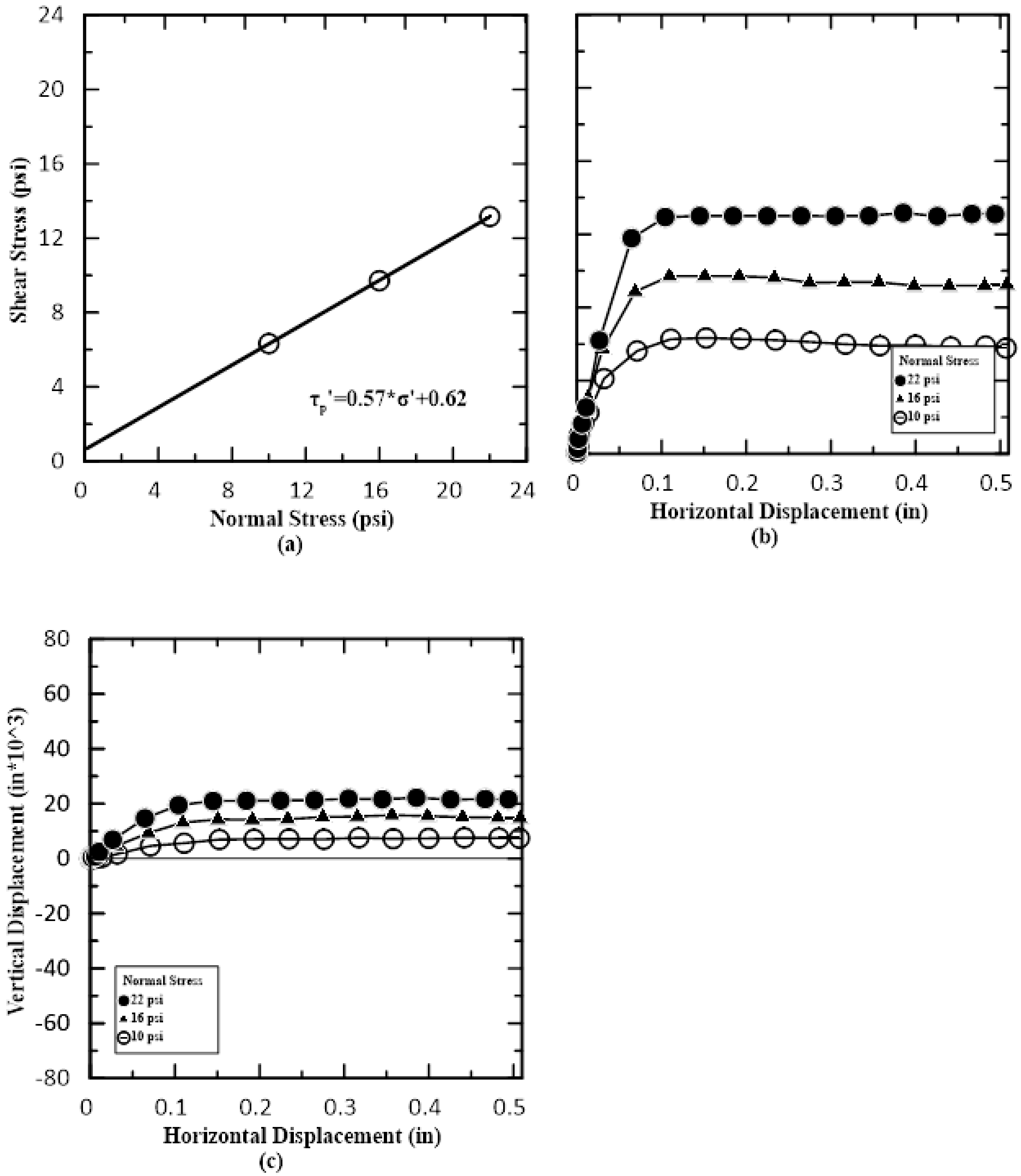

Figure 139. Large direct shear results for Soil 1 and Soil 2 mixtures at fine content = 20%, moisture content = 16.6%: (a) shear stress vs normal stress; (b) shear stress vs horizontal displacement; (c) vertical displacement vs horizontal displacement

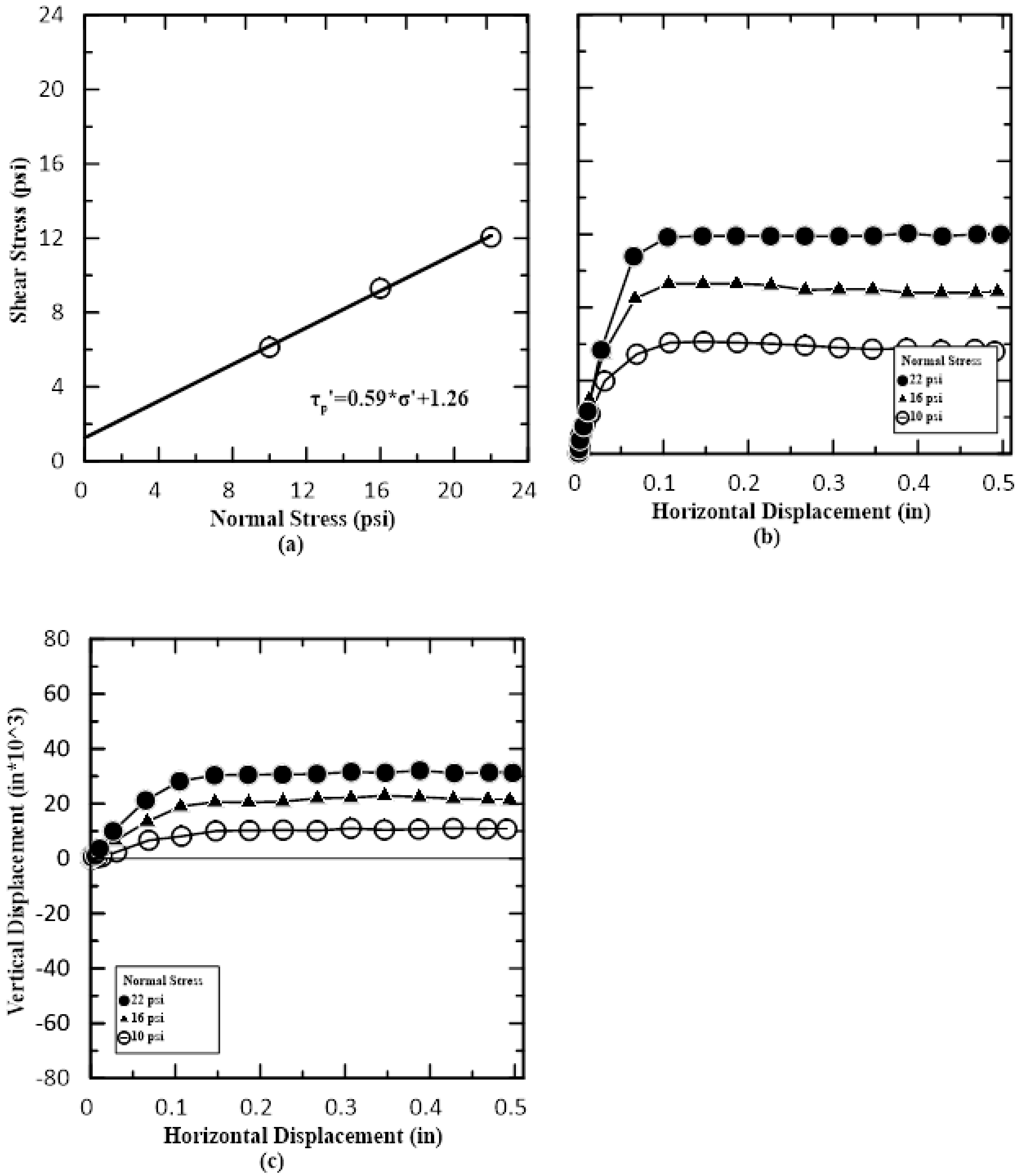

Figure 140. Large direct shear results for Soil 1 and Soil 2 mixtures at fine content = 20%, moisture content = 13.2%: (a) shear stress vs normal stress; (b) shear stress vs horizontal displacement; (c) vertical displacement vs horizontal displacement

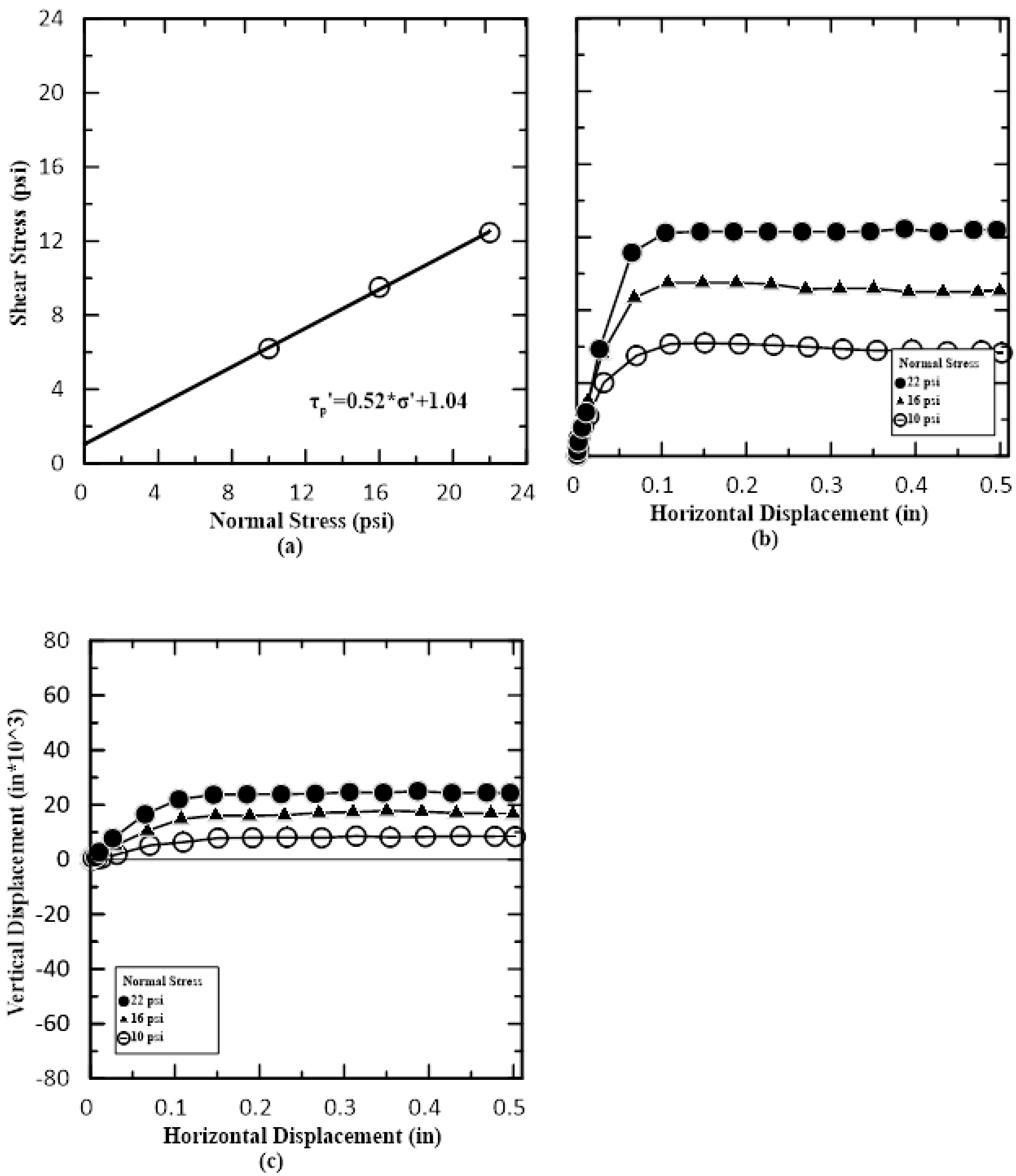

Figure 141. Large direct shear results for Soil 1 and Soil 2 mixtures at fine content = 20%, moisture content = 10.3%: (a) shear stress vs normal stress; (b) shear stress vs horizontal displacement; (c) vertical displacement vs horizontal displacement

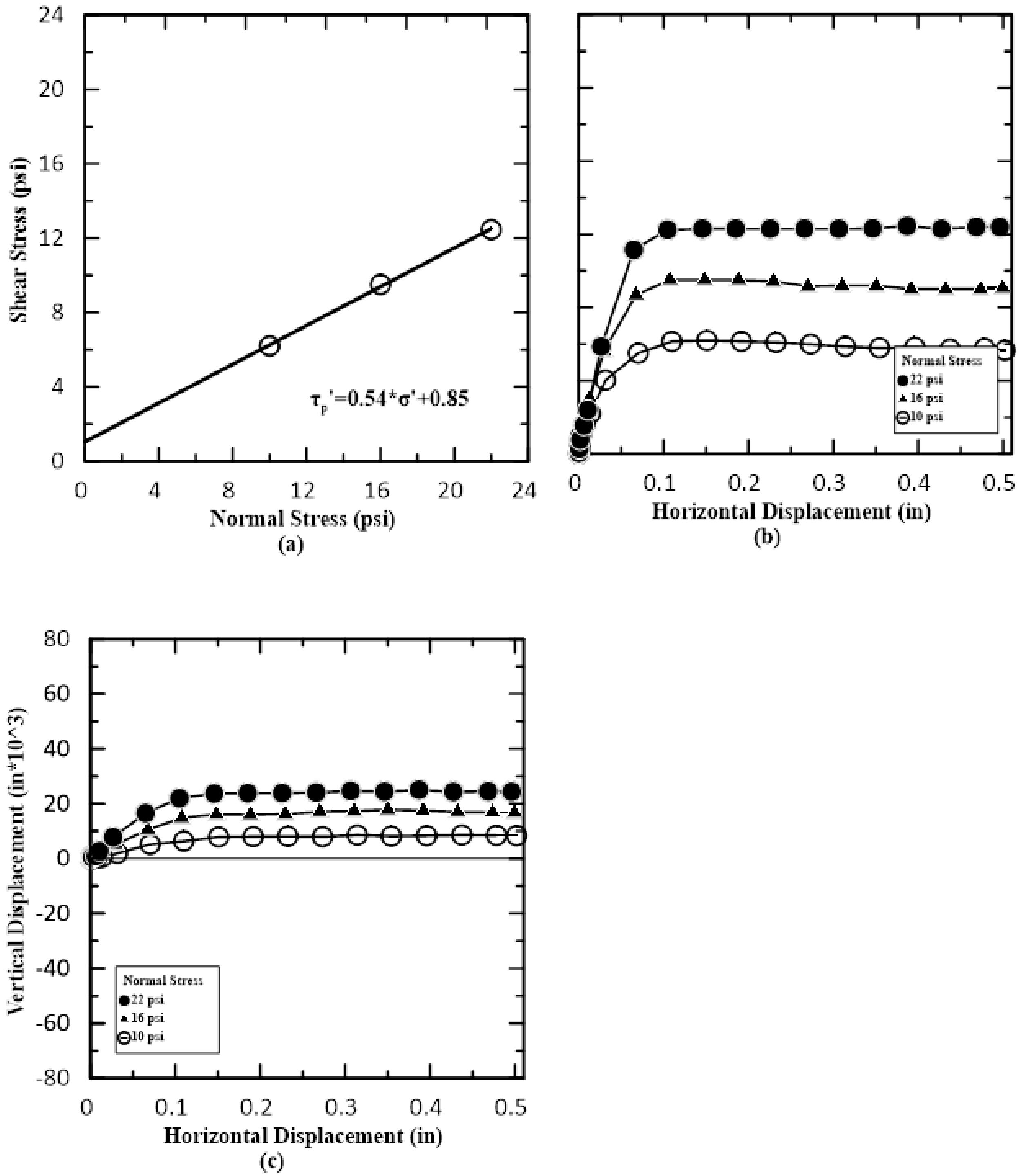

Figure 142. Large direct shear results for Soil 1 and Soil 2 mixtures at fine content = 30%, moisture content = 15.8%: (a) shear stress vs normal stress; (b) shear stress vs horizontal displacement; (c) vertical displacement vs horizontal displacement

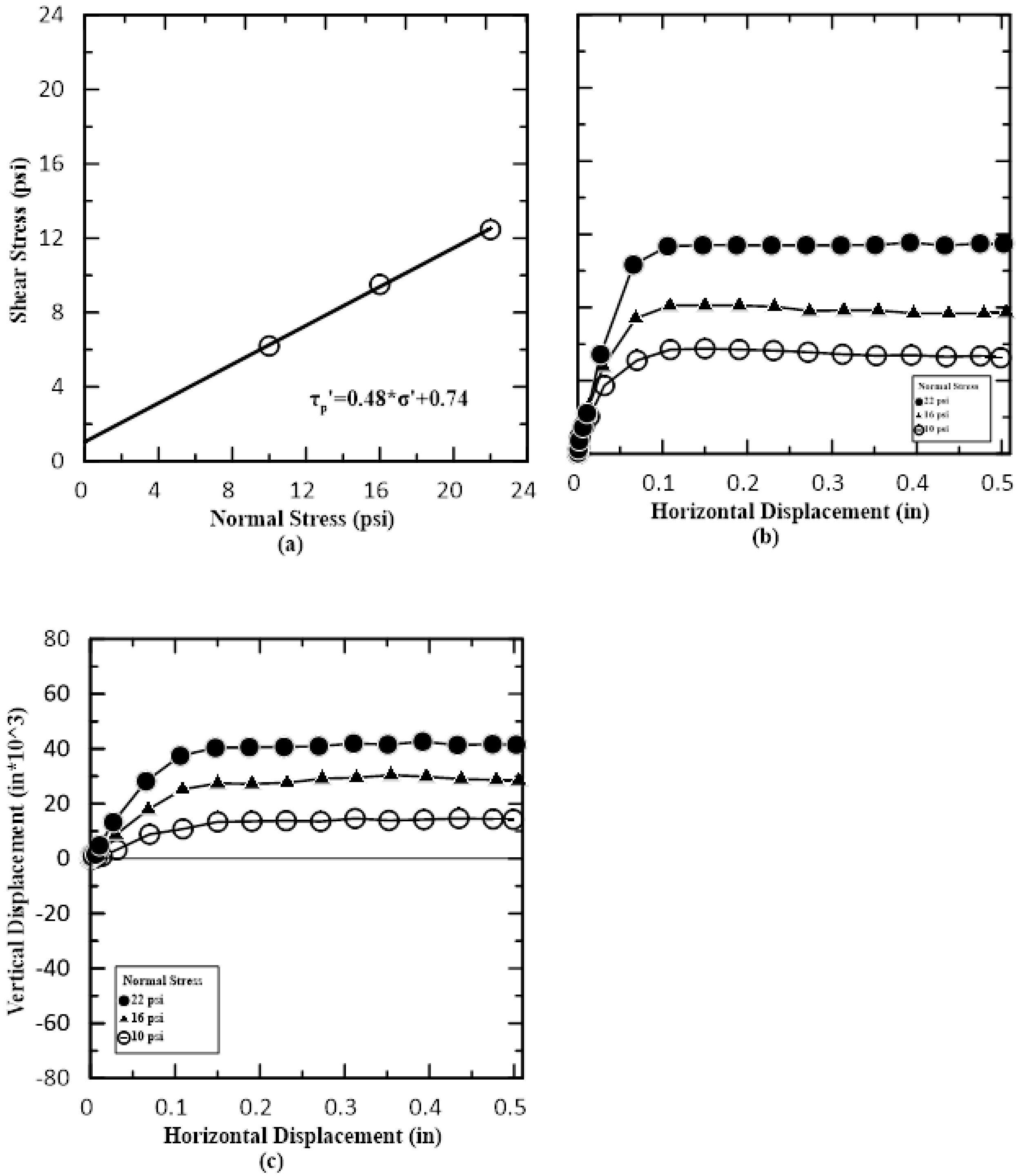

Figure 143. Large direct shear results for Soil 1 and Soil 2 mixtures at fine content = 30%, moisture content = 13.1%: (a) shear stress vs normal stress; (b) shear stress vs horizontal displacement; (c) vertical displacement vs horizontal displacement

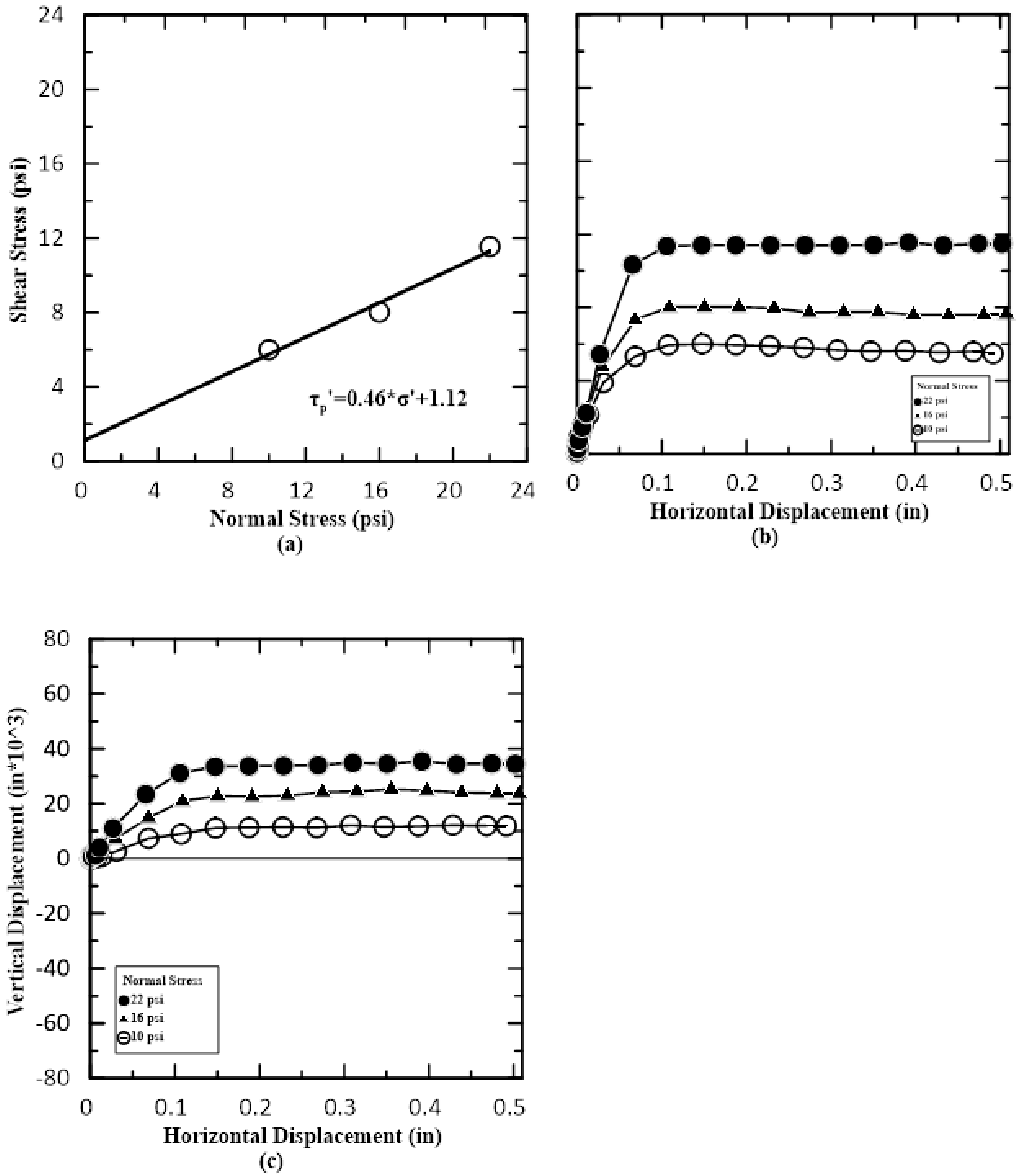

Figure 144. Large direct shear results for Soil 1 and Soil 2 mixtures at fine content = 30%, moisture content = 11.2%: (a) shear stress vs normal stress; (b) shear stress vs horizontal displacement; (c) vertical displacement vs horizontal displacement

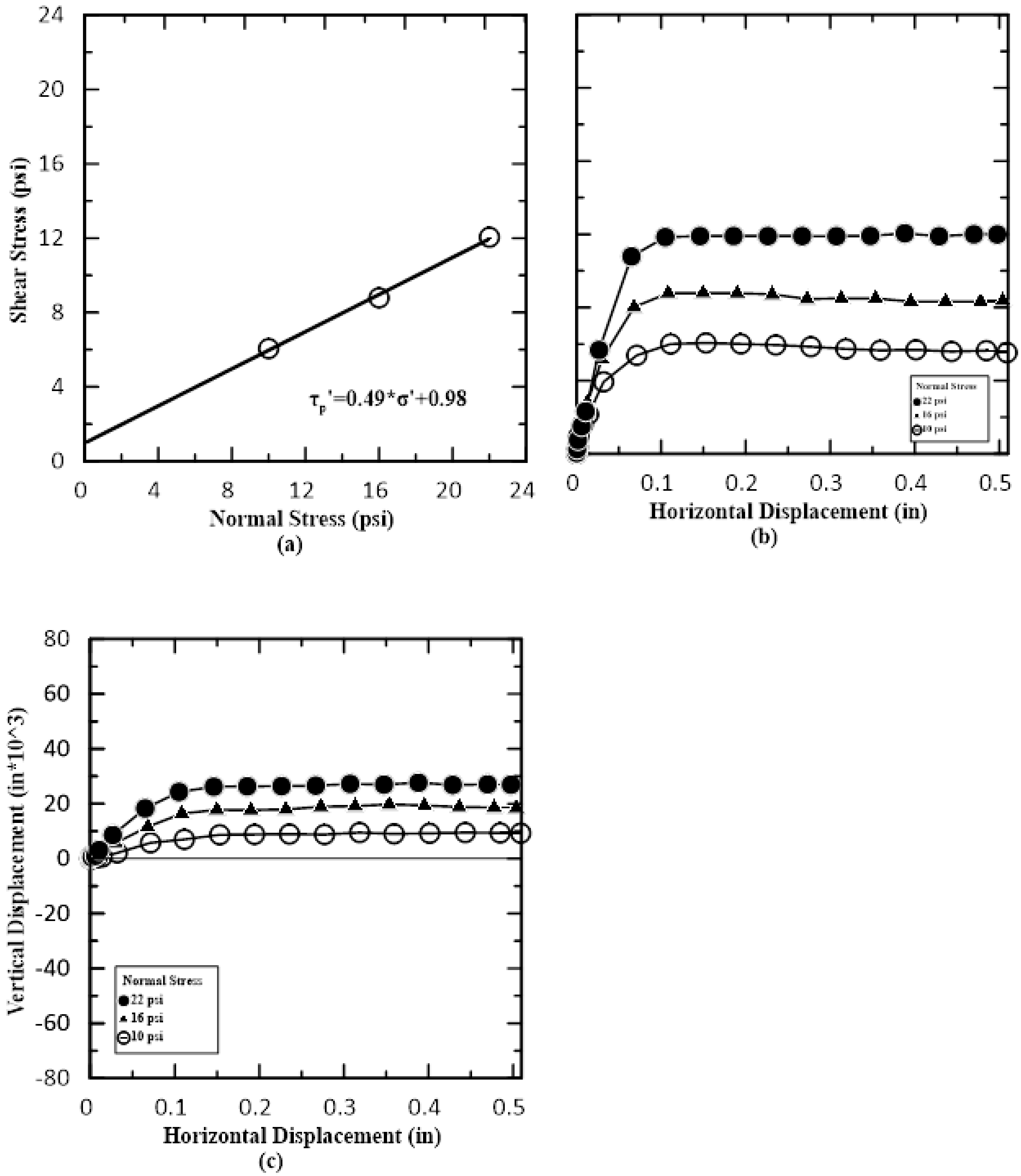

Figure 145. Large direct shear results for Soil 1 and Soil 2 mixtures at fine content = 40%, moisture content = 16.3%: (a) shear stress vs normal stress; (b) shear stress vs horizontal displacement; (c) vertical displacement vs horizontal displacement

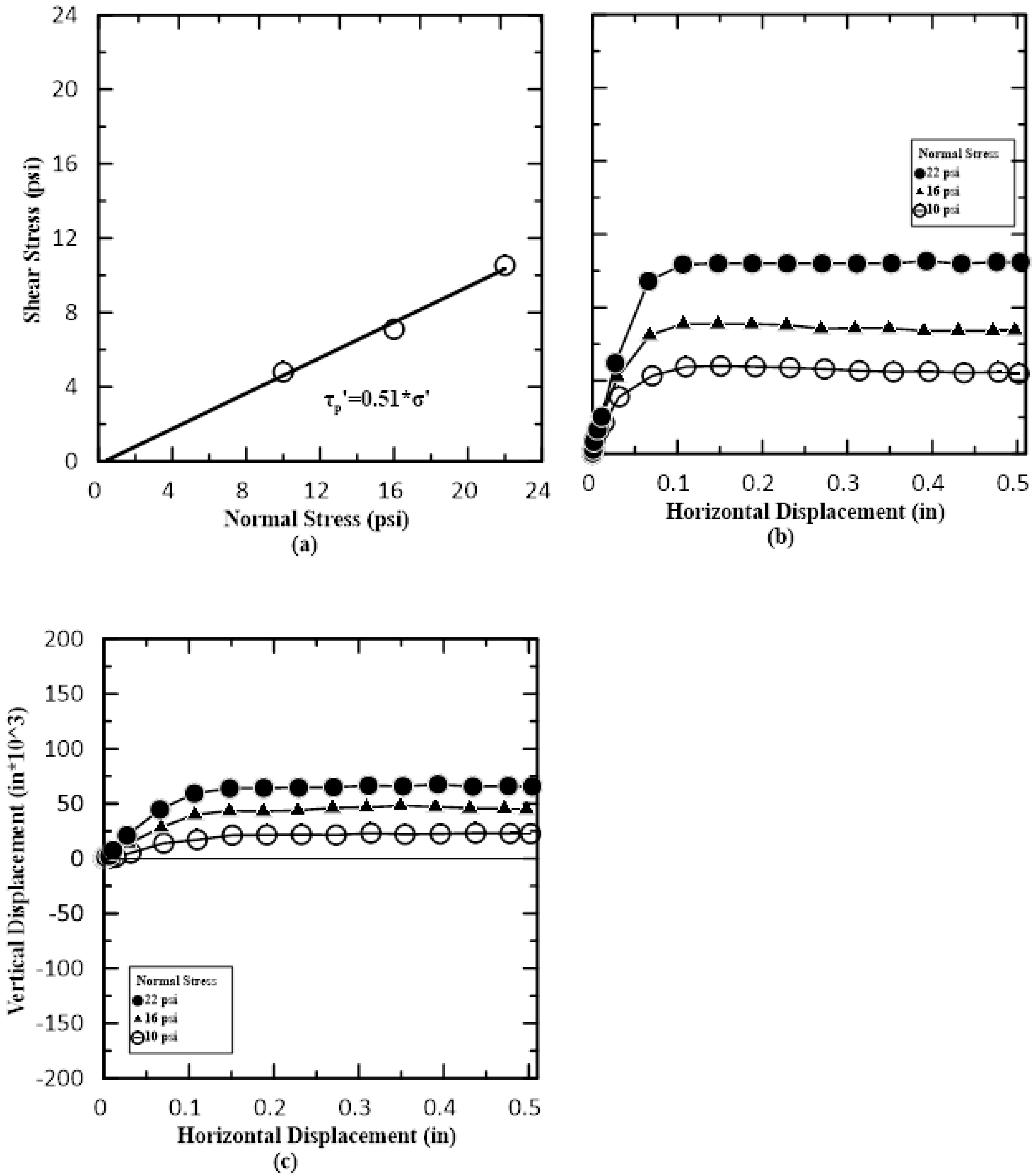

Figure 146. Large direct shear results for Soil 1 and Soil 2 mixtures at fine content = 40%, moisture content = 14.1%: (a) shear stress vs normal stress; (b) shear stress vs horizontal displacement; (c) vertical displacement vs horizontal displacement

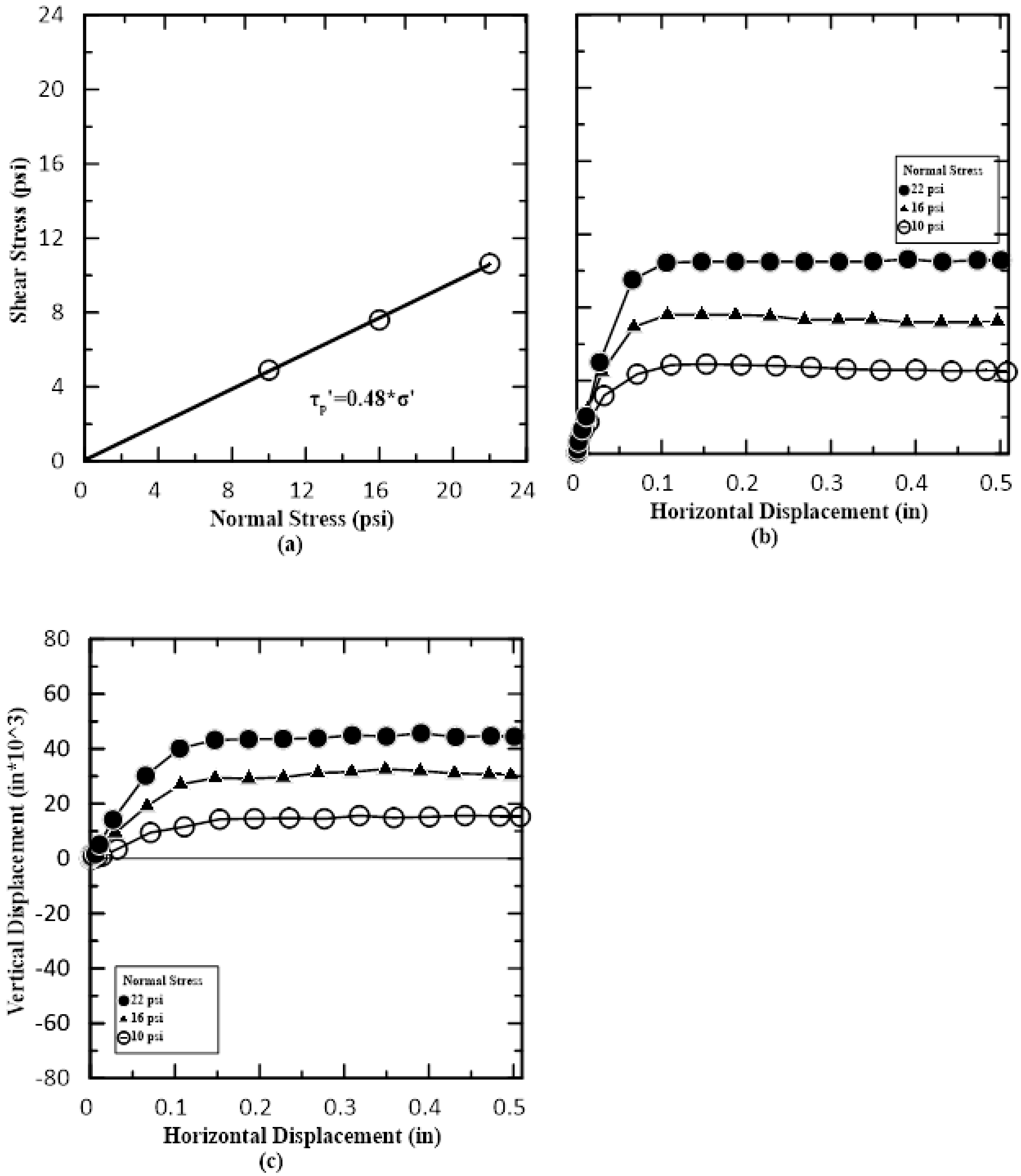

Figure 147. Large direct shear results for Soil 1 and Soil 2 mixtures at fine content = 40%, moisture content = 12.3%: (a) shear stress vs normal stress; (b) shear stress vs horizontal displacement; (c) vertical displacement vs horizontal displacement

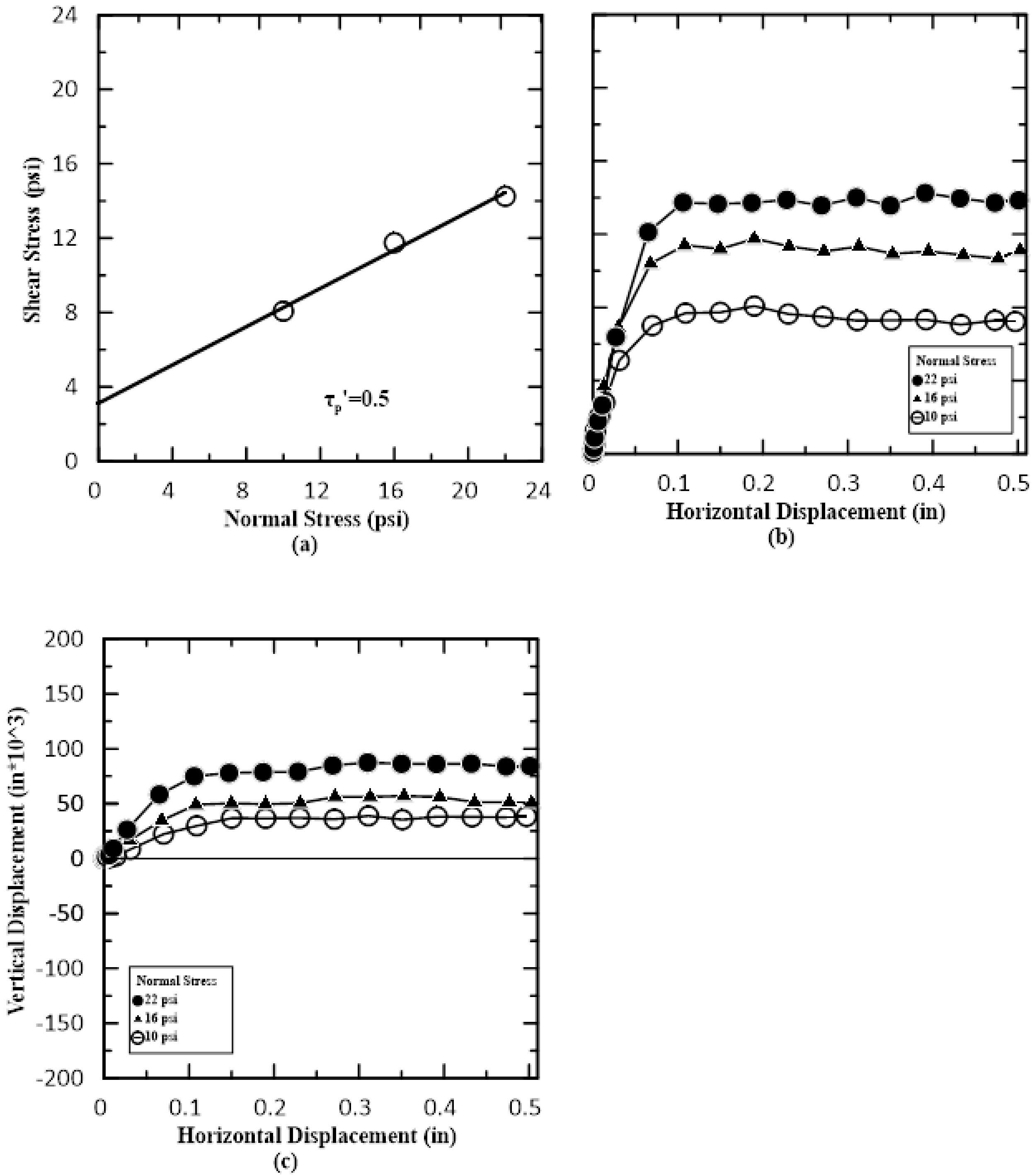

Figure 148. Large direct shear results for Soil 1 and Soil 3 mixtures at fine content = 10%, moisture content = 15%: (a) shear stress vs normal stress; (b) shear stress vs horizontal displacement; (c) vertical displacement vs horizontal displacement

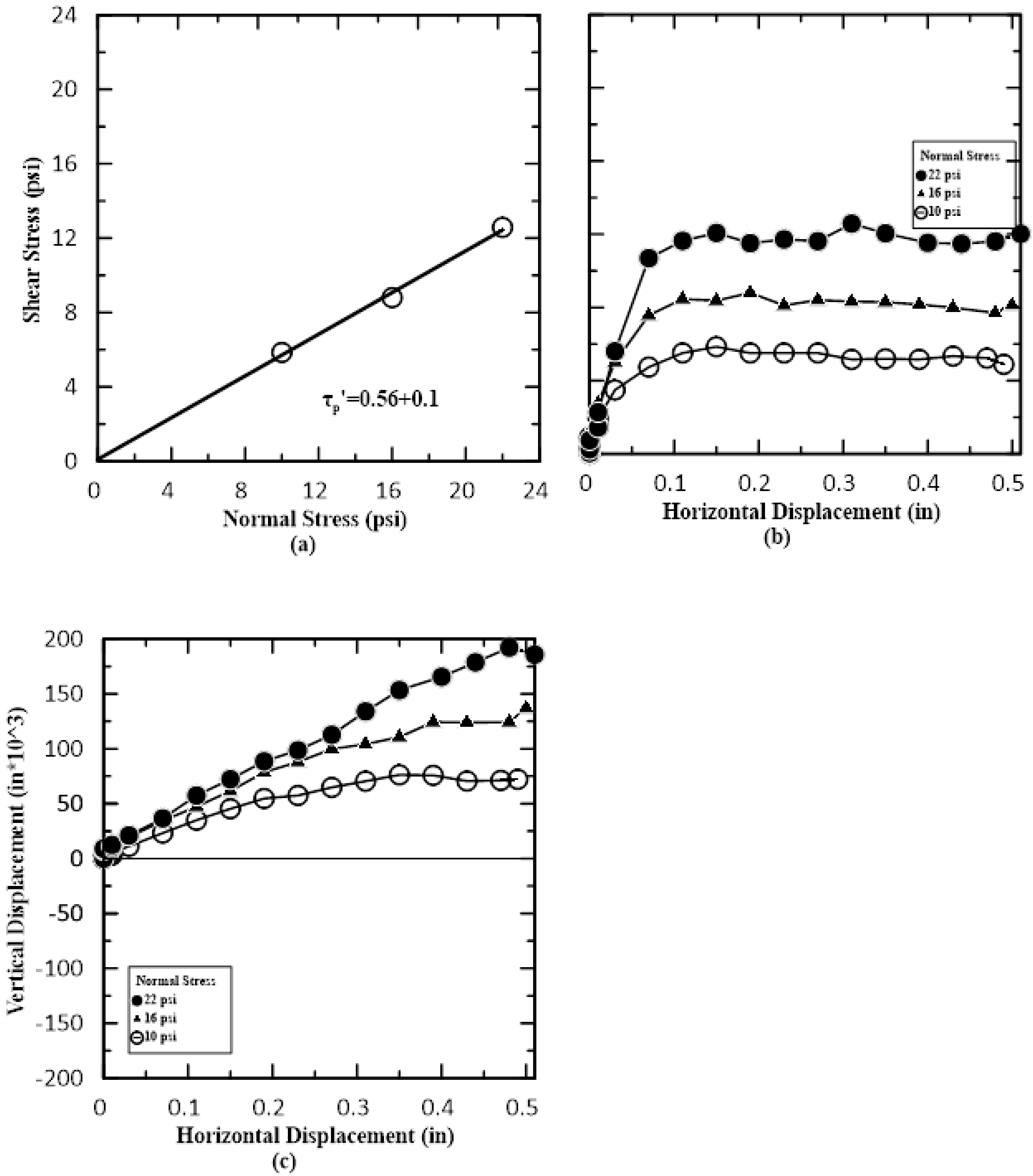

Figure 149. Large direct shear results for Soil 1 and Soil 3 mixtures at fine content = 10%, moisture content = 12.2%: (a) shear stress vs normal stress; (b) shear stress vs horizontal displacement; (c) vertical displacement vs horizontal displacement

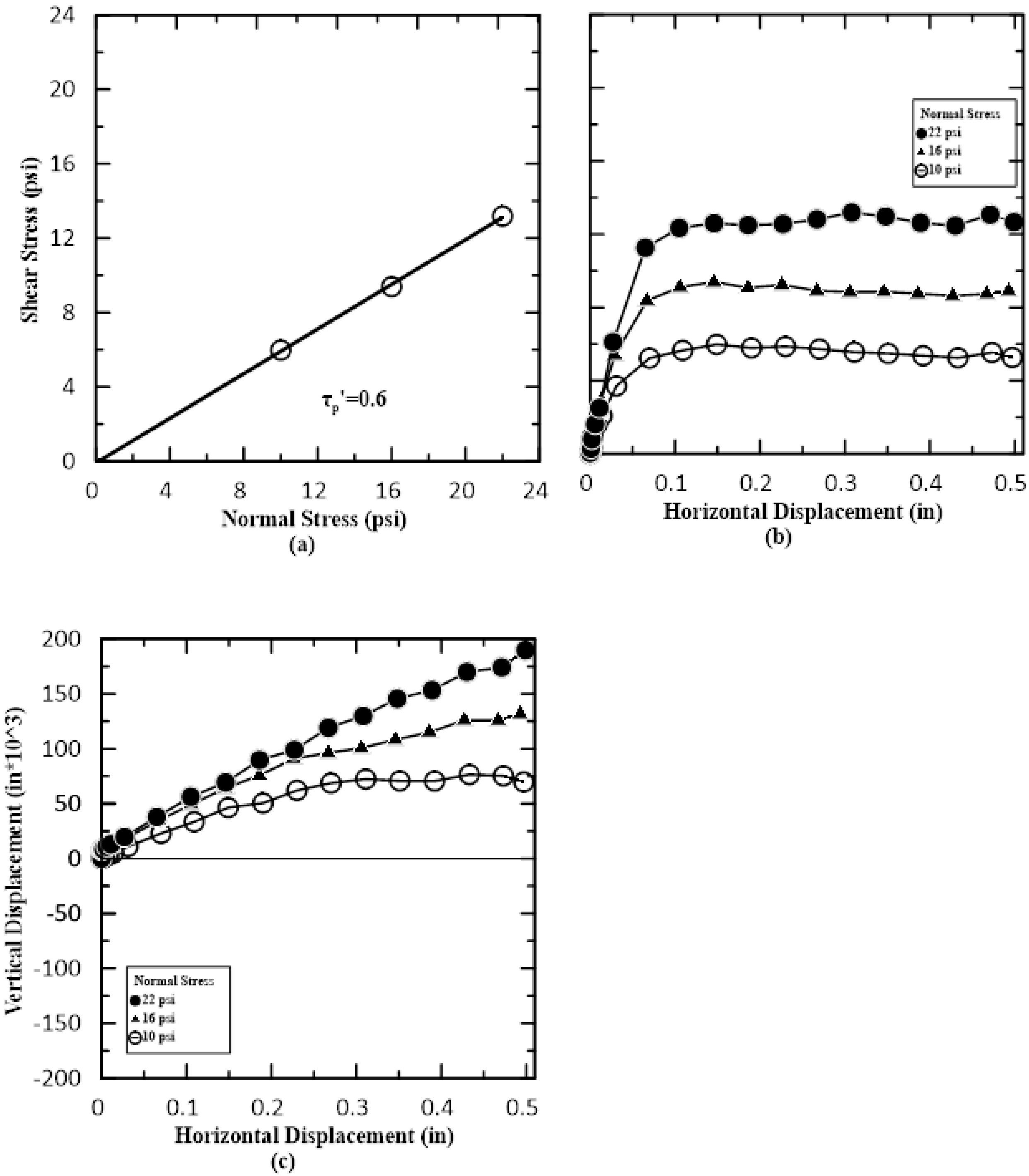

Figure 150. Large direct shear results for Soil 1 and Soil 3 mixtures at fine content = 10%, moisture content = 10.3%: (a) shear stress vs normal stress; (b) shear stress vs horizontal displacement; (c) vertical displacement vs horizontal displacement

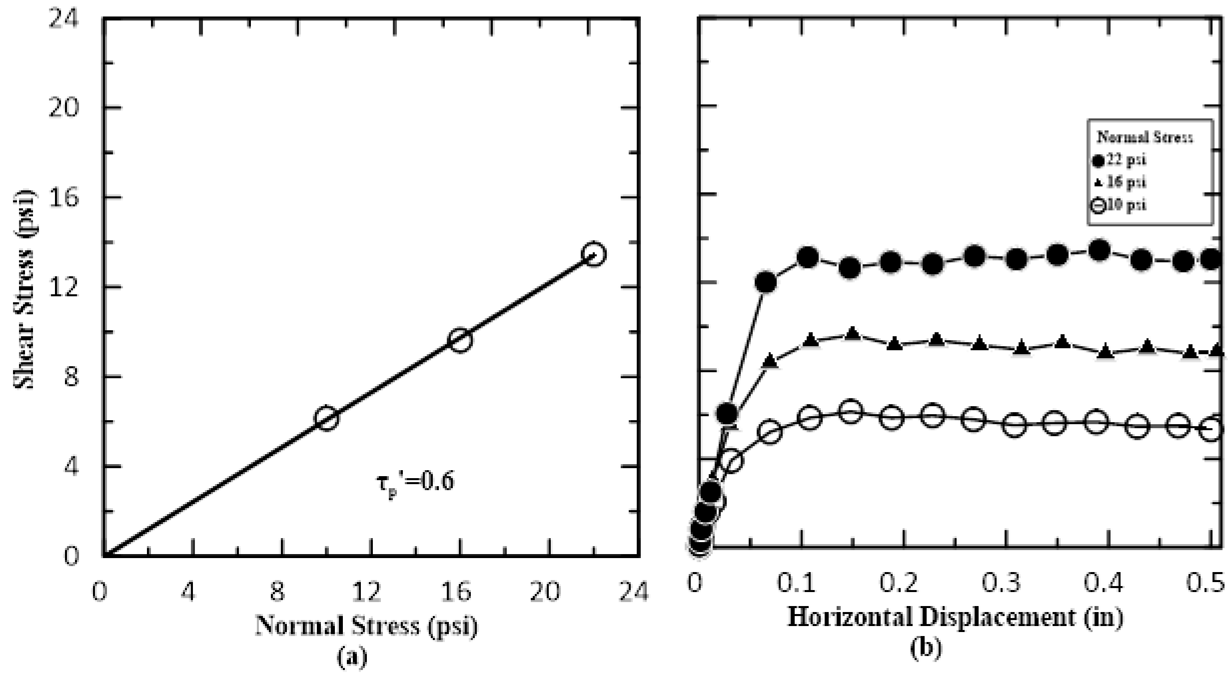

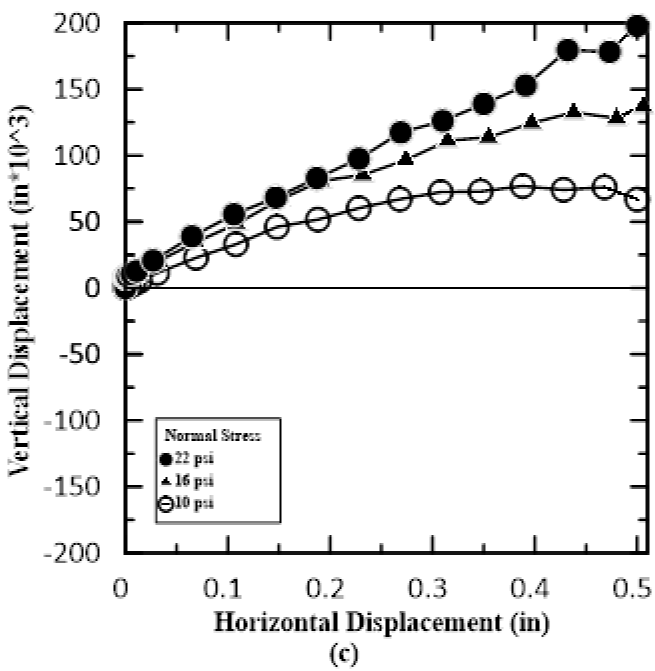

Figure 151. Large direct shear results for Soil 1 and Soil 3 mixtures at fine content = 50%, moisture content = 17.3%: (a) shear stress vs normal stress; (b) shear stress vs horizontal displacement; (c) vertical displacement vs horizontal displacement

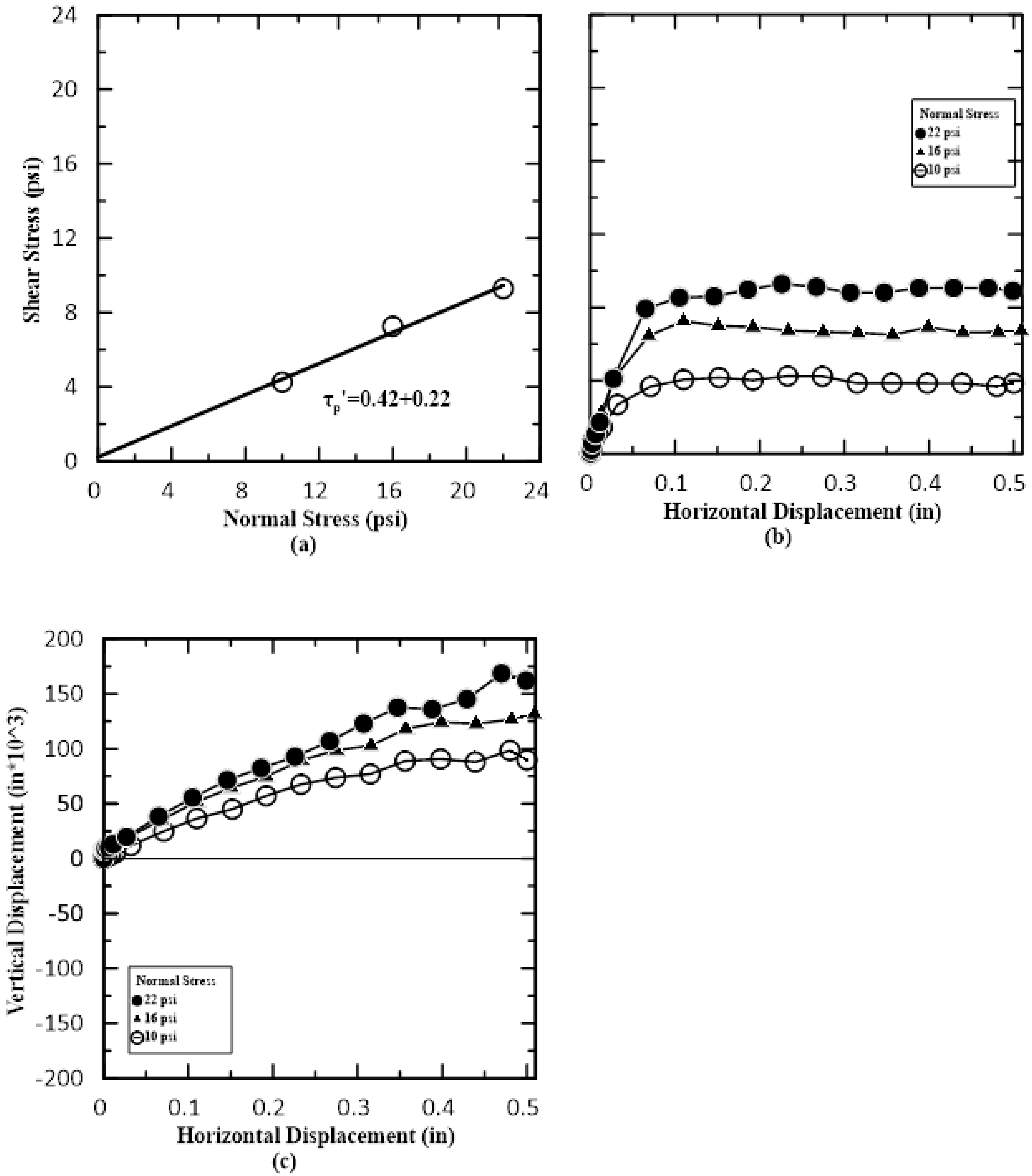

Figure 152. Large direct shear results for Soil 1 and Soil 3 mixtures at fine content = 50%, moisture content = 15.2%: (a) shear stress vs normal stress; (b) shear stress vs horizontal displacement; (c) vertical displacement vs horizontal displacement

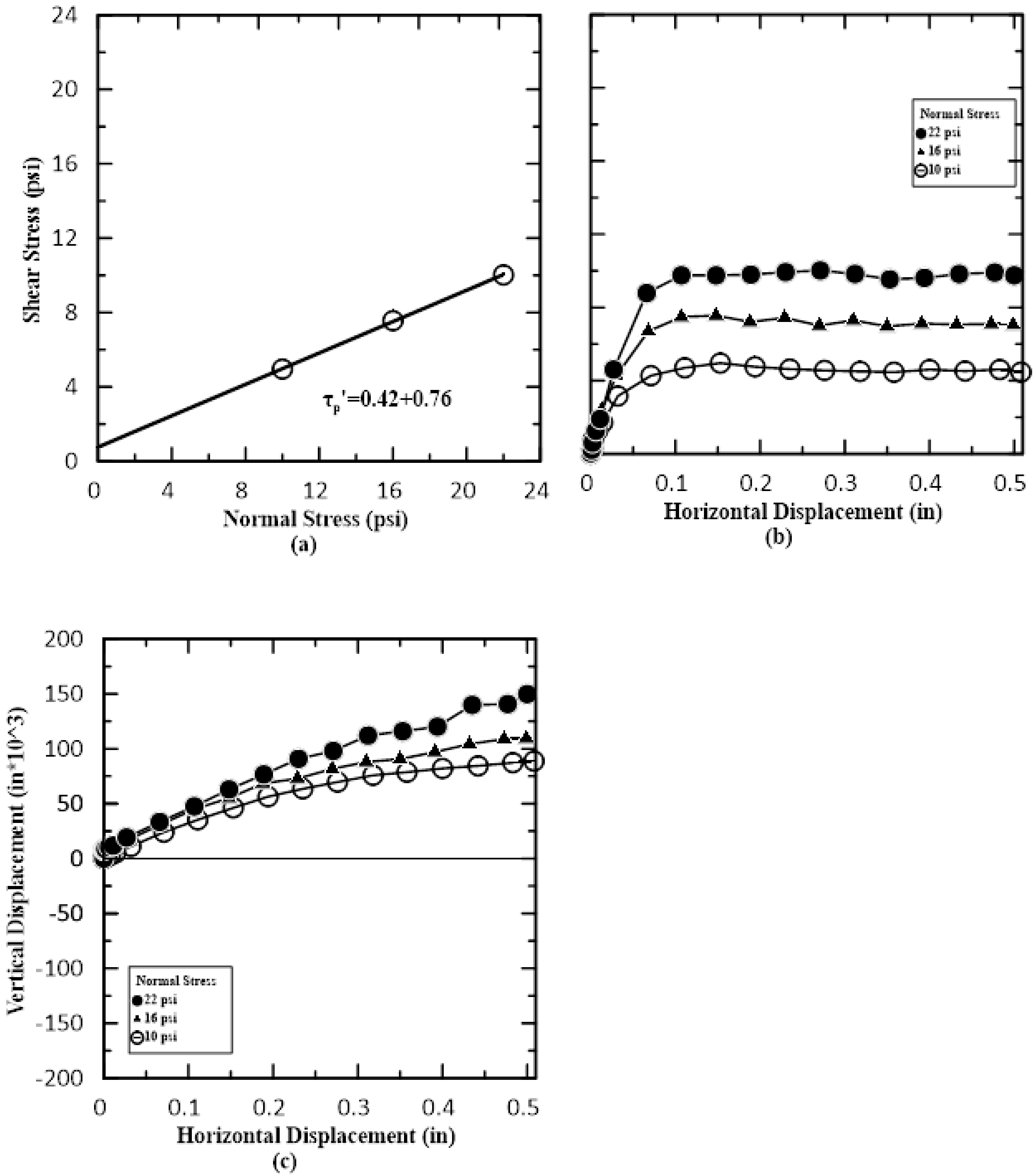

Figure 153. Large direct shear results for Soil 1 and Soil 3 mixtures at fine content = 50%, moisture content = 13%: (a) shear stress vs normal stress; (b) shear stress vs horizontal displacement; (c) vertical displacement vs horizontal displacement

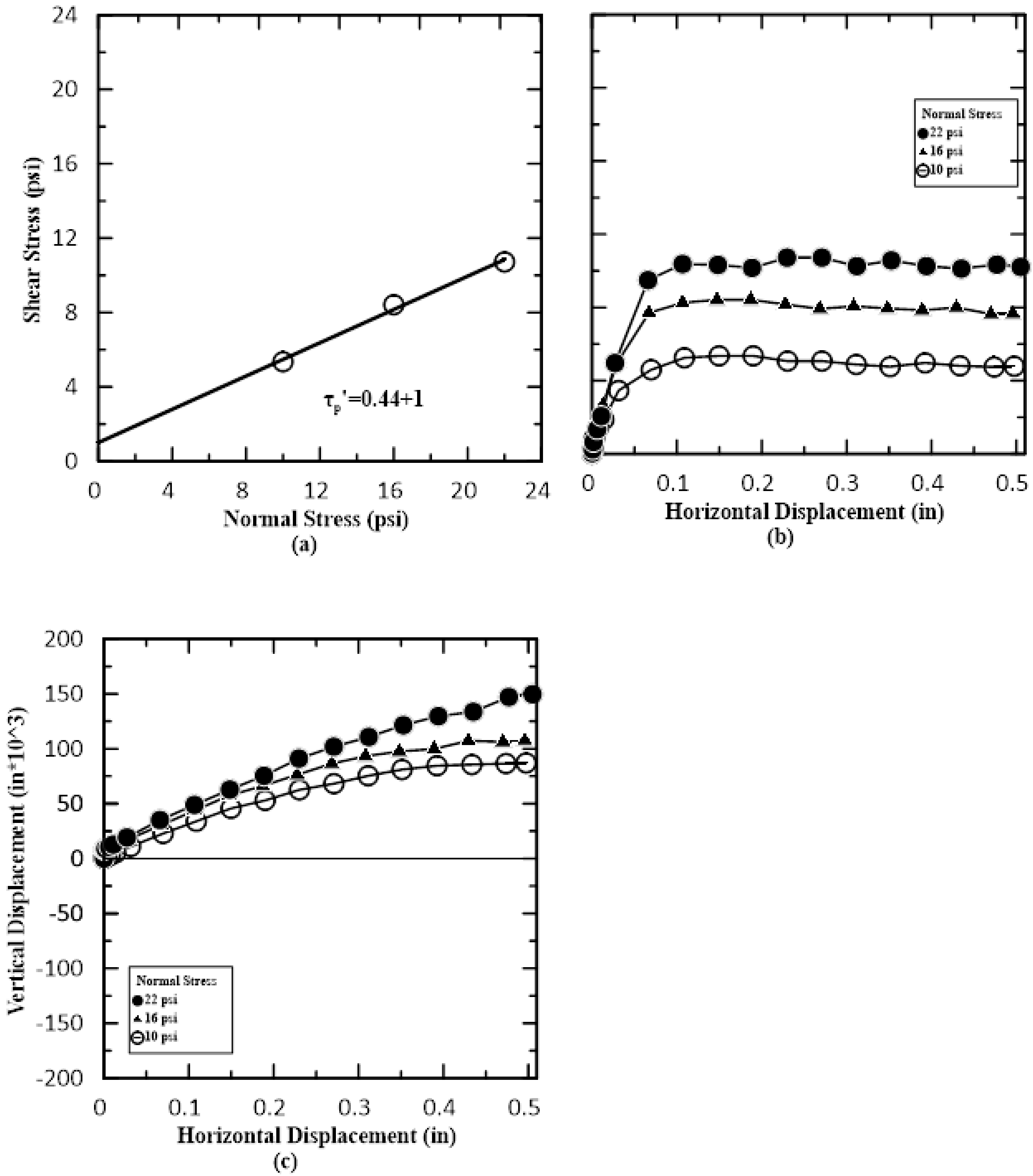

Figure 154. Large direct shear results for Soil 1 and Soil 3 mixtures at fine content = 70%, moisture content = 16.2%: (a) shear stress vs normal stress; (b) shear stress vs horizontal displacement; (c) vertical displacement vs horizontal displacement

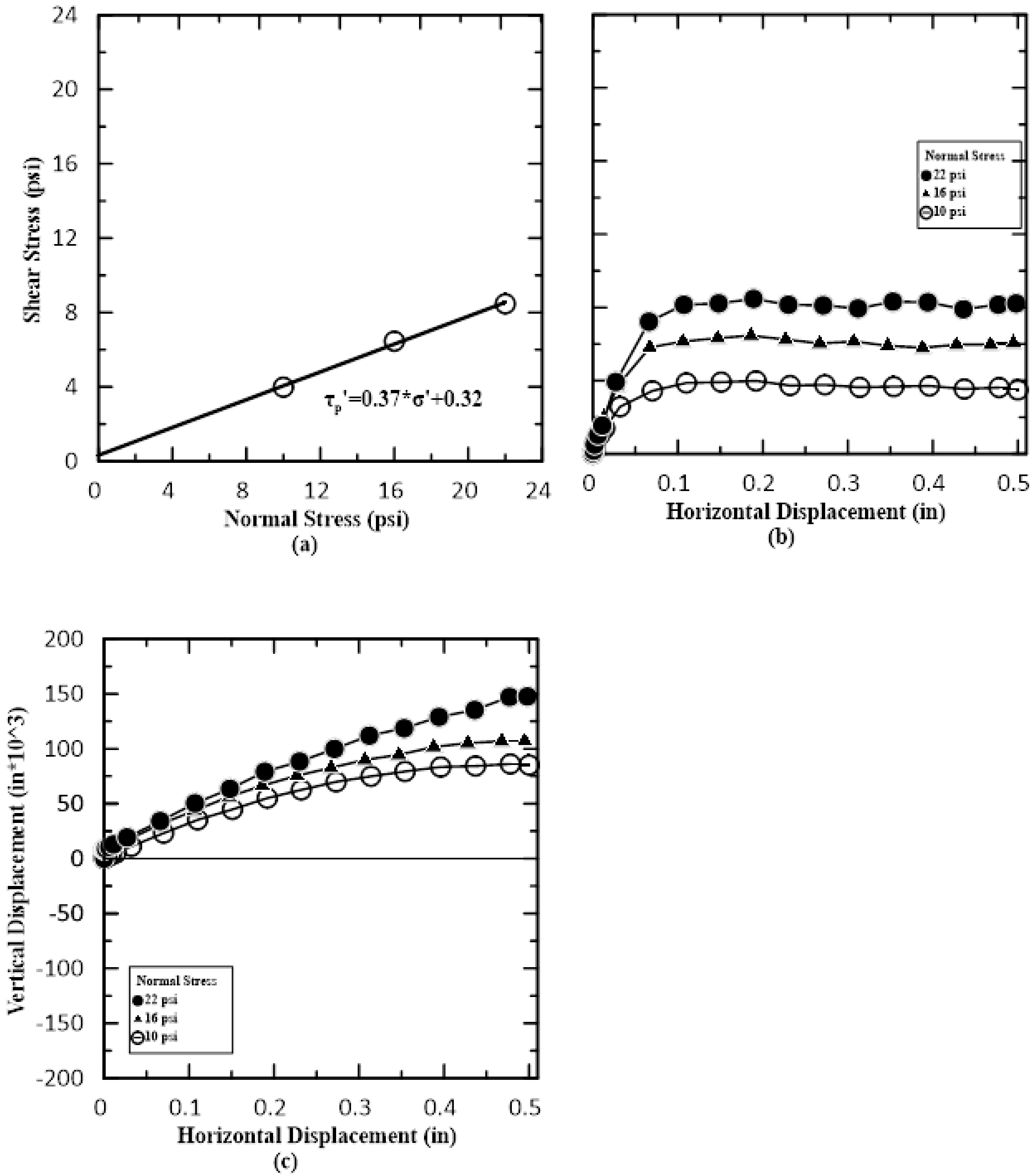

Figure 155. Large direct shear results for Soil 1 and Soil 3 mixtures at fine content = 70%, moisture content = 14.2%: (a) shear stress vs normal stress; (b) shear stress vs horizontal displacement; (c) vertical displacement vs horizontal displacement

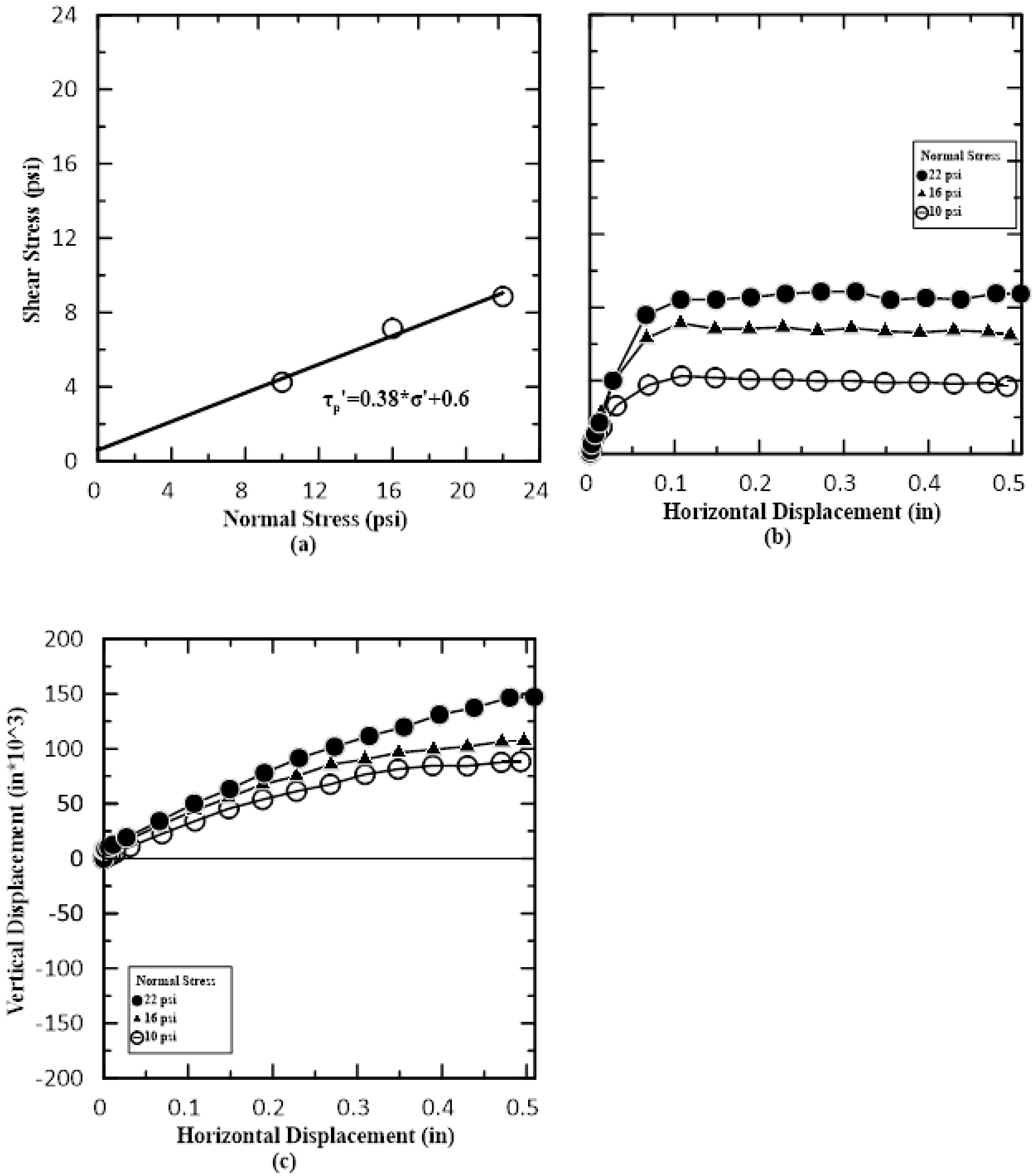

Figure 156. Large direct shear results for Soil 1 and Soil 3 mixtures at fine content = 70%, moisture content = 12%: (a) shear stress vs normal stress; (b) shear stress vs horizontal displacement; (c) vertical displacement vs horizontal displacement

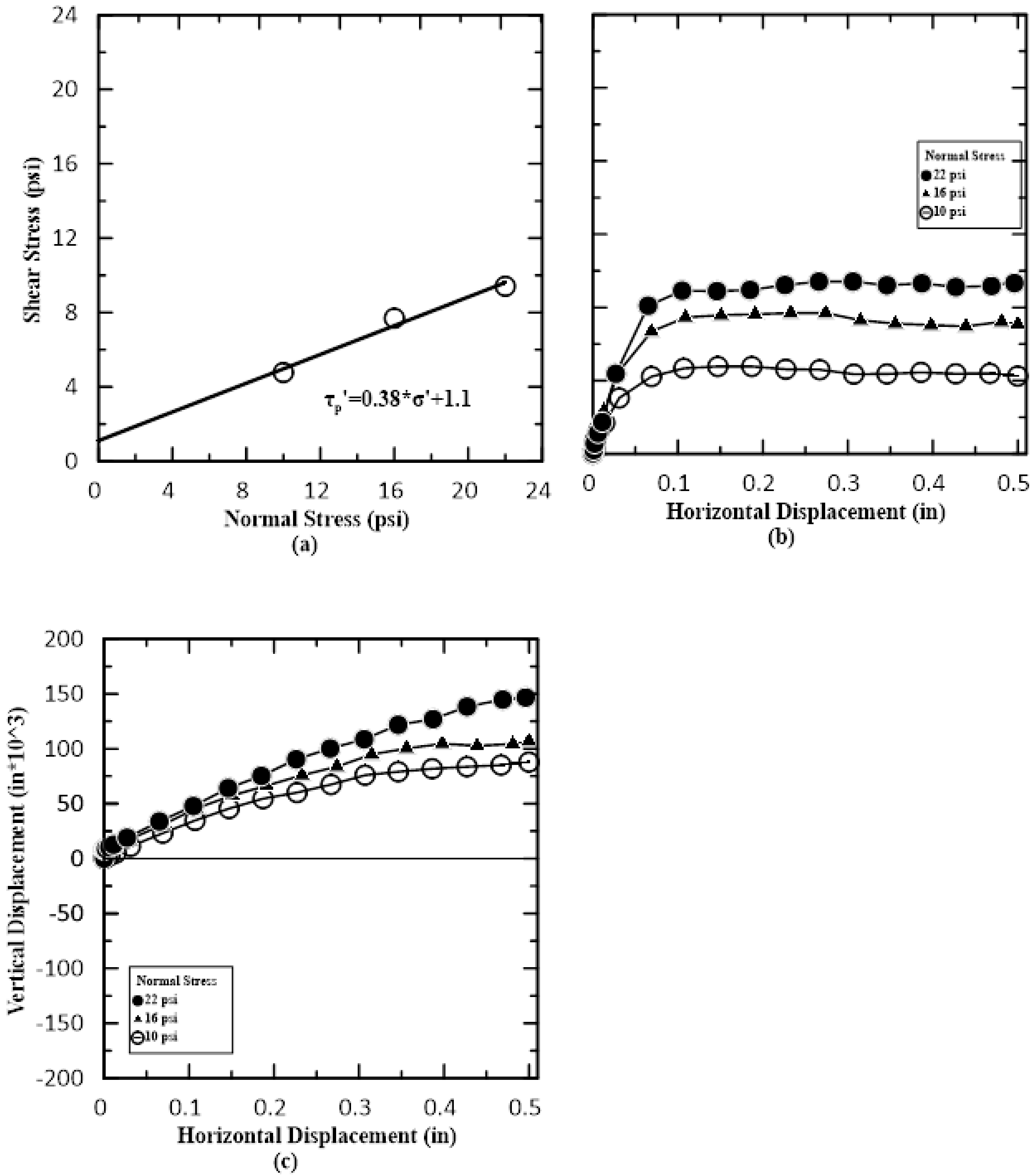

Figure 157. Large direct shear results for Soil 1 and Soil 4 mixtures at fine content = 10%, moisture content = 13.2%: (a) shear stress vs normal stress; (b) shear stress vs horizontal displacement; (c) vertical displacement vs horizontal displacement

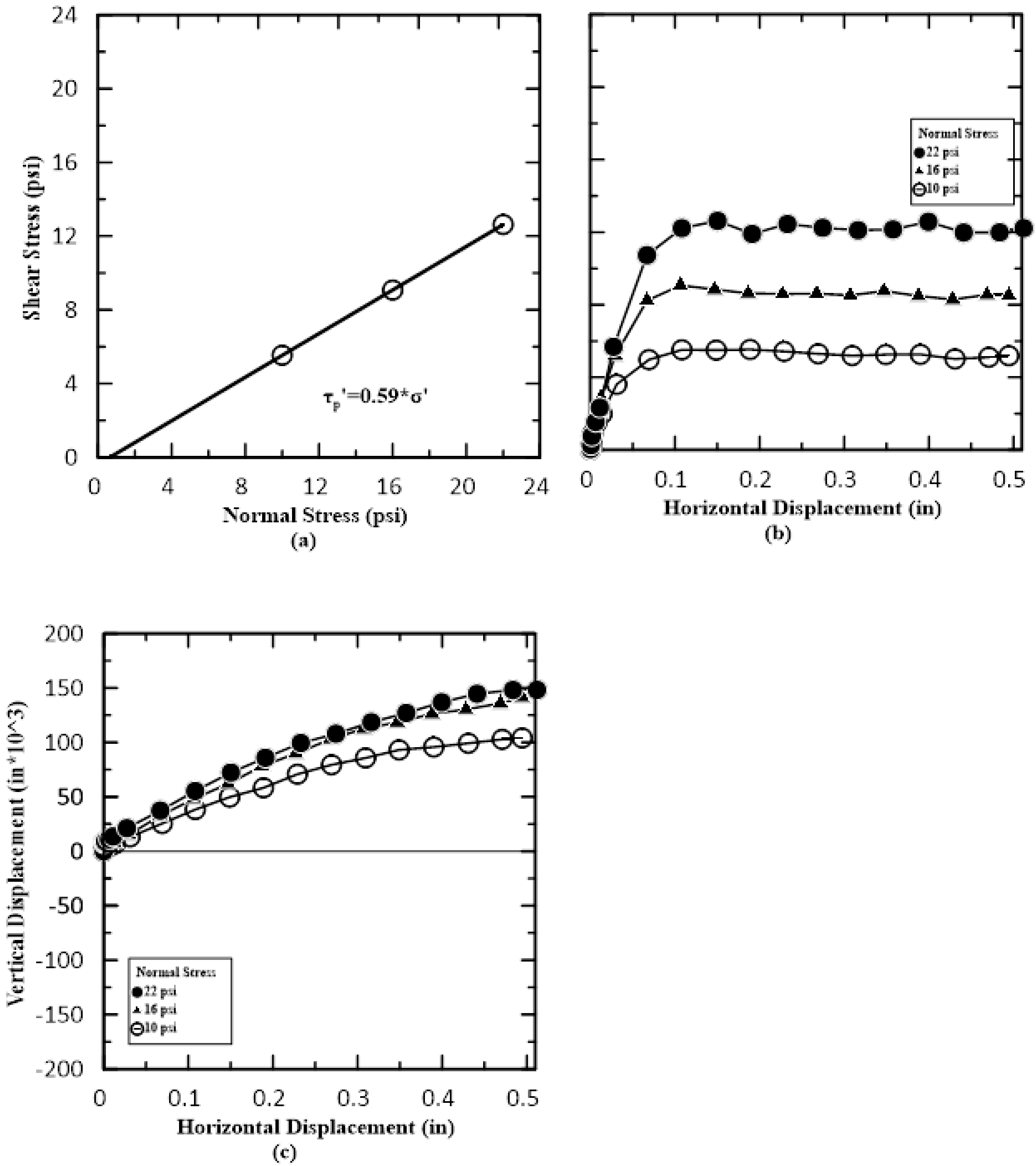

Figure 158. Large direct shear results for Soil 1 and Soil 4 mixtures at fine content = 10%, moisture content = 11.2%: (a) shear stress vs normal stress; (b) shear stress vs horizontal displacement; (c) vertical displacement vs horizontal displacement

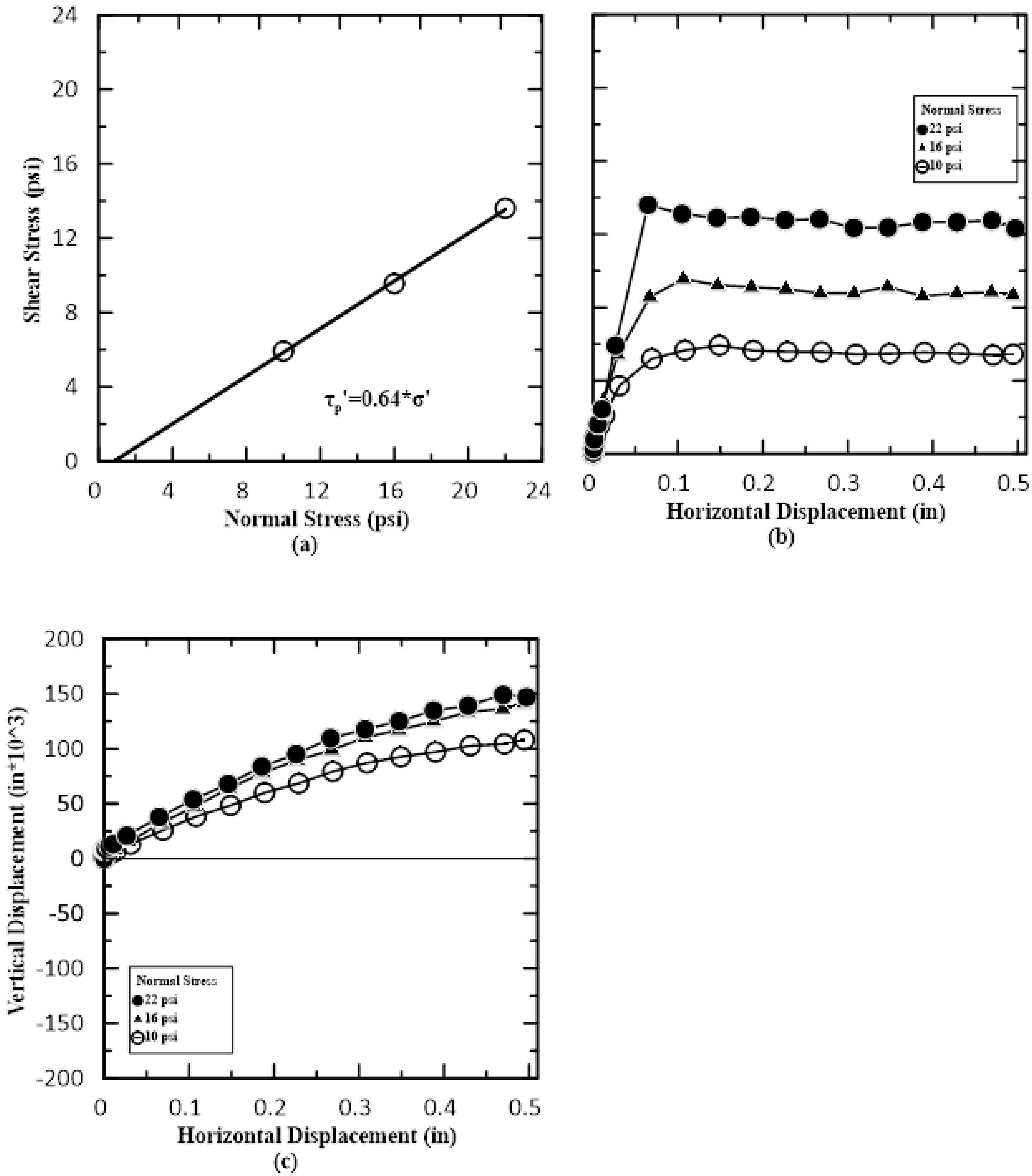

Figure 159. Large direct shear results for Soil 1 and Soil 4 mixtures at fine content = 10%, moisture content = 9.2%: (a) shear stress vs normal stress; (b) shear stress vs horizontal displacement; (c) vertical displacement vs horizontal displacement

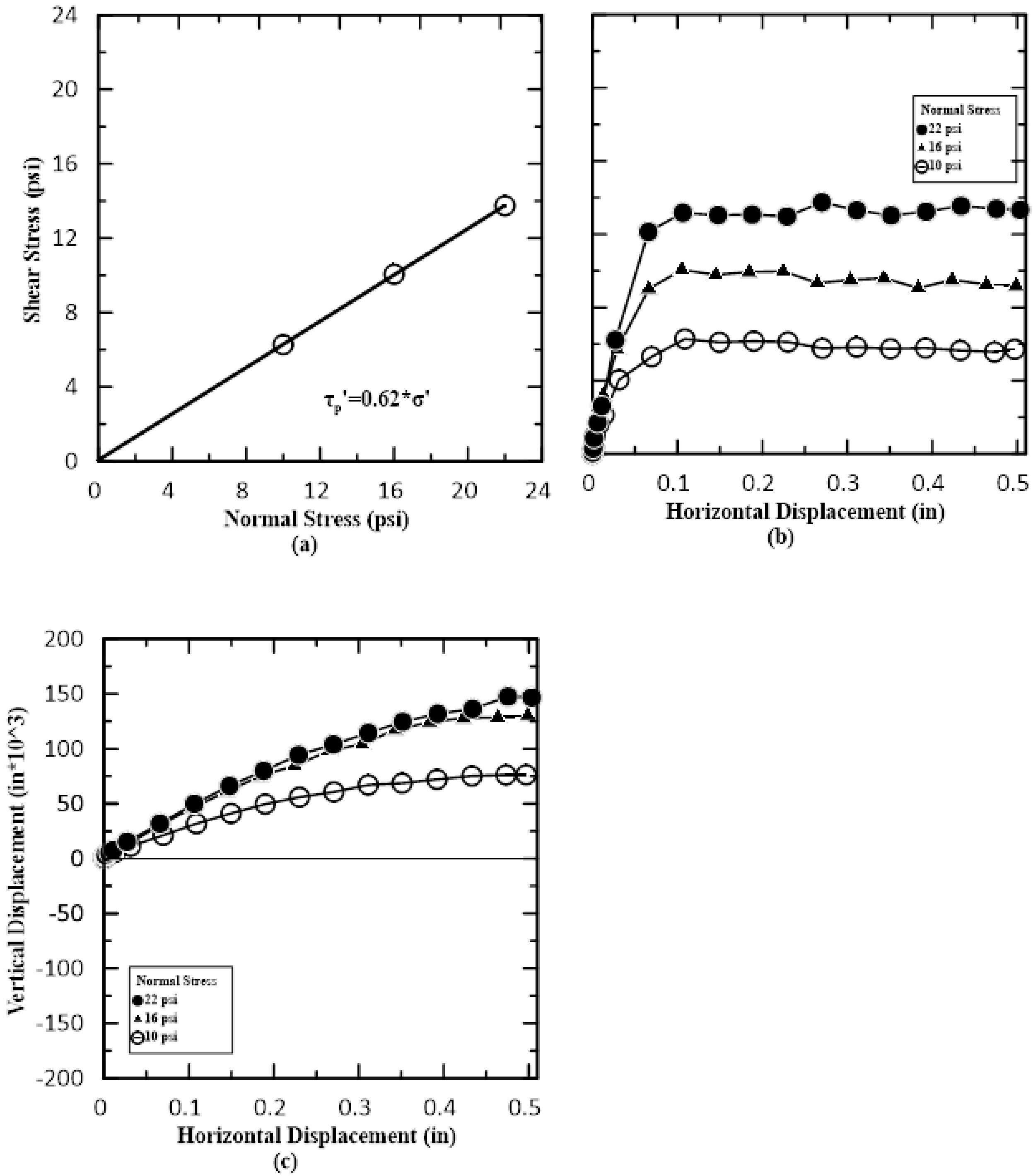

Figure 160. Large direct shear results for Soil 1 and Soil 4 mixtures at fine content = 50%, moisture content = 16.3%: (a) shear stress vs normal stress; (b) shear stress vs horizontal displacement; (c) vertical displacement vs horizontal displacement

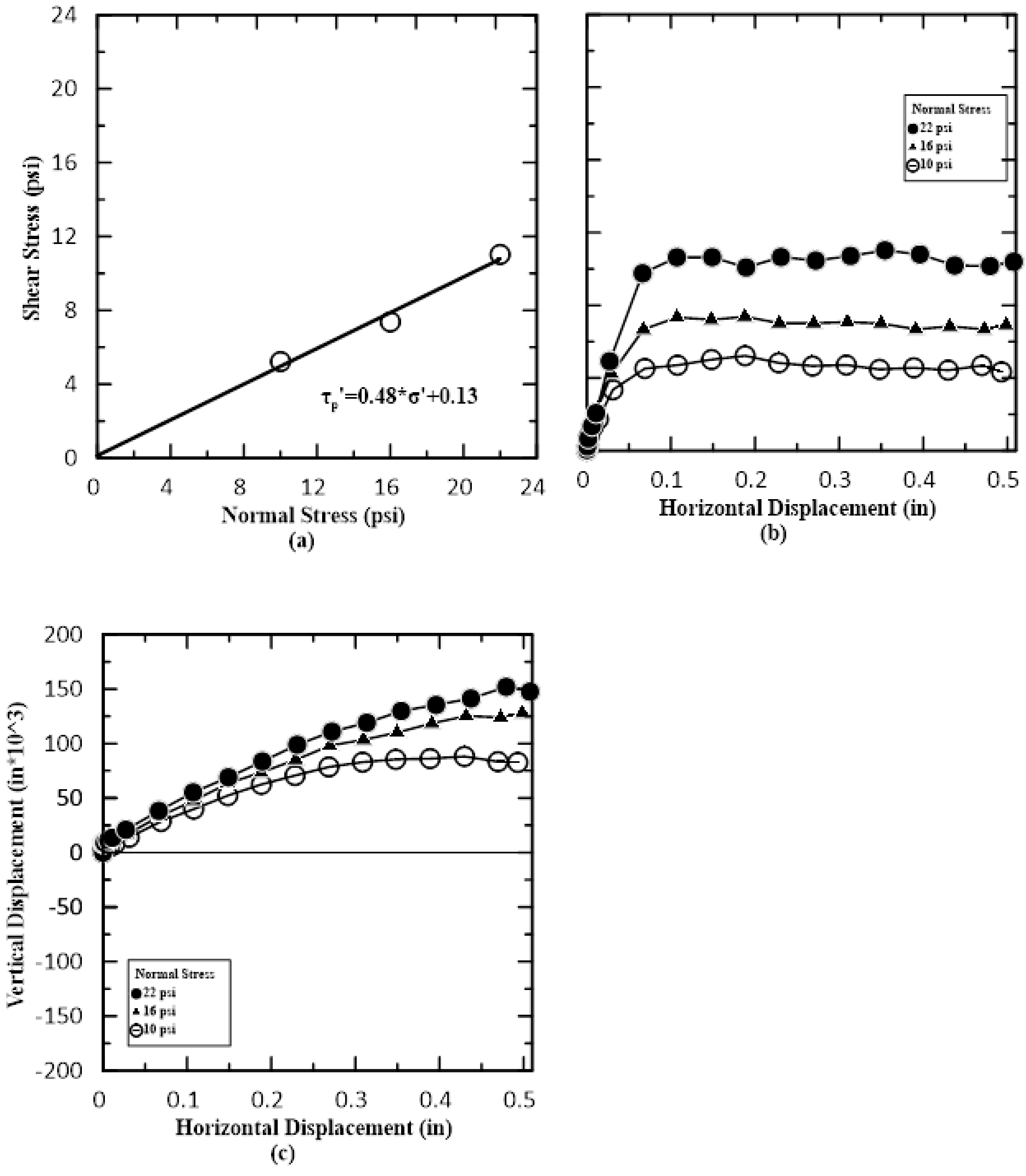

Figure 161. Large direct shear results for Soil 1 and Soil 4 mixtures at fine content = 50%, moisture content = 14.2%: (a) shear stress vs normal stress; (b) shear stress vs horizontal displacement; (c) vertical displacement vs horizontal displacement

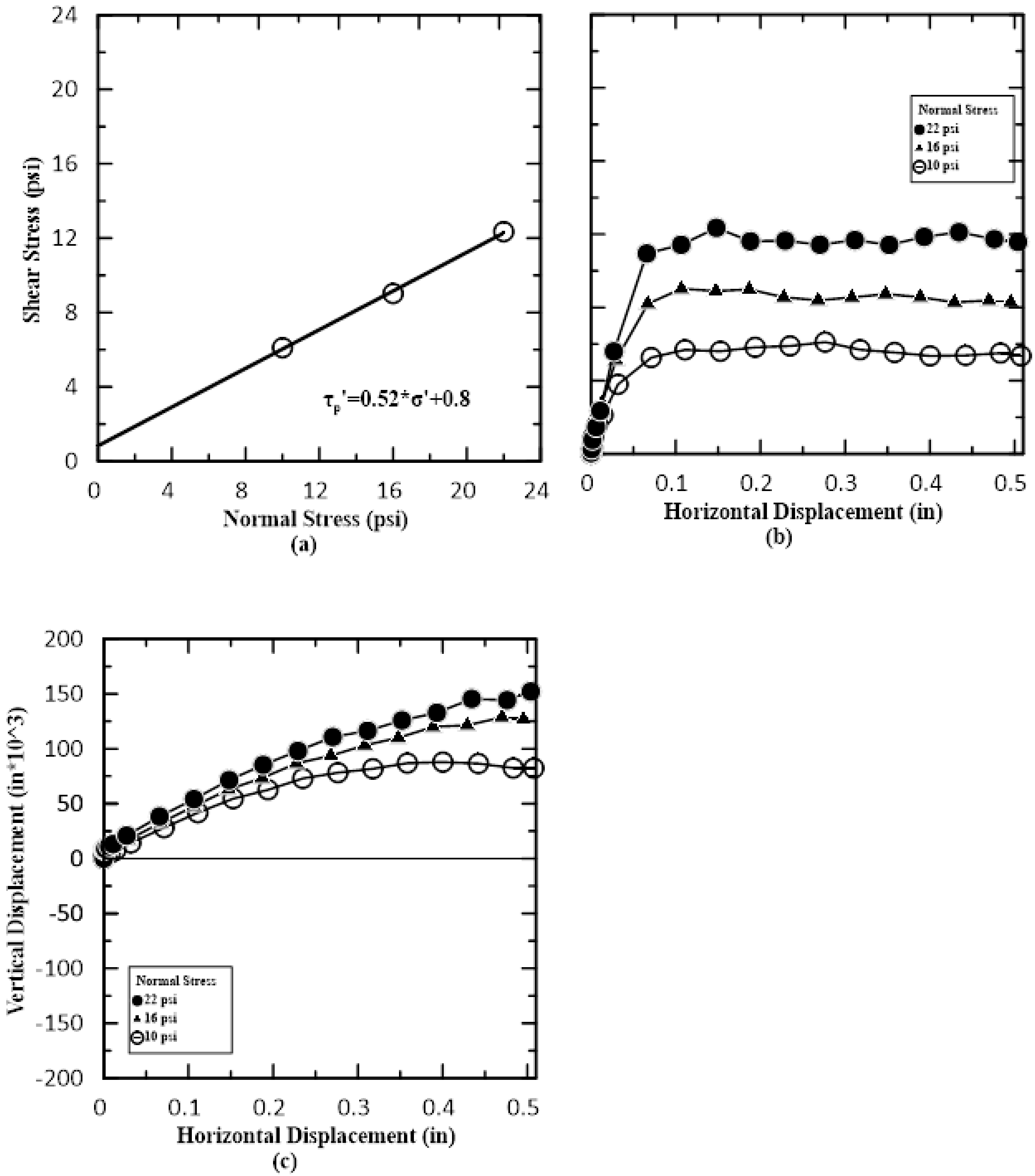

Figure 162. Large direct shear results for Soil 1 and Soil 4 mixtures at fine content = 50%, moisture content = 12.1%: (a) shear stress vs normal stress; (b) shear stress vs horizontal displacement; (c) vertical displacement vs horizontal displacement

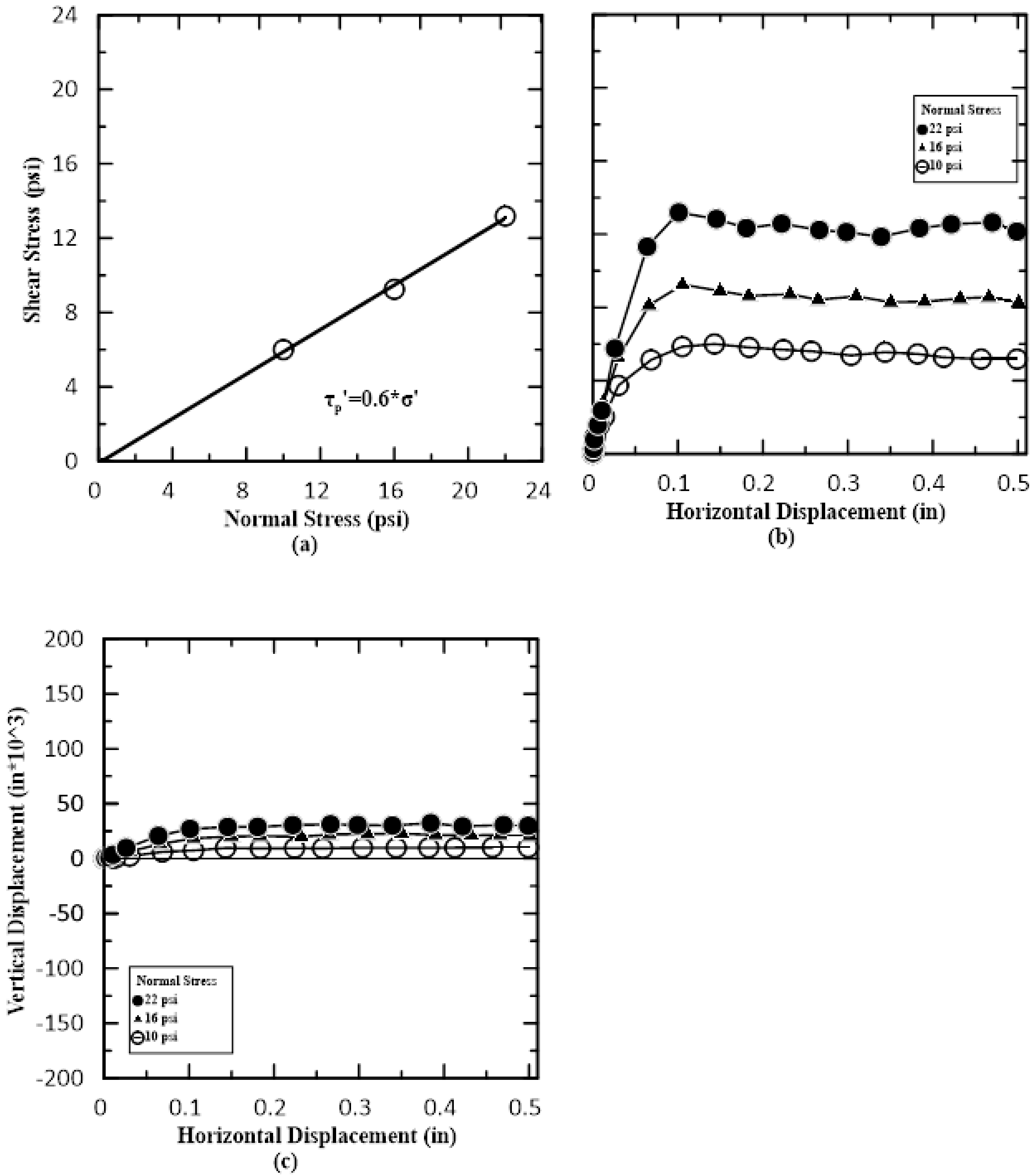

Figure 163. Large direct shear results for Soil 1 and Soil 4 mixtures at fine content = 70%, moisture content = 18.4%: (a) shear stress vs normal stress; (b) shear stress vs horizontal displacement; (c) vertical displacement vs horizontal displacement

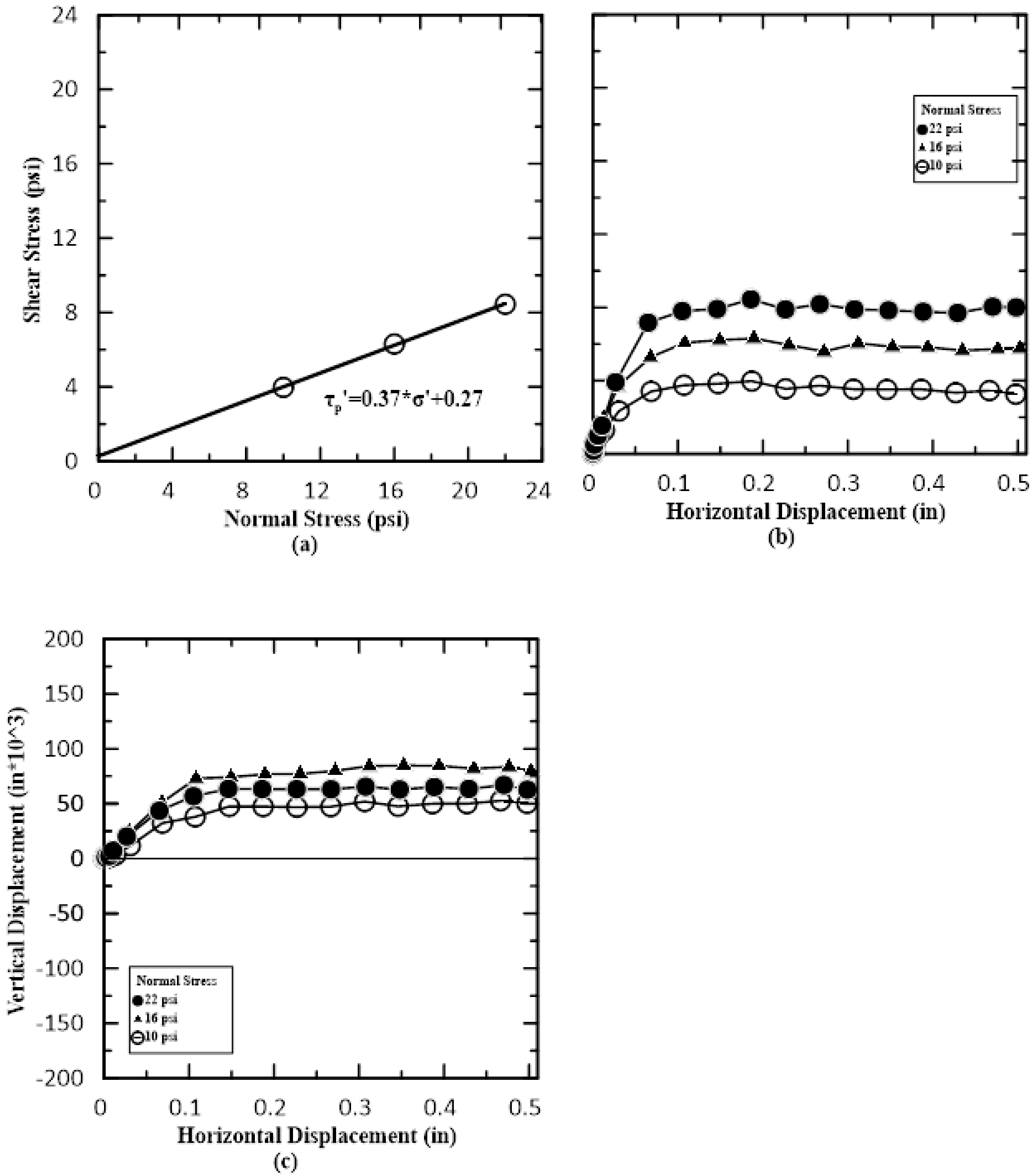

Figure 164. Large direct shear results for Soil 1 and Soil 4 mixtures at fine content = 70%, moisture content = 16.2%: (a) shear stress vs normal stress; (b) shear stress vs horizontal displacement; (c) vertical displacement vs horizontal displacement

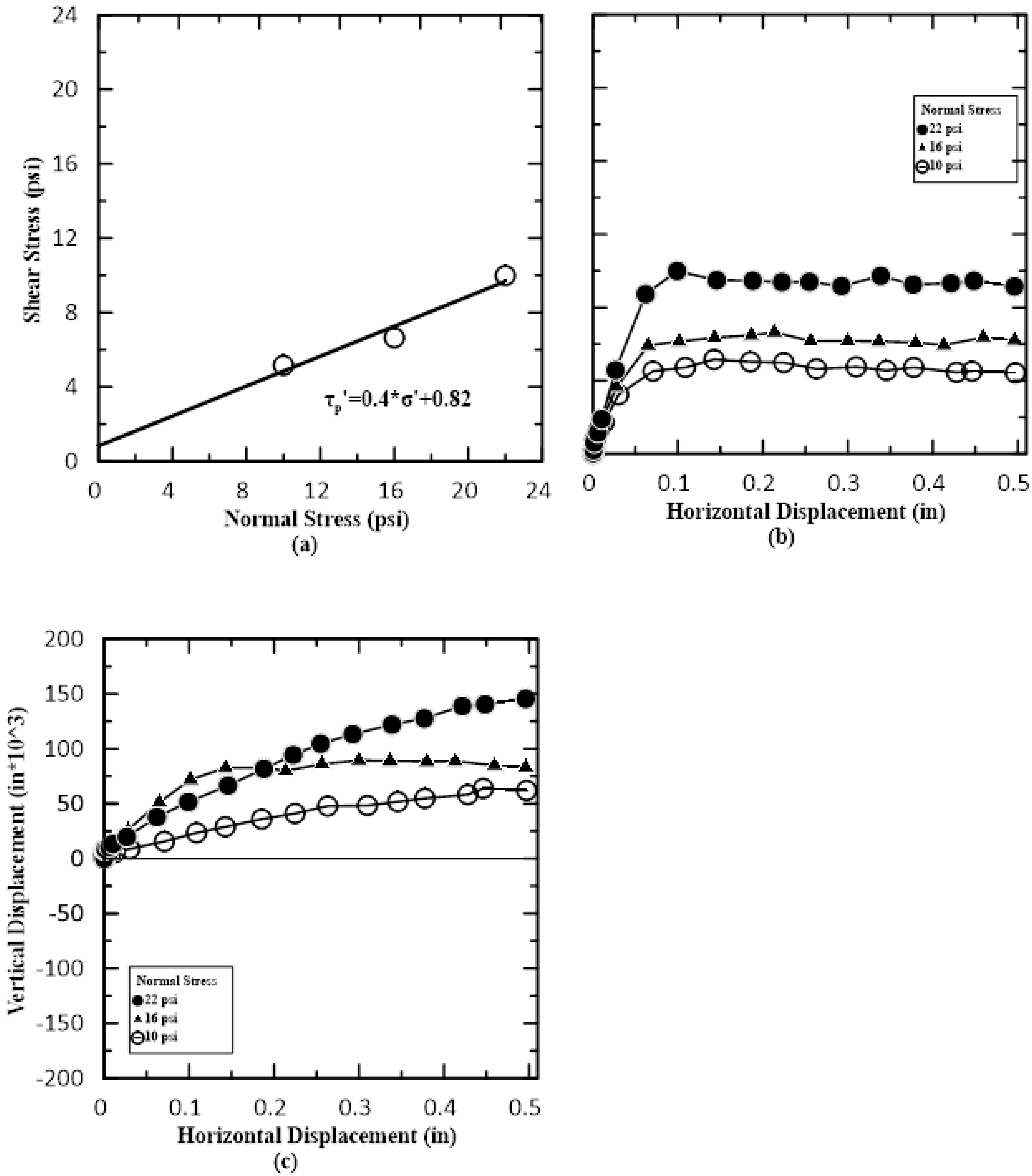

Figure 165. Large direct shear results for Soil 1 and Soil 4 mixtures at fine content = 70%, moisture content = 14.2%: (a) shear stress vs normal stress; (b) shear stress vs horizontal displacement; (c) vertical displacement vs horizontal displacement

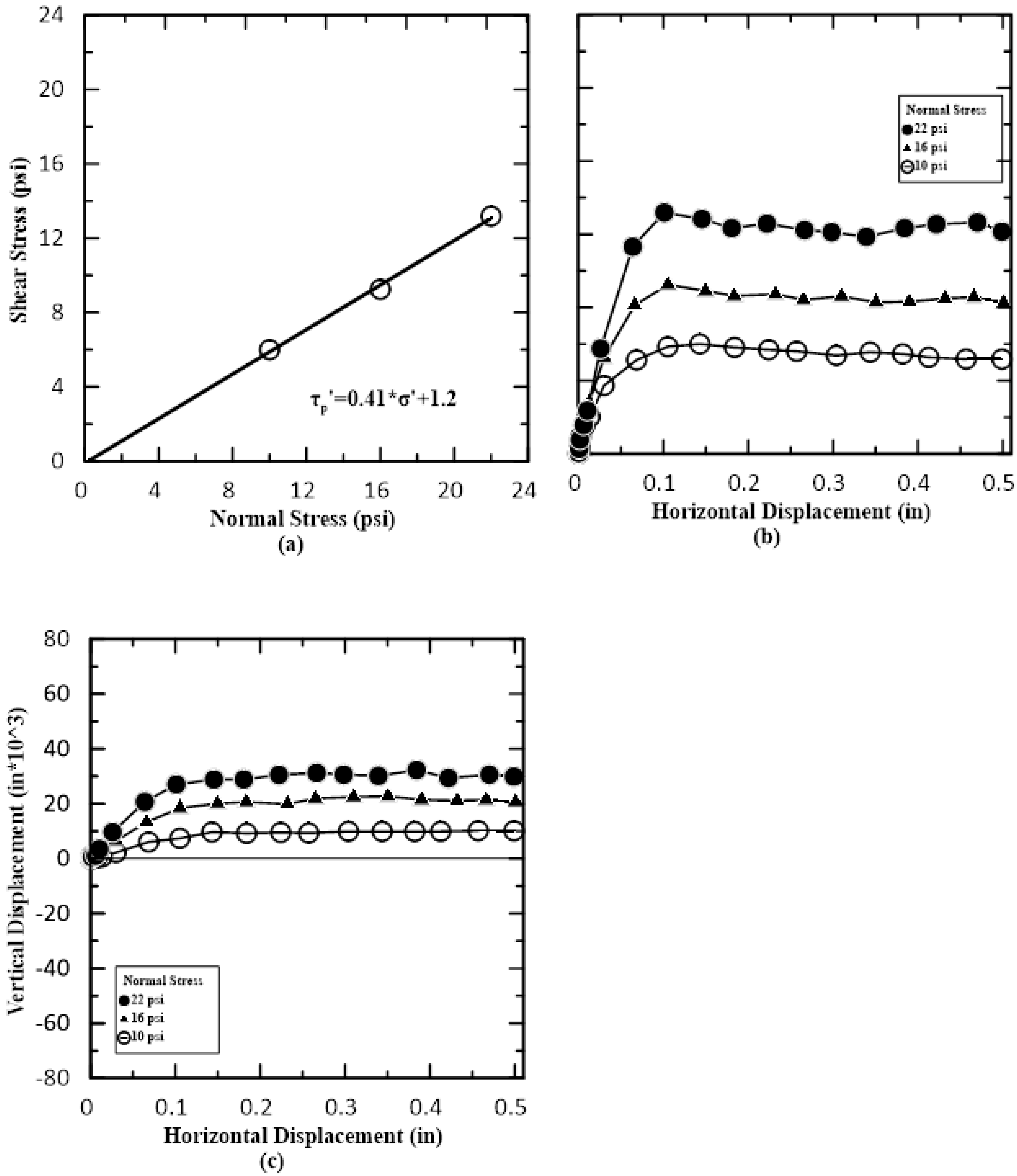

Figure 166. Large direct shear results for Soil 1 and Soil 5 mixtures at fine content = 10%, moisture content = 15.2%: (a) shear stress vs normal stress; (b) shear stress vs horizontal displacement; (c) vertical displacement vs horizontal displacement

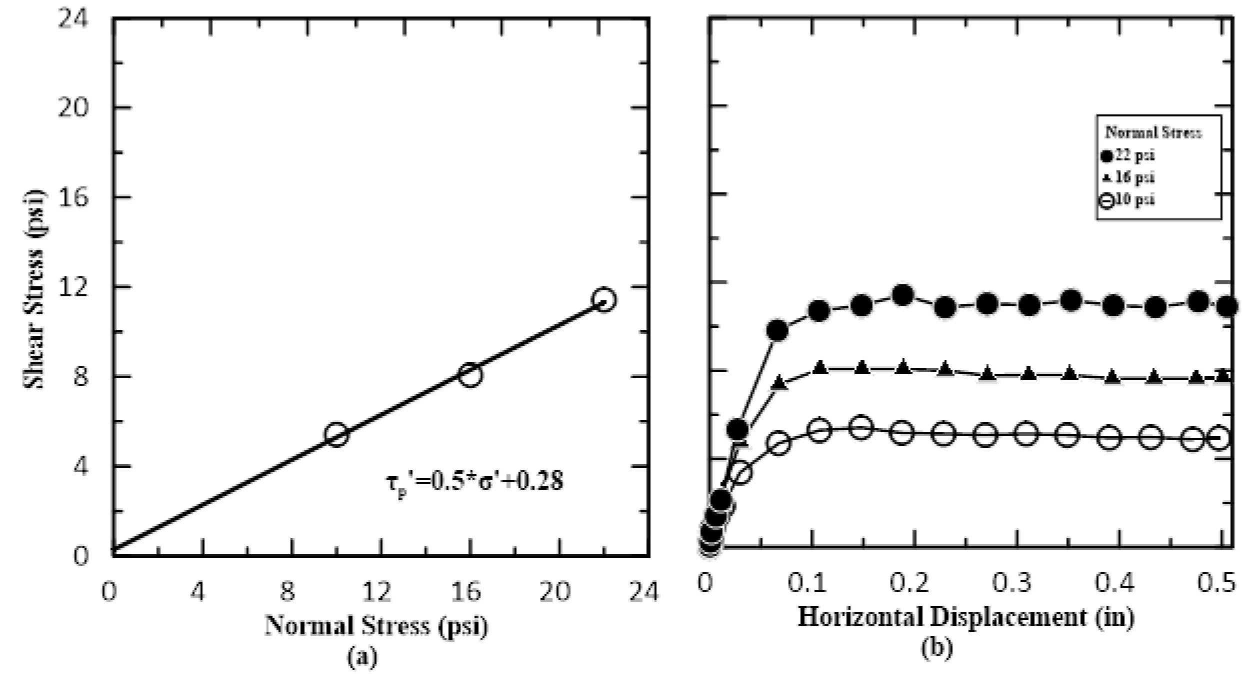

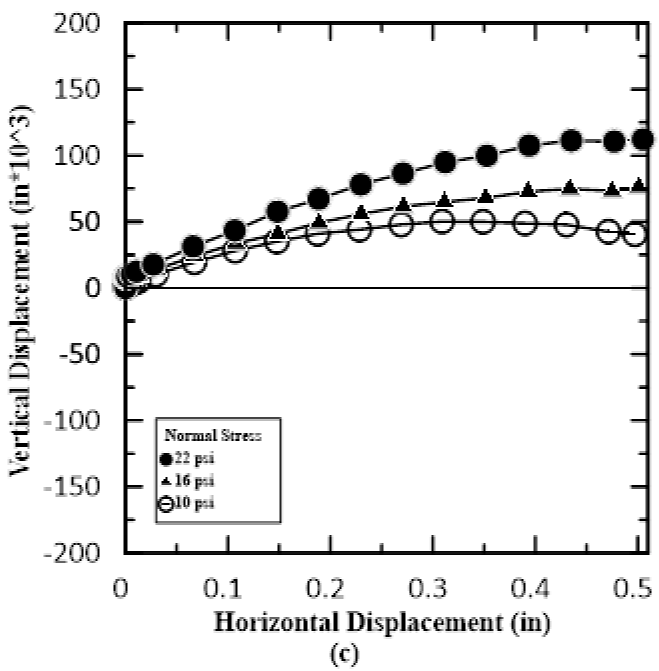

Figure 167. Large direct shear results for Soil 1 and Soil 5 mixtures at fine content = 10%, moisture content = 12%: (a) shear stress vs normal stress; (b) shear stress vs horizontal displacement; (c) vertical displacement vs horizontal displacement

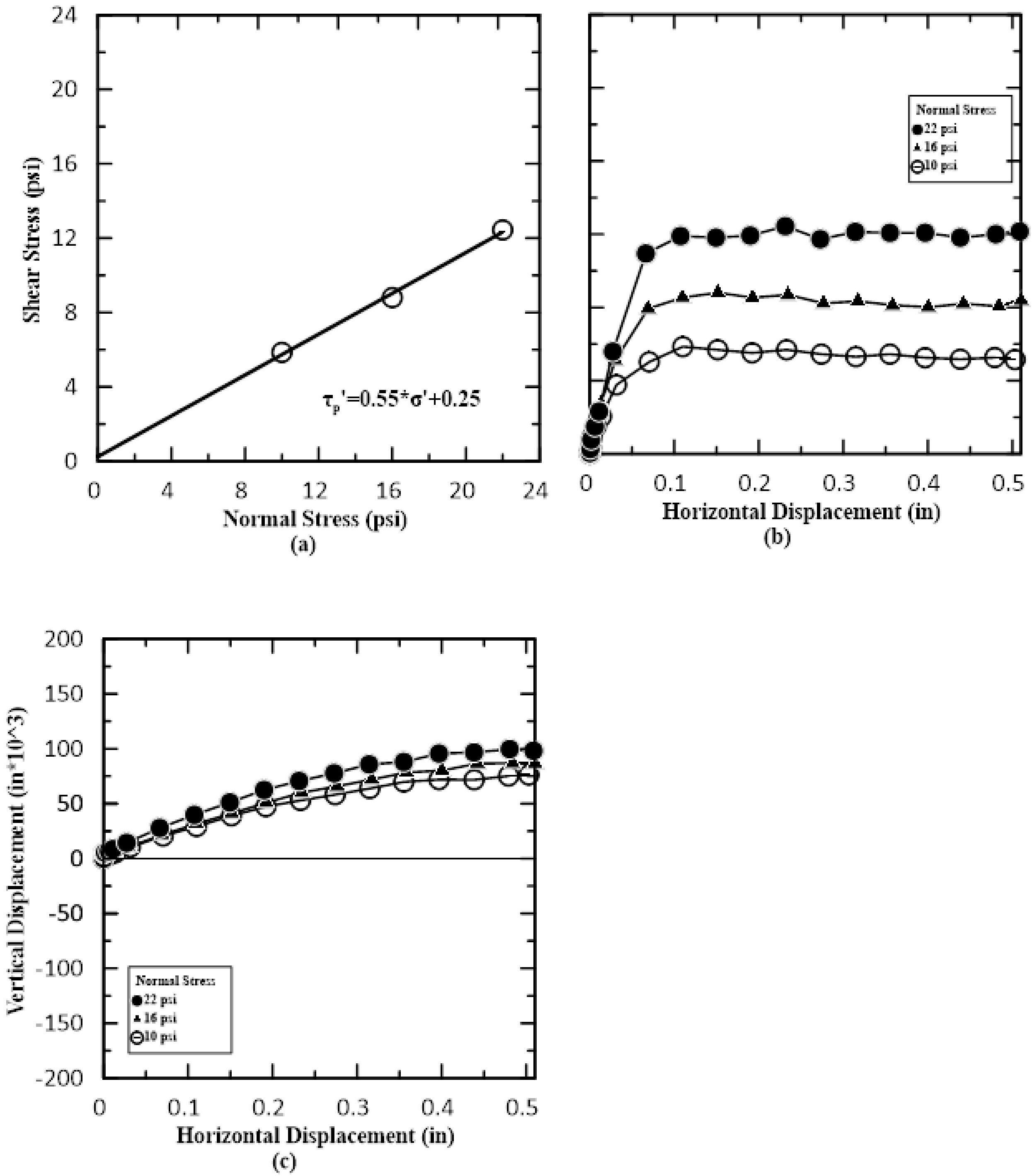

Figure 168. Large direct shear results for Soil 1 and Soil 5 mixtures at fine content = 10%, moisture content = 10%: (a) shear stress vs normal stress; (b) shear stress vs horizontal displacement; (c) vertical displacement vs horizontal displacement

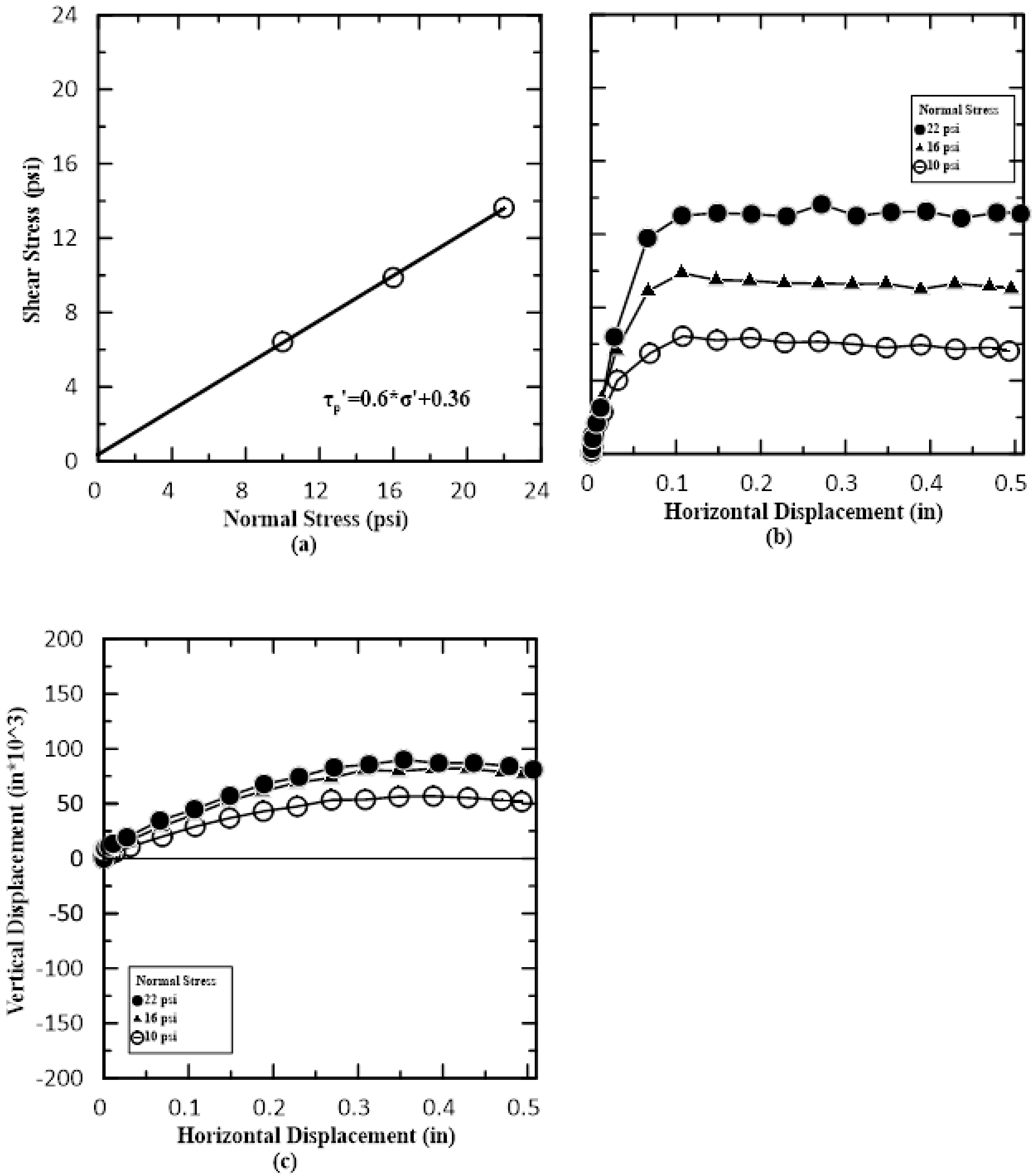

Figure 169. Large direct shear results for Soil 1 and Soil 5 mixtures at fine content = 50%, moisture content = 18.3%: (a) shear stress vs normal stress; (b) shear stress vs horizontal displacement; (c) vertical displacement vs horizontal displacement

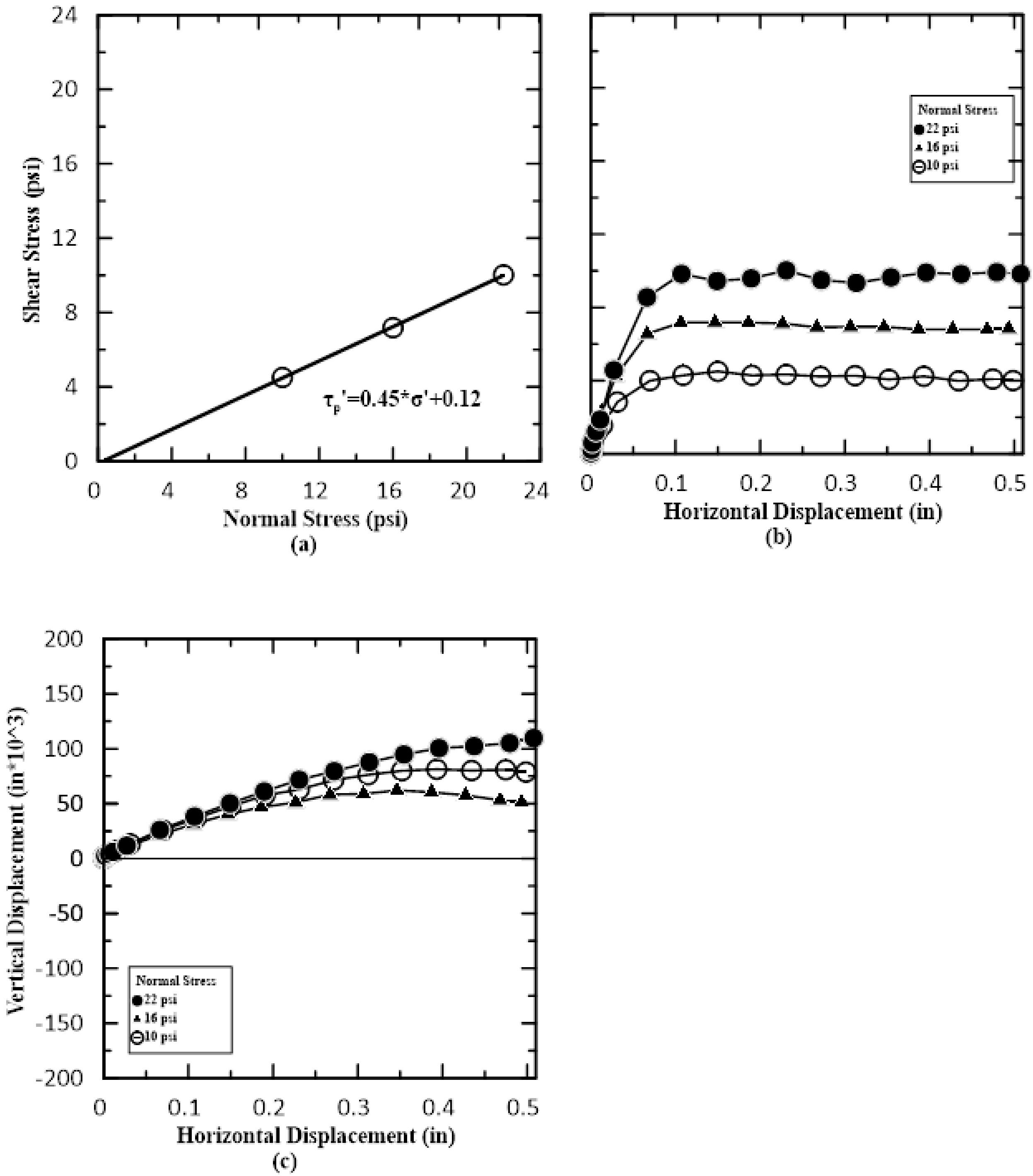

Figure 170. Large direct shear results for Soil 1 and Soil 5 mixtures at fine content = 50%, moisture content = 14.2%: (a) shear stress vs normal stress; (b) shear stress vs horizontal displacement; (c) vertical displacement vs horizontal displacement

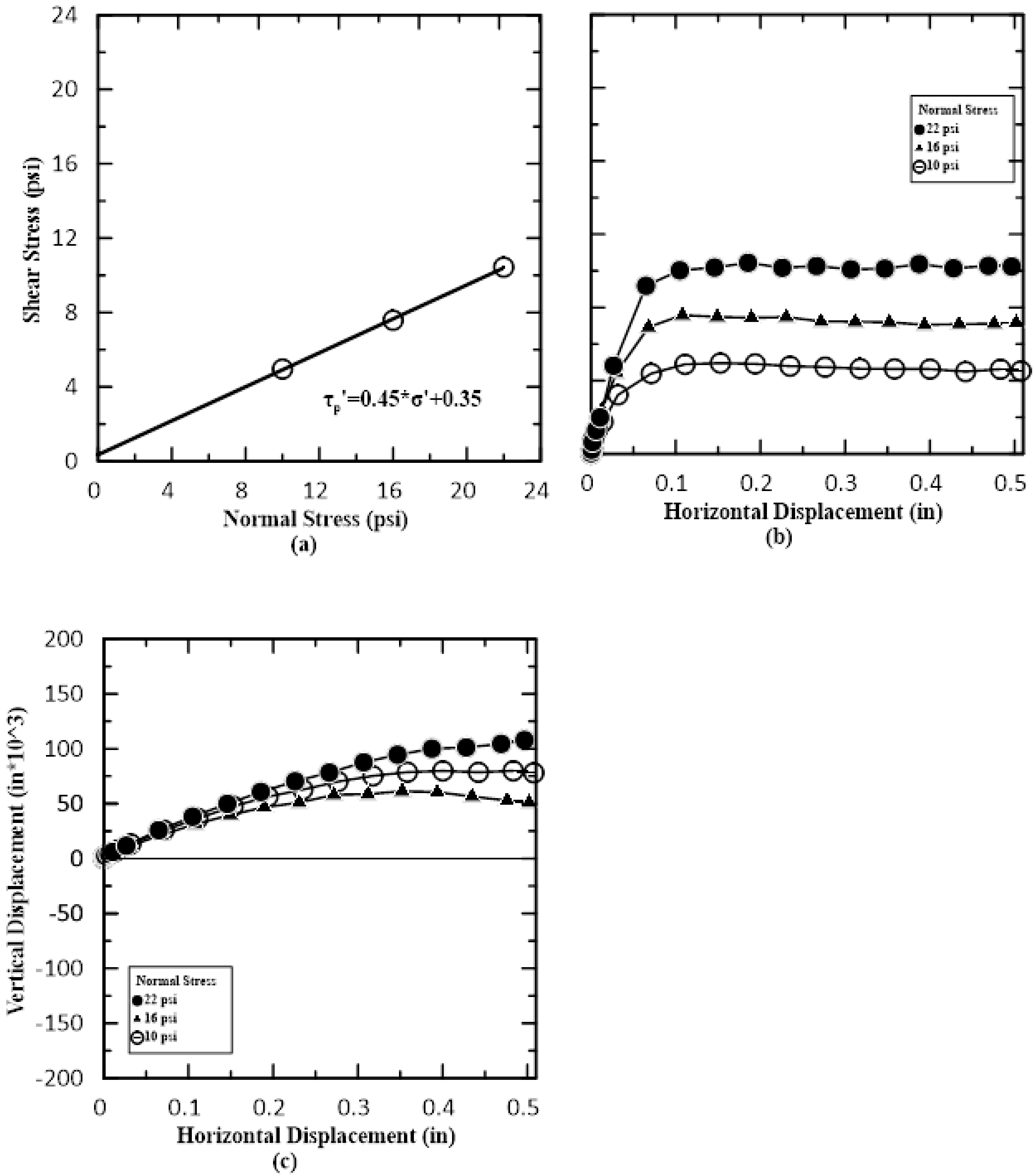

Figure 171. Large direct shear results for Soil 1 and Soil 5 mixtures at fine content = 50%, moisture content = 11%: (a) shear stress vs normal stress; (b) shear stress vs horizontal displacement; (c) vertical displacement vs horizontal displacement

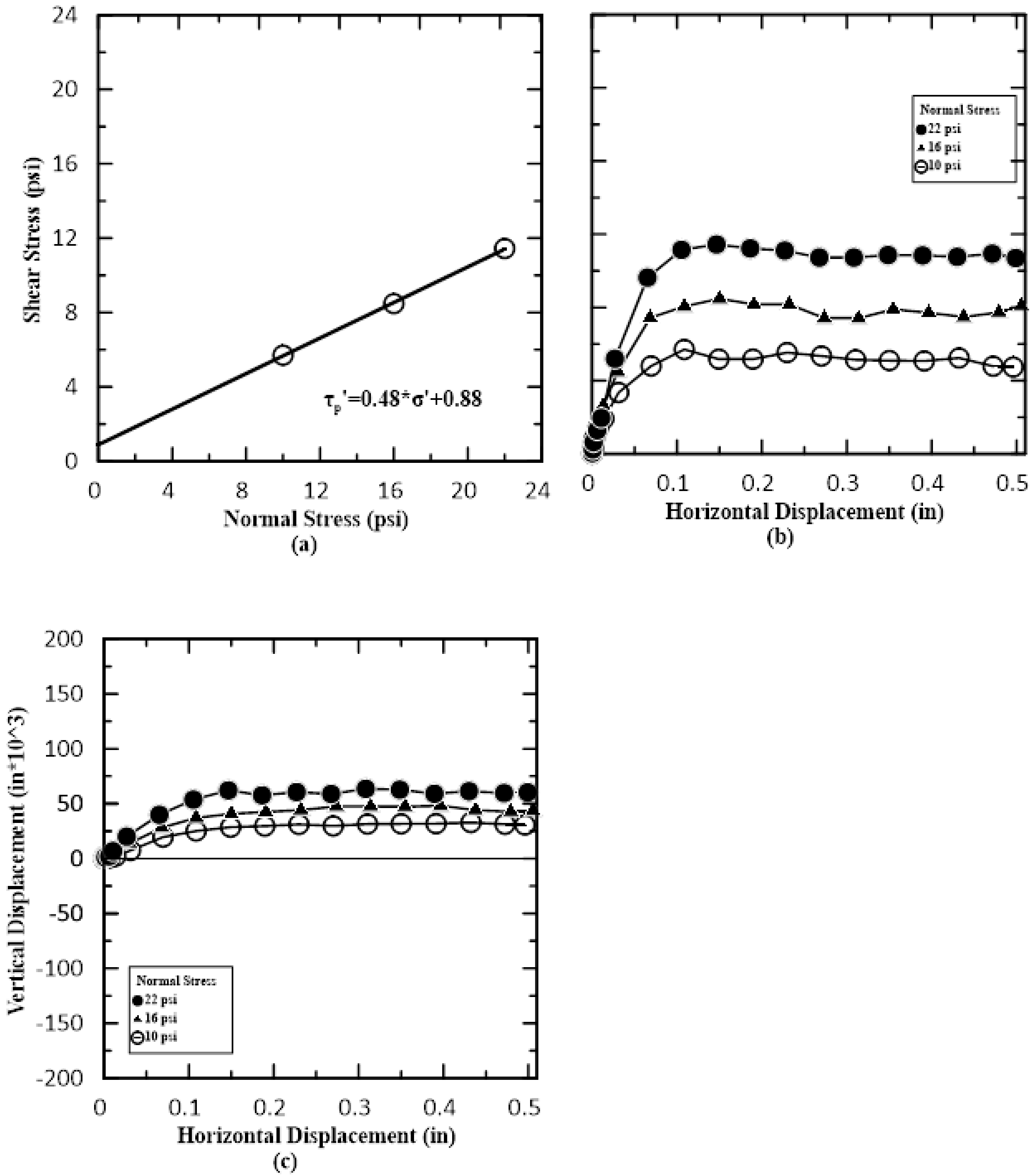

Figure 172. Large direct shear results for Soil 1 and Soil 5 mixtures at fine content = 70%, moisture content = 18.2%: (a) shear stress vs normal stress; (b) shear stress vs horizontal displacement; (c) vertical displacement vs horizontal displacement

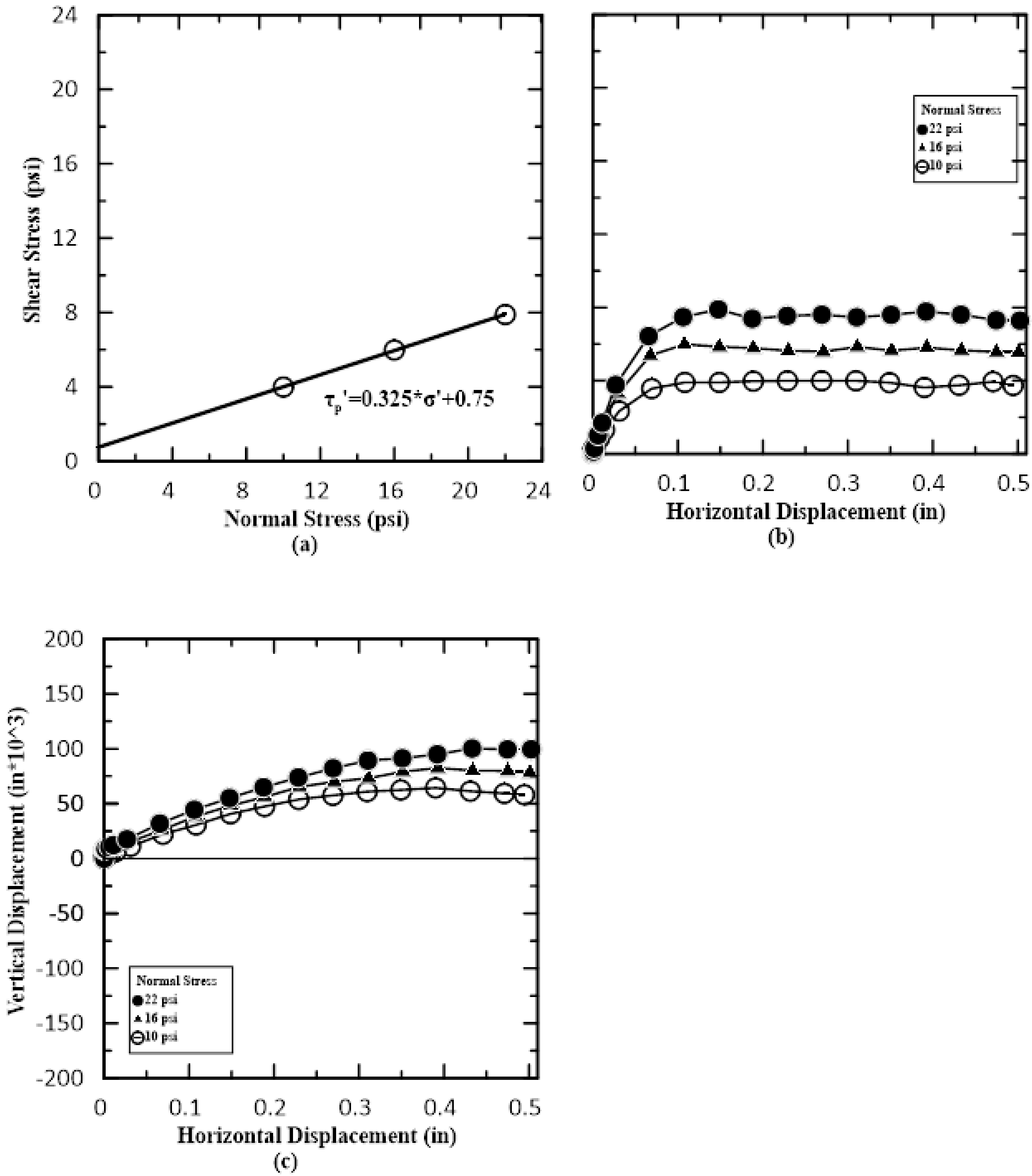

Figure 173. Large direct shear results for Soil 1 and Soil 5 mixtures at fine content = 70%, moisture content = 16.2%: (a) shear stress vs normal stress; (b) shear stress vs horizontal displacement; (c) vertical displacement vs horizontal displacement

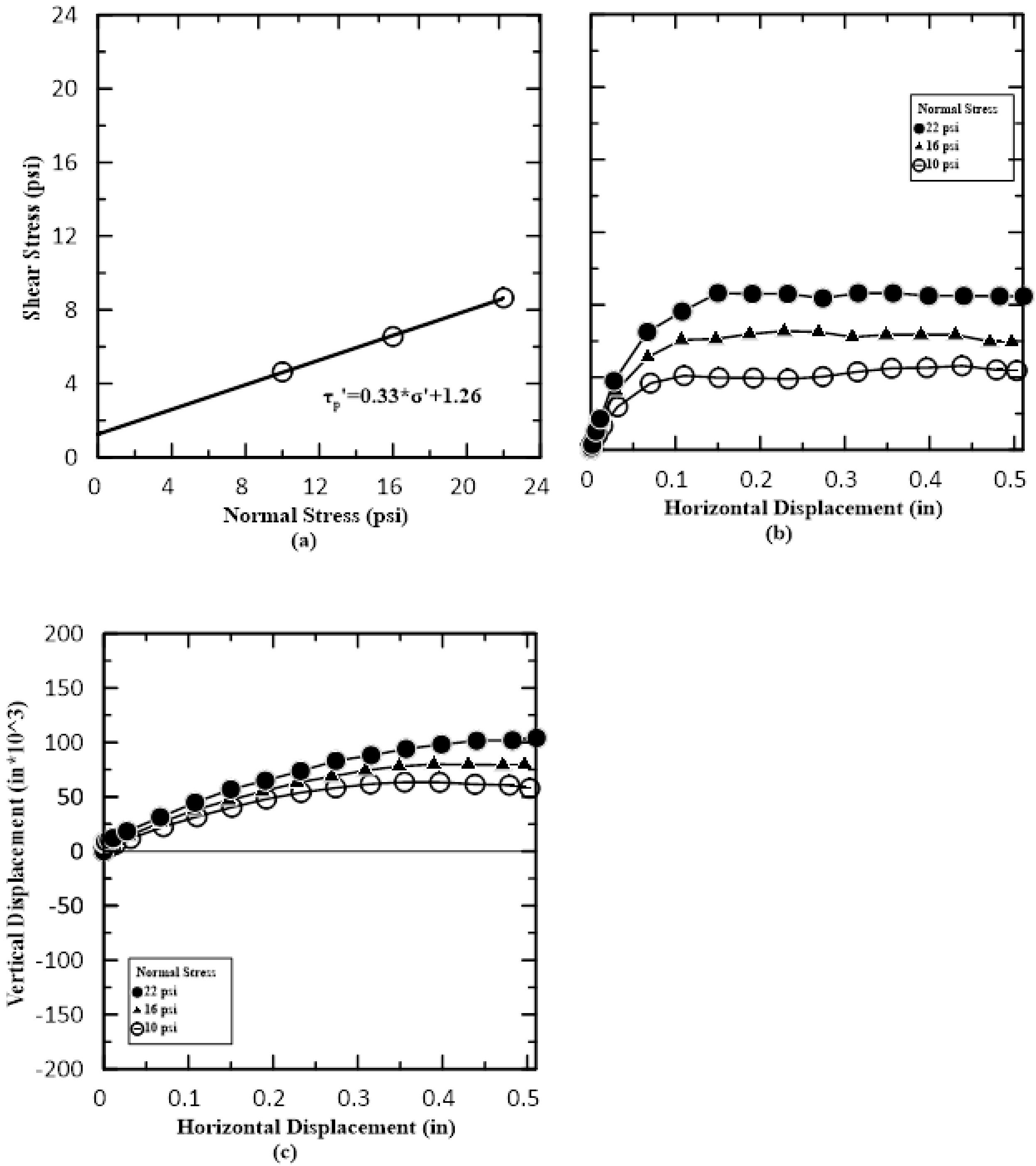

Appendix D
ANN Model Results

This section presents a comprehensive compilation of tables detailing the outcomes of the Artificial Neural Network (ANN) model across various phases of evaluation, encompassing training, validation, and testing. These tables encapsulate the results derived from the dataset sourced from soil direct shear test results, with a specific focus on predicting soil friction angles. The provided tables furnish a comprehensive overview of the model's performance and its capacity to generalize across different datasets. In addition to the prediction results, each table incorporates corresponding R-square values, thereby offering insights into the predictive accuracy and goodness-of-fit of the ANN model for the soil friction angle estimation. These tables collectively offer a valuable reference for the model's efficacy in capturing the complex relationships within the soil shear test data and its capability to provide accurate predictions.

Figure 174. Measured friction angle from direct shear vs predicted friction angle from ANN for Type 1 (2-5-1): a) Training; b) Validation; c) Testing; d) All data

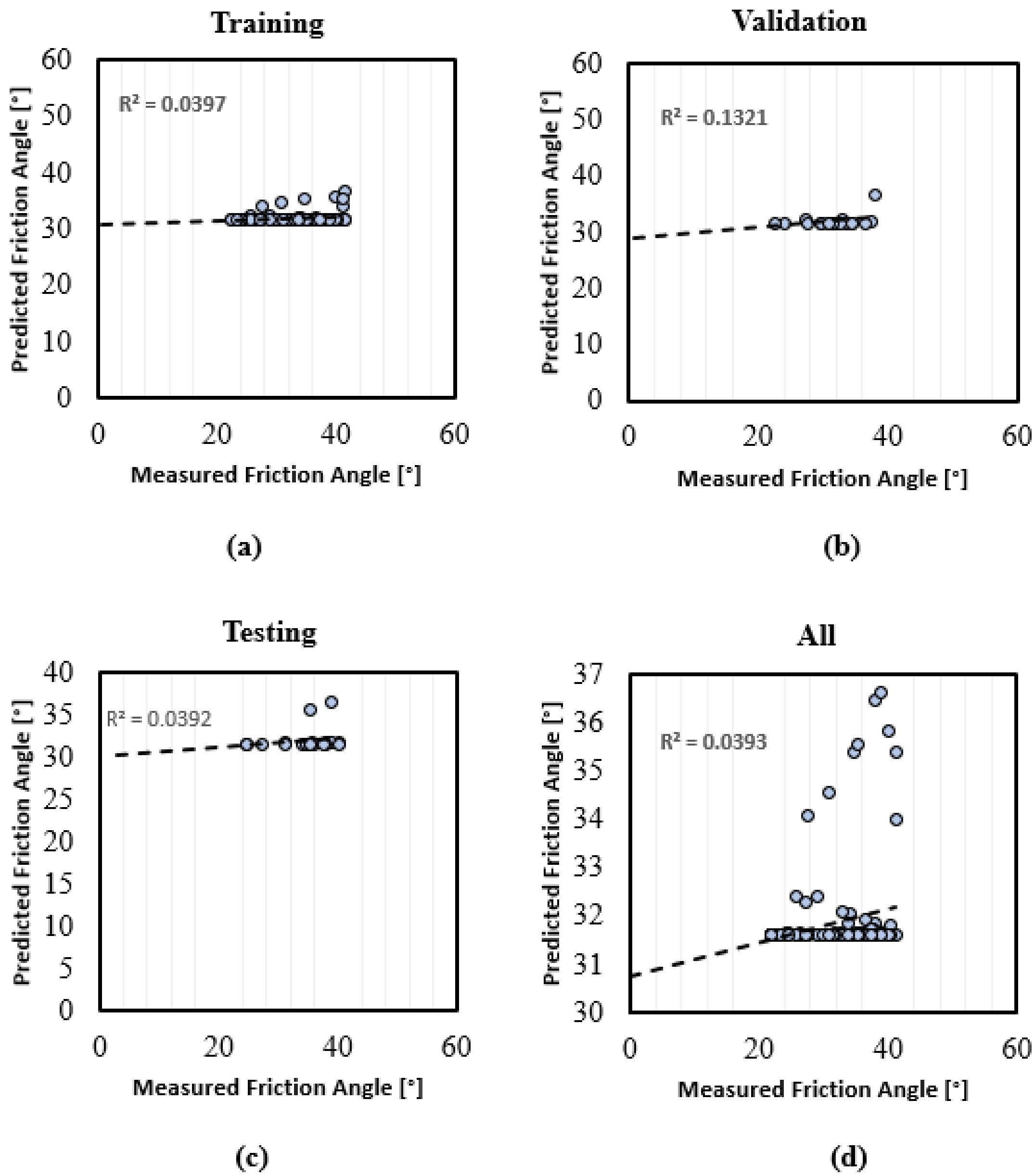

Figure 175. Measured friction angle from direct shear vs predicted friction angle from ANN for Type 1 (2-4-3-1): a) Training; b) Validation; c) Testing; d) All data

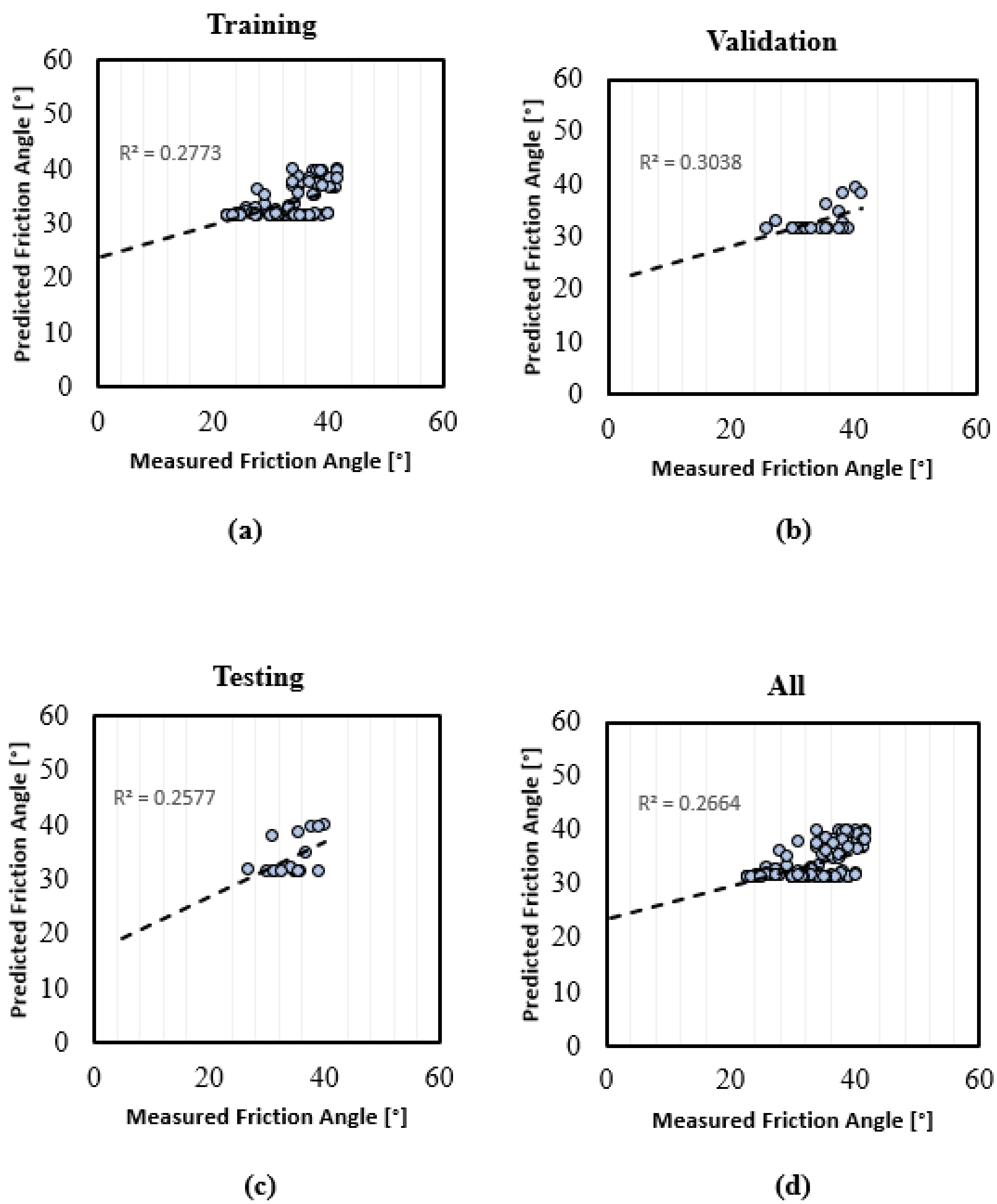

Figure 176. Measured friction angle from direct shear vs predicted friction angle from ANN for Type 2 (5-4-3-2-1): a) Training; b) Validation; c) Testing; d) All data

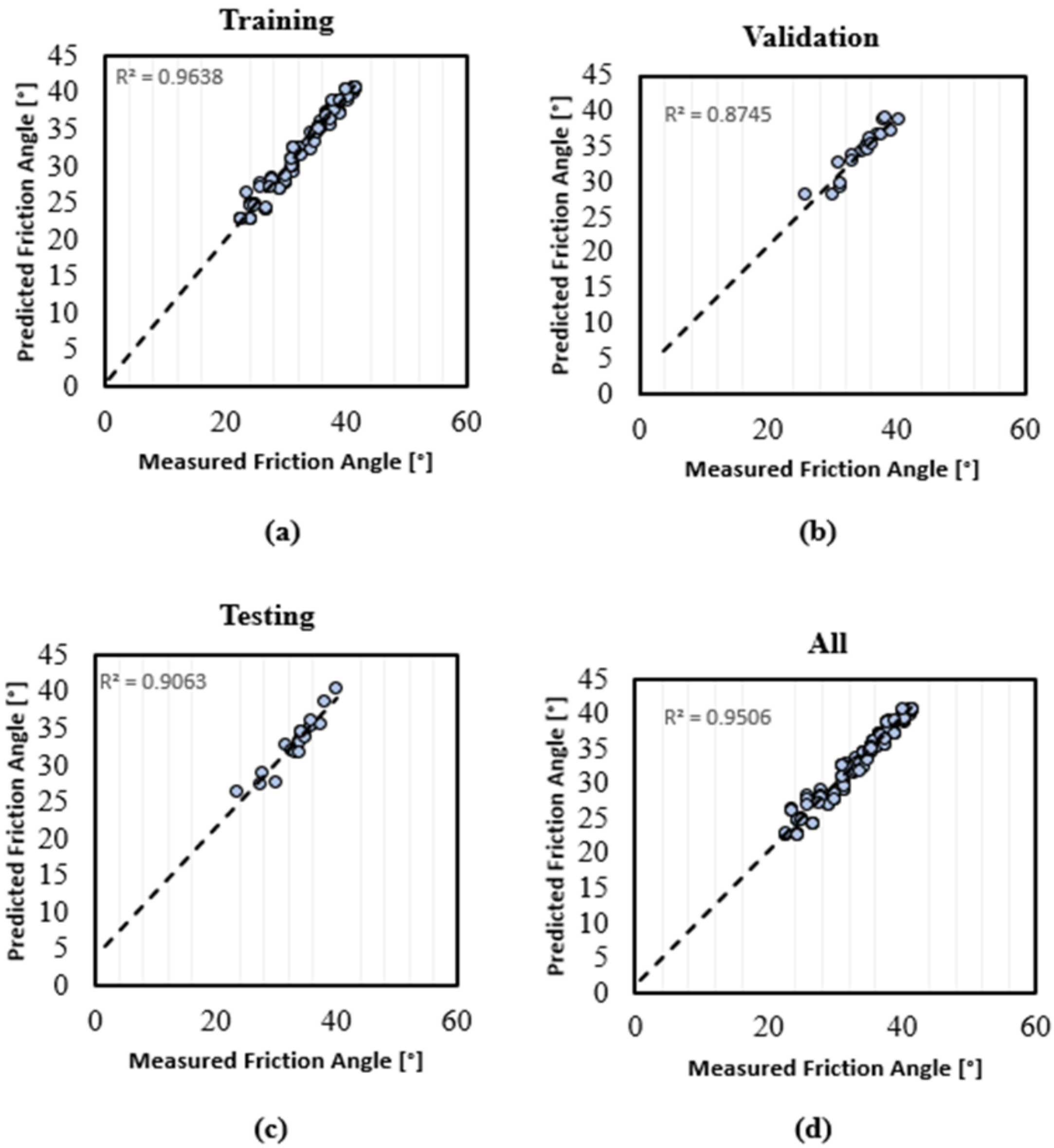

Figure 177. Measured friction angle from direct shear vs predicted friction angle from ANN for Type 2 (5-4-3-1): a) Training; b) Validation; c) Testing; d) All data

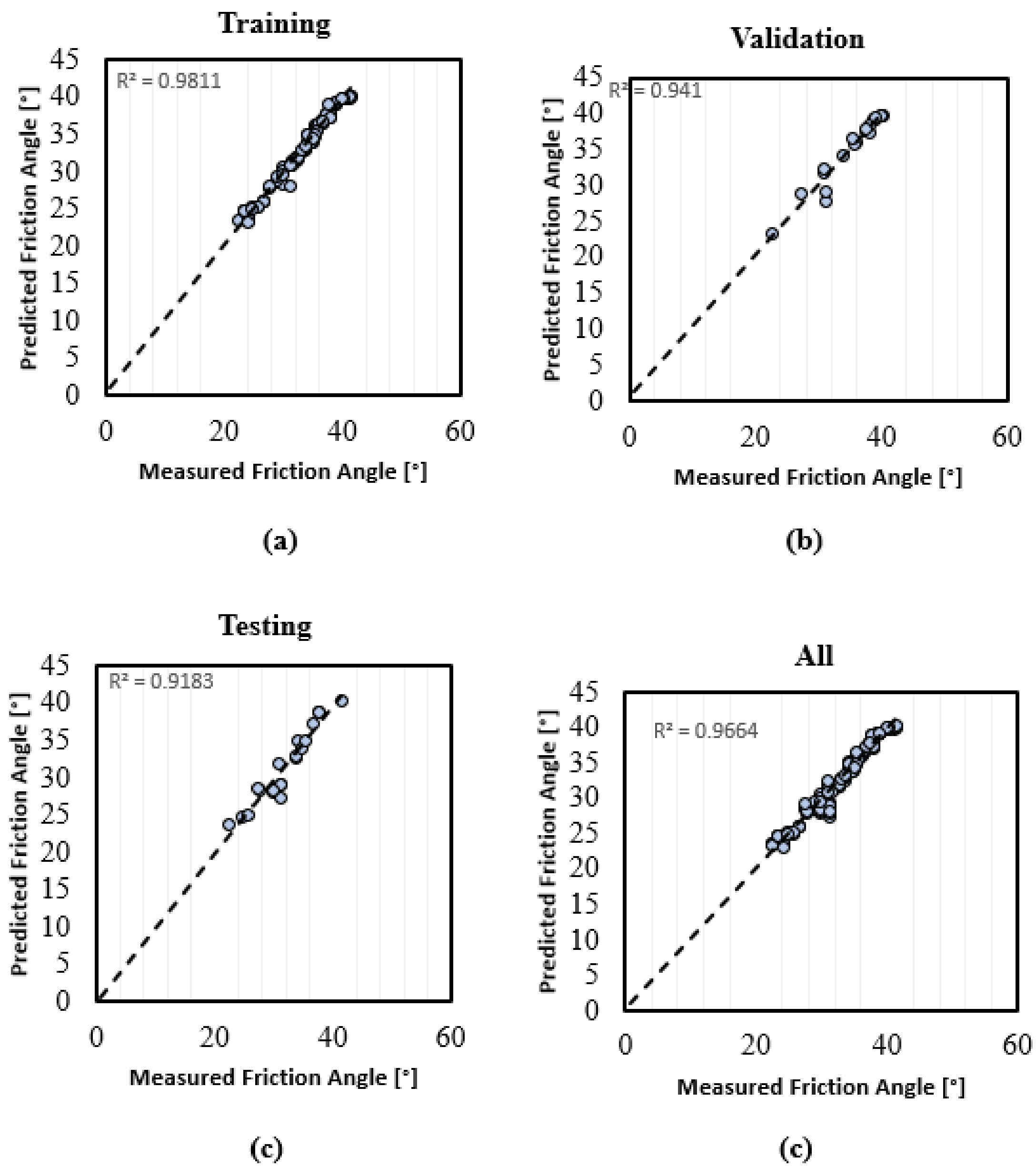

Figure 178. Measured friction angle from direct shear vs predicted friction angle from ANN for Type 3 (5-4-3-2-1): a) Training; b) Validation; c) Testing; d) All data

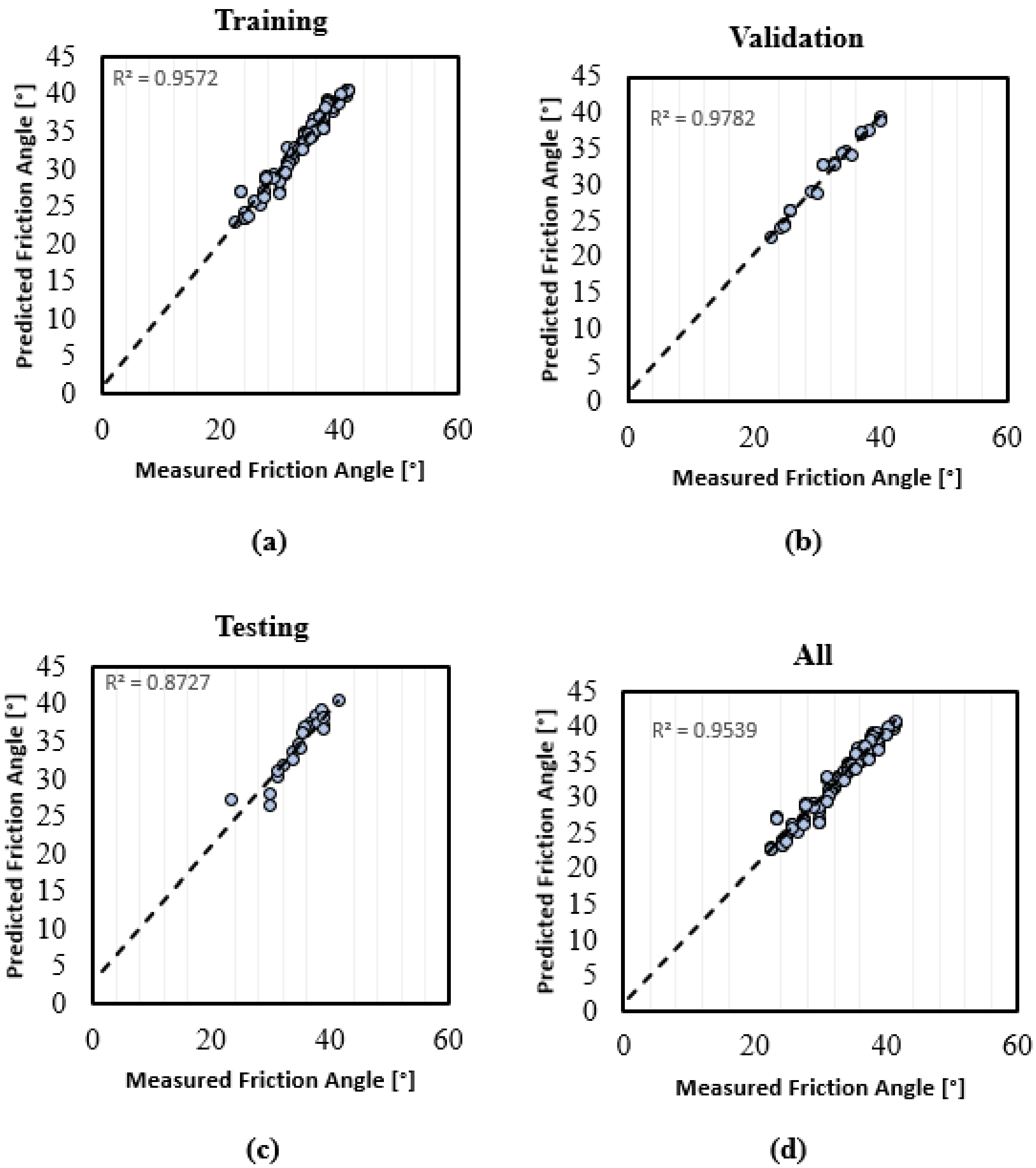

Figure 179. Measured friction angle from direct shear vs predicted friction angle from ANN for Type 3 (5-4-3-1): a) Training; b) Validation; c) Testing; d) All data

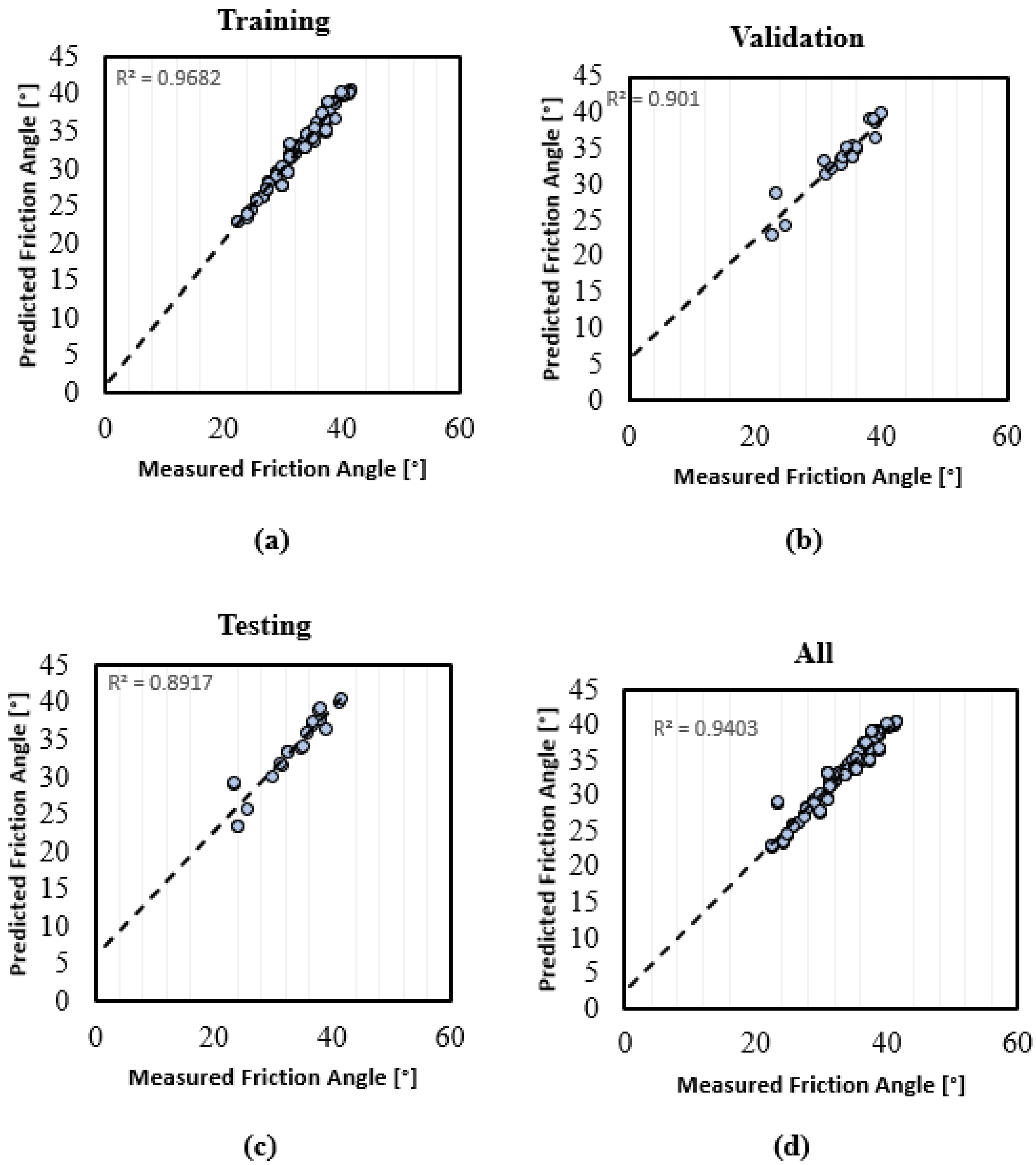

Figure 180. Measured friction angle from direct shear vs predicted friction angle from ANN for Type 4 (6-4-3-2-1): a) Training; b) Validation; c) Testing; d) All data

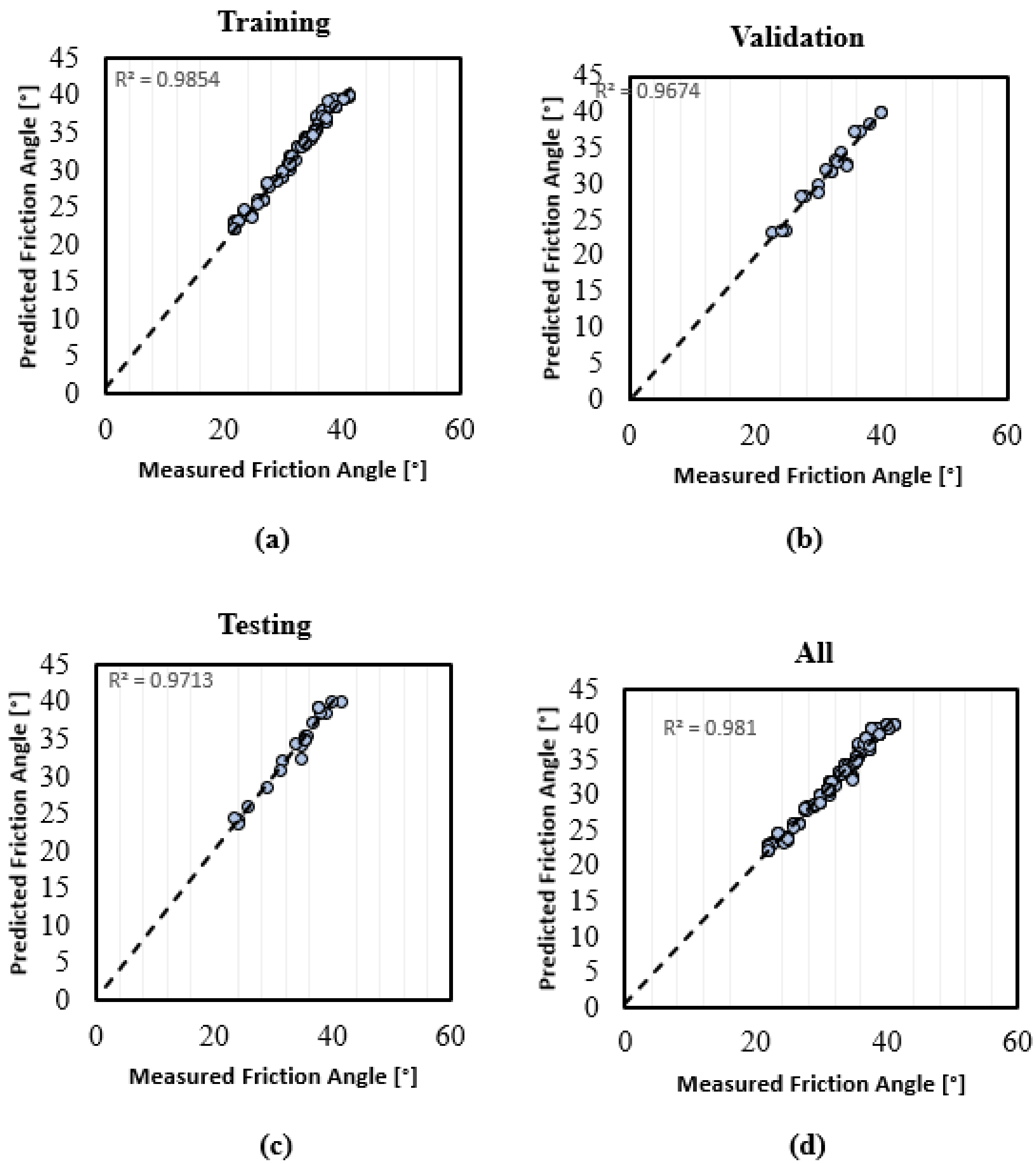

Figure 181. Measured friction angle from direct shear vs predicted friction angle from ANN for Type 4 (6-4-3-1): a) Training; b) Validation; c) Testing; d) All data

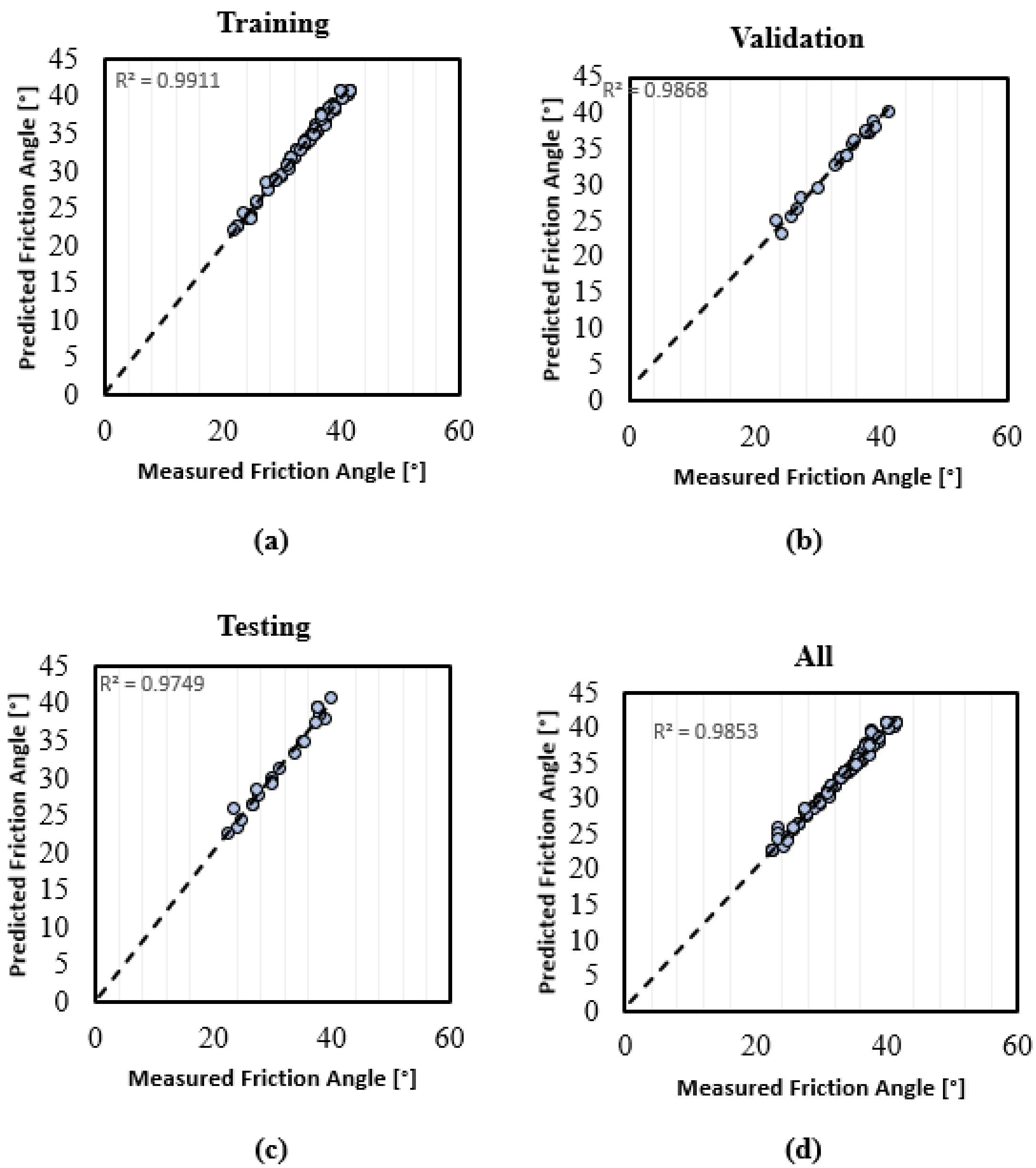

Figure 182. Measured friction angle from direct shear vs predicted friction angle from ANN for Type 5 (4-3-3-1): a) Training; b) Validation; c) Testing; d) All data

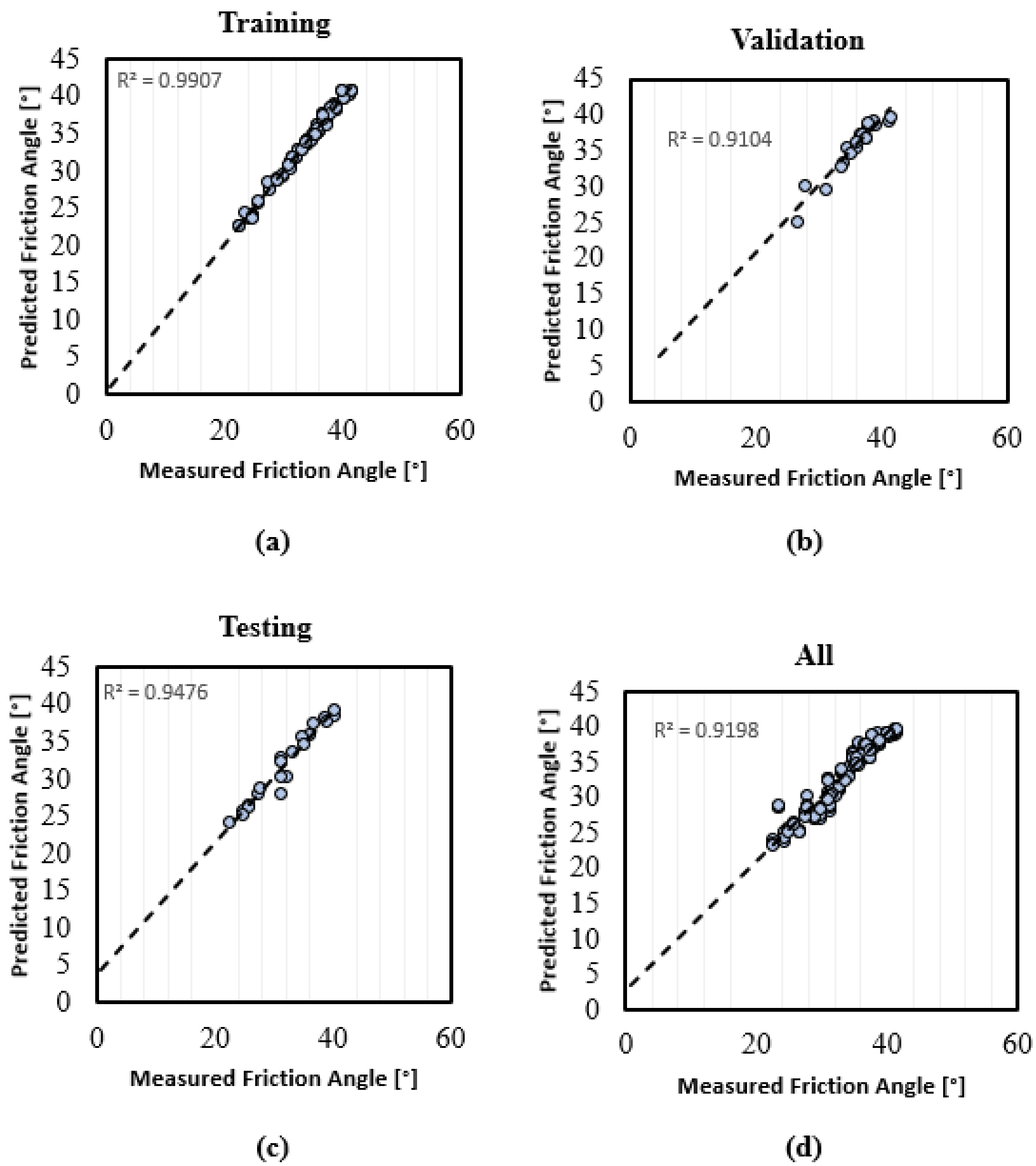

Figure 183. Measured friction angle from direct shear vs predicted friction angle from ANN for Type 5 (4-3-2-1): a) Training; b) Validation; c) Testing; d) All data

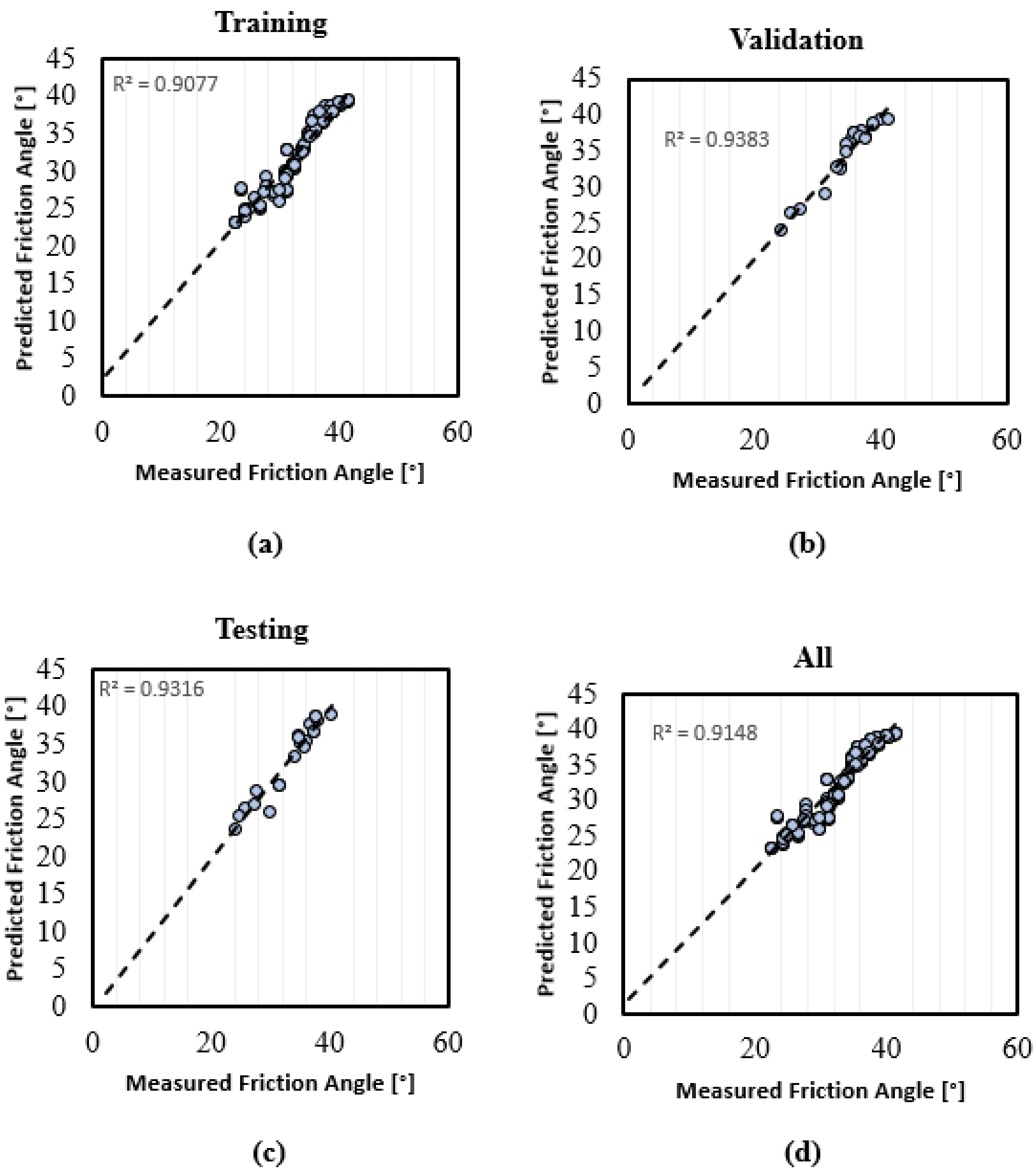

Figure 184. Measured friction angle from direct shear vs predicted friction angle from ANN for Type 6 (4-3-3-1): a) Training; b) Validation; c) Testing; d) All data

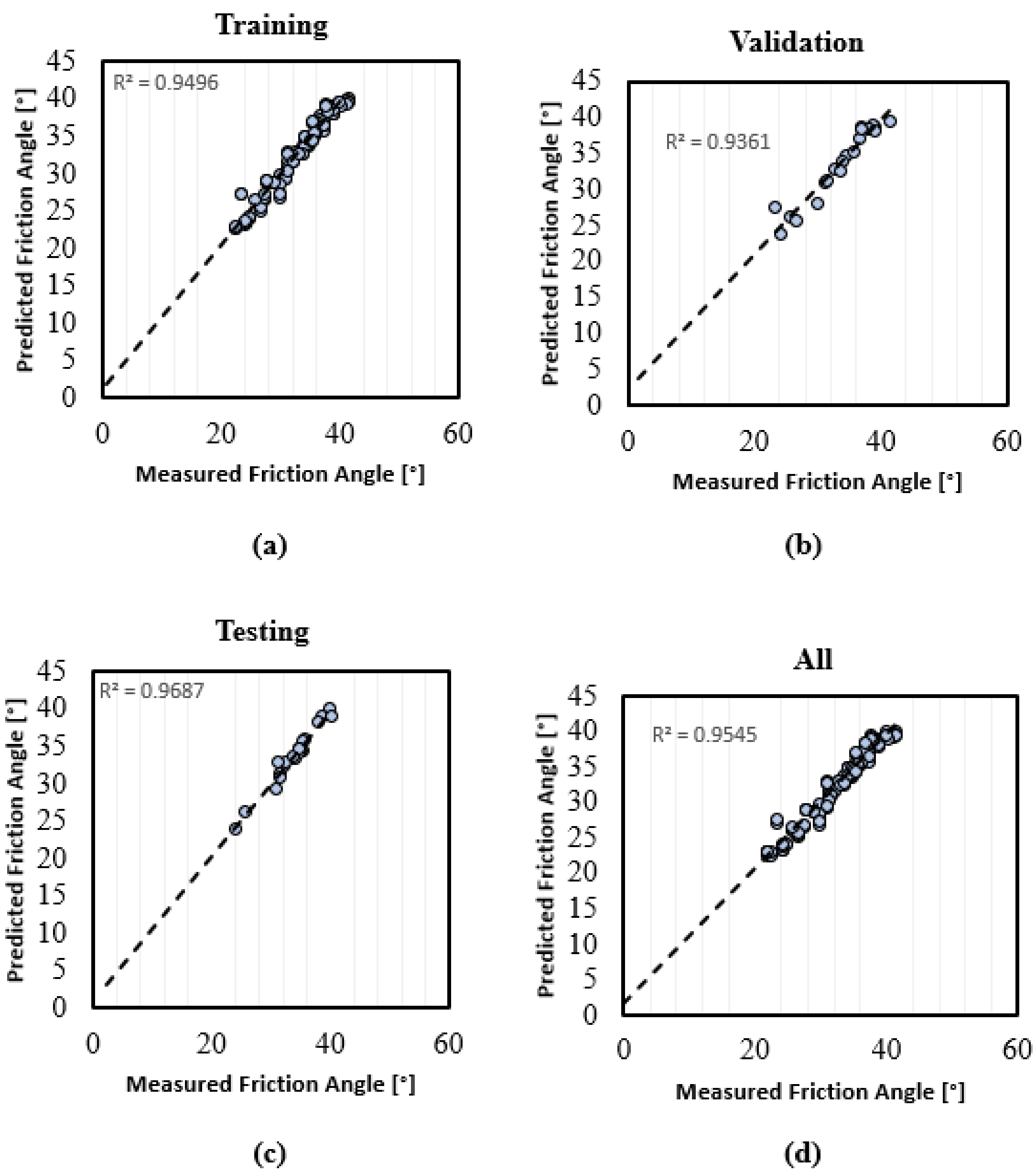

Figure 185. Measured friction angle from direct shear vs predicted friction angle from ANN for Type 6 (4-3-2-1): a) Training; b) Validation; c) Testing; d) All data

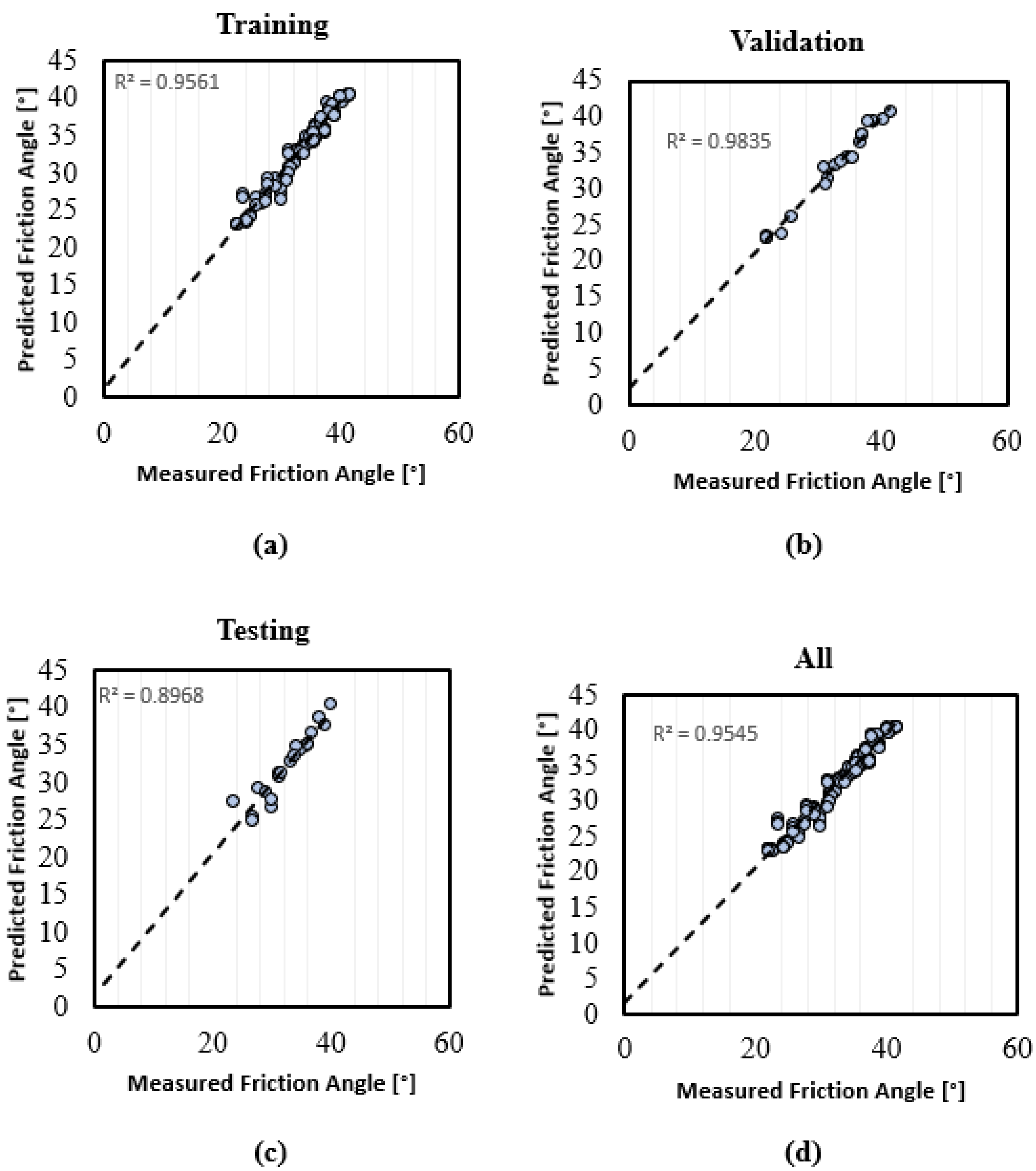

Figure 186. Measured friction angle from direct shear vs predicted friction angle from ANN for Type 7 (5-4-3-2-1): a) Training; b) Validation; c) Testing; d) All data

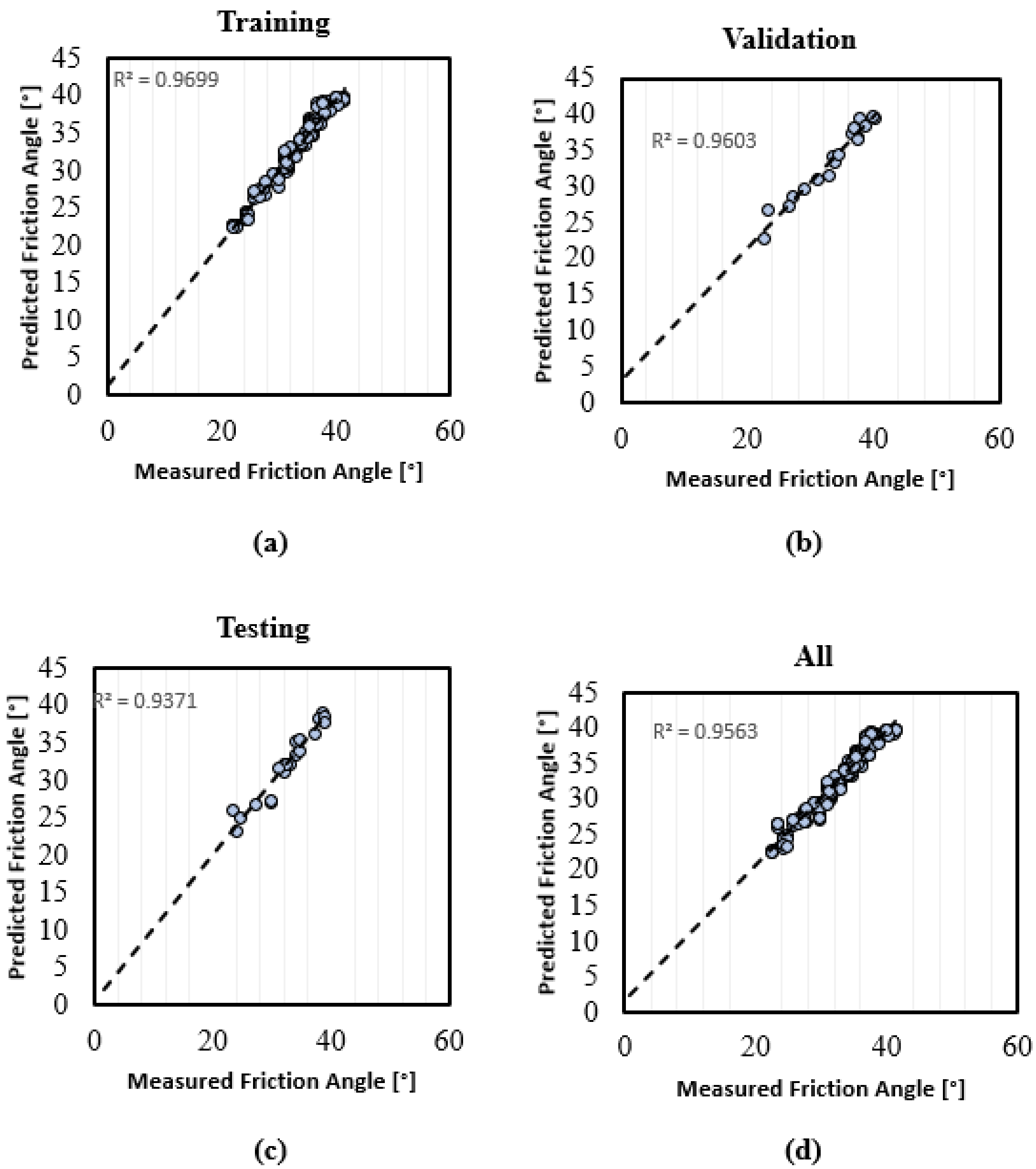

Figure 187. Measured friction angle from direct shear vs predicted friction angle from ANN for Type 7 (5-4-3-1): a) Training; b) Validation; c) Testing; d) All data